

AD 409 46



**USAAVLABS TECHNICAL REPORT 66-48**  
**PARAMETRIC ANALYSIS AND PRELIMINARY DESIGN**  
**OF A SHAFT-DRIVEN ROTOR SYSTEM**  
**FOR A HEAVY-LIFT HELICOPTER**

By

V. Bilezikjian

R. Huss

J. Brye

C. Kaysing

H. Childers

I. Sachs

W. Conway

C. Varner

H. Goldstein

J. Wilson

T. Hanson

CLEARINGHOUSE FOR FEDERAL SCIENTIFIC AND TECHNICAL INFORMATION			
Hardcopy	Microfiche	328	pp
\$7.00	\$1.50		
ARCHIVE COPY			

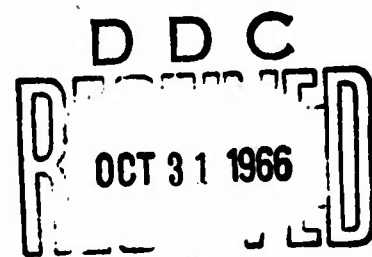
August 1966

code 1

**U. S. ARMY AVIATION MATERIEL LABORATORIES**  
**FORT EUSTIS, VIRGINIA**

**CONTRACT DA 44-177-AMC-276(T)**  
**LOCKHEED-CALIFORNIA COMPANY**  
**DIVISION OF LOCKHEED AIRCRAFT CORPORATION**  
**BURBANK, CALIFORNIA**

Distribution of this  
document is unlimited.



### Disclaimers

The findings in this report are not to be construed as an official Department of the Army position unless so designated by other authorized documents.

When Government drawings, specifications, or other data are used for any purpose other than in connection with a definitely related Government procurement operation, the United States Government thereby incurs no responsibility nor any obligation whatsoever; and the fact that the Government may have formulated, furnished, or in any way supplied the said drawings, specifications, or other data is not to be regarded by implication or otherwise as in any manner licensing the holder or any other person or corporation, or conveying any rights or permission, to manufacture, use, or sell any patented invention that may in any way be related thereto.

Trade names cited in this report do not constitute an official endorsement or approval of the use of such commercial hardware or software.

### Disposition Instructions

Destroy this report when no longer needed. Do not return it to originator.

ACCESSION FOR	
CFSTI	WHITE SECTION <input checked="" type="checkbox"/>
DDC	BUFF SECTION <input type="checkbox"/>
UNANNOUNCED	
CLASSIFICATION	<i>for Statement</i>
BY <i>fm</i>	<i>on file</i>
DISTRIBUTION/AVAILABILITY CODES	
DIST.	AVAIL. and/or SPECIAL
1	



**DEPARTMENT OF THE ARMY**  
**U. S. ARMY AVIATION MATERIEL LABORATORIES**  
**FORT EUSTIS, VIRGINIA 23604**

This report has been reviewed by the U. S. Army Aviation Materiel Laboratories, and basic technical data presented herein are considered to be sound. However, assumptions dependent upon design philosophy and/or engineering judgment are those of the contractor and do not necessarily reflect the views of the U. S. Army Aviation Materiel Laboratories. This report is published for the dissemination of information and the stimulation of ideas.

**Project 1F131001D157  
Contract DA 44-177-AMC-276(T)  
USAAVLABS Technical Report 66-48  
August 1966**

**PARAMETRIC ANALYSIS AND PRELIMINARY DESIGN  
OF A SHAFT-DRIVEN ROTOR SYSTEM  
FOR A HEAVY-LIFT HELICOPTER**

**Final Report  
LR 19143**

**by**

<b>V. Bilezikjian</b>	<b>R. Huss</b>
<b>J. Brye</b>	<b>C. Kaysing</b>
<b>H. Childers</b>	<b>I. Sachs</b>
<b>W. Conway</b>	<b>C. Varner</b>
<b>H. Goldstein</b>	<b>J. Wilson</b>
<b>T. Hanson</b>	

**Prepared by**

**Lockheed-California Company  
Division of Lockheed Aircraft Corporation  
Burbank, California**

**for**

**U. S. ARMY AVIATION MATERIEL LABORATORIES  
FORT EUSTIS, VIRGINIA**

<b>Distribution of this document is unlimited</b>
---



## ABSTRACT

A parametric analysis and a preliminary design study were conducted by the Lockheed-California Company to determine the optimum characteristics of a shaft-driven rotor which would result in the lightest gross weight helicopter capable of lifting military loads in the 12- to 20-ton range.

Helicopter configurations considered included single-rotor and tandem-rotor arrangements, both with internal cargo and with a cargo pod. Types of rotors analyzed were articulated, teetered, rigid, and matched-stiffness. Existing turbine engines or growth versions thereof were considered.

In the parametric analysis, group weight equations were developed and a computer program was utilized to determine the rotor characteristics for each helicopter configuration. For a given set of rotor parameters consisting of rotor radius, thrust/solidity coefficient, and tip speed, the program computed the power plant rating, fuel required, and the empty weight corresponding to the helicopter which would satisfy the most critical mission requirements with the minimum gross weight. The performance of the resulting configuration was determined.

Preliminary design studies of the rotor system, rotor controls, rotor/propulsion arrangement, and the general arrangement were made; corresponding drawings were included. Rotor loads were developed through the use of a performance/trim program and a coupled dynamic response analysis. The dynamic and aeroelastic investigation of the rotor system was based on whirl tower tests, dynamic model tests, and analytical studies. A structural design analysis of the rotor system, including fatigue and weight analysis, was prepared. A stability and control study of the helicopter was conducted, based on the requirements of MIL-H-8501A "General Requirements for Helicopter Flying and Ground Handling Qualities."

The results of the overall study indicate that there is negligible difference in rotor weight between the articulated, teetered, and the Lockheed rigid-rotor systems. The Lockheed matched-stiffness rotor system results in a 4- to 6-percent reduction in helicopter gross weight. This rotor system weight is approximately 10 percent of the transport gross weight. The matched-stiffness single-rotor configuration results in a gross weight of approximately 4,000 pounds less than that of the matched-stiffness tandem-rotor configuration based on the design refinement discussed in Section 6.

## FOREWORD

This report describes the analytical studies performed by the Lockheed-California Company under Contract DA 44-177-AMC-276(T). The program was sponsored by the U.S. Army Aviation Materiel Laboratories (USAAVLABS), Fort Eustis, Virginia, under the technical monitorship of Mr. J. E. Yeates, Mr. W. E. Nettles, and Lt. Nelson Solow.

Part 1 was initiated in January 1965 under the direction of Dr. Richard M. Carlson of Lockheed's Advanced Design Division - Rotary Wing. It was completed in April of 1965. Part 2 was initiated in May 1965 and was completed in October 1965. The parametric and rotor system preliminary design studies were conducted under the guidance of Mr. A. R. Yackle with contributions from the following:

Aerodynamics:	R. Prouty, H. Childers, J. Brye
Structures:	C. Kaysing
Weights:	R. Huss
Loads:	H. Goldstein, J. Gaidelis, R. London, W. Conway
Dynamics:	R. Donham, V. Bilezikjian, I. Sachs
Design:	T. Hanson, M. Salmun
Propulsion:	F. Hiersch, J. Wilson
Project:	C. Varner

Thanks are due to USAAVLABS for support in providing data resulting from previous efforts in this area and for help and advice in planning and conducting the program.

<u>Figure</u>		<u>Page</u>
18	Comparison of 0-Degree, -5-Degree, and -10-Degree Twist of Rectangular Blades - Sea Level Standard Day	64
19	Comparison of Fuel Requirements in Forward Flight for Tapered and Untapered Blades, Matched-Stiffness Rotor	65
20	Forward Flight Power Required for Matched-Stiffness Single-Rotor Helicopter - Sea Level Standard Day, $f_0 = 180$ Square Feet	66
21	Forward Flight Power Required for Matched-Stiffness Single-Rotor Helicopter - Sea Level Standard Day, $f_0 = 100$ Square Feet	67
22	Forward Flight Power Required for Matched-Stiffness Single-Rotor Helicopter - Sea Level Standard Day, $f_0 = 80$ Square Feet	68
23	Forward Flight Power Required for Matched-Stiffness Single-Rotor Helicopter - Sea Level Standard Day, $f_0 = 200$ Square Feet	69
24	Forward Flight Power Required for Matched-Stiffness Single-Rotor Helicopter - 5000 Feet, Standard Day, $f_0 = 80$ Square Feet	70
25	Forward Flight Power Required for Matched-Stiffness Single-Rotor Helicopter - 10,000 Feet, Standard Day, $f_0 = 80$ Square Feet	71
26	Forward Flight Power Required for Matched-Stiffness Single-Rotor Helicopter - 15,000 Feet, Standard Day, $f_0 = 80$ Square Feet	72
27	Forward Flight Power Required for Matched-Stiffness Single-Rotor Helicopter - 20,000 Feet, Standard Day, $f_0 = 80$ Square Feet	73
28	Fuel-Power Relationship, 501-M26 Engine - Sea Level Standard Day, 140 Knots	74
29	Fuel-Power Relationship, 501-M26 Engine - 5000 Feet, Standard Day, 140 Knots	75

<u>Figure</u>		<u>Page</u>
30	Fuel-Power Relationship, 501-M26 Engine - 10,000 Feet, Standard Day, 140 Knots	76
31	Fuel-Power Relationship, 501-M26 Engine - 15,000 Feet, Standard Day, 140 Knots	77
32	Fuel-Power Relationship, 501-M26 Engine - 20,000 Feet, Standard Day, 140 Knots	78
33	Fuel-Power Relationship, 501-M26 Engine - Sea Level Standard Day, Hover	79
34	Ferry Range, Two 501-M26 Engines, Standard Day	80
35	Takeoff Weight vs Range for Matched-Stiffness Single-Rotor System, Standard Day, $f_o = 80$ Square Feet	81
36	Weight - Maximum Specific Range Relationships - One Allison 501-M26 Engine, Sea Level Standard Day	82
37	Weight - Maximum Specific Range Relationships - Two Allison 501-M26 Engines, Sea Level Standard Day	83
38	Maximum Specific Range - Payload Equivalent Flat Plate Area, Allison 501-M26 Engine, Sea Level Standard Day	84
39	Specific Range for Standard Mission Conditions - Two Allison 501-M26 Engines, $\theta_1 = -5$ Degrees	85
40	Power Requirements for Standard Mission Forward Flight Conditions - $\theta_1 = -5$ Degrees	86
41	Effect of Cruise Speed on Mission Radius	88
42	Effect of Cruise Speed on Payload	89
43	Effects of Power Limits, Stall Limits, and Payload Equivalent Drag Area on Maximum Speed - Maximum Speed vs Payload Equivalent Drag Area	91
44	Corrected Available Engine Horsepower vs True Airspeed	92
45	Effects of Power Limits, Stall Limits, and Payload Equivalent Drag Area on Maximum Speed - Velocity vs Total Horsepower Required	93

## CONTENTS

<u>Section</u>	<u>Page</u>
ABSTRACT	111
FOREWORD	v
LIST OF ILLUSTRATIONS	viii
LIST OF TABLES	xvii
LIST OF SYMBOLS	xix
SUMMARY	1
1 PARAMETRIC STUDY	3
2 DESIGN LAYOUT	96
3 STATIC AND DYNAMIC ANALYSES	141
4 STRUCTURAL DESIGN AND WEIGHT ANALYSES	213
5 STABILITY AND CONTROL STUDY	248
6 CONFIGURATION REFINEMENT	262
BIBLIOGRAPHY	308
DISTRIBUTION	311

## ILLUSTRATIONS

<u>Figure</u>		<u>Page</u>
S-1	Shaft-Driven Matched-Stiffness Rotor and Transmission System - Heavy-Lift Helicopter	2
1	General Arrangement, Heavy-Lift Helicopter - Single Rotor, Internal Cargo, Parametric Study	5
2	General Arrangement, Heavy-Lift Helicopter - Single Rotor, Cargo Pod, Parametric Study	7
3	General Arrangement, Heavy-Lift Helicopter - Tandem Rotor, Internal Pod, Parametric Study	9
4	General Arrangement, Heavy-Lift Helicopter - Tandem Rotor, Cargo Pod, Parametric Study	11
5	Solution Gross Weight Determination Program 2477 Flow Diagram, Executive Program	25
6	Solution Gross Weight Determination Program 2477 Flow Diagram, Mission Subroutine	26
7	Output Summary Sheet for Solution Gross Weight Determination Program	33
8	Normalized Fuel Flow Horsepower for 501-M26 Engine	35
9	Dynamic Pressure Distribution in a Rotor Downwash	39
10	Gross Weight and Blade Loading Limited Flight Speed	41
11	Typical Plot of Solution Gross Weight Program Results	43
12	Typical Plot Used in Establishing Solution Limiting Line on Solution Gross Weight Program Results	44
13	Typical Cross Plot for Determining Tip Speed	47
14	Typical Plot for Radius Determination	49
15	Typical Mission Breakdown Computer Output Sheet	50
16	Comparison of Tapered and Rectangular Blade Rotor in Out-of-Ground-Effect Hover	62
17	Comparison of 0-Degree, -5-Degree, and -10-Degree Twist of Rectangular Blades - 6000 Feet, 95°F	63

<u>Figure</u>		<u>Page</u>
46	Hover Limits for Matched-Stiffness Single-Rotor Helicopter - $\theta_1 = -5$ Degrees	94
47	Maximum Hover Power - 501-M25 Engine	95
48	Rotor System Schematic	101
49	Rotor Weight vs Center-of-Gravity Travel and Flexure Stress	107
50	Rotor Assembly, Heavy-Lift Helicopter	109
51	Main Rotor Blade Segment, Heavy-Lift Helicopter	111
52	Spar/Flexure Assembly, Heavy-Lift Helicopter	115
53	Main Rotor Hub, Heavy-Lift Helicopter	117
54	Control Torque Tube Assembly, Heavy-Lift Helicopter	121
55	Gyro/Swash Plate Installation, Heavy-Lift Helicopter	123
56	General Arrangement - Rotor/Propulsion System, Heavy-Lift Helicopter	127
57	Main Rotor Blade Segment, Alternate Design	131
58	Flexure Assembly, Alternate Design	133
59	General Arrangement, Heavy-Lift Helicopter - Single-Rotor, Cargo Pod, Design Study	139
60	Variation of Two-Dimensional Section $C_{L_{max}}$ with Mach Number	147
61	Maximum Mean Rotor Lift Coefficient vs Advance Ratio	149
62	V-n Diagram	150
63	Flapwise Bending Moment vs Rotor Azimuth - Heavy-Lift Mission, 72,325 Pounds, 95 Knots, Rotor Station 165	157
64	Chordwise Bending Moment vs Rotor Azimuth - Heavy-Lift Mission, 72,325 Pounds, 95 Knots, Rotor Station 165	158
65	Flap Bending Moment vs Blade Station - Heavy-Lift Mission, 72,325 Pounds, 95 Knots	159



<u>Figure</u>		<u>Page</u>
66	Chord Bending Moment vs Blade Station - Heavy-Lift Mission, 72,325 Pounds, 95 Knots	160
67	Cyclic Flap Bending Moment vs Load Factor - Heavy-Lift Mission, 72,325 Pounds, 95 Knots	161
68	Steady Flap Bending Moment vs Load Factor - Heavy-Lift Mission, 72,325 Pounds, 95 Knots	162
69	Cyclic Chord Bending Moment vs Load Factor - Heavy-Lift Mission, 72,325 Pounds, 95 Knots	163
70	Steady Chord Bending Moment vs Load Factor - Heavy-Lift Mission, 72,325 Pounds, 95 Knots	164
71	Cyclic Flap Bending Moment vs Load Factor - Transport Mission, 59,325 Pounds, 110 Knots	165
72	Steady Flap Bending Moment vs Load Factor - Transport Mission, 59,325 Pounds, 110 Knots	166
73	Cyclic Chord Bending Moment vs Load Factor - Transport Mission, 59,325 Pounds, 110 Knots	167
74	Steady Chord Bending Moment vs Load Factor - Transport Mission, 59,325 Pounds, 110 Knots	168
75	Cyclic Flap Bending Moment vs Load Factor - 29,705 Pounds, 130 Knots	169
76	Steady Flap Bending Moment vs Load Factor - 29,705 Pounds, 130 Knots	170
77	Cyclic Chord Bending Moment vs Load Factor - 29,705 Pounds, 130 Knots	171
78	Steady Chord Bending Moment vs Load Factor - 29,705 Pounds, 130 Knots	172
79	Centrifugal Force Per Blade vs Blade Station	173
80	Flap Bending Moment vs Blade Station - Takeoff from 10-Degree Slope, 72,325 Pounds	178



<u>Figure</u>		<u>Page</u>
81	First Mode Flapping Bending Moment Distribution	180
82	First Mode In-Plane Bending Moment Distribution	183
83	Flap Bending Moment Spectra at Main Rotor Blade Station 75	186
84	Chord Bending Moment Spectra at Main Rotor Blade Station 75	187
85	Flap Bending Moment Spectra at Main Rotor Blade Station 165	188
86	Chord Bending Moment Spectra at Main Rotor Blade Station 165	189
87	Flight Resonance Analysis of Heavy-Lift Helicopter - Minimum Gross Weight	204
88	Flight Resonance Analysis of Heavy-Lift Helicopter - Maximum Gross Weight	205
89	Main Rotor Frequency Spectrum, Heavy-Lift Helicopter - Collective Angle = 5 Degrees, $\theta_1 = -5$ Degrees	207
90	Main Rotor Frequency Spectrum, Heavy-Lift Helicopter - Collective Angle = 10 Degrees, $\theta_1 = -5$ Degrees	208
91	Main Rotor Frequency Spectrum, Heavy-Lift Helicopter - Collective Angle = 15 Degrees, $\theta_1 = -5$ Degrees	209
92	Blade Cantilever Flapping Mode Shapes	210
93	Blade Cantilever In-Plane Mode Shapes	211
94	S-N Diagram - AM-350 Stainless Steel, $K_T = 1.0$	225
95	S-N Diagram - AM-350 Stainless Steel, $K_T = 2.0$	226
96	S-N Diagram - AM-350 Stainless Steel, $K_T = 3.0$	227
97	S-N Diagram - AM-350 Stainless Steel, $K_T = 4.0$	228
98	Cumulative Percentage of Fatigue Test Specimens Equalling or Exceeding a Ratio of Test Life to Calculated Life	229

<u>Figure</u>		<u>Page</u>
99	Stress Spectra at Main Rotor Blade Station 75	231
100	Stress Spectra at Main Rotor Blade Station 165	232
101	Calculated Life at Main Rotor Blade Station 75 - Transport Mission	233
102	Calculated Life at Main Rotor Blade Station 75 - Heavy-Lift Mission	234
103	Calculated Life at Main Rotor Blade Station 75 - Ferry Mission	235
104	Calculated Life at Main Rotor Blade Station 75 - Training	236
105	Calculated Life at Main Rotor Blade Station 165 - Transport Mission	237
106	Calculated Life at Main Rotor Blade Station 165 - Heavy-Lift Mission	238
107	Calculated Life at Main Rotor Blade Station 165 - Ferry Mission	239
108	Calculated Life at Main Rotor Blade Station 165 - Training	240
109	Calculated Life at Main Rotor Blade Station 75 - Composite	241
110	Calculated Life at Main Rotor Blade Station 165 - Composite	242
111	Variation in Design Stress at Main Rotor Blade Station 75 with K - 3600-Hour Life for Composite Mission Profile No. 2, 40-Percent Reduction in S-N Data	243
112	Variation in Ultimate Design Stress at Main Rotor Blade Station 165 with K - 3600-Hour Life for Composite Mission Profile No. 2, 40-Percent Reduction in S-N Data	243

<u>Figure</u>		<u>Page</u>
113	Rotor Blade Stiffness and Weight Distribution	244
1 4	Main Rotor Pitch Mass Moment of Inertia	245
1 5	Cyclic Control System Schematic	249
1 6	Directional Control System Schematic	251
117	Helicopter Response to Control Inputs - Hovering, 33,000 Pounds, 20-Inch-Aft-Center-of-Gravity Offset	256
118	Helicopter Response to Control Inputs - 130 Knots, 33,000 Pounds, 0-Center-of-Gravity Offset	257
119	Helicopter Response to Control Inputs - 130 Knots, 33,000 Pounds, 20-Inch-Aft-Center-of-Gravity Offset	258
120	Helicopter Response to Control Inputs - Hovering, 72,325 Pounds, 20-Inch-Aft-Center-of-Gravity Offset	259
121	Helicopter Response to Control Inputs - 95 Knots, 72,325 Pounds, 0-Center-of-Gravity Offset	260
122	Helicopter Response to Control Inputs - 95 Knots, 72,325 Pounds, 20-Inch-Aft-Center-of-Gravity Offset	261
123	Rotor Group Weight	266
124	Horizontal Stabilizer Weight	268
125	Tail Rotor Weight	270
126	Landing Gear Weight	274
127	Engine Accessories Weight	277
128	Drive System Weight	281
129	Flight Controls Weight	284
130	Hydraulics and Electrical Group Weight	287
131	Weight Summary	290
132	Output Summary Sheet for Solution Gross Weight Deter- mination - Refined Configuration	296

<u>Figure</u>		<u>Page</u>
133	Matched-Stiffness Blade Loading Limit - Tip Speed Relationship	298
134	Typical Plot of Solution Gross Weight Determination Program - Refined Configuration	299
135	Typical Plot Used in Establishing Solution Limiting Line on Solution Gross Weight Program Results - Refined Configuration	301
136	Typical Plot Used in Selecting Refined Configuration	302

## TABLES

<u>Table</u>		<u>Page</u>
I	Mission Requirements	14
II	Comparison of U.S. Engines - 3,000- to 20,000-SHP Class	16
III	501-M26 Engine Constants	36
IV	Configuration Comparison - External Cargo Helicopters, $\theta_1 = -5$ Degrees	53
V	Adjustments of Computer Results Shown in Table IV	54
VI	Matched-Stiffness Single-Rotor System Description and Weight Breakdown	55
VII	Mission Breakdown and Comparison - Single Matched-Stiffness Rotor	57
VIII	Effect of Single-Point Variations - Single Matched-Stiffness Rotor	58
IX	Design Weights	142
X	Structural Design Load Conditions	156
XI	Power-Off Flight - Heavy-Lift Mission Autorotation at $l_g$	174
XII	Definition of Missions	185
XIII	Summary of 80-Degree-of-Freedom System	196
XIV	Summary of 22-Degree-of-Freedom System	198
XV	Dynamic Equations of Equilibrium for Matched-Stiffness/Flexure Hub Rotor	199

<u>Table</u>		<u>Page</u>
XVI	Symbols for 10 x 10 Equations	201
XVII	Instrument Requirements for CL 875 Based on MIL-H-8501A	253
XVIII	Cases Investigated on the Analog Computer	254
XIX	Rotor Group Weight	265
XX	Tail Rotor Weight	269
XXI	Fuselage Weight	272
XXII	Landing Gear Weight	273
XXIII	Engine Accessories and Nacelle Group	276
XXIV	Fuel System Weight	278
XXV	Drive System Weight	279
XXVI	Flight Controls Weight	283
XXVII	Hydraulics and Electrical System Weight	286
XXVIII	Configuration Description External Cargo Helicopter, $\theta_1 = -5$ Degrees	304
XXIX	Adjustments of Computer Results Shown in Table XXVIII	304
XXX	Description of Matched-Stiffness Single- and Tandem-Rotor Systems and Weight Breakdown Comparison	305

### SYMBOLS

A	Area
$A_0$	Static angular position of flexure, radians
$A_1$	Maximum centrifugal restoring moment possible
$A_1$	Cyclic pitch, radians
$A_0, A_1, A_2$ , etc	Coefficients for curve for $C_{L_{max}}$ as a function of local Mach number
$a_0$	Coning angle
$a_2$	Second harmonic flapping angle
$a_n$	Flapping coefficients
AR	Aspect Ratio
B	Effective radius ratio
B	Tip loss factor
b	Number of blades
$B_0$	Flapping displacement due to static load
$B_1$	Cyclic pitch, radians
$B_f$	Relative blade flapping with respect to the torque tube
BL	Blade loading
BM	Bending moment
BR	Effective rotor radius
C	Blade chord
C	Damping, ft-lb/radian/sec
c	Distance from neutral axis to fiber in question
$C_D$	Drag coefficient
$C_L$	Lift coefficient
$C_{L_{ro}}$	Design mean lift coefficient
$C_L/\alpha$	Lift-curve slope per radian

$C_M$	Moment coefficient to account for spanwise location of sweep angle
$C_{Q_0}/\sigma$	Rotor profile torque coefficient
$C_T$	Thrust coefficient
$C_T/\sigma$	Solidity factor
CF	Centrifugal force
CG	Center of gravity
$C(X)$	Circumference at X
DL	Disc Loading
d/e	Mechanical advantage of blade feathering to gyro tilt motion
E	Modulus of elasticity
E	Inplane displacement due to static load
e	Distance of effective in-plane pivot location from center line of hub
EI	Flexural stiffness, lb-in. <sup>2</sup>
$EI_a$	Flexure flap bending at the point where the flexure joins the hub
f	Function
f	1/rev flap bending stress
f	Stress
$f_o$	Equivalent drag area
$f_1$	First mode amplification factor
$f_b$	Unit stress at flexure corner for flapping moment of 100,000 in-lb
$F_{bu}$	Flapwise buckling stress
$f_s$	Shear stress
$f_{s-a}$	Alternate (cyclic) shear stress
$F_{se}$	Shear endurance stress
$f_t$	Unit Stress at flexure corner for centrifugal force of 100,000 lb
$F_{tu}$	Ultimate tensile strength
FF	Fuel flow, lb/hr



$g$	Acceleration of gravity
GR	Gear ratio
$h$	Flexure thickness
$h$	Distance between WL through CG and ground line at the uphill MLG, ft
$h_F$	Distance of fuselage, transmission, and shaft system CG from hub
$h_r$	Distance between CG and rotor hub, ft
HLH	Heavy-lift helicopter
HOGE	Hover out-of-ground effect
$I$	Moment of inertia, slug-ft <sup>2</sup>
$I_{eb}$	Moment of inertia of one blade about the effective pivot location
$I_{zg}$	Polar moment of inertia of the gyro, slug-ft <sup>2</sup>
$I_{\theta F}$	Pitch moment of inertia of fuselage, transmission, and shaft
$I_{\phi F}$	Roll moment of inertia of fuselage, transmission, and shaft
$J$	Polar moment of inertia
$K$	Equation constant (usage defined at point of usage)
$K$	Control gyro mechanical advantage (gyro angle/blade angle)
$K$	Fatigue quality index
$K_c$	Fuel flow equation constant
$K_{DW}$	Correction factor for rotor thrust due to impingement of downwash on fuselage
$K_G$	Control spring stiffness as seen by the control gyro swash plate
$K_G$	Torsional stiffness, lb-in. <sup>2</sup>
$K_i$	Fuel weight to transport weight adjustment factor for current iteration
$K_T$	Notch factor
$K_v$	Fuel flow equation constant

$K_{\theta}$	Rotor stiffness on the shaft, ft-lb/radian
$K_{\theta_0}$	Flapping stiffness of blade outboard of feathering bearing
$K_e$	In-plane stiffness of blade outboard of feathering bearing
$K_{\theta}$	Rotor stiffness
$L$	Fuselage length, ft
$L_G$	Rolling moment on gyro
$lg$	Landing gear tread
$L_H$	Rolling moment on hub
$L_R$	Distance between rotors (tandem helicopter)
$L_{TR}$	Distance between main rotor and tail rotor
$M$	Mass, W/g
$M$	Bending moment
$M_A$	Aerodynamic effectiveness of cyclic feathering in producing moment
$M_b$	Flapwise bending
$M_C$	Chordwise bending moment, in.-lb
$M_f$	Feathering control moment
$M_f$	Moment on a fastener, in.-lb/ft of span
$M_f$	Flap bending moment, in.-lb
$M_G$	Swash plate damper
$M_H$	Pitching moment on hub
$M_t$	Rotational tip Mach number
$M_x$	Local Mach number
$M_{\dot{\theta}}$	Rotor aerodynamic damping in pitch
$M_{\dot{\phi}}$	Rotor aerodynamic damping in roll
M.S.	Margin of safety
$N$	Axial load
$n$	Load factor
$N_1$	Integer number
nm	Nautical mile

NRP	Normal rated power
$NRP \frac{V}{n}$	Normal rated power for velocity V and altitude h
OGE	Out-of-ground effect
P	Load on a fastener
P	Laplace operator
PL	Payload
Q	Main rotor torque
q	Rate of pitch, radians/sec
$Q_b$	Chordwise bending
$q_c$	Cyclic in-plane root moment
$q_g$	Rate of precession of the gyro, radians/sec
$Q_s$	Tail rotor drive shaft torque
QTR	Tail rotor torque
R	Main rotor radius, ft
r	Distance from the hub to a point on the rotor less than the full radius
$R_c$	Radius of curvature
$R_H$	Vector sum of $L_H$ and $M_H$
$R_M$	Mean radius
RHP	Required horsepower
RM	Mission radius
RP	Rated horsepower
RPSL	Maximum rated horsepower at sea level
S	Stress
$S_{eb}$	Blade static unbalance about effective pivot location
$S_\beta$	Blade static unbalance in flapping
SFC	Specific fuel consumption
SHP	Shaft horsepower

T	Thrust or rotor lift
t	Time of mission, hr
T <sub>TR</sub>	Tail rotor thrust
t <sub>1</sub> , t <sub>2</sub> , etc	Coefficients as defined in NACA Report No. 716
U	Blade section local velocity, fps
U(X)	Area unit weight at X
V	Flight velocity, ft/sec
V <sub>c</sub>	Cruise speed
V <sub>D</sub>	Design speed
V <sub>K</sub>	Flight velocity, knots
V <sub>T</sub>	Tip speed, ft/sec
v <sub>1</sub>	Induced velocity at front rotor of a tandem rotor helicopter, ft/sec
v <sub>2</sub>	Downwash velocity
$\left(\frac{v_2}{v_1}\right)$	Computer expression for ratio of downwash velocity to induced velocity
W	Design gross weight, lb
W <sub>ACC</sub>	Engine accessories group weight, lb. Includes air induction, exhaust and cooling systems, engine lubrication system, engine controls, starting system, and engine section or nacelle group
W <sub>ACE</sub>	Weight of air conditioning, external cargo, lb
W <sub>ACI</sub>	Weight of air conditioning, internal cargo, lb
W <sub>AUX</sub>	Weight of auxiliary gear, lb
W <sub>b</sub>	Blade weight, lb
W <sub>B</sub>	Fuselage weight, including vertical stabilizer, lb
W <sub>BASIC</sub>	Component weight plus oil weight plus crew less fuel tanks, lb
W <sub>BE</sub>	Fuselage weight, single rotor, external cargo, lb
W <sub>BI</sub>	Fuselage weight, single rotor, internal cargo, lb
W <sub>BTE</sub>	Fuselage weight, tandem rotor, external cargo, lb
W <sub>BTI</sub>	Fuselage weight, tandem rotor, internal cargo, lb

W <sub>C</sub>	Weight of crew, lb
W <sub>DS</sub>	Drive system weight, single-rotor helicopter, includes main and tail rotor gearboxes, interconnecting shafts, and all mounting provisions, lb
W <sub>DST</sub>	Drive system weight, tandem rotor, lb
W <sub>E</sub>	Engine weight, lb
W <sub>F</sub>	Fuel weight, lb
W <sub>F</sub>	Weight of fuselage, transmission, and shaft system, lb
W <sub>FC</sub>	Flight controls weight, lb
W <sub>FCT</sub>	Flight controls weight, tandem rotor, lb
W <sub>FE</sub>	Furnishings weight, external cargo, lb
W <sub>FI</sub>	Furnishings weight, internal cargo, lb
W <sub>FS</sub>	Fuel system weight, including tanks and plumbing, lb
W <sub>FIXED</sub>	Specific weight dependent on mission requirements, lb
W <sub>HET</sub>	Weight of hydraulics and electrical, tandem rotor, lb
W <sub>HE</sub>	Weight of hydraulics and electrical, lb
W <sub>HL</sub>	Solution gross weight, heavy-lift mission, lb
W <sub>IE</sub>	Weight of instruments and electronics, lb
W <sub>LG</sub>	Landing gear weight, single rotor, lb
W <sub>LGS</sub>	Landing gear weight, straddle type, single rotor, lb
W <sub>LGT</sub>	Landing gear weight, tandem rotor, lb
W <sub>LGST</sub>	Landing gear weight, tandem rotor, straddle type, lb
W <sub>OIL</sub>	Engine oil weight, lb
W <sub>RG</sub>	Rotor and hub group weight, lb
W <sub>RGT</sub>	Rotor and hub group weight, tandem rotor, lb
W <sub>RO</sub>	Residual fuel and oil weight, lb
W <sub>ST</sub>	Horizontal stabilizer weight, lb
W <sub>T</sub>	Solution gross weight, transport mission, lb
W <sub>TR</sub>	Tail rotor weight
W <sub>L</sub>	Water line
X	Spanwise blade section location, nondimensional
X	Fore and aft translation of entire system, positive forward

Y Lateral translation of entire system, positive right

$\frac{Z}{R}$  Ratio of height of rear rotor above front rotor plane  
to rotor radius

## SUBSCRIPTS

Allow	Allowable
Avail	Available
Ave	Average
b	Blade
CF	Centrifugal force
cf	Centrifugal
D	Design
e	Equivalent
F	Fuselage and shaft
G	Control gyro
H	Hub
HL	Heavy-lift mission
K	Constant, usage explained in text
MR	Main rotor
n	Load factor
q	Rate of pitch
R	Rotor
REQ	Required
SL	Sea level

T	Transport mission
TR	Tail rotor
t	Trim lg
X,Y,Z	Axis of rotation
Leg 1	Warm-up
Leg 2	Hover
Leg 3	Outbound
Leg 4	Hover
Leg 5	Inbound

Numbers such as 165 or 270, mean blade stations or azimuth angles, as applicable



### SYMBOLS FOR COMPUTER INPUTS AND OUTPUTS

ALF 270	Retreating blade angle of attack, degrees
ALT. $F_t$	Altitude, ft. (0.11111099 E-06 indicates warm-up leg. A negative sign indicates 95° day)
CLROHL	Rotor design mean lift coefficient at sea level standard day with heavy-lift mission solution gross weight
CLROT	Same as CLROHL except for transport mission
CT/SIGMA	Input used in determining solidity
DELPHI	Delta payload, payload change during each leg
FO	Parasite area
HP	Horsepower calculated for each leg (0 for warm-up)
IHP	Induced horsepower used in calculating d (fuel flow, with respect to time)
j	Number of the leg of the mission
K, TR	Constant added to main rotor radius to determine first approximation of tail rotor thrust for sizing the tail rotor
LEG 1	Warm-up
LEG 2	Hover
LEG 3	Outbound
LEG 4	Hover
LEG 5	Inbound
MR	Main rotor
MAXRP	Maximum rated power required by missions converted to rated power at sea level static standard day conditions
PCSRPC	Percent of maximum rated power calculated for each leg
PCXRP	Percent maximum rated power (for warm-up calculations)
SIGMA	Solidity, blade area/disc area
T	Flight time, hr (calculated from $V_K$ and distance or input in minutes)

TR	Tail rotor
V <sub>K</sub>	Flight velocity, knots
W	Engine weight
W <sub>B</sub>	Fuselage weight
W <sub>BASIC</sub>	Empty weight plus crew and oil
W <sub>CREW</sub>	Crew weight
W <sub>DS</sub>	Tail rotor drive shaft weight
W <sub>EMPTY</sub>	Empty weight (less fuel tanks)
W <sub>ES</sub>	Engine section weight
W <sub>FAVAILT</sub>	Fuel weight available for transport mission
W <sub>FLEG</sub>	Fuel used each leg
W <sub>FREQHL</sub>	Heavy-lift mission fuel weight required
W <sub>FREQT</sub>	Transport mission fuel weight required
W <sub>GBT</sub>	Tail rotor gearbox weight
W <sub>HL</sub>	Solution heavy-lift mission weight
W <sub>I</sub>	Weight iteration identification
W <sub>LEG</sub>	Weight of aircraft used for power calculations in each leg
W <sub>LG</sub>	Landing gear weight
W <sub>MRD</sub>	Main rotor drive shaft weight
W <sub>O</sub>	Initial gross weight
W <sub>OIL</sub>	Oil weight (for engines and transmission)
W <sub>RG</sub>	Rotor group weight
W <sub>RUN</sub>	Initial gross weight for specific run
W <sub>RUNHL</sub>	Initial gross weight for heavy-lift mission
W <sub>RUNT</sub>	Initial gross weight for transport mission
W <sub>ST</sub>	Stabilizer weight
W <sub>T</sub>	Solution transport mission weight
W <sub>TR</sub>	Tail rotor weight
XRPVH	Maximum rated power per engine that can be used for flight condition

### GREEK SYMBOLS

(Alpha)	$\alpha$	Angle of attack
	$\alpha_o$	Wake skew angle measured from the normal to the tip path plane below the rotor
	$\alpha_{270}$	Retreating blade angle of attack
(Beta)	$\beta$	Angle between gyro arm and blade
	$\beta_o$	Effective fixed cone angle, radians
	$\bar{\beta}_o$	Flapping displacement due to perturbational load, positive up
	$\Delta\beta$	Blade overcone angle outboard of feathering bearing angle, positive up
(Delta)	$\delta$	Vertical blade displacement
	$\delta$ or $\Delta$	Increment
(Epsilon)	$\bar{\epsilon}$	In-plane displacement due to perturbational load, positive aft
	$\epsilon_x$ or $y$	Angular deflection component of all blade toward front or toward the right side of rotor
(ETA)	$\eta$	Lateral CG offset with respect to rotor shaft
(THETA)	$\theta$	Pitch attitude
	$\theta$	Blade incidence angle, degrees
	$\theta$	Mean blade pitch angle, radians
	$\theta$	Angle formed by attitude of vehicle with ground plane when downhill MLG just clears the ground
	$\theta_1$	Angle for zero centrifugal restoring moment, radians
	$\theta l_c$	Longitudinal cyclic pitch angle, radians
	$\theta l_s$	Lateral cyclic pitch angle, radians
(LAMBDA)	$\theta_s$	Angle of ground lines with horizontal
	$\lambda$	Inflow ratio
	$\lambda$	Blade sweep forward, positive forward
(Mu)	$\mu$	Advance ratio or tip speed ratio

(Nu)	$\nu$	Expression in load factor criteria, defined as $B^3 + 3/2B\mu_n^2 + 4/3\pi\mu_n^3$
(RHO)	$\rho$	Density
(SIGMA)	$\sigma$	Solidity ratio, blade area/disc area
	$CT/\sigma$	Solidity factor
(PHI)	$\phi$	Roll attitude
(PSI)	$\psi$	Rotor blade azimuth position
	$\psi^1$	Blade sweep angle
	$\psi_0$	Control gyro cant angle to blade
(OMEGA)	$\Omega$	Rotor speed, radians per second
	$\Omega$	Rotational velocity of the gyro
	$\Omega R$	Rotor tip speed
(KAPPA)	$\kappa$	Longitudinal CG offset with respect to rotor shaft

## SUMMARY

This report presents the results of studies conducted for the U.S. Army Aviation Materiel Laboratories by the Lockheed-California Company under Contract DA 44-177-AMC-276(T) to determine the characteristics of a shaft-driven helicopter capable of lifting military loads in the 12-20-ton range.

The studies were conducted in two parts: (1) a parametric analysis and configuration determination of the rotor system and (2) a rotor system preliminary design.

Part 1 of this study covered the parametric analysis during which the helicopter component weight equations were derived, the solution gross weight computer program routine was developed, the rotor system characteristics were determined, and the performance of the rotor system was analyzed. Part 2 covered the preliminary design phase of the program which included design of the rotor system components, a rotor/propulsion system arrangement, static and dynamic loads analyses including a dynamic and aeroelastic investigation of the rotor system, structural and weight analyses, fatigue analysis, and stability and control study. Additional studies were conducted to refine the weight equations for high gross weight vehicles and to determine any associated changes in rotor system characteristics or gross weight.

The characteristics of the single matched-stiffness rotor system resulting from the additional studies of Part 2 of this program are summarized as follows:

Design gross weight	74,727 lb
Transport mission weight	62,500 lb
Number of blades	5
Rotor diameter	104 ft
Blade chord	38.0 in.
Blade section	NACA 0012

Rotor tip speed	730 fps
Mean blade lift coefficient	0.484
Aspect ratio	16.5

The rotor system is illustrated in Figure S-1 and consists of the hub (which is the central fitting integral with the transmission), the five matched-stiffness spar/flexures, and the rotor blade segments. The control system consists of the gyro-swash plate assembly, the five control torque tubes, and the pitch links which connect the gyro to the control torque tube. The transmission configuration as shown is arranged for a three-engine system. This is a typical arrangement only, as the number and type of engines can be varied as circumstances dictate.

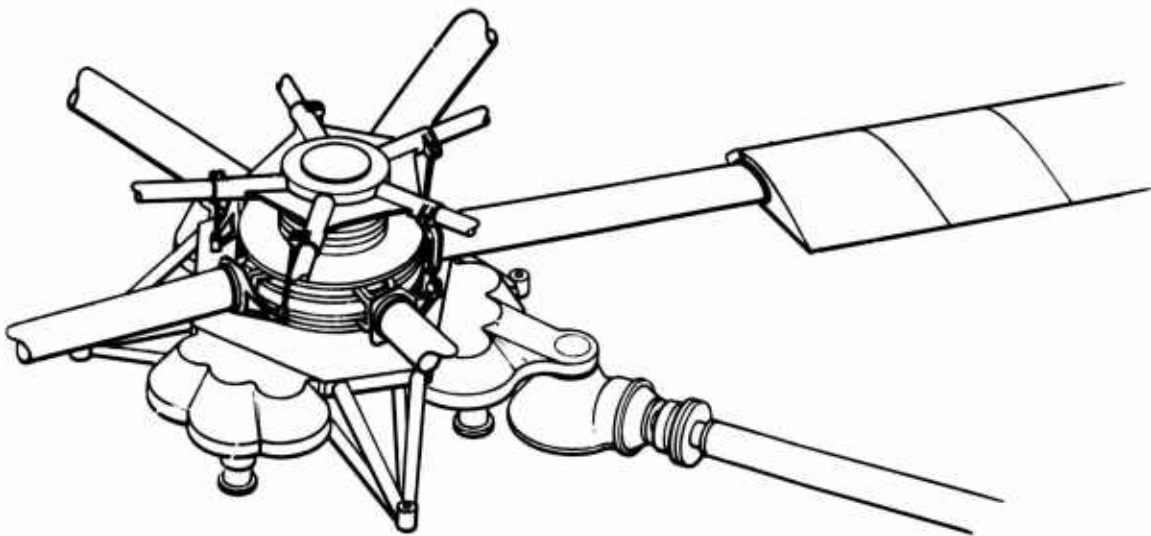


Figure S-1. Shaft-Driven Matched-Stiffness Rotor and Transmission System - Heavy-Lift Helicopter

## SECTION 1

### PARAMETRIC STUDY

#### INTRODUCTION

A parametric analysis of a shaft-driven heavy-lift helicopter (HLH) rotor system was conducted to determine the optimum rotor characteristics of a helicopter which would perform the transport, heavy-lift, and ferry missions specified by the Statement of Work. This analysis was conducted in conjunction with a preliminary design study of the rotor system.

The overall helicopter configuration was established in sufficient detail to provide weight and drag data used in the rotor analysis. The major effort was placed on rotor analysis and design, determination of propulsion requirements, and an empirical performance analysis. The helicopter configurations considered in the parametric analysis were:

- Single rotor - internal cargo (Figure 1)
- Single rotor - cargo pod (Figure 2)
- Tandem rotor - internal cargo (Figure 3)
- Tandem rotor - cargo pod (Figure 4)

The helicopter configuration selected for the preliminary design effort is presented in Section 2 (Figure 59).

For identification purposes the heavy-lift helicopter is referred to as Lockheed Model CL 875.

#### BASIC DESIGN ANALYSIS

The following paragraphs present the design considerations used in the study:

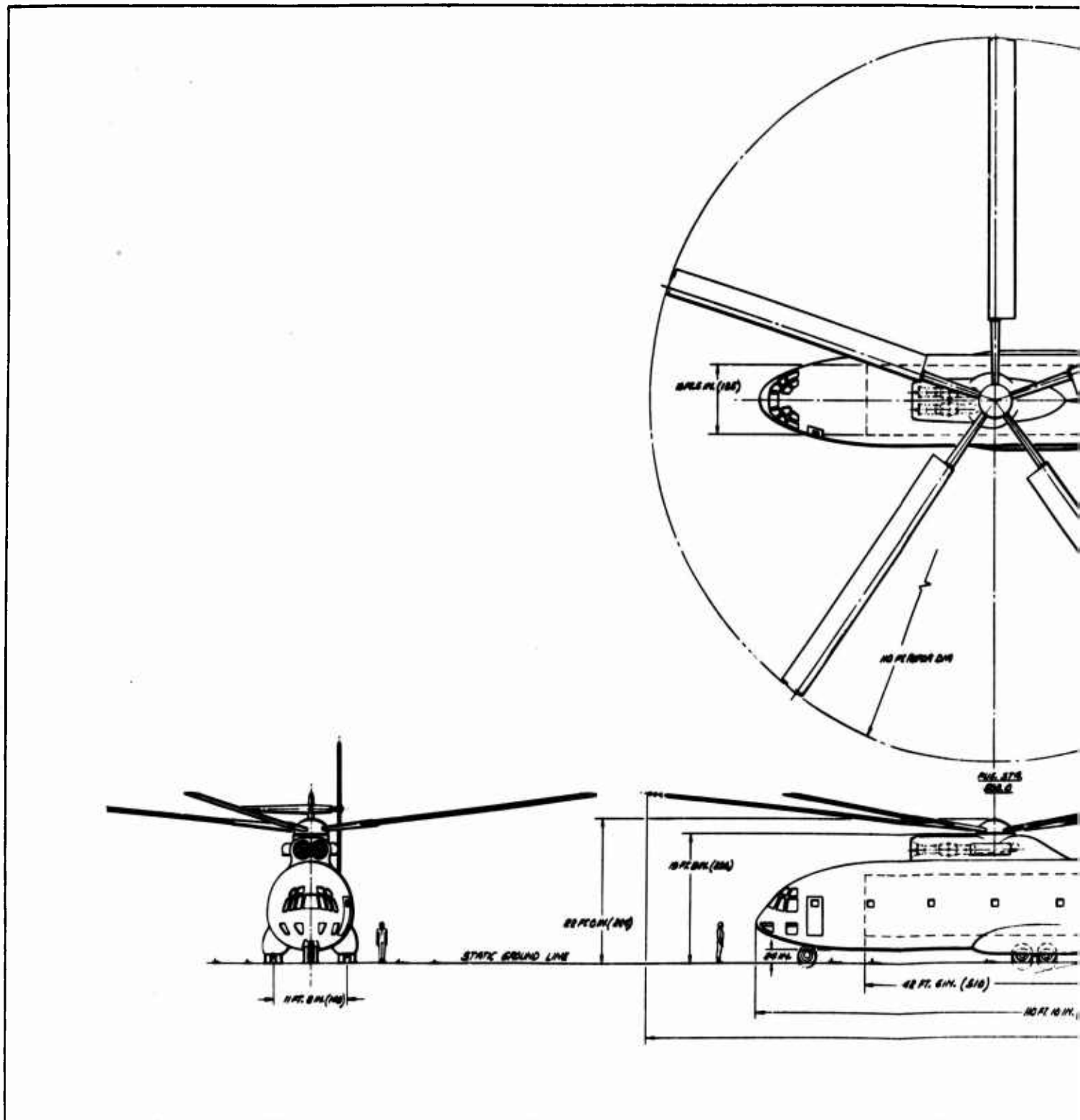
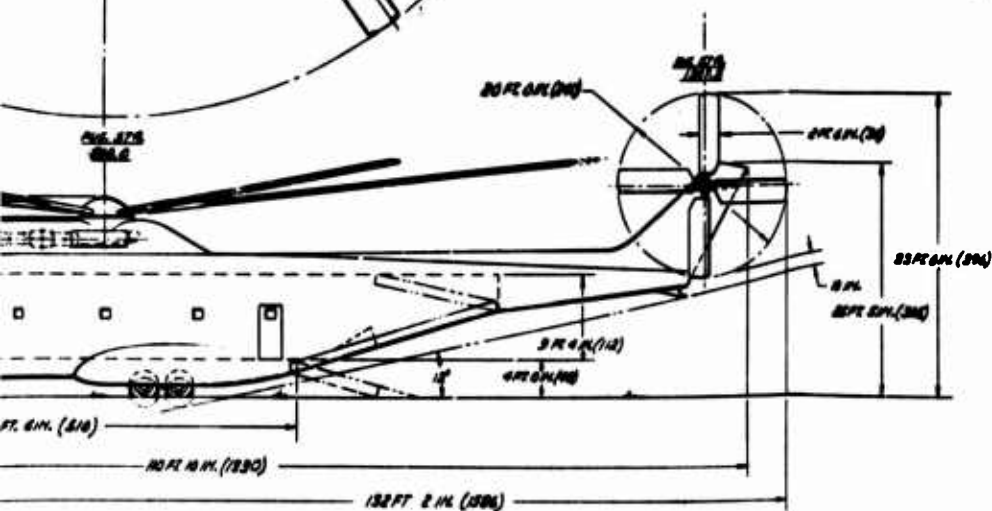
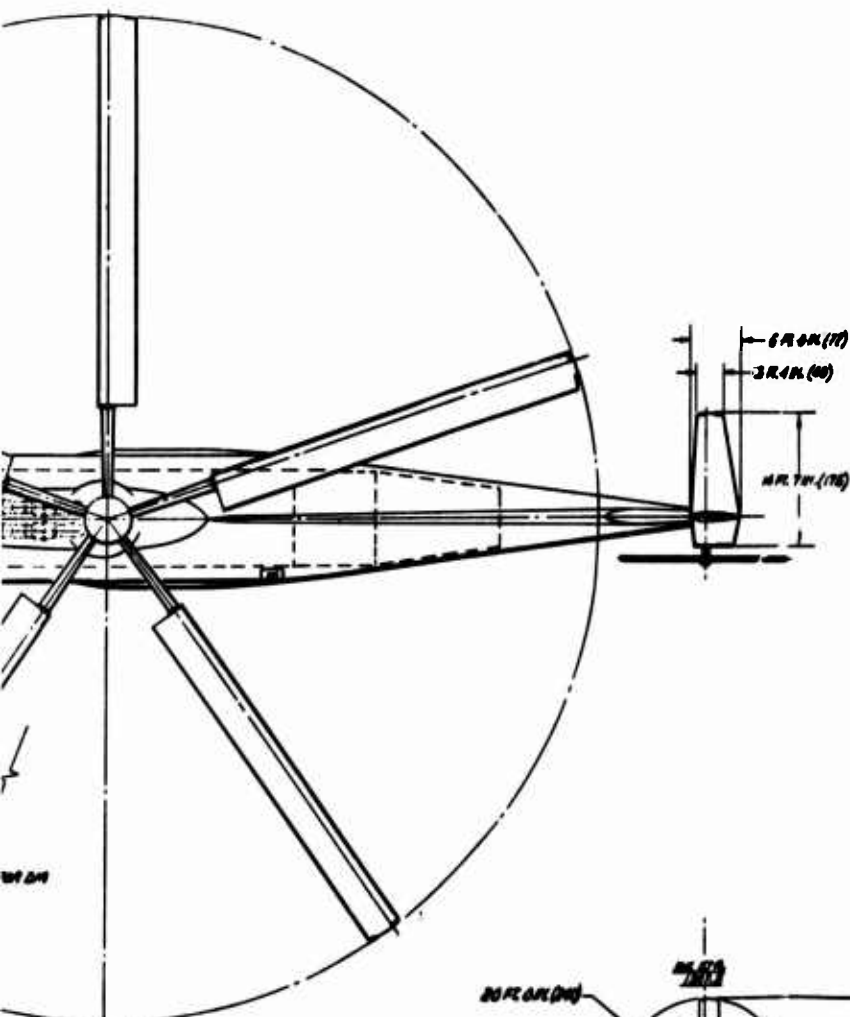


Figure 1. General Arrangement, Heavy-Lift Helicopter - Single Rotor, Internal Cargo, Parametric Study





<b>ADVANCED DESIGN</b>		DESIGNED - CALIFORNIA, CA.
<b>GENERAL ARRANGEMENT - H.L.H.</b>		CONSTRUCTION - CALIFORNIA, CA.
<b>SINGLE MOTOR - INTERNAL GEAR</b>		
DESIGNED BY	W. H. H. H.	
CHECKED BY	W. H. H. H.	
DATE	10/1/54	
CL 875-4	10/1/54	CL 875-4

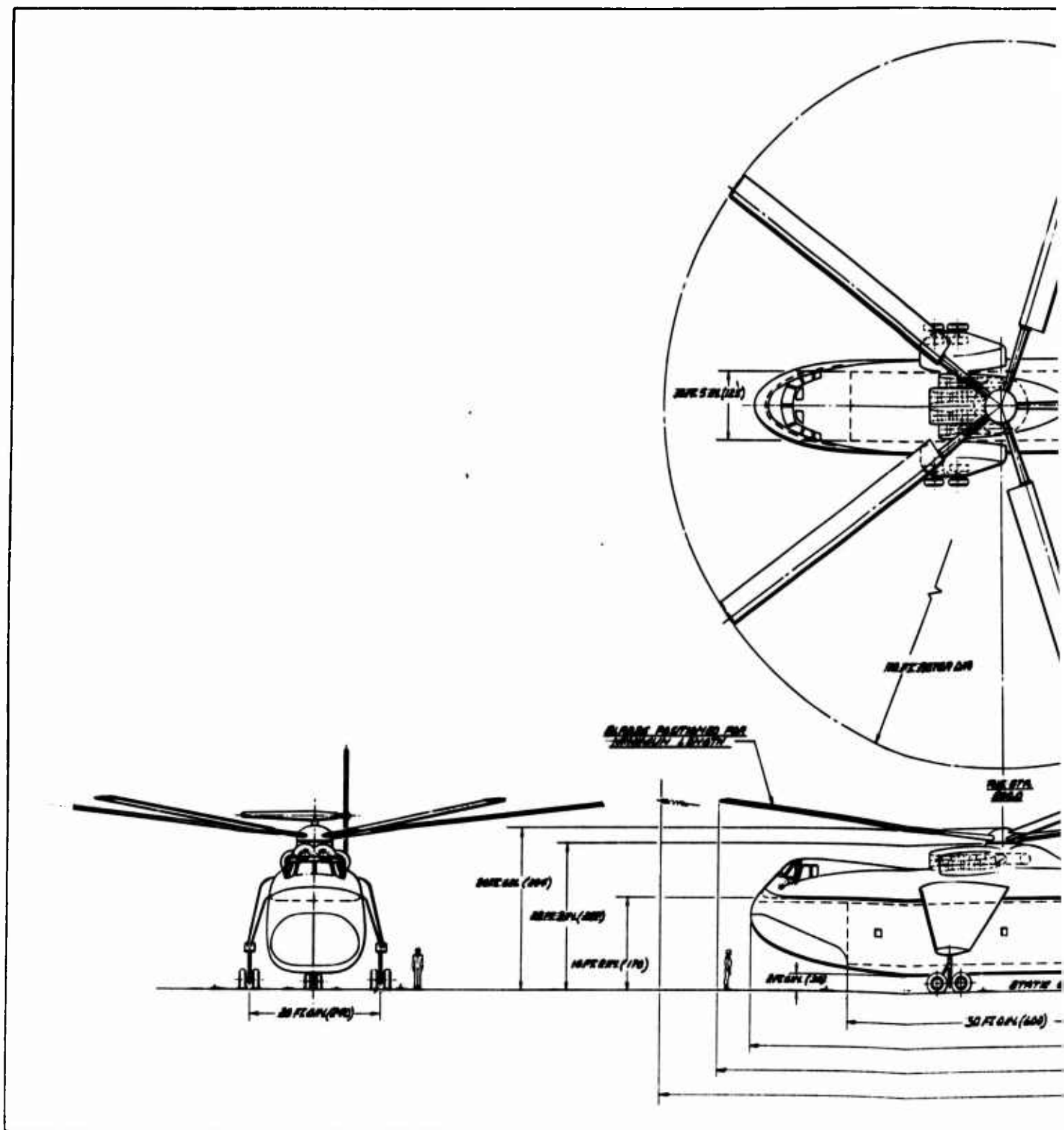
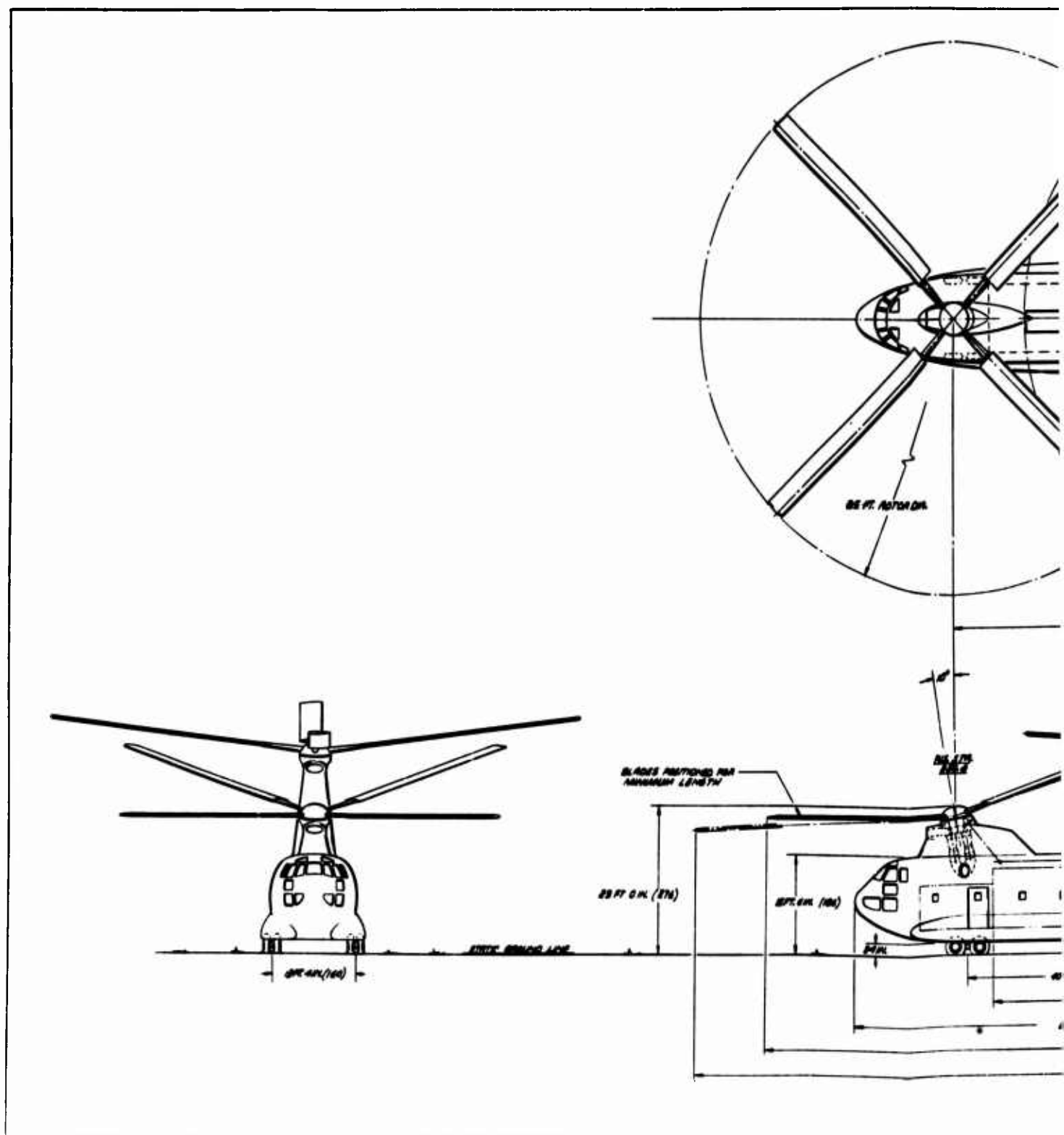
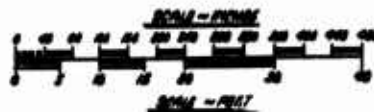



Figure 2. General Arrangement, Heavy-Lift Helicopter - Single Rotor, Cargo Pod, Parametric Study





**Figure 3. General Arrangement, Heavy-Lift Helicopter - Tandem Rotor, Internal Pod, Parametric Study**



<b><u>ADVANCED DESIGN</u></b>		<b>UNITED - SAFETY CO.</b> SUNSHINE CALIFORNIA	
<b><u>GENERAL ARRANGEMENT N.H.M.</u></b> <b><u>TANDEM MOTOR INTERNAL P.D.</u></b>			
<b><u>100 Power</u></b>	<b><u>6 Stage</u></b>		
<b><u>115 Cycle</u></b>	<b><u>N.H.M.</u></b>		
<b><u>2-1/2" Dia.</u></b>	<b><u>100% Eff.</u></b>		
<b><u>CL 875-7</u></b>	<b><u>M. H. TAYLOR</u></b>	<b><u>CL 875-7-1</u></b>	

B

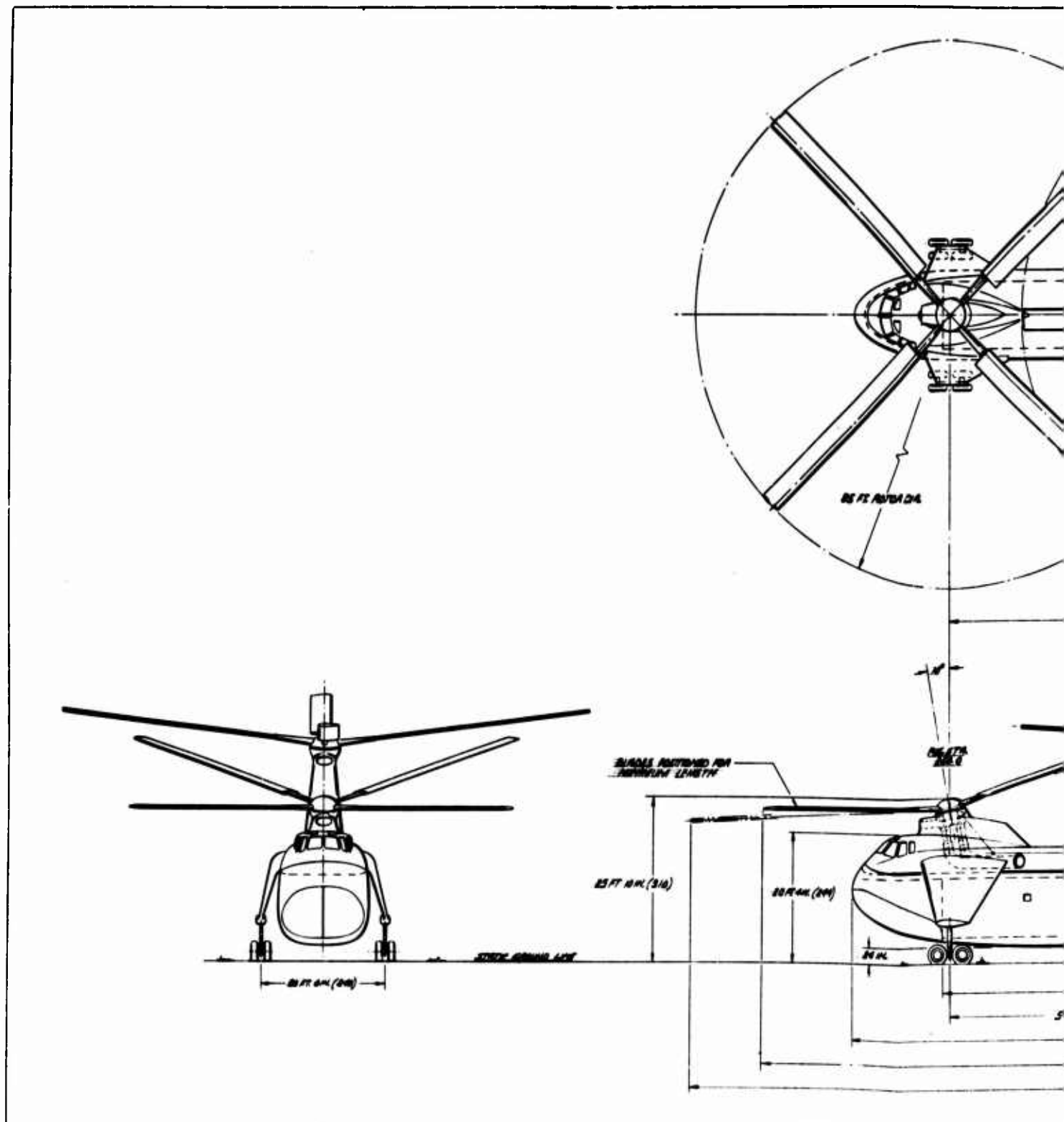
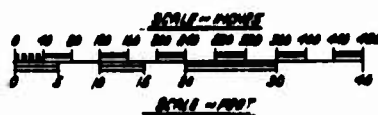




Figure 4. General Arrangement, Heavy-Lift Helicopter - Tandem Rotor, Cargo Pod, Parametric Study

P



<b>ADVANCED DESIGN</b>		ADDRESS - NEW YORK CO. 00000000000000000000	
<u>GENERAL ARRANGEMENT - M-L M</u>			
<u>TANDEM MOTOR - CARGO ASD</u>			
			
CL 875-B		CL 875-B-1	

### Contractually Fixed Characteristics

The heavy-lift helicopter parametric analysis conducted by the Lockheed-California Company is based on a vehicle having the following characteristics:

- Turbine powered
- Safe autorotation at design gross weight
- Design load factor of +2.5g to -0.5g at design gross weight
- Minimum crew of one pilot, one copilot, and one crew chief
- All components to be designed for 1200 hours between major overhauls and 3600-hour service life
- Multiengine capability

### Mission Requirements

The mission requirements for the heavy-lift helicopter are itemized in Table I.

### Rotor System Characteristics

The rotor systems considered were:

- Stiff in-plane (conventional rigid rotor)
- Articulated
- Teetered
- Matched-stiffness

The variables used in selecting the optimum rotor system include:

- Number of rotors (independent variable)
- Rotor diameter (independent variable)
- Blade airfoil section (independent variable)
- Rotor tip speed (independent variable)



TABLE I MISSION REQUIREMENTS			
ITEM	MISSION		
	TRANSPORT	HEAVY-LIFT	FERRY
Payload, tons	12 (Outbound Only)	20 (Outbound Only)	NA
Radius, nm	100	20	-
Range, nm	-	-	1500 (No Payload - STOL Takeoff)
V Cruise, knots	110 (12-Ton Payload)	95 (20-Ton Payload)	Best Speed for Range
Hovering Time, min	130 (No Payload)	130 (No Payload)	NA
	3 at Takeoff 2 at Mid-point (With Payload)	5 at Takeoff 10 at Destination (With Payload)	NA
Hovering Capability	6000 ft, 950F (OGE)	Sea Level, 590F (OGE)	NA
Cruise Altitude	Sea Level Standard Atmosphere	Sea Level Standard Atmosphere	Best Altitude for Range
Reserve Fuel	10% Initial Fuel	10% Initial Fuel	10% Initial Fuel
Fuel Allowance (Start, Warm-up, Takeoff)	MIL-C-5011 A	MIL-C-5011 A	MIL-C-5011 A
Design Load Factor, g	+2.5 to -0.5	+2.5 to -0.5	+2.0 to -0.5

- Blade aspect ratio (independent variable)
- Thrust/solidity coefficient (independent variable)
- Gross weight (dependent variable)
- Number of blades (dependent variable)
- Mean blade lift coefficient (dependent variable)
- Blade chord (dependent variable)

Independent variables are defined as those variables necessary for definition of the helicopter. The dependent variables can each be defined in terms of one or more independent variables, i.e., blade chord is dependent on (defined by) rotor diameter and blade aspect ratio.

#### Propulsion Systems Summary

For this study, engines in the 3,000- to 20,000-hp range were considered, and the engine whose power, fuel consumption, and power/weight ratio provided the lowest gross weight within the design limits for each configuration was determined. A comparison of the rated power and specific fuel consumption (SFC) for some engines of U.S. manufacture in this class size is provided in Table II. Only free turbine-type engines were considered because of the difficulties which are entailed in helicopter operation with a fixed-shaft engine.

The analysis conducted by Lockheed showed that the 6000-foot, 95°F hover requirement should be the critical point for engine sizing for the heavy-lift helicopter. The rotor power required at 6000 feet, 95°F, for the recommended design is approximately 8000 horsepower.

Engines Considered - A discussion of each engine considered in the study follows:

Allison 501-M26: This engine is based on the T56-A-18, currently under development by the Navy for antisubmarine warfare (ASW) aircraft. The T56-A-18 will utilize an air-cooled turbine which will operate at a turbine inlet temperature of 2070°F. A turbine capable of this operating temperature has been demonstrated by Allison. The variable geometry compressor necessary for free turbine operation has been demonstrated in the 501-M25. Although the 501-M26 is an advanced engine, it will utilize these demonstrated components.

<b>TABLE II</b> <b>PERFORMANCE OF U. S. ENGINES</b> <b>3,000- TO 20,000-SHP CLASS</b>								
ENGINE	SEA LEVEL STANDARD DAY				6000 FEET, 95°F		WEIGHT (LB)	OUTPUT SPEED (RPM)
	TAKEOFF (SHP)	TAKEOFF (SFC)	MIL (SHP)	MIL (SFC)	TAKEOFF (10 MIN) (SHP)	MIL (30 MIN) (SHP)		
501-M26	5,450	0.479	5,450	0.479	3,715	3,715	1,030	13,000
240	18,800	0.510	NA	NA	NA	NA	4,100	NA
LTC4B-11A	3,750	0.523	3,400	0.533	2,640	2,300	640	16,000
JFTD12A-3	4,050	0.695	3,200	0.725	2,700	2,130	870	9,000
Advanced JFTD12	4,750	0.626	4,050	0.647	3,170	2,700	955	9,000
FT3C-7	20,000	0.51	15,000	0.54	13,300	10,000	13,800	4,500
T64-GE-12 (AAFSS)	3,435	0.480	3,435	0.480	2,650	2,470	688	13,600
T64/S4B	3,900	0.475	3,435	0.480	2,900	2,470	688	13,600
T64/S5A	4,500	0.490	4,000	0.490	3,120	3,070	720	13,600

- T64 Series: The T64 turboshaft/turboprop engine was developed with Navy funds for the CH53A, CV-7A, XC-142A and XV-9A vehicles. The T64-12 is the first of a series of growth versions of the basic T64 engine and is planned for later versions of the listed aircraft. The present development schedule calls for military qualification test in December 1967. An increase in shaft horsepower is accomplished through a 12-percent increase in airflow and the resulting higher combustion and turbine inlet temperatures.

Two growth versions of the T64-12 have been proposed for the Advanced Aerial Fire Support System (AAFSS) program. They are the T64-GE-12 (AAFSS) and the T64/S4B. The shaft horsepower increase is achieved by a change in the turbine inlet temperature and first-stage turbine cooling. Both engines incorporate titanium compressors. Availability would be determined by the development of the AAFSS program.

Two additional engines, still in the study stage, are the T64/S5A and T64/S5B. Both engines would use air-cooled blades in both stages of the gas generator turbine. These engines could be qualified 2 to 3 years after the T64-12. The T64/S5A would have a military power rating of 4,500-5,000 shaft horsepower and would incorporate a stronger power turbine shaft to take the higher torque loads. The T64/S5B would have a military and maximum shaft horsepower rating of 3,900.

- GEL/S1: This is a shaft version of the GEL/J1 turbojet engine now under development. It could be used as a single-engine design for the HLH, but, as such, would not meet the multi-engine requirement. Furthermore, it is felt that the GEL project is far too preliminary to permit use of this engine in this study. Since performance figures are classified, this engine is not listed in Table II.
- Model 240: This free-turbine, aft-drive version of the J79-GE-7 turbojet was developed for marine applications where weight penalties are not as high as in aircraft. As such, this engine has a low power-to-weight ratio. Since the fuel consumption is low, a version of this engine with aircraft technology applied to the turbine design could possibly be utilized for a single-engine HLH design.

- ITC4B-11A: This engine is a growth version of the T-55L-9 and utilizes an air-cooled turbine, transonic compressor, and higher turbine inlet temperature. It has a slightly higher fuel consumption than does the T64-GE-12 (AAFSS) with the same power.
- JFTD12A-3: This engine is used in the S-64 Skycrane and is a free-turbine, aft-drive version of the J60(JT12) turbojet. Because of the low pressure ratio in this engine, fuel consumption is high; however, the JFTD12A-3 features light weight and availability without additional development.
- Advanced JFTD12: This is an advanced version of the JFTD12A-3 engine. It will utilize the production JT12A-5 turbojet for a gas generator with the JFTD12A-3 power turbine but has a high fuel consumption.
- FT3C-7: This engine is an aft-drive, free-turbine version of the J57 (JT3C) turbojet. It supplies more than enough power for a single-engine HLH but is quite heavy because it was developed for stationary and marine applications.

Propulsion Augmentation - Various means of power augmentation were considered for use in the HLH. The most promising means of augmentation are:

- Reheat
- Water/alcohol injection
- Short-duration high-power rating

Reheat between the turbines as a means of increasing power has several significant drawbacks. To operate in this mode, the power turbine must be equipped with a variable geometry nozzle diaphragm which increases complexity and weight. Since an additional diffuser and combustor are necessary for this device, a pressure drop is induced which increases specific fuel consumption at all power settings.

Water/alcohol injection seems promising as a means of increasing hot day power available. Power increases up to 30 percent at 6000 feet, 95° F can be achieved. However, specific liquid consumption is quite high during augmentation. To realize a 10-percent power increase, a water flow rate of nearly 50 percent of the fuel flow is required. The

special tanking, valving, and line complicate the aircraft configuration. The water used for the injection system must be "de-ionized" to prevent compressor contamination. The logistics of this special liquid and the necessity for adding de-ionizing equipment increases the complexity of the system. The Lockheed P3-A "Orion" presently uses a water/alcohol injection system in its T56-A10W engines for takeoff augmentation, but because of the problems discussed, Lockheed is seriously considering the installation of the higher power T56-A-14 engine and the elimination of the water/alcohol system.

Short-duration high-power rating is the most promising method of power augmentation. This can be done by utilizing short-time overspeed and/or high turbine inlet temperature with a penalty of slightly shortened turbine life. Because of the relatively constant variation of specific fuel consumption with power, a 10-percent increase in power can be obtained with only a 10-percent increase in fuel consumption. Since this augmentation scheme utilizes the aircraft fuel system, no weight penalty is incurred, except possibly a small increase in turbine weight.

Power increases obtained by these methods are only useful for short periods of time. Such power increases are applicable to the HLH for improving 6000-foot, 95°F hover capability but are not useful in any other part of the basic mission.

Any of the power augmentation schemes would result in reduced fuel consumption for the missions by reducing the engine size required. However, since basically this is a rotor system parametric study and power augmentation is not an accepted concept for helicopters, it was not considered in the parametric study except for engines which had 10-minute ratings.

#### WEIGHT ANALYSIS

For the parametric study, statistical equations were developed for use in predicting the weights of the functional groups of a heavy-lift helicopter. Equations were developed for the following functional groups:

- Rotor and hub group
- Tail group (including tail rotor and horizontal stabilizer)
- Body group
- Landing gear group

- Propulsion group (including engine, engine accessories, drive system, and fuel system)
- Flight controls group
- Hydraulics and electrical group
- Electronics
- Furnishings
- Instruments and electronics
- Air conditioning
- Auxiliary gear group

The weight equations were based on statistical data for contemporary helicopters available during the parametric study. Since the assumptions and methods used in the derivations of the equations are varied and are subject to revisions depending on additional statistical data or state-of-the-art technology, no attempt is made in this section to substantiate the derivation of the equations used in the parametric study.

The primary purpose in developing the weight equations was to establish the component weights used in the iteration of gross weight. In some cases, they serve as a guide in determining the effect on weight of varying certain parameters.

For this study the component weights were determined as a function of gross weight or other parameters and are summarized as follows:

#### Rotor and Hub Group

Matched-stiffness

$$W_{RG} = f(W, b, R, c, \Omega R)$$

Articulated, rigid, and teetered

$$W_{RG} = f(W, BL)$$

#### Tail Rotor (Single Rotor Only)

Horizontal stabilizer

$$W_{ST} = f(W, V_C)$$

Tail rotor

$$W_{TR} = f(T_{TR}, BL_{TR})$$

#### Fuselage Group

$$W_B = f(W, R, n)$$

#### Landing Gear Group

$$W_{LG} = f(W)$$

#### Propulsion Group

Engine

$$W_E = \text{Actual engine weight}$$

Engine accessories

$$W_{ACC} = f(W_E)$$

Fuel system

$$W_{FS} = f(W_F)$$

Drive System

$$W_{DS} = f(Q, Q_S, Q_{TR}, GR_{TR})$$

#### Flight Controls Group

$$W_{FC} = f(W, V_C)$$

#### Equipment Group

$$W_{FE} = f(W) \text{ AND } W_{FIXED}$$



For the above equations

$W_{XX}$	=	Specific component weight
$W$	=	Design gross weight
$b$	=	Number of blades
$\Omega R$	=	Rotor tip speed
$C$	=	Blade chord
$R$	=	Rotor radius
$BL$	=	Blade loading (main rotor)
$V_C$	=	Cruise speed
$T_{TR}$	=	Tail rotor thrust
$BL_{TR}$	=	Blade loading (tail rotor)
$W_E$	=	Engine weight
$W_F$	=	Fuel capacity in pounds
$Q$	=	Main rotor torque
$Q_S$	=	Tail rotor drive shaft torque
$Q_{TR}$	=	Tail rotor torque
$GR_{TR}$	=	Gear ratio (tail rotor gearbox)
$W_{FIXED}$	=	Specific weight dependent on mission requirements

#### Gross Weight

Summing of the component weights gives the weight empty. To this weight are added the crew weight and the engine oil weight. A three-man crew is assumed; at 200 pounds per man, this results in a weight of 600 pounds.

Engine oil weight is determined by

$$W_{OIL} = 0.04 W_E$$

In the determination of the transport gross weight, the fuel weight is a variable; hence, the fuel tank weight is also a variable until the maximum amount of fuel required has been determined. In the program, the basic weight is defined as the weight of all weight-empty items (except the fuel tanks) plus the weight of the crew and of the engine oil. Using this definition of basic weight, the gross weight is then the sum of the basic weight, fuel and fuel tank weight (sized for the transport mission), and the payload weight.

#### Additional Weight Studies

Following completion of the weight study conducted during Part 1 of this program, additional statistical information was acquired on component weights of contemporary helicopters. Preliminary design weight studies completed on large shaft-driven rotor systems also provided inputs. Using this information, the weight equations were reviewed and rederived, where necessary, to improve the accuracy of the results. The rederived equations and statistical substantiation are presented in Section 6.

#### PARAMETRIC ANALYSIS PROCEDURE

A digital computer program was developed which, for a given set of rotor parameters consisting of rotor radius, thrust/solidity coefficient, and tip speed, would compute the required power plant rating, the fuel required, and the empty weight corresponding to the helicopter which would satisfy the most critical mission requirement with the minimum gross weight. The takeoff gross weight of this helicopter for the heavy-lift mission is called the "solution gross weight". By utilization of the computer program printout of the solution gross weight and required sea level rating of the power plant, plots were made of the engine size and solution gross weights at constant tip speed for various values of rotor radius and thrust/solidity coefficient (Figure 11). For a given equivalent power plant rating, corresponding to an actual engine or group of engines, the combination of rotor parameters giving the minimum solution gross weight was determined within the limitations of (1) blade loading or design mean blade lift coefficient, (2) disc loading, and (3) tip speed.

The procedure was carried out for both single- and tandem-rotor helicopters having rigid, articulated, teetered, or matched-stiffness rotor systems. The distinction between the various rotors was in the

weight equations used to represent them. In this study, the rigid, articulated, and teetered rotors were all represented by the same weight equation based on statistical studies. The matched-stiffness rotor was represented by a separate weight equation based on recent Lockheed studies on this type of rotor.

By analysis it was determined that the 6000-foot, 95°F hover requirement should be the critical point for engine sizing for the heavy-lift helicopter with a corresponding rotor power requirement of approximately 8000 horsepower.

#### Methodology-Computer Logic

Figure 5 is a flow chart of the parametric study computer program. Blocks 1 through 5 describe the reading of constants required in the program and the reading and setup of the main rotor parameters and the mission matrix.

Initially a gross weight for the transport was assumed (Block 6). In subsequent iterations, the gross weight was taken from calculations in Block 26. The rotor solidity and number of blades were calculated in Block 7. If the helicopter was a single rotor system (Block 8), the tail rotor was sized (Block 9) and the total horsepower for the 6000-foot, 95°F hover requirement was determined (Block 10). Block 11 converts this power requirement to a sea level engine rating.

The mission subroutine depicted in Figure 6 is used to determine power, leg weights, and fuel requirements for the five parts of the transport mission (Block 13). If the required power for any part of the transport mission exceeded the power established in Block 11, the new power requirement was entered into Block 12. The total fuel weight for the transport mission, including reserve fuel, and the landing weight at the end of the heavy-lift mission (transport empty weight including fuel tank weight plus heavy-lift crew, oil, and estimated fuel reserve weights), were determined (Block 15). The mission subroutine was then used to calculate power, leg weights, fuel requirements and takeoff weights for the heavy-lift mission. However, the fuel weight was calculated in reverse order starting from the end of the mission (Block 17). If the required power plant rating (Block 18) was greater than that previously established in Blocks 11 or 14, the calculation was abandoned, the output flagged, and a new set of parameters selected (Block 6). The takeoff weight for the heavy-lift mission was then corrected for differences between estimated and calculated fuel reserve (Block 19) and used with the weight equations to determine the weight available for fuel in the transport mission (Blocks 20 through 22). An

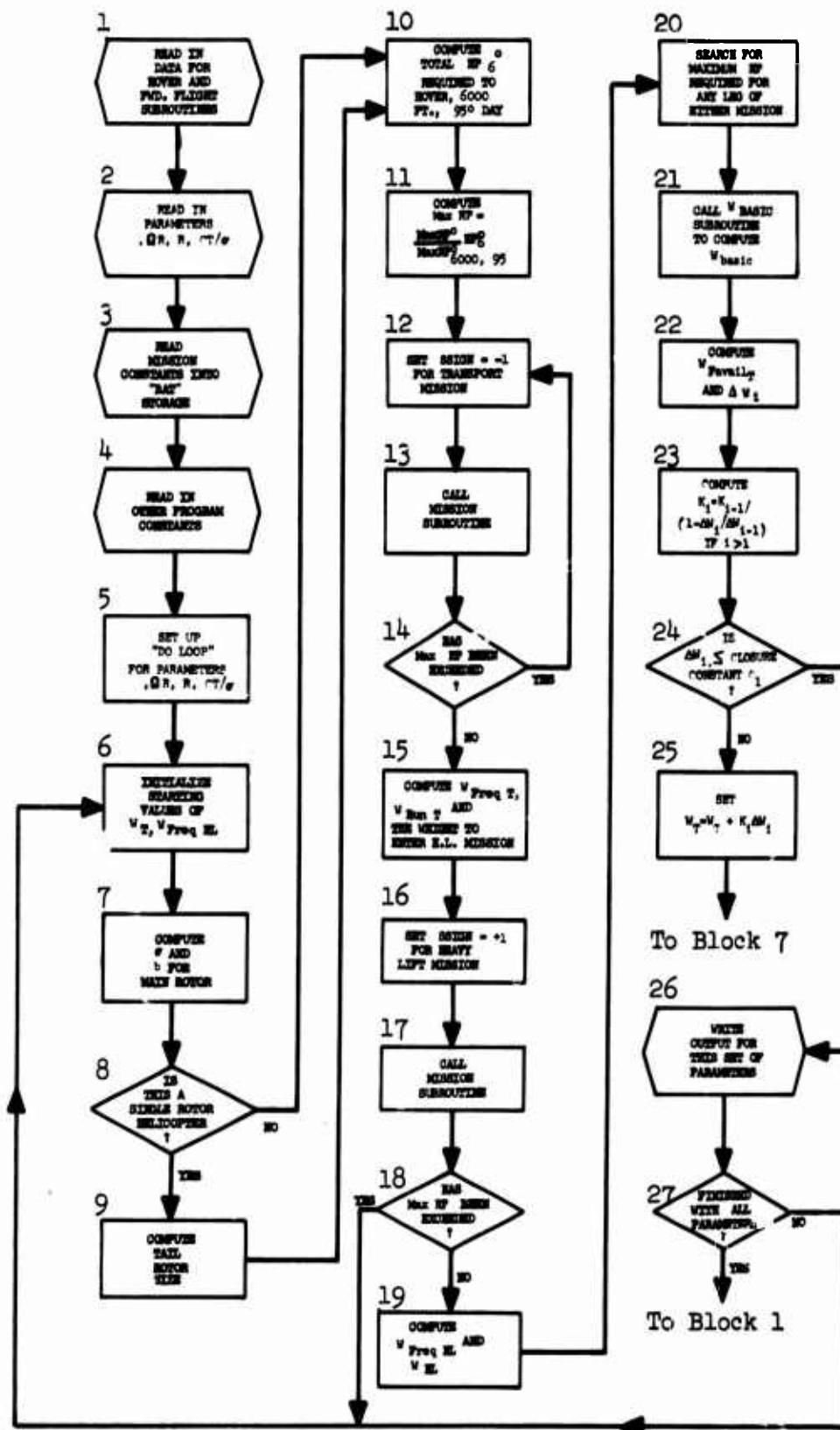
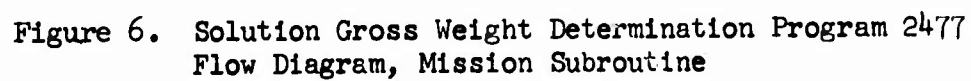


Figure 5. Solution Gross Weight Determination Program 2477  
Flow Diagram, Executive Program



iteration constant  $K_1$  was calculated in Block 23 for use in adjusting the difference between the fuel available and fuel required for the transport mission to a difference in the transport mission weight. The difference between the available fuel weight and required fuel weight was checked and, if found to be more than 200 pounds (Block 24), a new trial gross weight for the transport mission was used (Block 25) and the process was restarted at the point where calculation of solidity and number of blades occurred (Block 7). Otherwise, the weights and power were printed (Block 26) and the next set of rotor parameters was selected until all combinations had been used (Block 27).

#### Determination of Power Required - Single-Rotor Helicopter

Main Rotor Power in Hover - The Lockheed computer program for helicopter hovering performance was modified for use as a subroutine. This program makes use of the blade element strip theory. It computes the angle of attack and Mach number at 11 radius stations and uses airfoil data corresponding to the blade element conditions to determine rotor thrust and power. The airfoil characteristics were determined from the NASA whirl tower tests reported in References 1 and 2. The program uses a momentum balance procedure to determine the induced velocity at each blade element.

Tip losses were accounted for by using an effective radius,  $BR$ , in the integration for thrust. The factor,  $B$ , was determined from the equation

$$B = 1 - \sqrt{\frac{2 C_T}{b}}$$

Vertical drag on the fuselage was accounted for by correcting the weight-to-thrust ratio by multiplying the weight by 1.03 (see "Drag Analysis" discussed later in this section).

Tail Rotor Power in Hover - The tail rotor diameter was determined as a function of the main rotor torque at 6,000 feet, 95°F, by assuming a disc loading of 15 psf, 4 blades, a tip speed of 650 fps and a clearance between the rotors of 1 foot. The design solidity of the tail rotor was based on a design  $C_T/\sigma$  of 0.08 for the 6,000-foot, 95°F condition. This value of  $C_T/\sigma$  corresponds to the tail rotor's operating in hover at about 60 percent of its maximum thrust capability, thus leaving 40 percent for maneuvering. The power absorbed by the tail rotor sized in this way was computed with the same hovering program which was used for the main rotor.

Total Power Required - The total power required was obtained by adding the main rotor and tail rotor powers for the 6000-foot, 95°F condition.

The computer program for this study utilized the 501-M26 engine, corrected for losses, which has conservative characteristics for engines in this horsepower category. The equivalent sea level power ratings of other engines used in the study for comparison were obtained by multiplying the ratio of the 501-M26 sea level rating, corrected for losses, to the 501-M26 6000-foot, 95°F rating of a specific engine.

Forward Flight - Lockheed's computer program for power required in forward flight was used as a subroutine in the parametric analysis. This is a mathematical integration, force balance method similar to that used by NACA in preparation of Report 1266 (Reference 3). The program assumes a constant inflow velocity through the rotor disc, a constant tip-loss factor, a constant lift-curve slope, and a drag polar with empirical corrections for compressibility and stall. These corrections were obtained from the NACA work by Gessow, Crim, and Gustafson reported in References 4 and 5. Aeroelastic effects are neglected and the blades are assumed to be restrained at the hub by springs which simulate the rotor stiffness characteristics.

#### Determination of Power Required - Tandem-Rotor Helicopter

Hover Power - The hover power required by the tandem-rotor helicopter was calculated by a procedure based on that used for the single-rotor helicopter but corrected for induced interference effects due to rotor overlap. The increase in induced power due to this overlap was based on Heyson's work (Reference 6). An overlap of 35 percent was assumed for all tandem configurations, and the corresponding increase in induced power was 8.7 percent. It should be noted that Sweet (Reference 7) has demonstrated excellent experimental correlation with Heyson's theoretical work. The induced velocity ratio was evaluated from the results of the work of Castles and DeLeeuw given in Reference 8 for an overlap ratio of 0.35 and with the center of the rear rotor in the plane of the front rotor ( $\frac{Z}{R}$  of zero) for all flight conditions. The choice of a constant  $\frac{Z}{R}$  implies that the front rotor is trimmed for no flapping by the rear rotor position.

Forward Flight Power - The power requirement for forward flight of the tandem-rotor helicopter as determined by the computer program was used for the fuel weight calculations of the cruise portions of the transport and heavy-lift missions. This procedure made use of the main rotor portion of the single-rotor forward flight subroutine to calculate

the front rotor power by assuming that the rotor carries half of the weight and overcomes half of the parasite drag. The rear rotor had the additional requirement of climbing through the front rotor downwash imposed upon it. The value of this downwash at the rear rotor center was determined by using an expression for the ratio of this velocity to the induced velocity  $\left(\frac{v_2}{v_1}\right)$  based on the work of Castles and DeLeeuw reported in Reference 8. The computer used an expression of the form

$$\left(\frac{v_2}{v_1}\right)^2 = C_2 \alpha_D^2 + C_1 \alpha_D + C_0$$

where  $C_0$ ,  $C_1$  and  $C_2$  are functions of the overlap and the height ratio of the rear rotor with respect to the no-flapping plane of the front rotor. For an overlap of 35 percent and a height ratio of zero, the constants are

$$C_0 = 0$$

$$C_1 = 3.274 \times 10^{-3}$$

$$C_2 = 0.2444 \times 10^{-3}$$

The downwash velocity at the rear rotor,  $v_2$ , due to the front rotor is obtained by

$$v_2 = \left(\frac{v_2}{v_1}\right)^2 \times v_1$$

where  $v_1$  is the induced velocity of the front rotor. The forward flight subroutine is used to calculate the power required by the rear rotor, assuming it represents the main rotor of a helicopter with half the weight and drag of the actual tandem helicopter, climbing at the angle determined by the forward speed and the downwash velocity,  $v_2$ .

#### Determination of Fuel Required

The fuel weight for each of the five parts of the transport mission given in Table I, Mission Requirements, was determined by using

$$W_F = (FF) t + \frac{1}{2} \frac{d(FF)}{dt} t^2$$



$W_F$  is represented by the enclosed area of the trapezoid in the following sketch:



Where  $FF_1$  is the fuel flow rate at the beginning of the leg and  $FF_2$  the fuel flow rate at the reduced weight of the end of the leg,  $h$  is given by

$$\frac{d(FF)}{dt} \quad ( - t )$$

and

$$FF = \text{Max RP} \times \text{SFC} \times \frac{\%FF}{100}$$

$$\%FF = K_C - K_V V_K + \left( \frac{d\%FF}{d\% \text{Max RP}} \right) \% \text{Max RP}$$

$$\% \text{Max RP} = \frac{\text{RHP} \times 100}{\text{Max RP}}$$

(See Table III for value of constants used in the program)

RHP is calculated by the appropriate hover or forward flight subroutine. Max RP was either the current computer program value or an integer number,  $N_1$ , times the engine rated thrust for the cruise portions if engine shutdown for cruise was being considered where

$$N_1 = \frac{\text{RHP}}{(\text{NRP}_h^V / \text{ENG})},$$

and is rounded up so that normal rated power would not be exceeded during cruise with engine shutdown.

Now

$$\frac{d(\text{FF})}{dt} = \frac{d(\text{FF})}{d(\% \text{Max RP})} \times \frac{d(\% \text{Max RP})}{dW} \times \frac{dW}{dt}$$

where

$$\frac{dW}{dt} = -\text{FF}$$

$$\frac{d(\text{FF})}{d(\% \text{Max RP})} = \frac{\text{Max RP} \times \text{SFC}}{100} \times \frac{d(\% \text{FF})}{d(\% \text{Max RP})}$$

$$\frac{d(\% \text{Max RP})}{dW} = \frac{3}{2} \frac{\text{iHP}}{W} \times \frac{100}{\text{Max RP}}$$

iHP = induced horsepower

t = time of mission portion in hours.

For the heavy-lift mission, which was calculated in reverse order starting from the end of the mission, the same fuel weight equations were used except for  $\frac{d(\text{FF})}{dt}$ , which was written above with a positive sign:

$$\frac{d(\text{FF})}{dt} = - \frac{d(\% \text{FF})}{d(\% \text{Max RP})} \times \frac{d(\% \text{Max RP})}{dW} (\text{FF}) \times \frac{dW}{dt}$$

The short vertical side,  $\text{FF}_2$ , of the preceding sketch represents the calculated fuel flow rate when starting from the end of the mission legs as with the heavy-lift mission.

The weight was adjusted by the fuel weight used and by the payload dropped in the previous leg before calculating power required for the next leg.

The total mission fuel weight required was determined by

$$W_F = \frac{\sum_{j=1}^5 W_{Fj}}{0.90}$$

where the subscript j indicates the mission leg, and the 0.90 is a factor for 10-percent reserve.

### Component Weight Equations

The basic weight, defined as empty weight plus the weight of engine oil and crew but without fuel tanks, was calculated from the component weight equations of "Weight Analysis" for the trial helicopter as a function of the rotor parameters, the takeoff weight for the heavy-lift mission, the installed power, the number of main rotors, the type of main rotor, the size of the main rotor, or the distance between main rotors. (External cargo fuselage with straddle-type landing gear was assumed as the configuration in the computer program).

In the solution gross weight determination program the engine weight was based on existing engines, as follows:

$$W_E = (\text{No. of engines}) \times (\text{Actual engine weight})$$

where

$$\text{Number of engines} = \frac{\text{Max RP}}{\text{RP}_{s1}}$$

For the 501-M26 engine used,  $\text{RP}_{s1} = 5219$  HP and the weight per hardware engine = 1030 pounds.

The component weight breakdown utilizes actual engine weight for the specific engine shown.

### Technique of Iteration

The difference between the fuel required for the transport mission and the fuel available at the trial gross weight was used as the parameter of iteration. If the difference was less than 200 pounds, the helicopter was considered to be matched to the mission requirements and the gross weight corresponding to the heavy-lift mission was printed out as the solution gross weight, as shown in Figure 7. If the fuel difference exceeded 200 pounds, a new trial gross weight was selected and the calculations were repeated.

### Computation of Ferry Range

The ferry range was calculated for the single-rotor configuration by considering the weight available for fuel and tankage to be  $1.25 \text{ WHL} - \text{WBASIC}$  which corrects for the fact that the ferry mission can be performed at a gross weight corresponding to a design load factor of 2.0.

THETA= -5.0											
CT/SIGMA	RADIUS	TIP SPEED	SIGMA	TRANSPORT WT, LBS	HEAVY LIFT WT, LBS	MAX RATED POWER	MAX ALPHA 270, DEG.	CLROT	CLORHL	BLADES	B.L.
0.055	47.0	650.0	0.0815	60452.2	73654.9	9271.6	8.556	0.36158	0.43909	4.00000	65.12325
0.065	47.0	650.0	0.0681	59936.8	73126.9	9000.2	9.973	0.42732	0.52135	3.00000	77.32427
0.075	47.0	650.0	0.0582	59070.1	72401.0	8804.9	11.409	0.49306	0.60433	3.00000	89.63079
0.085	47.0	650.0	0.0511	58762.0	72179.3	8803.2	12.835	0.55880	0.68639	3.00000	101.80132
0.055	49.0	650.0	0.0747	60416.1	73458.3	8915.7	8.459	0.36158	0.43963	4.00000	65.20331
0.065	49.0	650.0	0.0621	59387.8	72620.5	8575.1	9.886	0.42732	0.52253	3.00000	77.49048
0.075	49.0	650.0	0.0532	58669.1	72041.0	8411.6	11.322	0.49306	0.60543	3.00000	89.79458
0.085	49.0	650.0	0.0475	59382.7	72781.7	8998.9	12.704	0.55880	0.68488	2.00000	101.57008
0.055	47.0	700.0	0.0696	60095.1	72959.1	9395.2	8.018	0.36158	0.43897	3.00000	75.50704
0.065	47.0	700.0	0.0578	59005.6	72103.4	8974.8	9.393	0.42732	0.52217	3.00000	89.81009
0.075	47.0	700.0	0.0498	59005.6	0.	0.	0.	0.49651	0.	3.00000	0.
0.085	47.0	700.0	0.0446	59550.8	72782.6	9880.3	12.067	0.55880	0.68294	2.00000	117.47531
0.055	49.0	700.0	0.0635	59550.8	72488.5	8680.7	7.941	0.36158	0.44013	3.00000	75.70633
0.065	49.0	700.0	0.0528	58535.8	71746.3	8304.1	9.323	0.42732	0.52375	3.00000	90.09063
0.075	49.0	700.0	0.0463	59243.1	72477.0	9105.6	10.642	0.49306	0.60320	2.00000	103.75572
0.085	49.0	700.0	0.0409	59243.1	72496.7	9415.7	11.984	0.55880	0.68381	2.00000	117.62189
0.055	47.0	750.0	0.0607	60109.5	72505.7	9337.4	7.526	0.36158	0.43614	3.00000	84.12034
0.065	47.0	750.0	0.0505	59167.8	71867.0	9034.6	8.848	0.42732	0.51903	3.00000	102.48768
0.075	47.0	750.0	0.0444	60001.7	72729.5	10164.9	10.104	0.49306	0.59765	2.00000	118.01120
0.085	47.0	750.0	0.0394	60390.5	73169.3	10963.5	11.375	0.55880	0.67704	2.00000	133.68044
0.055	49.0	750.0	0.0558	60142.7	72573.3	9123.1	7.441	0.36158	0.43631	3.00000	84.15313
0.065	49.0	750.0	0.0472	60142.7	72717.9	9490.3	8.722	0.42732	0.51646	2.00000	102.02021
0.075	49.0	750.0	0.0405	59552.3	72356.5	9695.9	10.039	0.49306	0.59907	2.00000	118.29106
0.085	49.0	750.0	0.0362	60178.2	73024.9	10482.3	11.303	0.55880	0.67809	2.00000	133.89528

Figure 7. Output Summary Sheet for Solution Gross Weight Determination Program

The maximum nautical miles per pound of fuel was determined for several weights between the takeoff weight and basic weight at altitudes of up to 20,000 feet by the overlay of semilog plots as described in "Performance of the Rotor System." The maximum nautical miles per pound for each of these weights, using engine shutdown where possible and not exceeding blade loading or retreating blade stall speed limits, was then plotted versus its corresponding weight. The area under this curve (between the starting weight minus, warm-up and takeoff fuel, and the basic weight, plus fuel tanks and 10-percent reserve), was taken as the ferry range (Figure 34).

### Power Plant Analysis

Engine Performance - Values of engine fuel flow and horsepower were obtained from a manufacturer's chart for the 501-M26 engine. These data, corrected for losses and with the fuel flow increased by 5 percent, were normalized with the fuel flow at the maximum sea level static rated power. These results were plotted as %FF (fuel flow) versus %Max RP (maximum rated power) for different speeds (Figure 8). Maximum rated power was military power (30-minute rating) in the case of the 501-M26 engine.

In the region from 30 percent of power to normal rated power, the fuel flow, horsepower relationship was represented by a linear relationship (Figure 8) of this form

$$\%FF = K + \frac{d(\%FF)}{d(\%Max RP)} (\%Max RP)$$

The slope of this line,  $\frac{d(\%FF)}{d(\%Max RP)}$ , was assumed constant with forward speed and a linear relationship for K was determined as a function of flight speed. This resulted in

$$\%FF = K_C - K_V V_K + \frac{d(\%FF)}{d(\%Max RP)} (\%Max RP)$$

These normalized engine data for the 501-M26 were used in the computer program. Table III shows the values of the constants used.

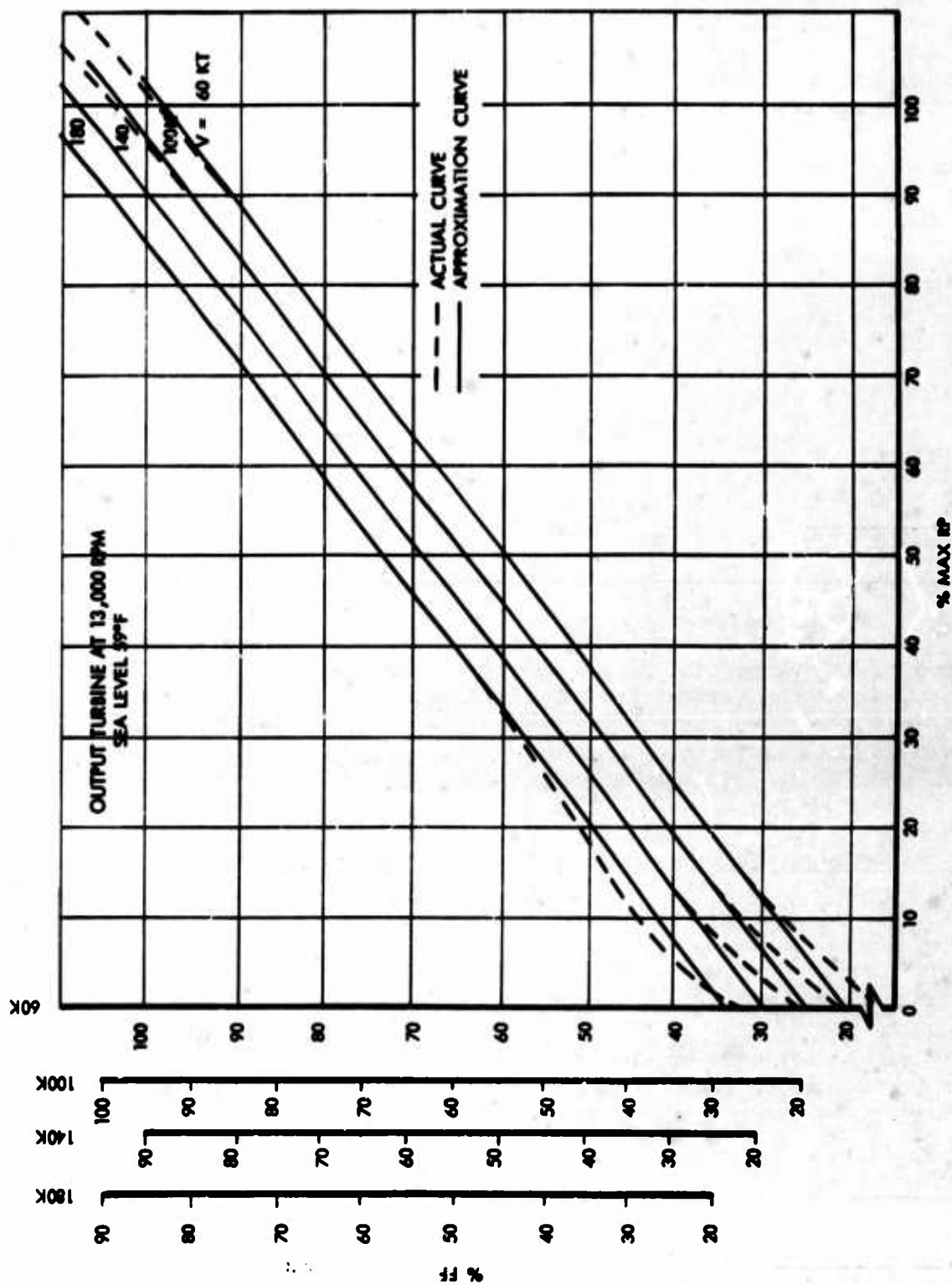


Figure 8. Normalized Fuel Flow Horsepower for 501-M26 Engine

TABLE III	
501-M26 ENGINE CONSTANTS	
$RP_{6000\text{-ft, } 95^{\circ}\text{F (Corrected)}}$	3526
$RP_{SL}$	5219
Weight, lb	1030
SFC	0.525
K	21.2
$K_V$	0.00664
$\frac{d(\%FF)}{d(\%Max\ RP)}$	0.775

The propulsion system installation losses (per engine) were assumed to be 2.4 percent of the delivered horsepower plus 200 more horsepower for the twin engine installation. The fixed portion of these losses was proportional to the engine size. These losses are derived as follows for one 501-M26 engine:

Inlet losses -	0.4% (for assumed 0.997 recovery)
Transmission loss -	2.0% + 30 HP (for windage)
Power extraction -	70 HP (for accessories and hydraulic pump)
<b>TOTAL</b>	<b>2.4% + 100 HP</b>

These losses were applied over the entire flight regime. No attempt was made to include variation of inlet to get maximum static recovery. A bellmouth inlet was assumed.

#### Drag Analysis

Frontal Drag - The equivalent drag area,  $f_o$ , used in the mission matrix of the computer program was assumed to be 80 square feet for the basic helicopter (inbound legs), based on the drag breakdown shown below.

The transport mission outbound leg was assumed to be done with  $f_o$  equal to 100 square feet and the heavy-lift mission outbound leg with  $f_o$  equal to 180 square feet.

The additional 20 square feet of  $f_o$  used for the outbound leg of the transport mission was considered to be representative of some type of drag-reducing cargo enclosure, such as a semi-streamlined pod or rectangular-type cargo pod equipped with double vanes on the side, and bottom corners at the front and rear ends.

The additional 100 square feet of  $f_o$  used for the outbound leg of the heavy-lift mission was used as being representative of a large un-faired load. (It could not be expected that any attempts at fairing a bulky load would be made for the short distance of the heavy-lift mission outbound cruise.)

A drag breakdown based on the configuration of Figure 2 for an external-cargo-type helicopter follows. Figures are given in square feet.

Fuselage	9.63
Cabin	1.95
Pylon and nacelles	3.14
Main rotor hub	13.10
Hub, nacelle, fuselage interference	2.62
Tail	1.74
Tail rotor hub	0.36
Main landing gear fairing	1.20
Main landing gear and wheels	36.44
Tail landing gear	<u>8.51</u>
TOTAL	78.69

Vertical Drag - The downwash factor,  $K_{DW}$ , of 1.03 was used to allow for the rotor downwash impingement on the fuselage. This factor multiplied by the weight gave the thrust used in the hover power required calculations and in determining the design mean lift coefficients,  $\left(C_{L_{ro}}\right)_T$  and  $\left(C_{L_{ro}}\right)_{HL}$ . A strip analysis was performed for the helicopter configuration of Figure 2.



The effective drag area, 3.1 percent of rotor area, was determined from the variation of dynamic pressure/disc loading ratio with radius station, the distance below the rotor, and the representative drag coefficients as given in Figure 9. Since percent download is given by

$$\frac{\left[ \sum C_D A \left( \frac{q}{DL} \right) \right] \frac{W}{\pi R^2} \times 100\%}{W} = \frac{\sum C_D A \left( \frac{q}{DL} \right) \times 100\%}{\pi R^2}$$

where

$\frac{q}{DL}$  = dynamic pressure/disc loading ratio (from Figure 9)

A = planform area of the segment

$\sum C_D A \left( \frac{q}{DL} \right)$  = effective drag area,

the download correction ratios are equal to these area ratios and are independent of weight, W.

Figure 9 represents a fairing of data presented in NACA TN 4239 (Reference 9) and drag coefficients in a rotor downwash as presented in WADD TR 61-124 (Reference 10).

#### Main Rotor Characteristics

The main rotor characteristics were based on the following assumptions:

- Number of blades, b, determined by the solidity,  $\sigma$ , and a blade aspect ratio of 16,  $AR_b$ , so that  $b = \pi AR_b \sigma$  to nearest integer
- Data for an NACA 0012 airfoil in tabular form based on whirl tower tests were used for the hover program. These airfoil data were input into the forward flight program as follows:

$$C_{D_0} = 0.009$$

$$C_{D_1} = 0.000$$

$$C_{D_2} = 0.400$$

$$C_L/\alpha = 6.00/\text{radian}$$

$$\text{Stall angle} = 14 \text{ degrees}$$

$$\text{Drag divergence Mach no.} = 0.81$$

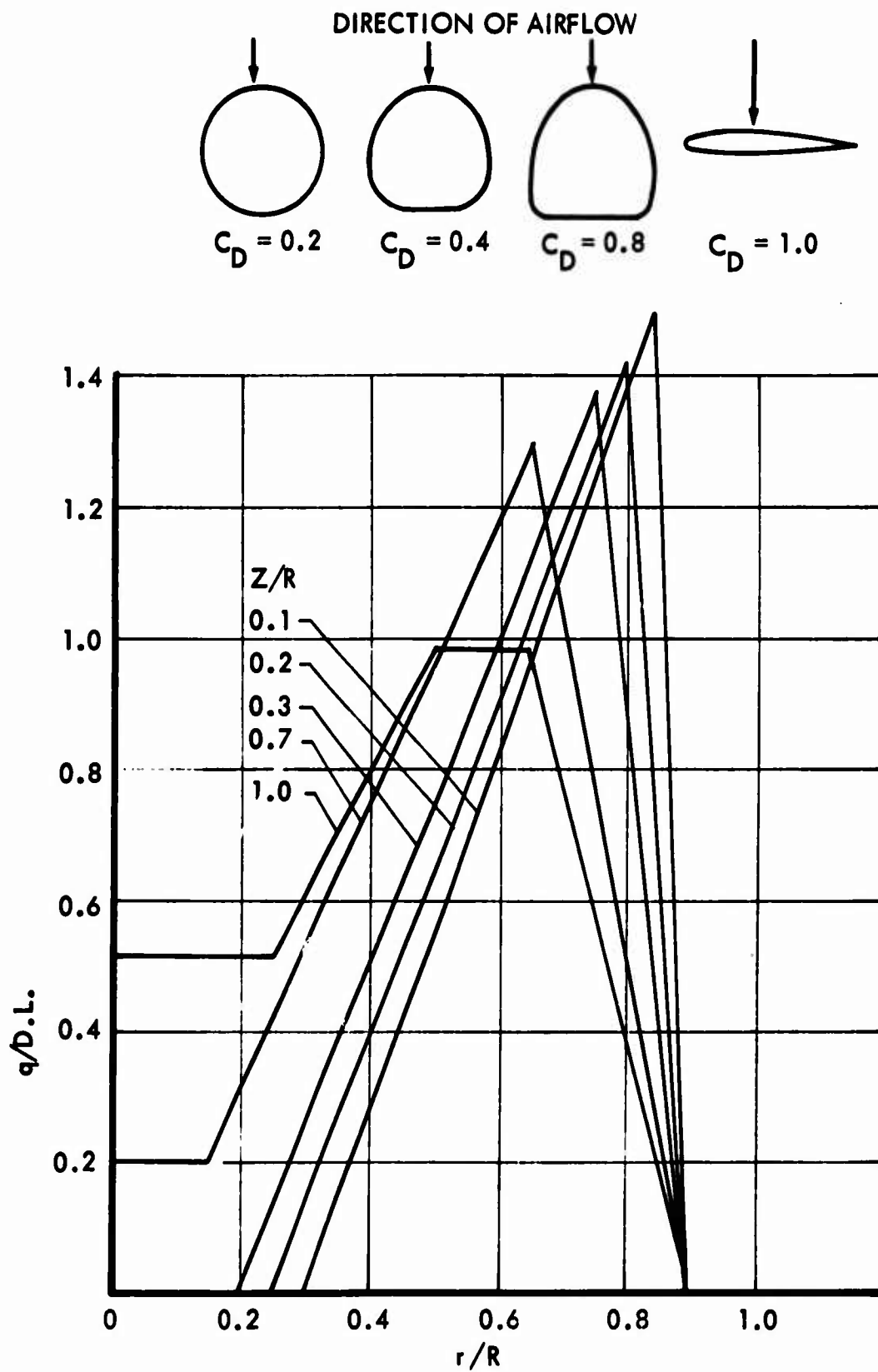


Figure 9. Dynamic Pressure Distribution in a Rotor Downwash

- The rotor radius was assumed to be effective for lift only to  $B \times R$ .
- The blade cutout at the center of the blade was 15 percent of the radius for the rigid, articulated, and teetered rotors, and 20 percent for the matched-stiffness rotors. The larger cutout was used for the matched-stiffness rotor because of the torsional flexure length needed at the hub for feathering and cyclic pitch changes.
- Blade loading used in the rotor weight equation and the computer output for the single-rotor helicopter was

$$BL = \frac{W_{HL}}{\sigma \pi R^2}$$

and for the tandem-rotor helicopter was

$$BL = \frac{W_{HL}}{2 \sigma \pi R^2}$$

#### Matched-Stiffness Blade Loading (Limitations)

For the parametric study, a blade loading limit of 77 psf was established for the matched-stiffness rotor at the 95-knot outbound speed for the heavy-lift mission. This limit was based on wind tunnel measurements (Reference 11) which showed that, for the centrifugal loads which were used in developing the design synthesis type rotor group weight equation, the second harmonic in-plane loads would exceed design limits if higher blading loadings were used. During the design study of the rotor system, this relationship was investigated and was found to be a function of advance ratio, and the results are presented in Section 6.

Figure 10 shows the effect of gross weight on the maximum forward speed due to the second harmonic in-plane blade loading limitations based on wind tunnel data (Reference 11). These limits were established on the horsepower versus flight speed plots (Figures 20 through 27). These speed limit lines were not exceeded during the ferry range determination.

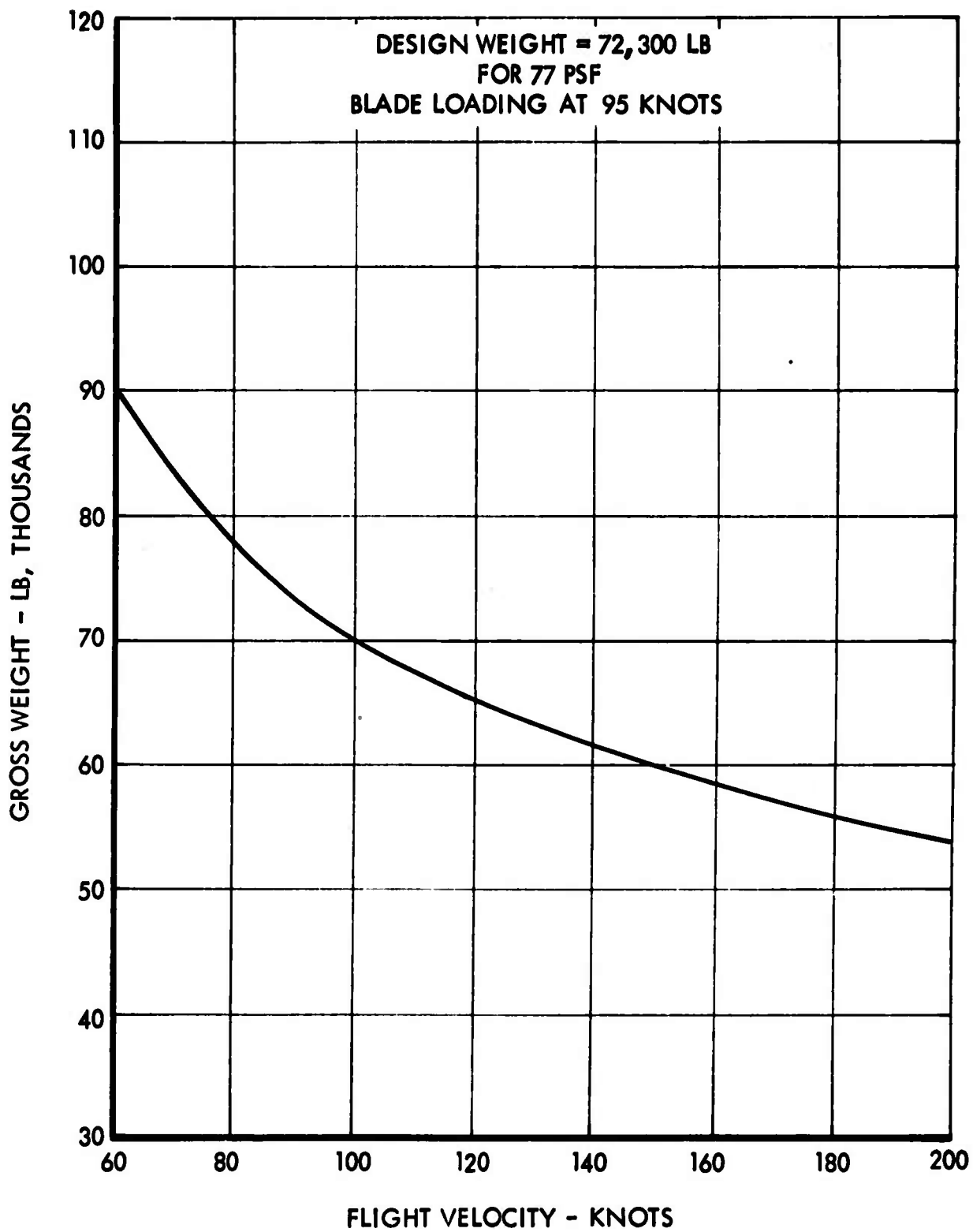


Figure 10. Gross Weight and Blade Loading Limited Flight Speed

Since the 95-knot speed at  $W_{HL}$  was the limiting condition, solution limiting lines of  $BL = 77 \text{ psf}$  could be established on the Max RP versus solution gross weight plots to indicate the limiting condition for the matched-stiffness rotors by cross-plotting  $BL$  versus  $W_{HL}$  (Figures 11 and 12).

It is not necessary to consider a  $\left(C_{L_{r_0}}\right)_T = 0.50$  line (see following section) when a 77-psf line for the limit line is considered.

#### Design Mean Lift Coefficient Limitation

A design mean lift coefficient of 0.50 was used for the transport mission weight as an upper limit in determining the usable solutions for the rigid, articulated, and teetered rotors in order to conform with current practice for helicopters designed to hover at 6000 feet, 95°F.

#### Retreating Blade Stall Limits

All solutions plotted on the Max RP versus  $W_{HL}$  plot with  $\left(C_{L_{r_0}}\right)_T \leq 0.50$  had a maximum retreating blade angle of attack ( $\text{Max } \alpha_{270}$ ) for mission requirements of less than  $14^\circ$  (i.e., the stall angle).

In the determination of ferry range for the optimum single matched-stiffness rotor, forward speeds at a given weight and altitude in excess of the stall limit line ( $\alpha_{270} = 14^\circ$ ) were not used.

#### RESULTS OF PARAMETRIC ANALYSIS

For a given set of rotor parameters and a given helicopter configuration, the computer program printed out the takeoff gross weight for the heavy-lift mission and the required sea level rating of the power plant. These values were then entered on plots such as are shown in Figure 11. From these plots, for a given configuration and engine size, the rotor radius, thrust/solidity coefficient, and tip speed can be chosen which result in the lowest helicopter gross weight. This gross weight and the corresponding rotor parameters represent the optimum matching of the helicopter to the power plants considered for the mission requirements used in this study.

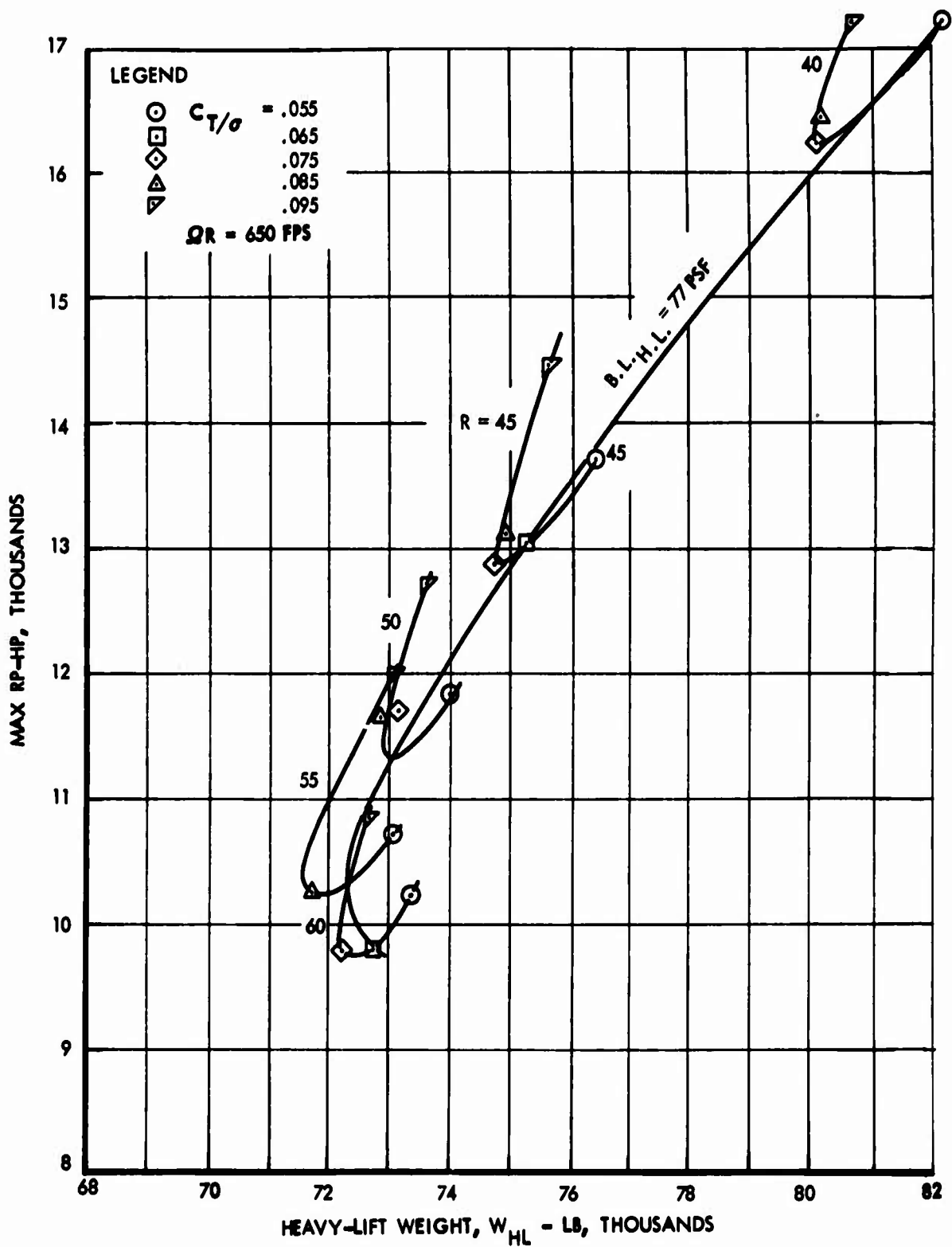


Figure 11. Typical Plot of Solution Gross Weight Program Results

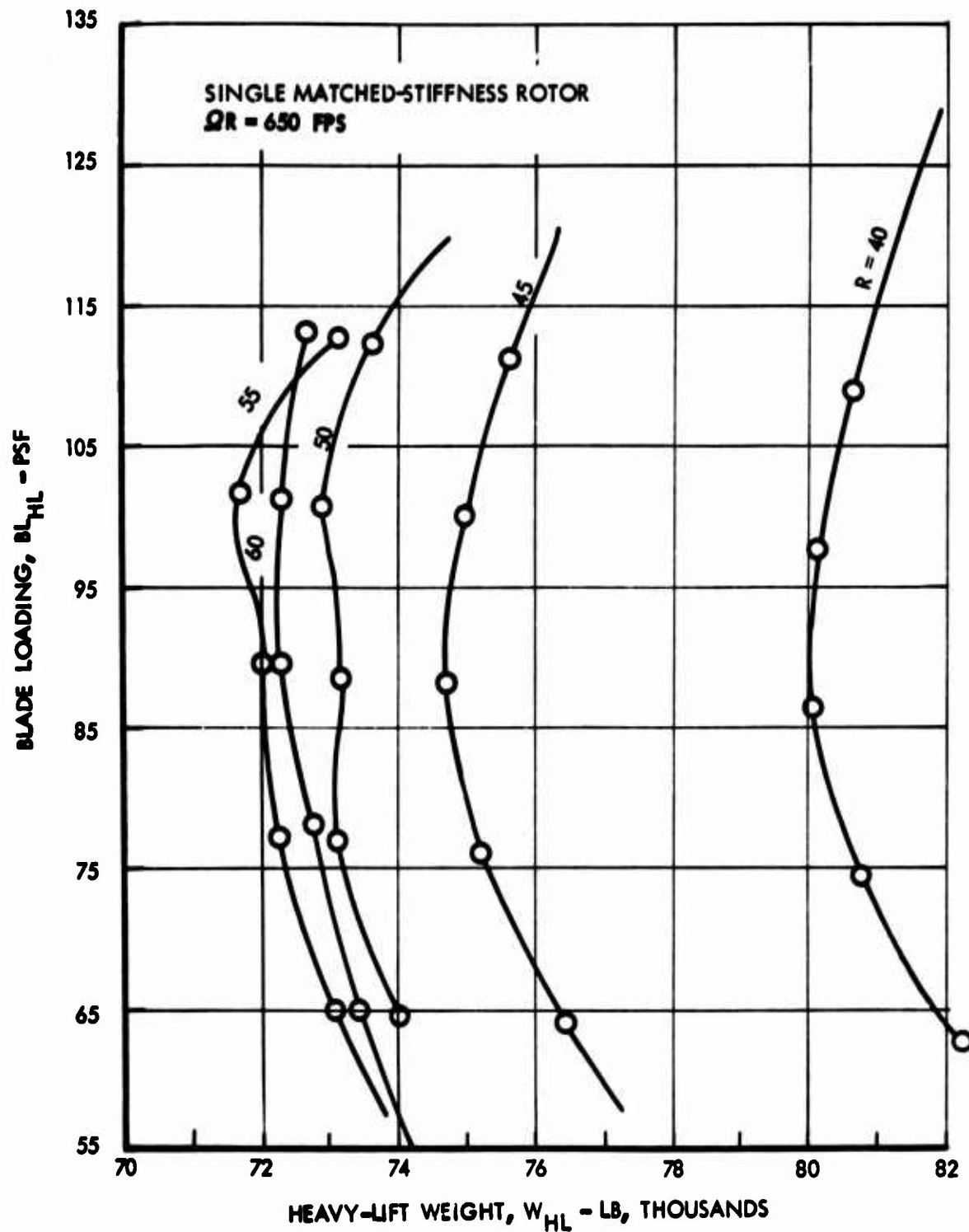


Figure 12. Typical Plot Used in Establishing Solution Limiting Line On Solution Gross Weight Program Results

Solution gross weights were determined for each of the following configurations:

- Single rotor (articulated, teetered, and rigid)
- Single rotor (matched-stiffness)
- Tandem rotor (articulated, teetered, and rigid)
- Tandem rotor (matched-stiffness)

The study indicates that there is negligible difference in the rotor weights of the articulated, teetered, and rigid-rotor systems. The matched-stiffness rotor system, however, resulted in from 8- to 12-percent reduction in vehicle gross weight. The matched-stiffness rotor system, therefore, is the recommended system.

The use of the matched-stiffness rotor system results in the minimum helicopter gross weight which is essentially the same for both the single-rotor and tandem-rotor arrangements. Characteristics of these two rotor systems are summarized as follows:

	<u>Single Rotor</u>	<u>Tandem Rotor</u>
Design gross weight, lb	72,300	72,500
Transport mission weight, lb	59,300	59,600
Number of blades	5	3
Rotor diameter, ft	110	97
Blade section	0012	0012
Rotor tip speed, fps	650	700
Mean blade lift coefficient	0.520	0.446
Blade chord, ft	3.4	3.2
Aspect ratio	16.2	15.1

The foregoing comparison indicates that other considerations are necessary to select the optimum number of rotors for the heavy-lift helicopter.



### Parameters Used in the Computer Program

The basic parameters consisting of tip speed, rotor radius, and thrust/solidity coefficient were entered into the program. Various combinations of the values of the parameters shown below were used.

- Tip speed,  $\Omega R = 600, 650, 700, 750, \text{ and } 800 \text{ fps}$
- Thrust/solidity coefficient,  $C_T/\sigma = 0.055, 0.065, 0.075, \text{ and } 0.085$
- Rotor radius:

Single rotor:

$R = 45, 50, 55, \text{ and } 60 \text{ ft}$

Tandem rotor:

Articulated, rigid, and teetered,  $R = 33, 35, 37, \text{ and } 39 \text{ ft}$

Matched-stiffness,  $R = 41, 43, 45, 47, \text{ and } 49 \text{ ft}$

Parameter values other than the foregoing were submitted when necessary to fill in areas needing better definition.

### Use of Computer Results

The results of the solution gross weight determination program described above were plotted as maximum rated power (Max RP) versus heavy-lift gross weight ( $W_{HL}$ ) at constant tip speeds ( $\Omega R$ ) as shown in Figure 11. Solution limit lines of 77 psf blade loading for the matched-stiffness single- and tandem-rotor configurations, or a  $\left(C_{L_{r_o}}\right)_T$  limit line of 0.50 for the articulated, teetered, and rigid single- and tandem-rotor configurations, were established on these plots by crossplots of BL or  $\left(C_{L_{r_o}}\right)_T$  versus  $W_{HL}$  at lines of constant R (rotor radius).

The type and number of engines nearest the minimum weight points of these plots could then be used to establish a plot of tip speed versus minimum  $W_{HL}$  at constant Max RP (Figure 13) for the configuration. The tip speed at or near the minimum weight was determined in this manner. A plot of the value of  $W_{HL}$  at the intersection of the

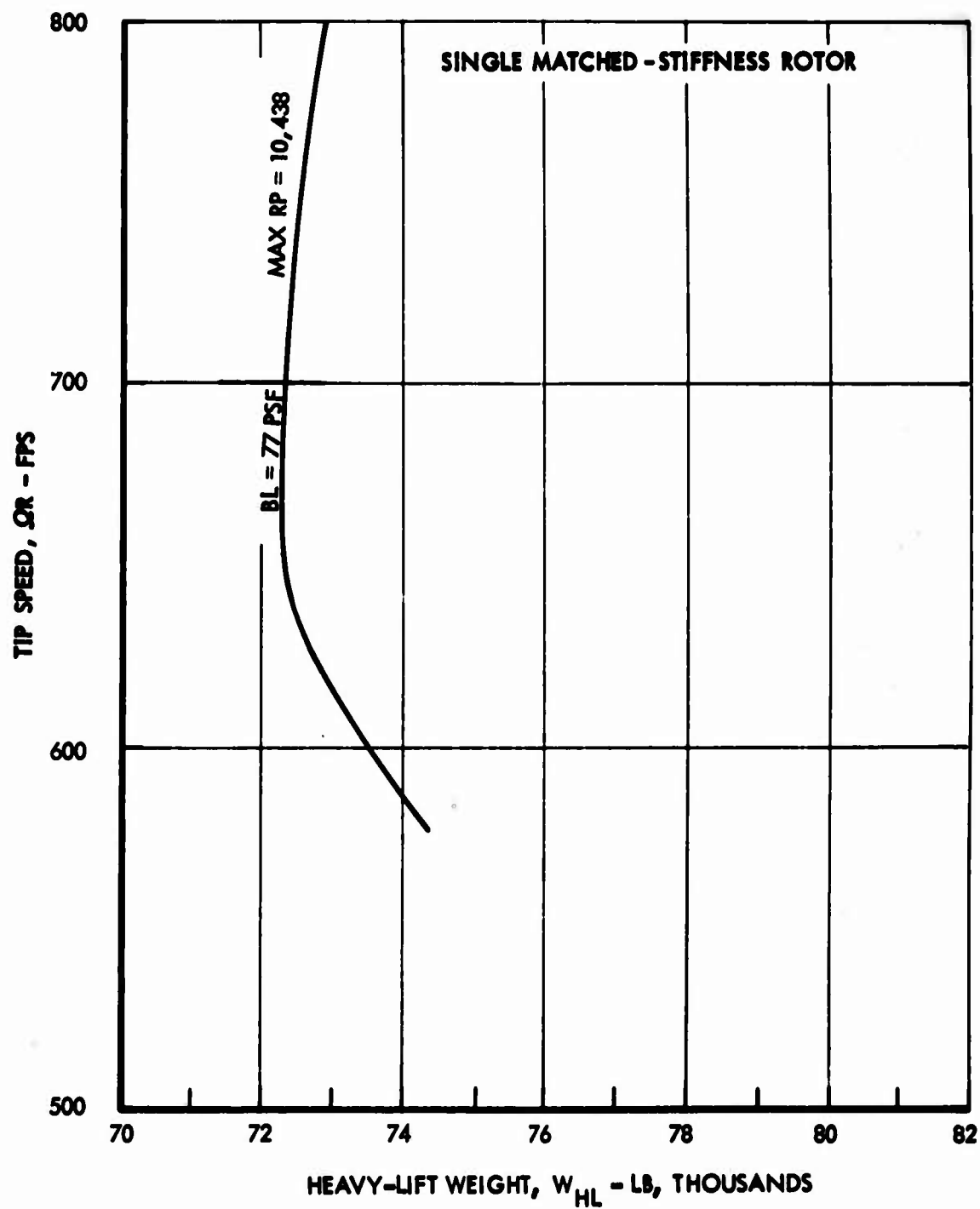


Figure 13. Typical Cross Plot for Determining Tip Speed

solution limit line and the lines of constant R on the Max RP versus  $W_{HL}$  chart for this optimum (minimum weight) tip speed versus the corresponding R was then established (Figure 14). From this plot the optimum R was determined at the minimum  $W_{HL}$ .

Once the optimum R was determined,  $\sigma$  could be calculated with the  $W_{HL}$  which corresponded to the optimum tip speed and the Max RP corresponding to the number and type of engines using either

$$\sigma = \frac{W_{HL}}{\pi R^2 \times BL}$$

for the matched-stiffness configurations or

$$\sigma = \frac{(C_T)_T}{\left(\frac{C_T}{\sigma}\right)_T}$$

for the articulated, teetered, rigid rotor configurations where

$$(C_T)_T = \frac{W_T \times K_{DW}}{\rho_o \pi R^2 \Omega_R^2}$$

and

$$\frac{C_T}{\sigma} = \frac{(\bar{C}_{L_{r0}})_T \times B^3}{6} = \frac{0.50 \times 0.97^3}{6}$$

The transport weight was then determined from the computer output summary sheet (Figure 7) for the corresponding parametric values and the heavy-lift weight.

To verify the results of the computer program and to obtain complete weight and mission breakdowns, these and other significant parameters for the matched-stiffness single rotor were submitted to the solution gross weight determination program, and output sheets such as those shown in Figure 15 were obtained. It will be noted that the Max RP is 154 horsepower less than the 10,438 horsepower which is representative of the two 501-M26 engines used. This was considered to be an

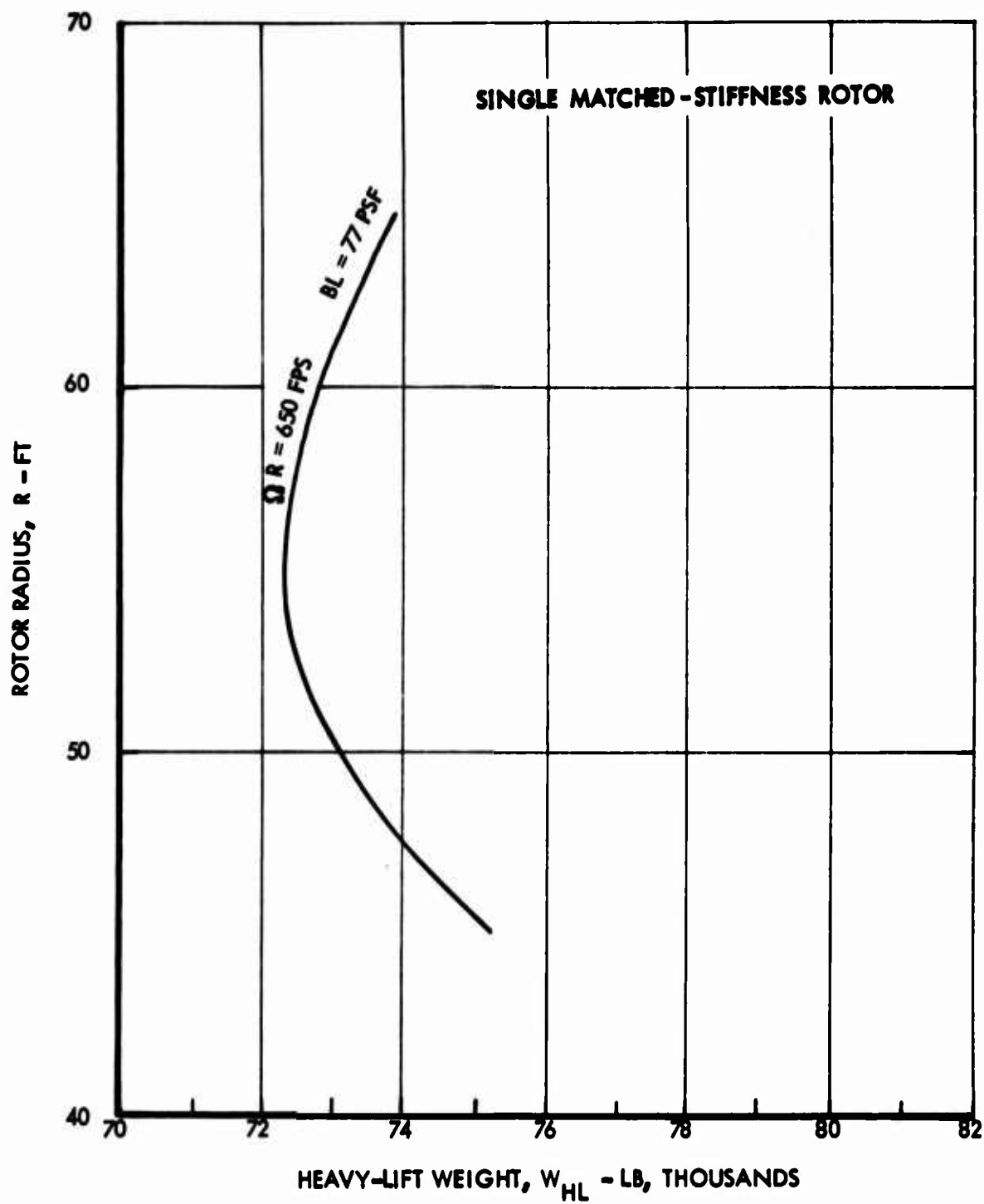


Figure 14. Typical Plot for Radius Determination

RADIUS, NR	TIP SPEED, NR	INIST, NR	SIGNA, NR	NO OF BLADES, NR
35.0000	650.0000	-5.00000	0.0968730	5.0000

RADIUS, TR	TIP SPEED, TR	SIGNA, TR	NO OF BLADES, TR	0-L, TR	N, TR	C7/SIGNA, TR
9.0079	650.3000	0.2403908	4.	15.0000	12.0000	0.0000000

TRANSPORT MISSION CONSTANTS

	LEG 1	LEG 2	LEG 3	LEG 4	LEG 5
PCIRP	0.0734999E 02	0.	0.1100000E 03	0.	0.1300000E 03
VR	0.3333333E-01	0.4999999E-01	0.9000001E 00	0.3333333E-01	0.76923077E 00
T, HRS	0.	0.	0.8999999E 03	0.	0.8000000E 02
FO	0.11111099E 04	0.	0.	0.	0.
ALT, FT	0.52190000E 04	0.52190000E 04	0.0999999E 03	0.52190000E 04	0.0999999E 03
DIST	0.	0.	0.4652999E 04	0.2399999E 05	0.44630000E 04
SRPM	0.5014199E 05	0.5895543E 05	0.56399743E 05	0.32280253E 05	0.30237088E 05
DELPL	0.	0.63676413E 04	0.42799751E 04	0.60030974E 04	0.34680044E 04
WLEG	0.	0.	0.84227848E 01	0.	0.69517165E 01
ALF270	0.15999984E 03	0.18656902E 03	0.25556879E 04	0.11969910E 03	0.20431644E 04
WFLEG	0.07349999E 02	0.01911058E 02	0.41614354E 02	0.58368334E 02	0.34581073E 02
PCIRPC	0.	0.42381907E 04	0.26445429E 04	0.39275711E 04	0.28425169E 04
IMP					

HEAVY LIFT MISSION CONSTANTS

	LEG 1	LEG 2	LEG 3	LEG 4	LEG 5
PCIRP	0.0734999E 02	0.	0.9500000E 02	0.	0.1300000E 03
VR	0.3333333E-01	0.3333333E-01	0.21052631E-00	0.16666666E-00	0.15384615E-00
T, HRS	0.	0.	0.1800000E 03	0.	0.8000000E 02
FO	0.11111099E 04	0.	0.	0.	0.
ALT, FT	0.52190000E 04	0.52190000E 04	0.2000000E 02	0.52190000E 04	0.2000000E 02
DIST	0.	0.	0.46340000E 04	0.4000000E 05	0.46820000E 04
SRPM	0.72304204E 05	0.72144207E 05	0.71771590E 05	0.71093423E 05	0.30341097E 05
DELPL	0.	0.81985465E 04	0.52089158E 04	0.00323903E 04	0.39726344E 04
WLEG	0.	0.	0.93412481E 01	0.	0.64386422E 01
ALF270	0.15999984E 03	0.37261739E 03	0.67796735E 03	0.73252704E 03	0.41573163E 03
WFLEG	0.07349999E 02	0.79714767E 02	0.50646478E 02	0.7809224E 02	0.34626070E 02
PCIRPC	0.	0.57190853E 04	0.33152498E 04	0.55555864E 04	0.28481223E 04
IMP					

MGC	5577.768	WROD	3984.412	WFREQ	5627.678
USF	175.509	WDS	157.609	WFRML	2620.937
WTR	536.216	WGB	182.215	WT	59302.00
WB	7074.096	WCAFE	4042.511	WHL	72295.25
WLG	3759.353	WEMPT	28572.947	MAX RP	10284.853
WE	2029.775	WCREW	600.000	MAX AL270	9.34125
WES	1055.483	WOLL	81.191	CLROT	0.426396
		WBSIC	29256.138	CLROM	0.519821

MSFM ROTOR

Figure 15. Typical Mission Breakdown Computer Output Sheet

acceptable closure error for the installed power. Because of this closure error, however, the transport fuel  $(W_{FREQ})_T$  was adjusted upward by the increase in fuel which would be representative of the actual engines used.

$$\Delta W_{FREQ} = \Delta \text{Max RP} \times \frac{\partial W_F}{\partial \text{Max RP}} \times \frac{t}{0.90}$$

where

$$t = \text{the mission time in hours} = 1.78$$

and

$$\frac{\partial W_F}{\partial \text{Max RP}} = 0.1113$$

for Allison 501-M26.

Then

$$\Delta W_F = \frac{154 \times 0.1113 \times 1.78}{9} = 34 \text{ lb}$$

To check fuel weight available,

$$(W_{FAVAIL})_T = \frac{W_T - (W_{BASIC} + PL_T)}{1 + K_{FT}}$$

$$(W_{FAVAIL})_T = \frac{59,302 - (29,254 + 24,000)}{1.075} = 5630 \text{ lb}$$

$$(W_{FREQ})_T = 5627 + 34 = 5661$$

Thus,

$$(\Delta W_F)_T = 31 \text{ lb}$$

This is an acceptable error of closure. A hand calculation using the appropriate curves of nautical miles/pound versus weight, hover power versus weight, and corrected engine power versus corrected fuel flow yielded a  $(W_{FREQ})_T$  of 5720 pounds and  $(W_{FREQ})_{HL}$  of 2634 pounds (Table VII).

These quantities indicate the validity of the cross-plotting and the computer program results as well as the compatibility of the optimum parameters selected.

#### Results of Computer Analysis

A description of the rotor/propulsion system for each configuration studied is presented in Table IV. Adjustments to the computer results of Table IV are shown in Table V. These adjustments were required because the weight equations for the fuselage and tandem-rotor helicopter cross-shafting were revised, and engine and fuel adjustments were made to correspond to the actual engine selected. These data show that the lowest weight ( $W_{HL}$ ) configuration is the matched-stiffness single-rotor helicopter. Although the results in Table IV show little weight difference between the matched-stiffness single-rotor and the tandem-rotor configurations, the adjustments shown in Table V favor the single rotor.

The matched-stiffness single-rotor helicopter was selected as the recommended configuration. A complete weight breakdown and description of this recommended helicopter is shown in Table VI.

The component weights were determined by the computer program (Figure 15). The complete transport and heavy-lift mission breakdowns were determined from the computer results shown in Figure 15 and from the curves and data of the performance section shown in Table VII.

The effect of single-point variations on the transport mission weight for 6000-foot, 95°F hover out-of-ground effect (HOGE) and the transport and heavy-lift payload and fuel weight are shown in Table VIII. These were obtained by varying parameters and configurations which were of second-order effect and were not varied in the solution gross weight determination program.

It appears that the most significant result of the single-point variation studies is the improvement obtained by engine shutdown during cruise. This procedure results in a 989-pound reduction in fuel required for the transport mission. However, use of the engine shutdown option in the solution gross weight determination program shows that this results in only a 300-pound reduction in heavy-lift design gross weight. This weight reduction is less than the transport mission fuel weight reduction because it results only in a reduction of the installed power

TABLE IV											
CONFIGURATION COMPARISON											
EXTERNAL CARGO HELICOPTERS, $\theta_1 = -5$ Degrees											
CONFIGURATION	$W_{HL}$ (lb)	$W_T$ (lb)	NO. OF ENGINES AND TYPE	R (ft)	$\sigma$	$\Omega$ R (fps)	BL (lb/ft <sup>2</sup> )	$C_{L_{RO_T}}$	$C_{L_{HL}} Q_{HL}$	NO. BLADES	DL (lb/ft <sup>2</sup> )
Single Matched-Stiffness Rotor	72,300	59,300	(2) 501-M26	55	.0986	650	77.0	.426	.520	5	7.60
Single Rigid, Articulated, and Teetered Rotors	78,000	66,400	(4) T64-GE-12 (AAFSS)	49.6	.0868	750	119.8	.500	.586	4	10.08
Tandem Matched-Stiffness Rotor	72,500	59,600	(2) T64/S5A	48.3	.0641	700	77.0	.366	.446	3	5.63
Tandem Rigid, Articulated, and Teetered Rotors	80,200	68,300	(3) T64/S5A	39.0	.0724	750	132.4	.500	.586	4	9.60



TABLE V  
ADJUSTMENTS OF COMPUTER RESULTS SHOWN IN TABLE IV

CONFIGURATION	FUSELAGE (lb)	CROSS SHAFT (lb)	ENGINE (lb)	FUEL and FUEL TANK (lb)		PAYLOAD (lb)	
				HEAVY-LIFT MISSION	TRANSPORT MISSION	HEAVY-LIFT MISSION	TRANSPORT MISSION
Single Matched- Stiffness Rotor	-840	0	0	0	0	+840	+840
Single Rigid, Articulated, and Teetered Rotors	-230	0	-190	0	-210	+420	+630
Tandem Matched- Stiffness Rotor	0	+93	-200	-270	-630	+377	+737
Tandem Rigid, Articulated, and Teetered Rotors	0	+84	-304	-270	-630	+490	+850

TABLE VI  
MATCHED-STIFFNESS SINGLE-ROTOR SYSTEM  
DESCRIPTION AND WEIGHT BREAKDOWN

Gross Weight:	
Design (Heavy-Lift Mission Load Factor = 2.5), lb	72,300
Transport Mission, lb	59,300
Ferry Mission (Load Factor = 2.0), lb	90,300
Power Plant:	
Engine Number and Type (or Equivalent)	Two (2) 501-M26
Total Rated Power	
Sea Level Uncorrected	10,900 (30 min)
6000 ft, 95°F Uncorrected	7,430 (30 min)
Power Correction	-(2.4% + 200 hp)
Fuel Flow Increased by	5%
Transmission:	
Design Horsepower (3600-hr Life)	8,200
Main Rotor:	
Radius, ft	55.0
Solidity	.0986
Number of Blades	5
Blade Chord, in.	41.0
Blade Aspect Ratio	16.2
Tip Speed, fps	650
Disc Loading (Heavy-Lift Mission), psf	7.60
Design Mean Blade Lift Coefficient	
Transport	.426
Heavy-Lift	.520
Hover Horsepower, Transport,	
6000 ft, 95°F (Main Rotor Only)	6,263
Blade Loading, psf	77
Tail Rotor:	
Radius, ft	9.61
Solidity	.2484
Main Rotor to Tail Rotor Hub Distance, ft	65.61
Hover Horsepower, Transport,	
6000 ft, 95°F (Tail Rotor Only)	686
Equivalent Drag Areas:	
Inbound (Transport and Heavy-Lift) and Ferry, sq ft	80
Outbound Transport, sq ft	100
Outbound Heavy-Lift, sq ft	180
Ferry Mission Range (with 10% Reserve), nm:	2,600

TABLE VI (CONTINUED)

## Component Weights, lb:

Rotor Group	5,578
Tail Group	710
Tail Rotor	(536)
Horizontal Stabilizer	(174)
Body Group	7,074
Landing Gear Group	3,759
Flight Controls Group	1,250
Propulsion Group	7,860
Engines	(2,060)
Engines Accessories	(1,055)
Fuel System	(421)
Drive System	(4,324)
Equipment	<u>2,793</u>
Total (Weight Empty)	29,024

## Mission Weight, lb:

## Transport Mission

Crew	600
Fuel	5,620
Oil and Residual Fuel	81
Payload	<u>24,000</u>
Gross Weight	59,325

## Heavy-Lift Mission

Crew	600
Fuel	2,620
Oil and Residual Fuel	81
Payload	<u>40,000</u>
Gross Weight	72,325

## Ferry Mission

Crew	600
Fuel	56,800
Oil and Residual Fuel	81
Auxiliary Tanks	<u>3,839</u>
Gross Weight	90,344

TABLE VII

MISSION BREAKDOWN AND COMPARISON  
SINGLE MATCHED-STIFFNESS ROTOR

MISSION	WARM- UP FUEL	MISSION INITIAL HOVER		LEG OUTBOUND		MIDPOINT HOVER		INBOUND		TOTAL FUEL INCLUDING RESERVE
		AVERAGE WEIGHT	FUEL	AVERAGE WEIGHT	FUEL	AVERAGE WEIGHT	FUEL	AVERAGE WEIGHT	FUEL	
Computer Output (Figure 15) with Corrections for Max RP										
Transport Heavy-Lift	161 161	187 374		2,571 681		120 736		2,056 418		5,662 2,634
Check Calculations										
Transport Heavy-Lift	163 163	187 377		57,700 71,400	2,578 666	120 744	56,300 70,600	31,200 30,100	2,104 420	5,720 2,634
Optimum Cruise Speed										
Transport Heavy-Lift	163 163	187 377		57,700 71,400	2,498 661	120 744	56,400 70,600	31,300 30,100	2,110 421	5,640 2,630
Engine Shutdown (Computer Output with Corrections)										
Transport Heavy-Lift	163 163	187 377		2,074 687		120 745		1,646 335		4,650 2,560

TABLE VIII					
EFFECT OF SINGLE-POINT VARIATIONS SINGLE MATCHED-STIFFNESS ROTOR					
VARIATION	6000 Ft, 95°F HOVER INCREMENT (lb)	$W_{F_T}$ INCREMENT (lb)	$PL_T$ INCREMENT (lb)	$W_{F_{HL}}$ INCREMENT (lb)	$PL_{HL}$ INCREMENT (lb)
Standard*	0	0	0	0	0
Optimum nm/lb	0	-80	+80	-4	+4
Engine Shutdown (Standard)	0	-1012	+1012	-74	+74
Taper 3:1	+700	+20	+680	+5	-5
$\theta_1 = 0$	-600	+74	-674	+40	-40
$\theta_1 = -10^\circ$	+800	-45	+845	+6	-6

\*Standard is No Engine Shutdown,  $\theta_1 = -5^\circ$ , External Cargo Fuselage,  
Taper = 1:1, Missions Performed With Fixed Speeds per Table I,  $W_{HL} = 72,300$   $W_T = 59,300$

requirement caused by the reduced weight for the 6000-foot, 95°F hover requirement and, consequently, the engine weight. The effect of the reduced installed power on the heavy-lift mission fuel weight is slight because of the short duration of the mission.

No effect for the NACA 63015 airfoil is shown because this airfoil has essentially the same aerodynamic characteristics as the NACA 0012 airfoil which was used in the solution gross weight determination program. The difference lies in structural considerations.

Figures 16, 17 and 18 show the effect on hover performance of using rotor-blade taper and twist variations. The corresponding fuel weights were determined from Figure 33. The effect of twist on fuel consumption was determined from the solution gross weight determination program. The effect of taper on forward flight fuel consumption was determined from Figure 19 which was obtained from horsepower calculations of the computer program 1599, and from the corresponding fuel flows from Figure 28.

#### PERFORMANCE OF THE RECOMMENDED ROTOR SYSTEM

Performance characteristics of the single-rotor helicopter with a matched-stiffness rotor, which was found to be the lightest helicopter considered in this study, are summarized in this section. The important physical parameters of this helicopter are as follows:

Design gross weight	72,300 lb
Transport mission weight	59,300 lb
Number of blades	5
Rotor diameter	110 ft
Blade section	NACA 0012
Rotor tip speed	650 fps
Mean blade lift coefficient	0.520
Blade chord	3.4 ft
Blade aspect ratio	16.2
Blade twist	-5°

#### Equivalent drag areas

Transport outbound	100 sq ft
Heavy-lift outbound	180 sq ft
Ferry and inbound	80 sq ft

Rated military power (2 501-M26 engines) 10,900 hp

This helicopter will meet the requirements of the heavy-lift, transport, and ferry missions specified in the Statement of Work and will hover out of ground effect at 6000 feet, 95°F at the transport mission gross weight.

Speed/power plots for this configuration for the transport and heavy-lift missions are shown in Figures 20, 21, and 22.

It can be determined from these figures and the engine limit corresponding to military rated power, the transmission torque limit, and the blade loading limit (Figure 43) that the maximum speeds for the various missions are as follows:

Transport, outbound	140 knots
Heavy-lift, outbound	95 knots
Both missions, inbound	175 knots

#### Maximum Specific Range

A plot of maximum specific range as a function of gross weight and altitude was constructed to optimize the flight profile for the ferry mission (Figure 34). The determination of the maximum specific range was done with a graphical method using plots of power required as a function of the logarithm of speed (Figures 20 through 27) and plots of engine power as a function of the logarithm of fuel flow (Figures 28 through 32). The speed for maximum specific range was read off at the speed at which the slope of HP versus Log V was equal to the slope of HP versus Log FF. This procedure is based on the concept that at the speed for maximum specific range, the differential of specific range with respect to velocity is zero. Fuel/power relationship for hover is shown in Figure 33.

The stall limit, the blade loading limit, or power-limited speed condition, whichever occurred at the lowest speed, was used to determine the maximum specific range at the particular weight and altitude. This was done at altitudes of up to 20,000 feet with an equivalent fuselage drag area of 80 square feet for weights of from 30,000 to 100,000 pounds in 10,000-pound increments. Both one- and two-engine operations were considered. The envelope of these curves was then established. By determining the area under this curve between the takeoff weight and the landing weight with a 10-percent fuel reserve (integrating the specific range between weight limits), the ferry range was determined. Figure 34 was then used to establish a plot of range versus takeoff weight (Figure 35) by allowing for climb fuel where necessary at intermediate takeoff weights. A similar method was used to determine the maximum nautical miles per pound at sea level for several values of  $f_0$  and the results are plotted on Figures 36, 37 and 38.

#### Check of Calculations for Fuel Required

To check the computer results for the optimum configuration and to provide a base for other hand calculations, curves were constructed for specific range as a function of weight for the speeds and equivalent drag areas corresponding to the requirements of the transport and heavy-lift missions. These are shown in Figure 39 which was based on the curves in Figures 40 and 28 and the relationship

$$\text{Nautical Miles/pound} = \frac{V_K}{FF}$$

which is the specific range.

The results of these calculations are shown in Table VIII. These curves were used to check the output of the computer program. The correlation was excellent (Table VII).

#### Effect of Speed on Range and Payload

The effects of speeds other than those specified in the Statement of Work on mission radius and on payload were determined. Also, at the request of USAAVLABS, the effects of using equivalent drag areas of 200 square feet for outbound flight and 100 square feet for inbound flight were checked. These effects were determined by use of the speed/power relationships of Figures 23 and 21, respectively, and power/fuel relationships of Figures 28 and 33 at the corresponding mean standard mission cruise leg weight.



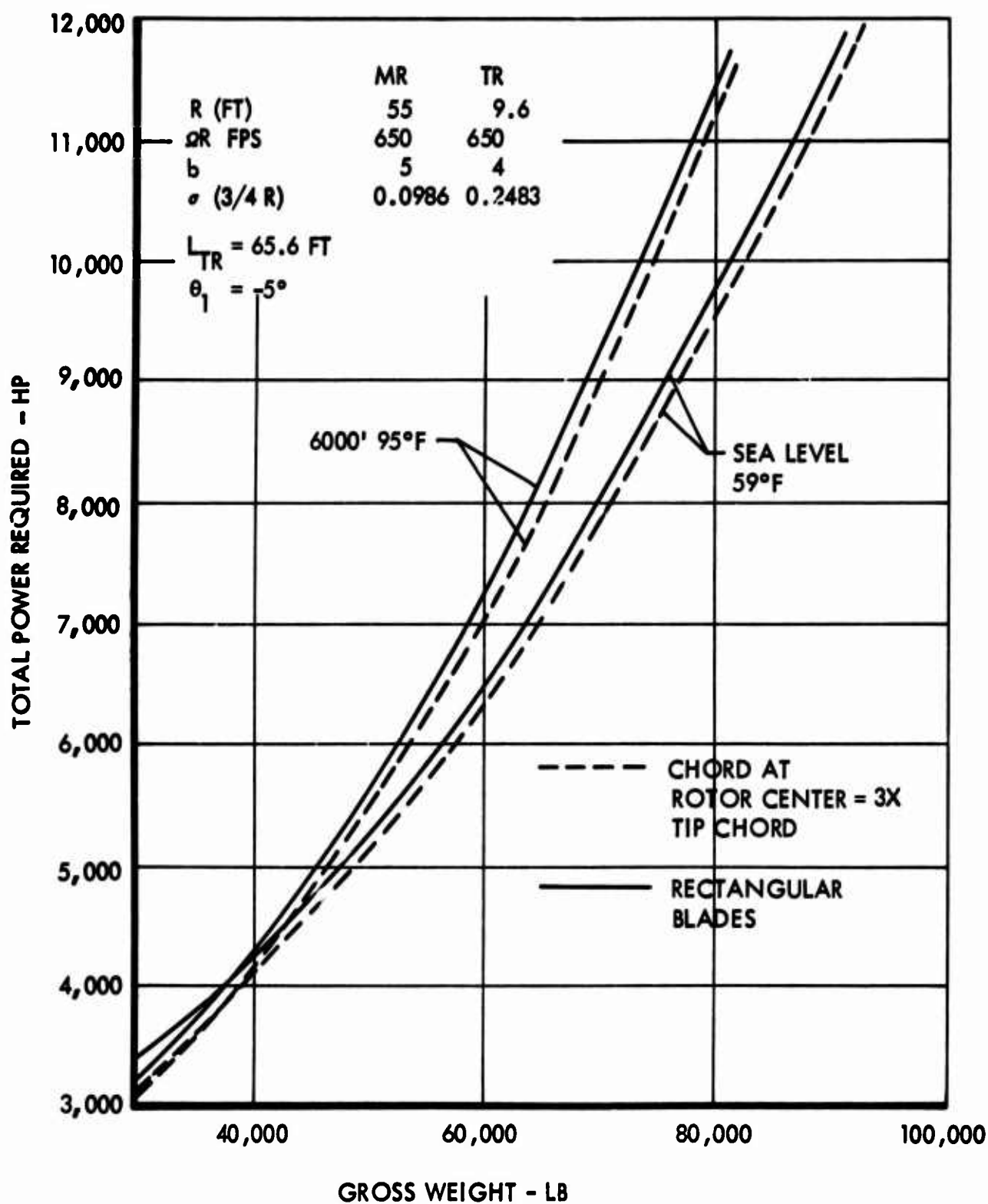


Figure 16. Comparison of Tapered and Rectangular Blade Rotor in Out-of-Ground-Effect Hover

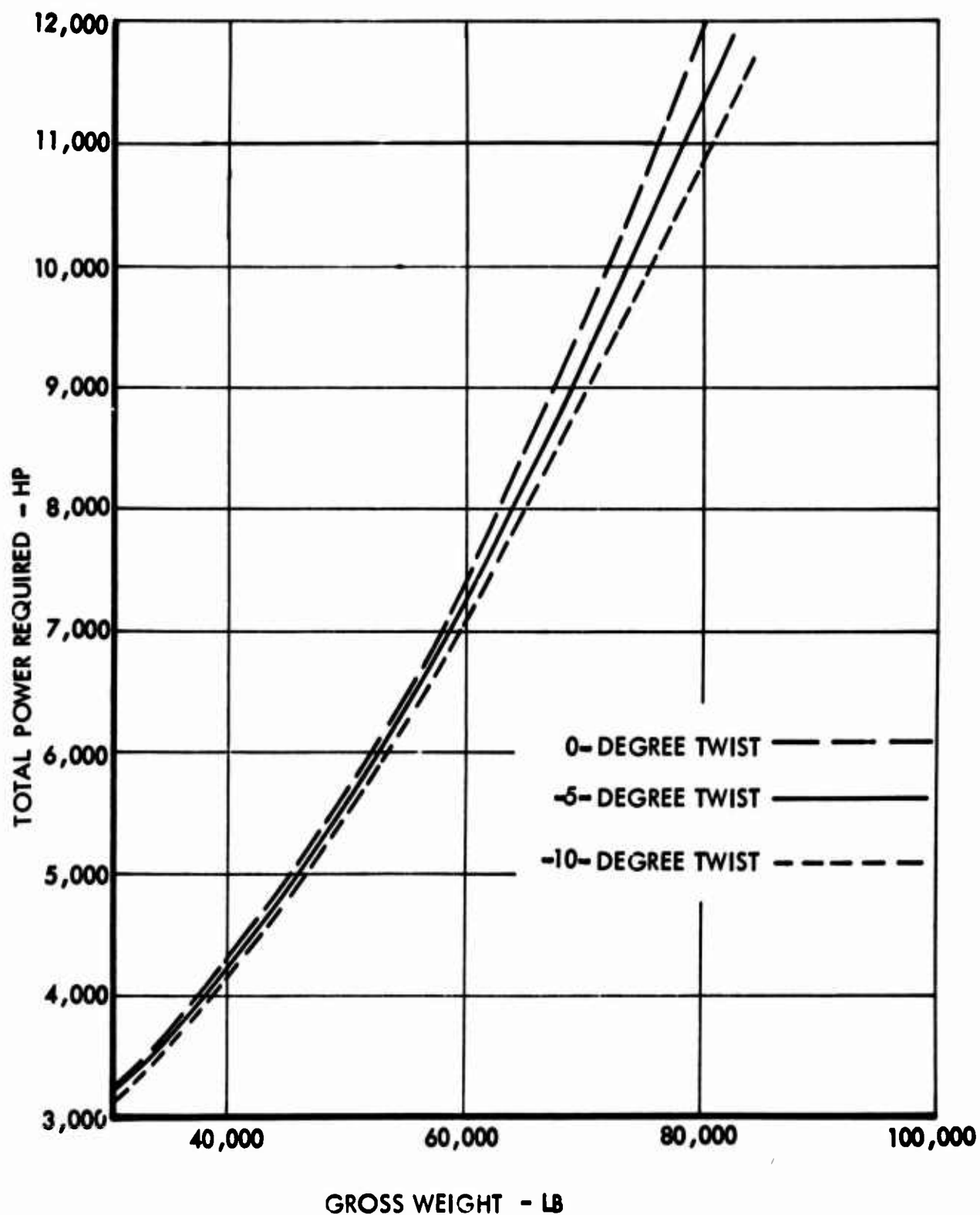


Figure 17. Comparison of 0-Degree, -5-Degree, and -10-Degree Twist of Rectangular Blades - 6000 Feet, 95°F

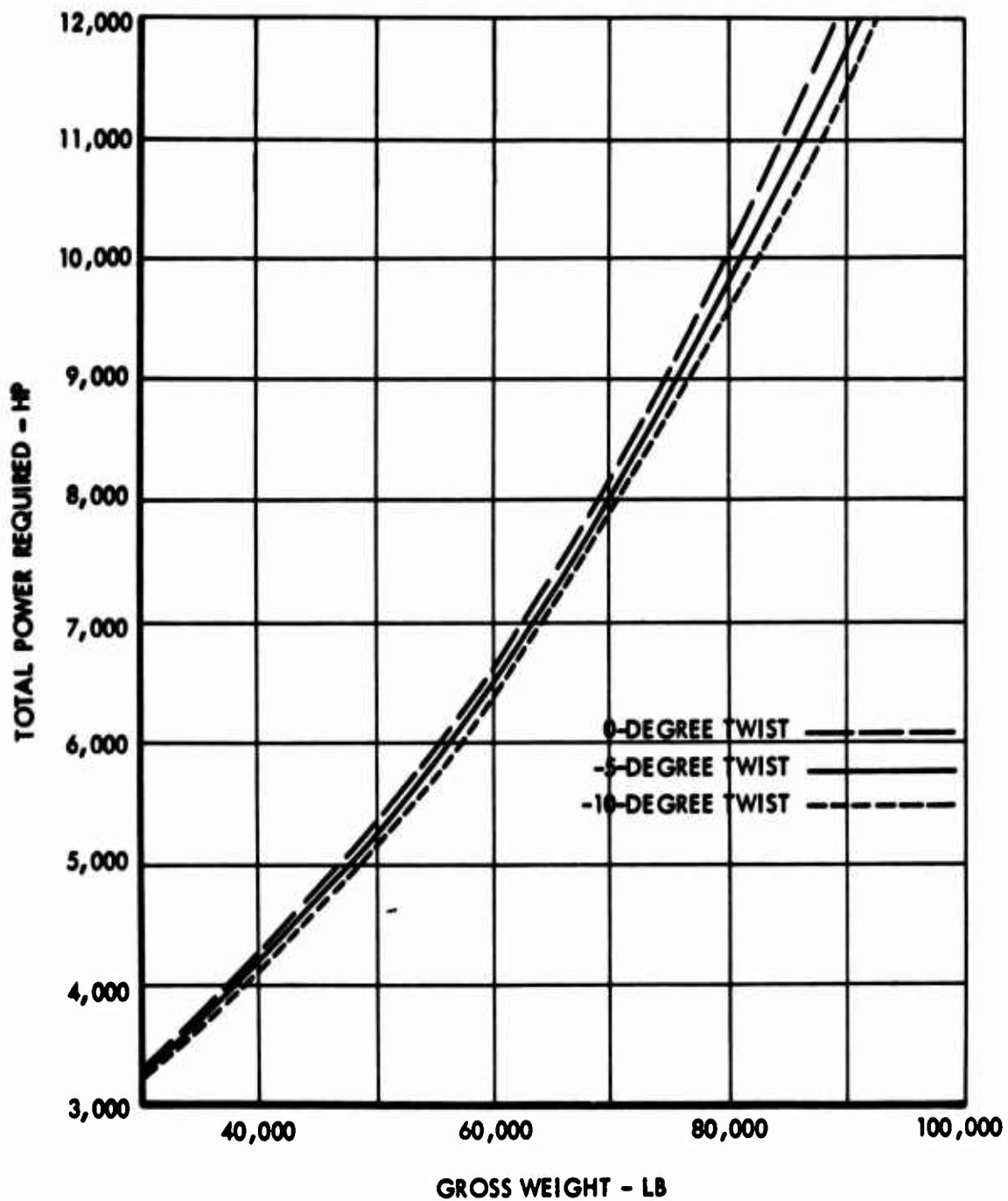


Figure 18: Comparison of 0-Degree, -5-Degree, -10-Degree Twist of Rectangular Blades - Sea Level Standard Day

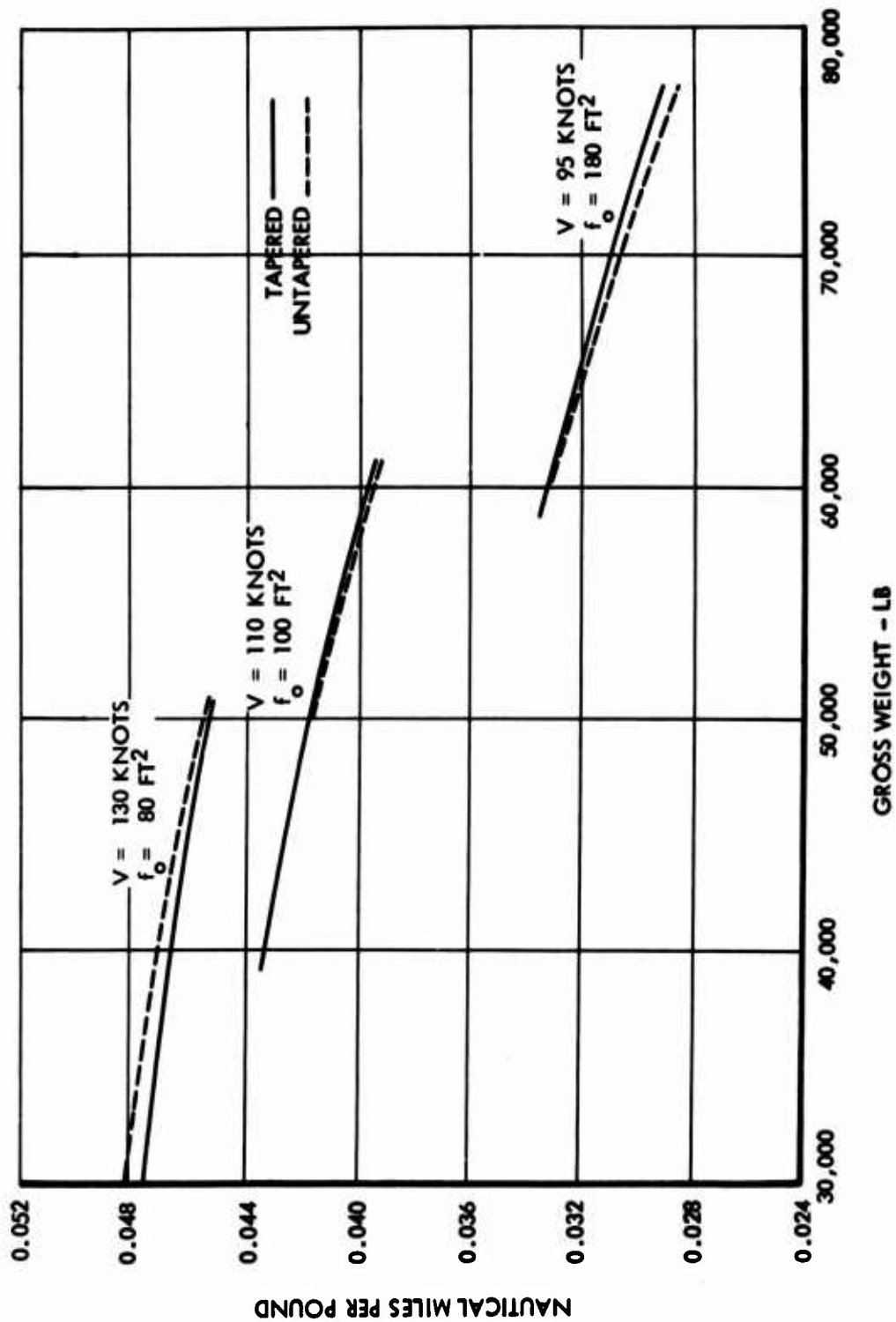


Figure 19. Comparison of Fuel Requirements in Forward Flight for Tapered and Untapered Blades, Matched-Stiffness Rotor

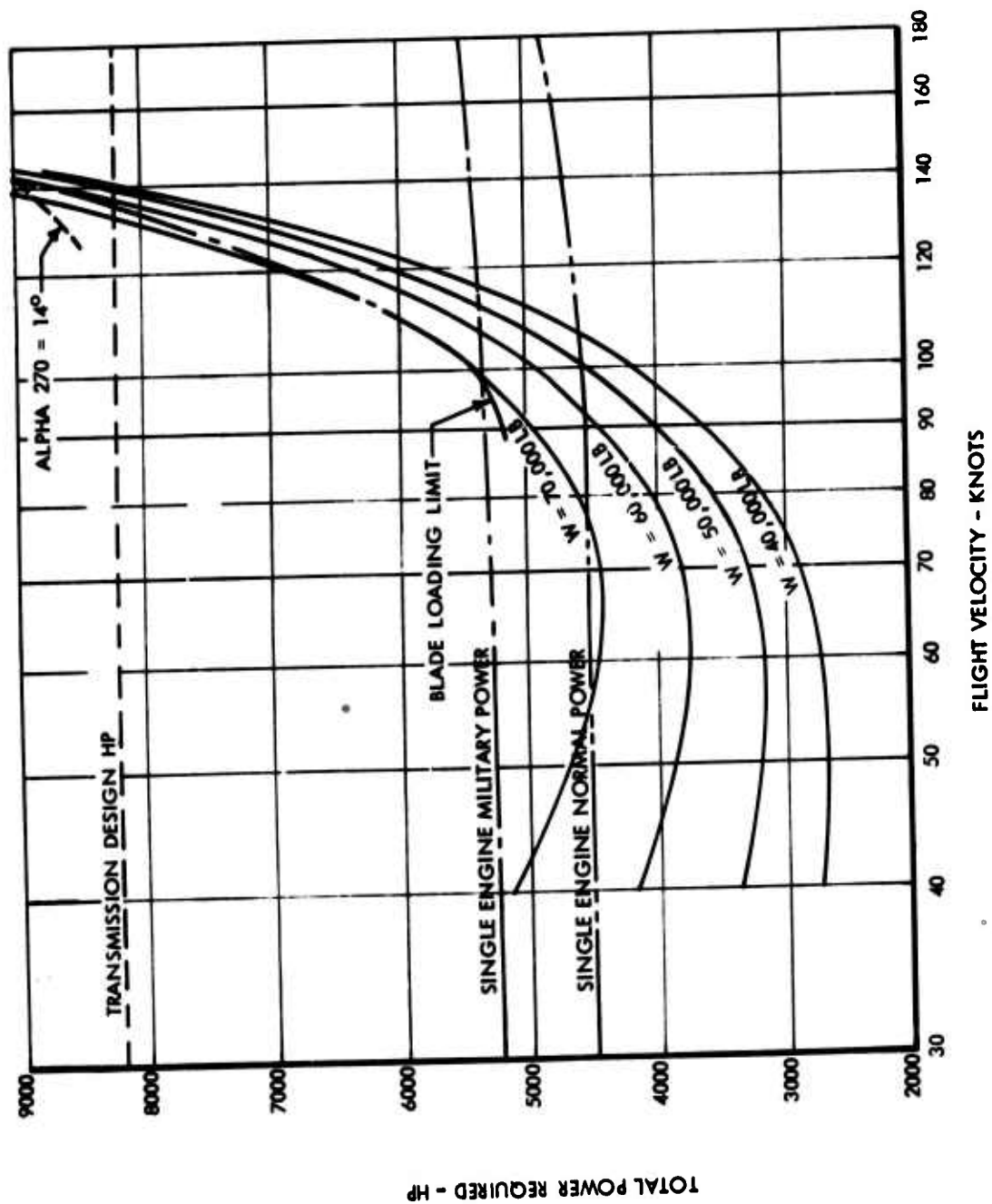


Figure 20. Forward Flight Power Required for Matched-Stiffness Single-Rotor Helicopter -  
Sea Level Standard Day,  $f_o = 180$  Square Feet

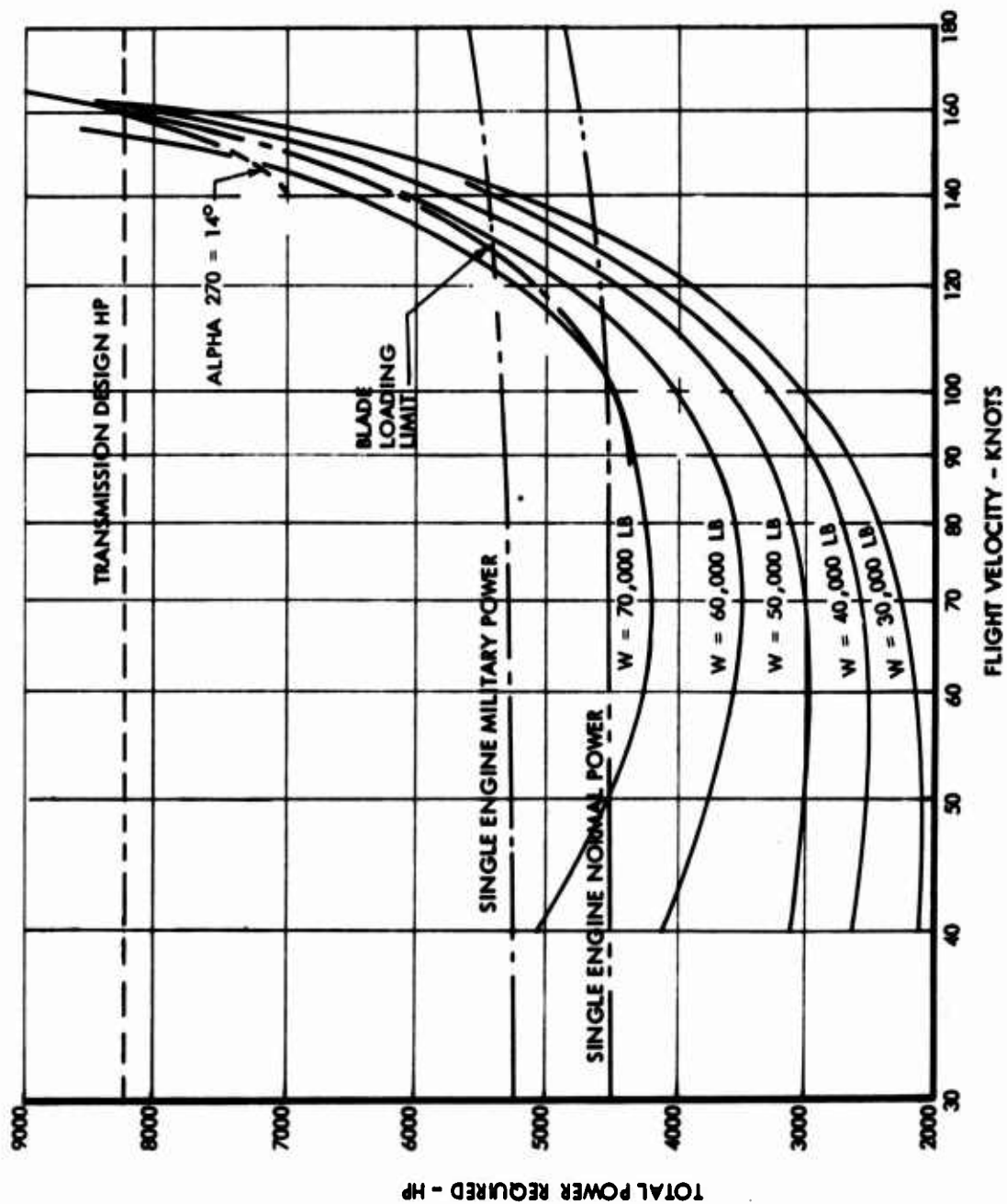


Figure 21. Forward Flight Power Required for Matched-Stiffness Single-Rotor Helicopter -  
Sea Level Standard Day,  $f_o = 100$  Square Feet

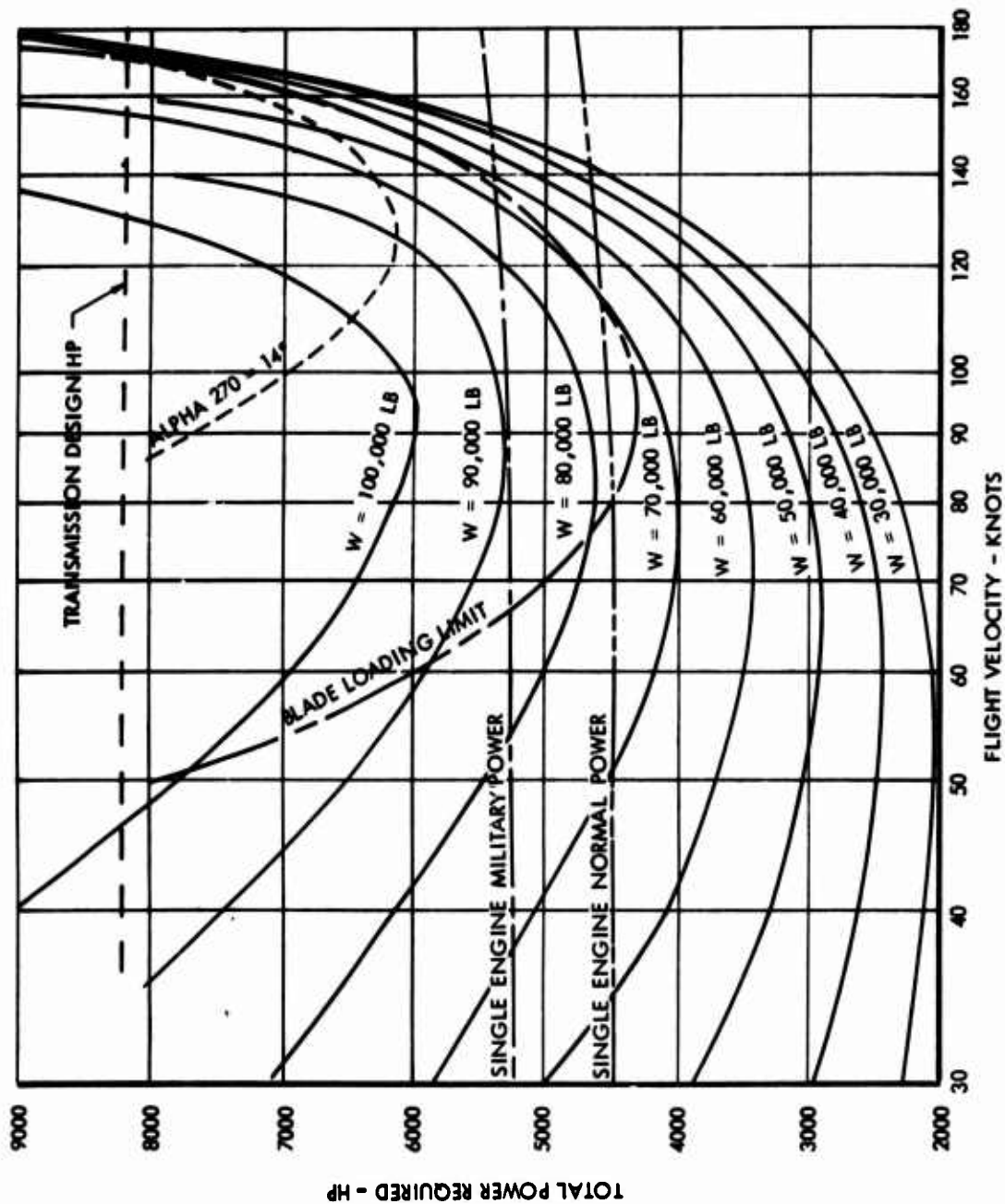


Figure 22. Forward Flight Power Required for Matched-Stiffness Single-Rotor Helicopter - Sea Level Standard Day,  $f_o = 80$  Square Feet

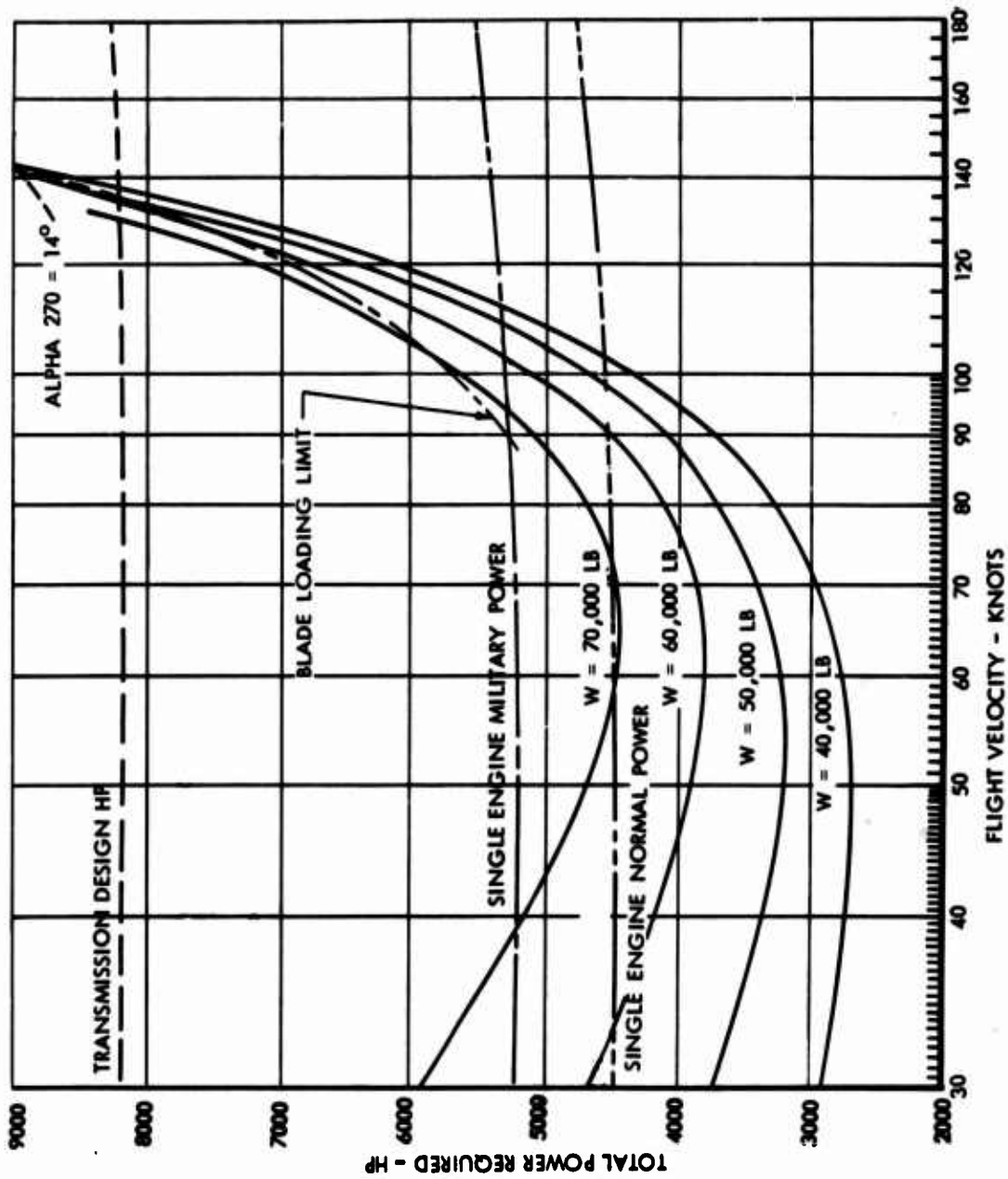


Figure 23. Forward Flight Power Required for Matched-Stiffness Single-Rotor Helicopter -  
Sea Level Standard Day,  $f_0 = 200$  Square Feet



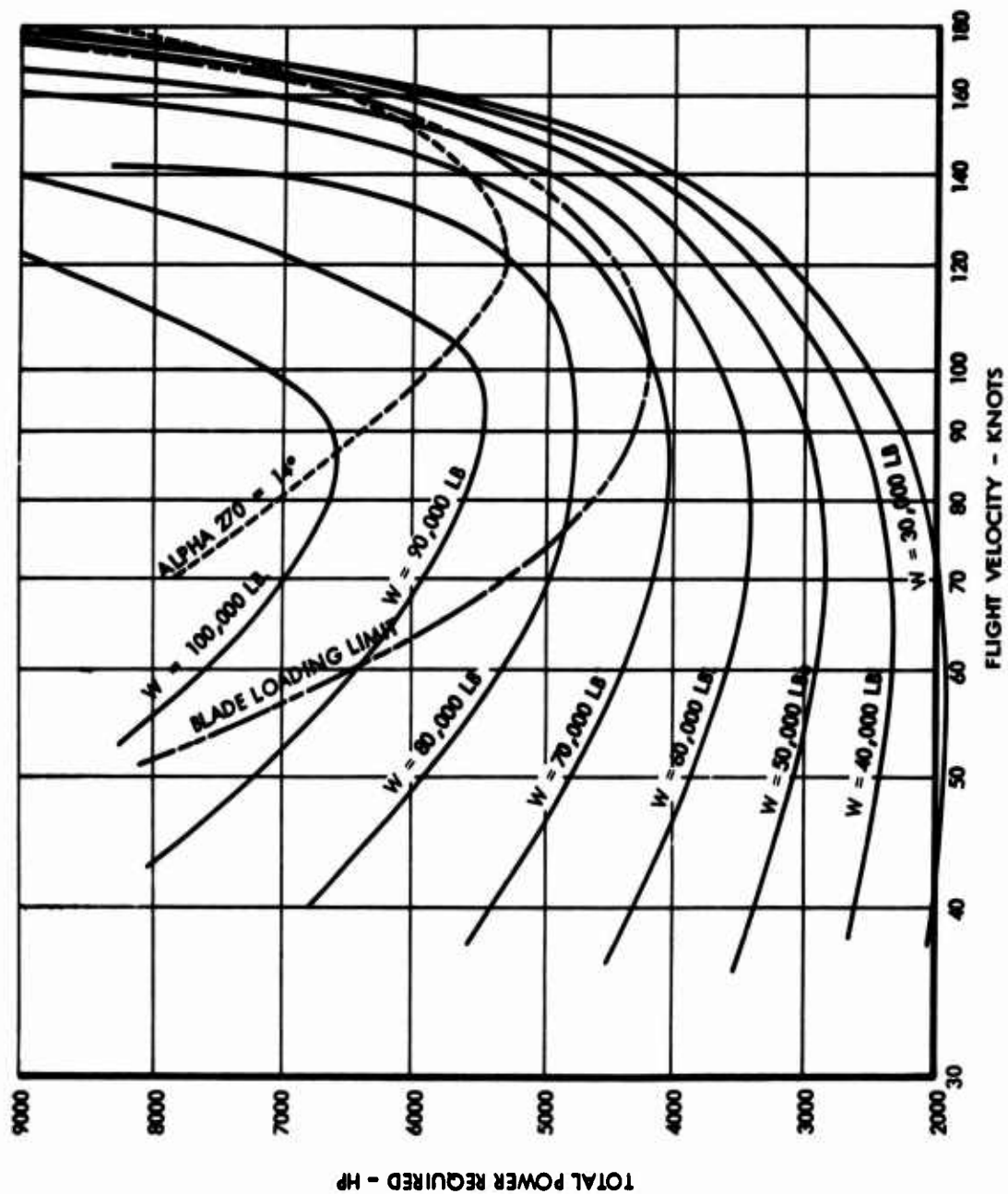


Figure 24. Forward Flight Power Required for Matched-Stiffness Single-Rotor Helicopter - 5000 Feet, Standard Day,  $f_o = 80$  Square Feet

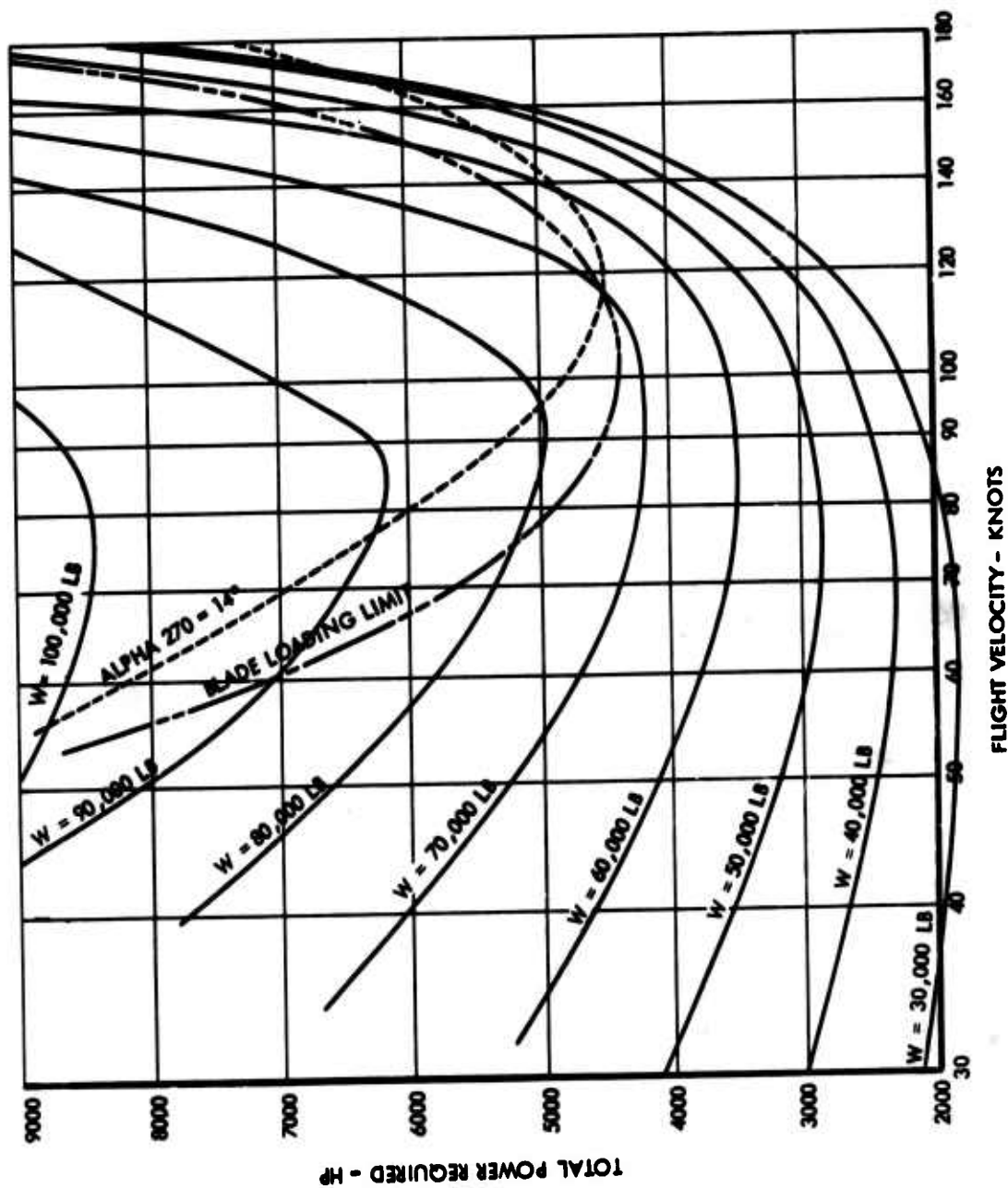


Figure 25. Forward Flight Power Required for Matched-Stiffness Single-Rotor Helicopter -  
10,000 Feet, Standard Day,  $f_o = 80$  Square Feet

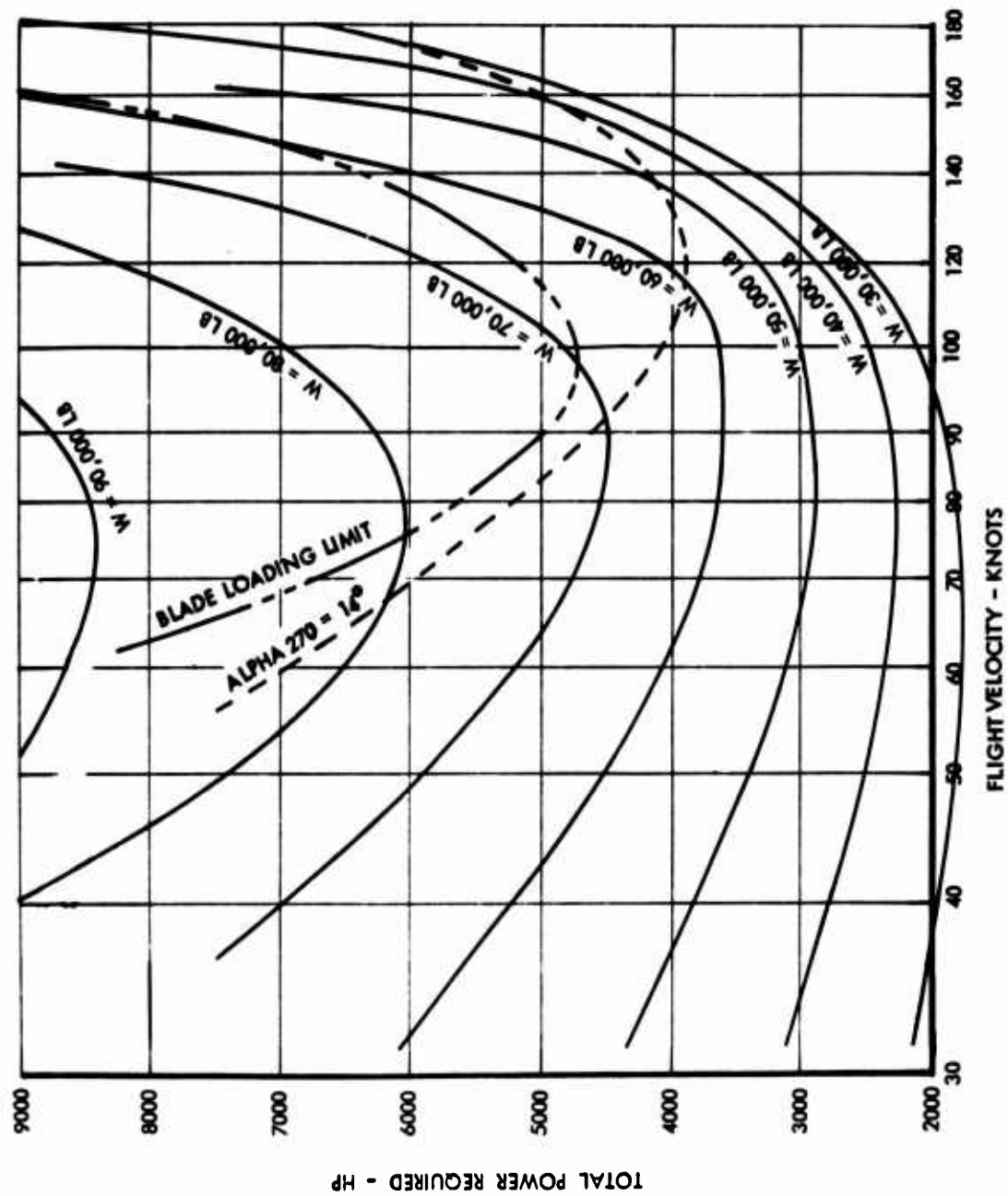


Figure 26. Forward Flight Power Required for Matched-Stiffness Single-Rotor Helicopter - 15,000 Feet, Standard Day,  $f_0 = 80$  Square Feet

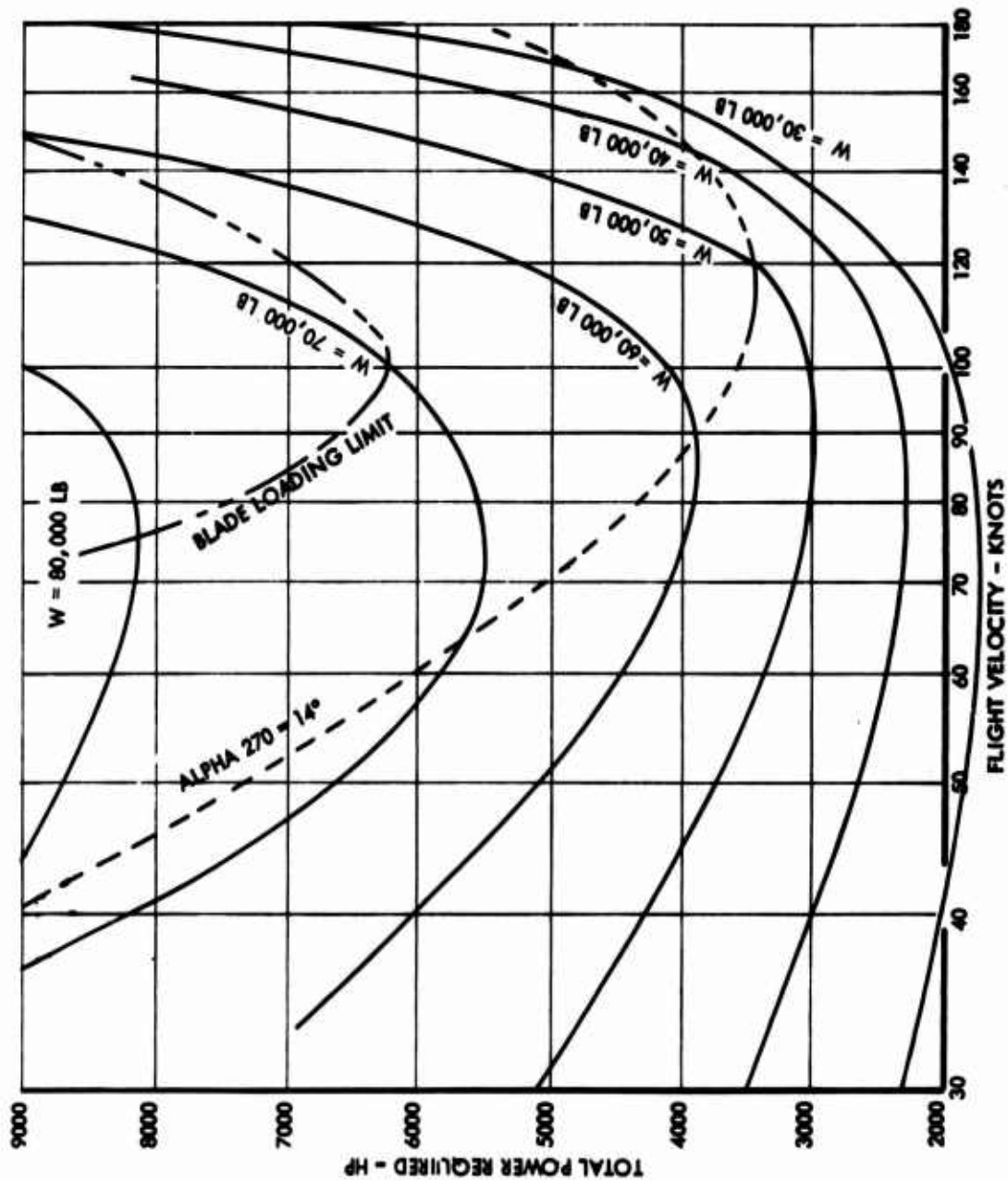


Figure 27. Forward Flight Power Required for Matched-Stiffness Single-Rotor Helicopter -  
20,000 Feet, Standard Day,  $f_o = 80$  Square Feet

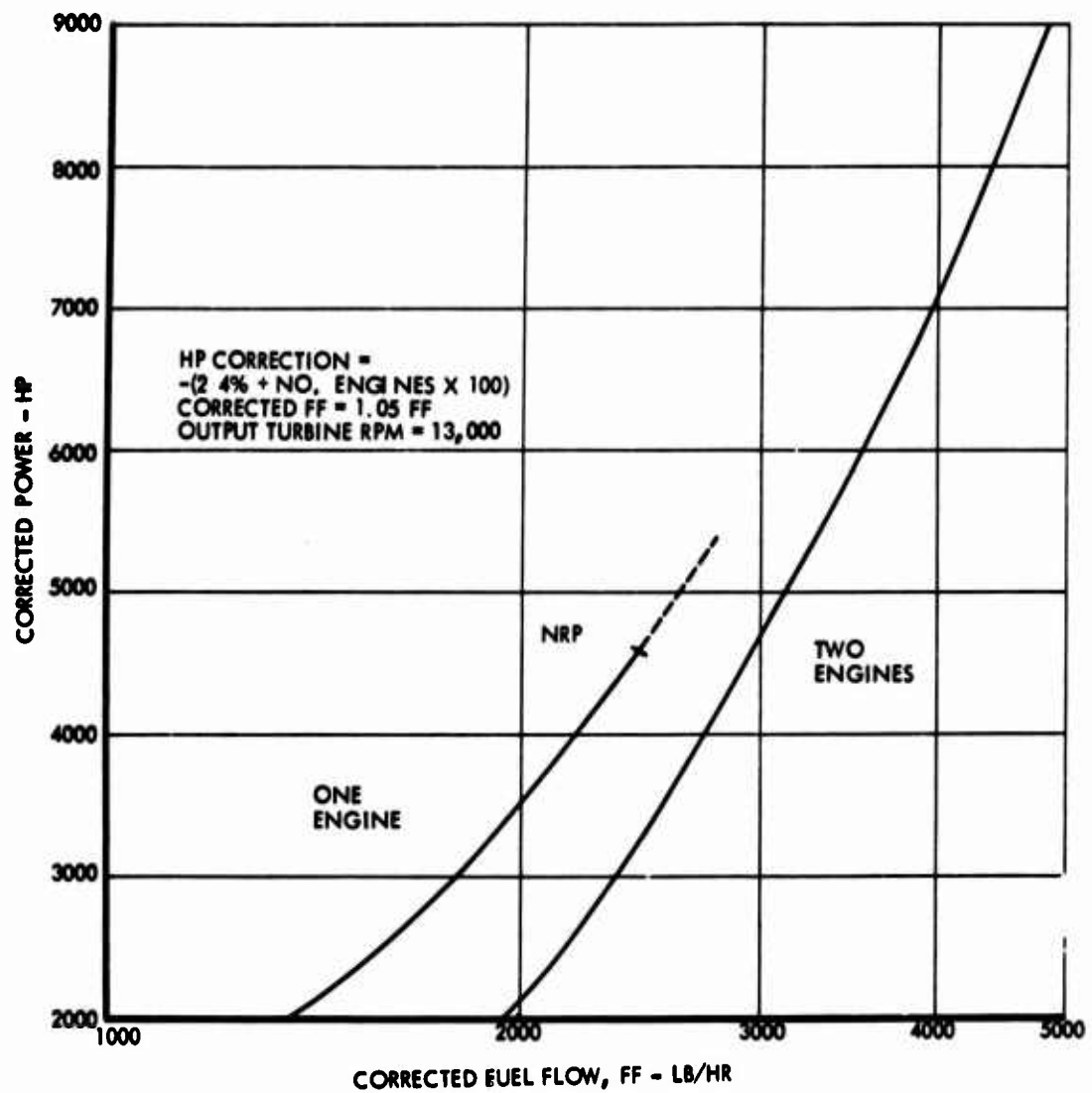


Figure 28. Fuel-Power Relationship, 501-M26 Engine -  
Sea Level Standard Day, 140 Knots

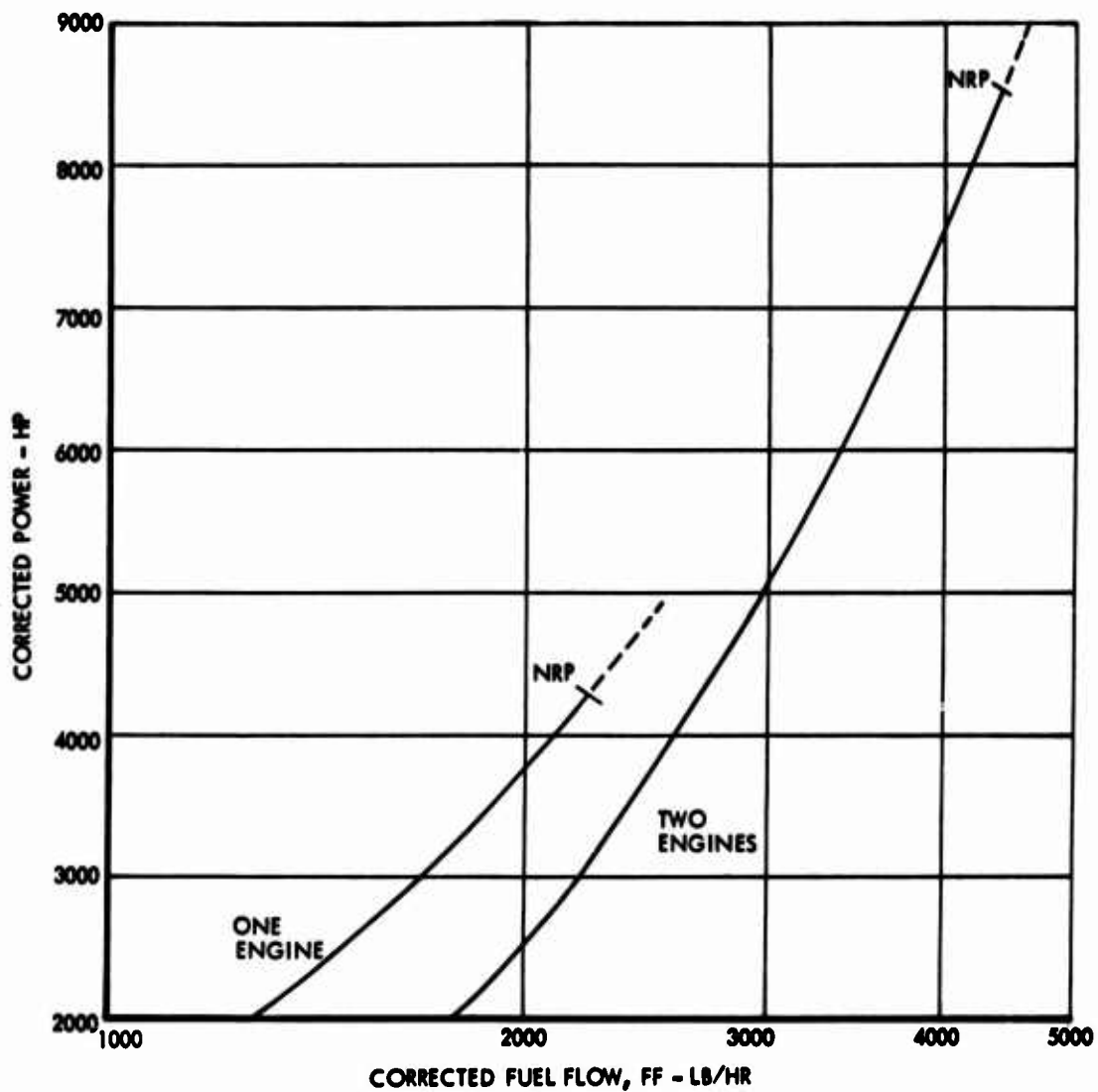


Figure 29. Fuel-Power Relationship, 501-M26 Engine -  
5000 Feet, Standard Day, 140 Knots

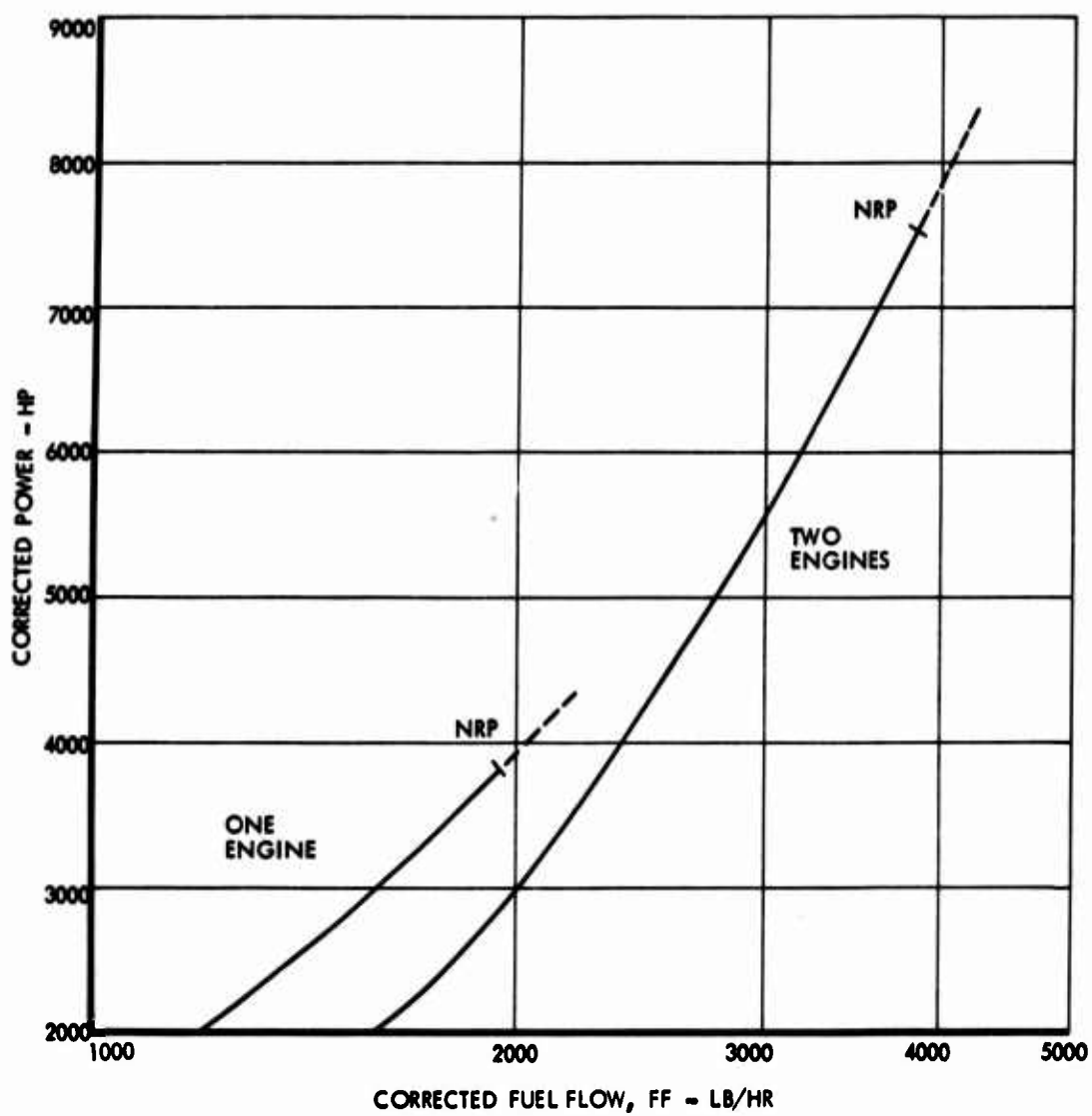


Figure 30. Fuel-Power Relationship, 501-M26 Engine -  
10,000 Feet, Standard Day, 140 Knots

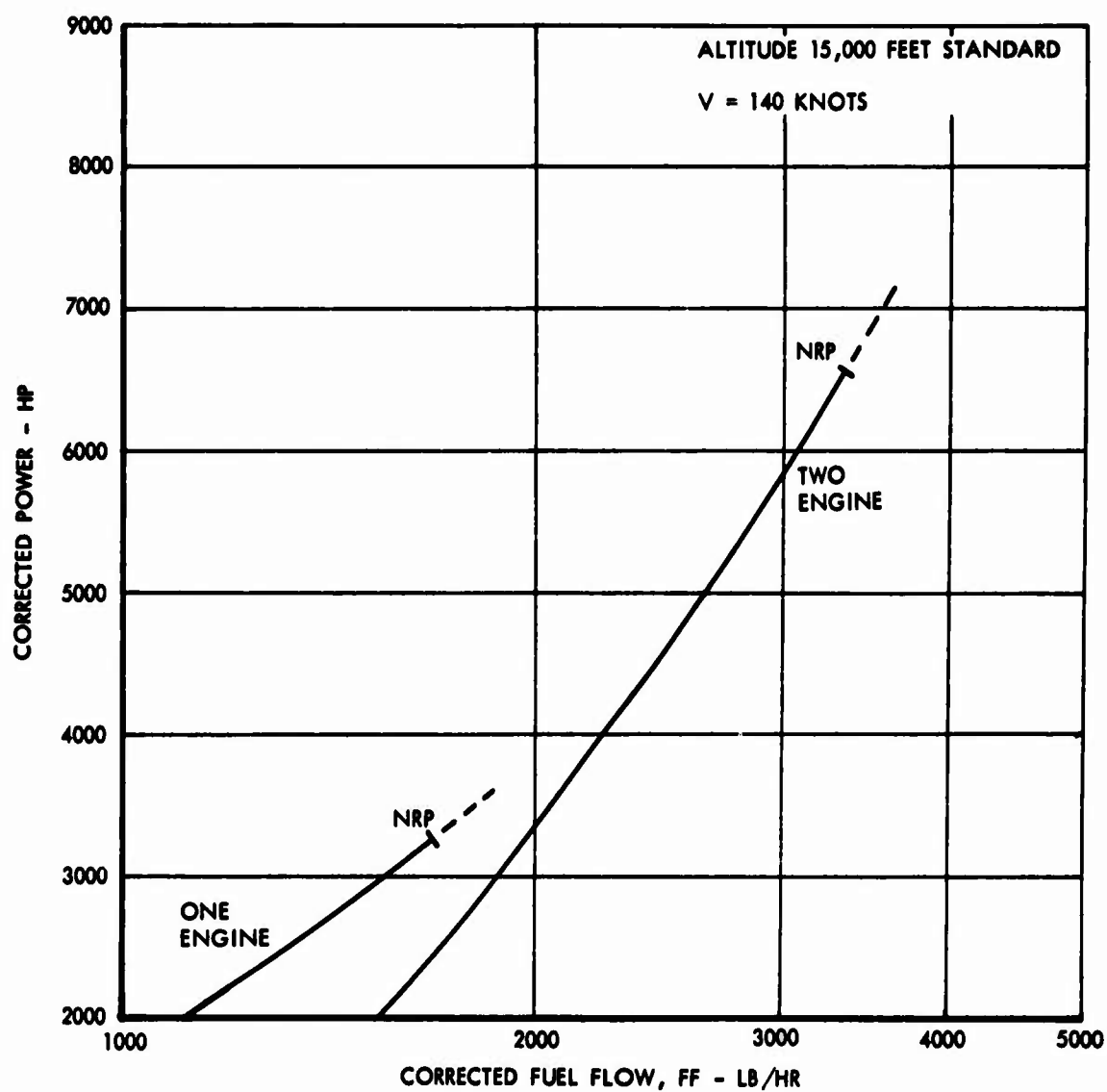


Figure 31. Fuel-Power Relationship, 501-M26 Engine -  
15,000 Feet, Standard Day, 140 Knots



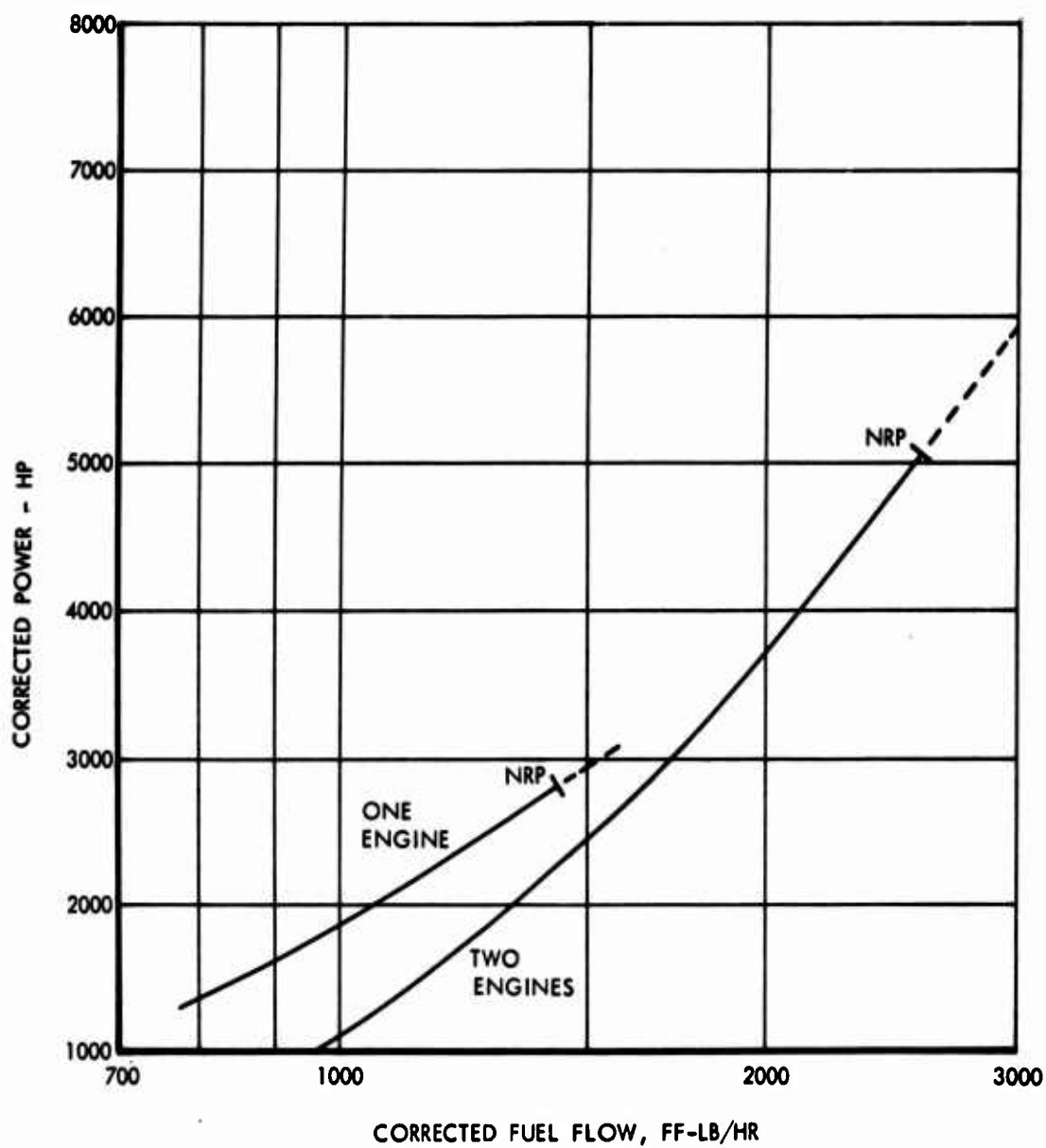


Figure 32. Fuel-Power Relationship, 501-M26 Engine -  
20,000 Feet, Standard Day, 140 Knots

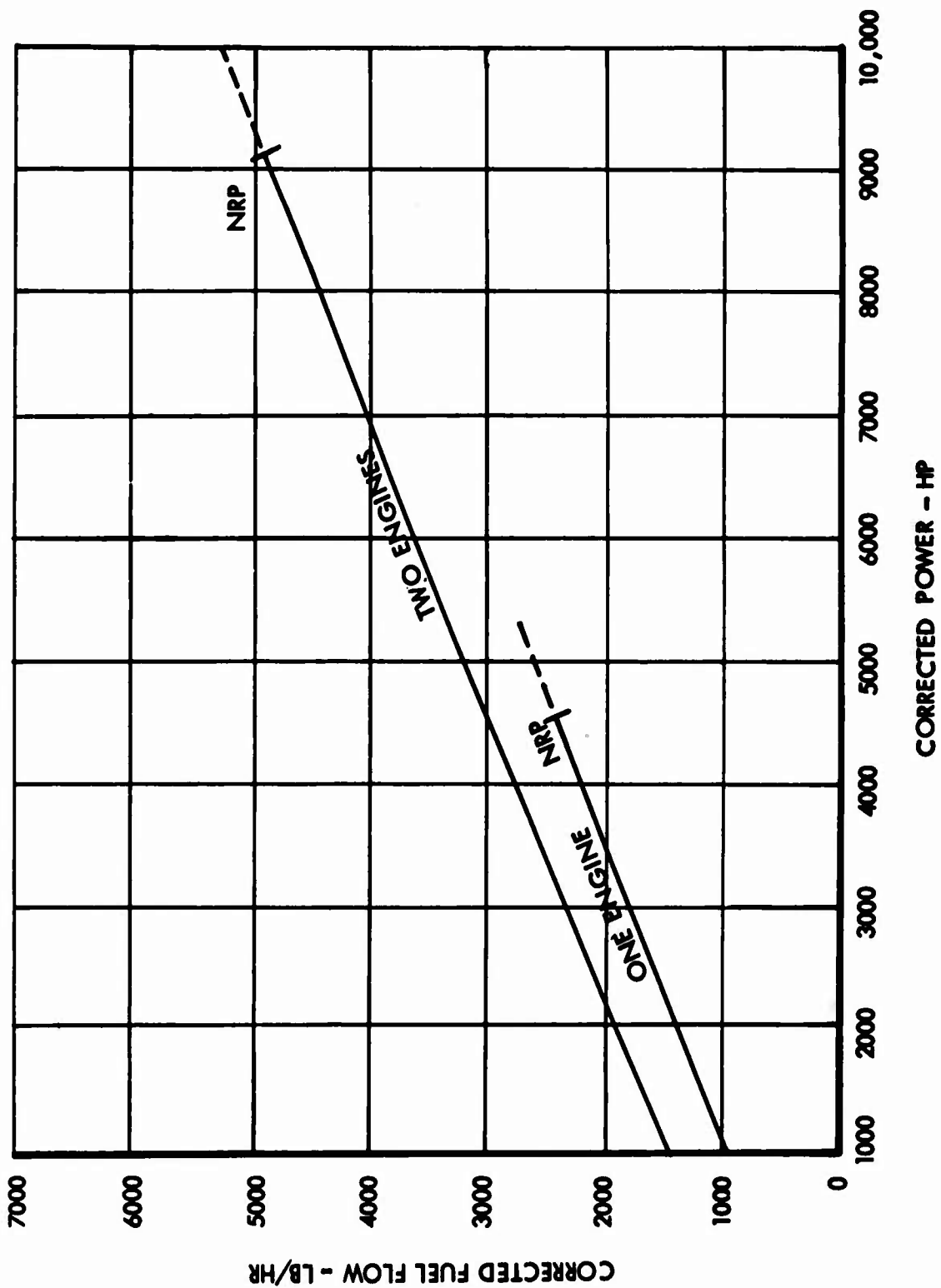


Figure 33. Fuel-Power Relationship, 501-M26 Engine - Sea Level Standard Day, Hover

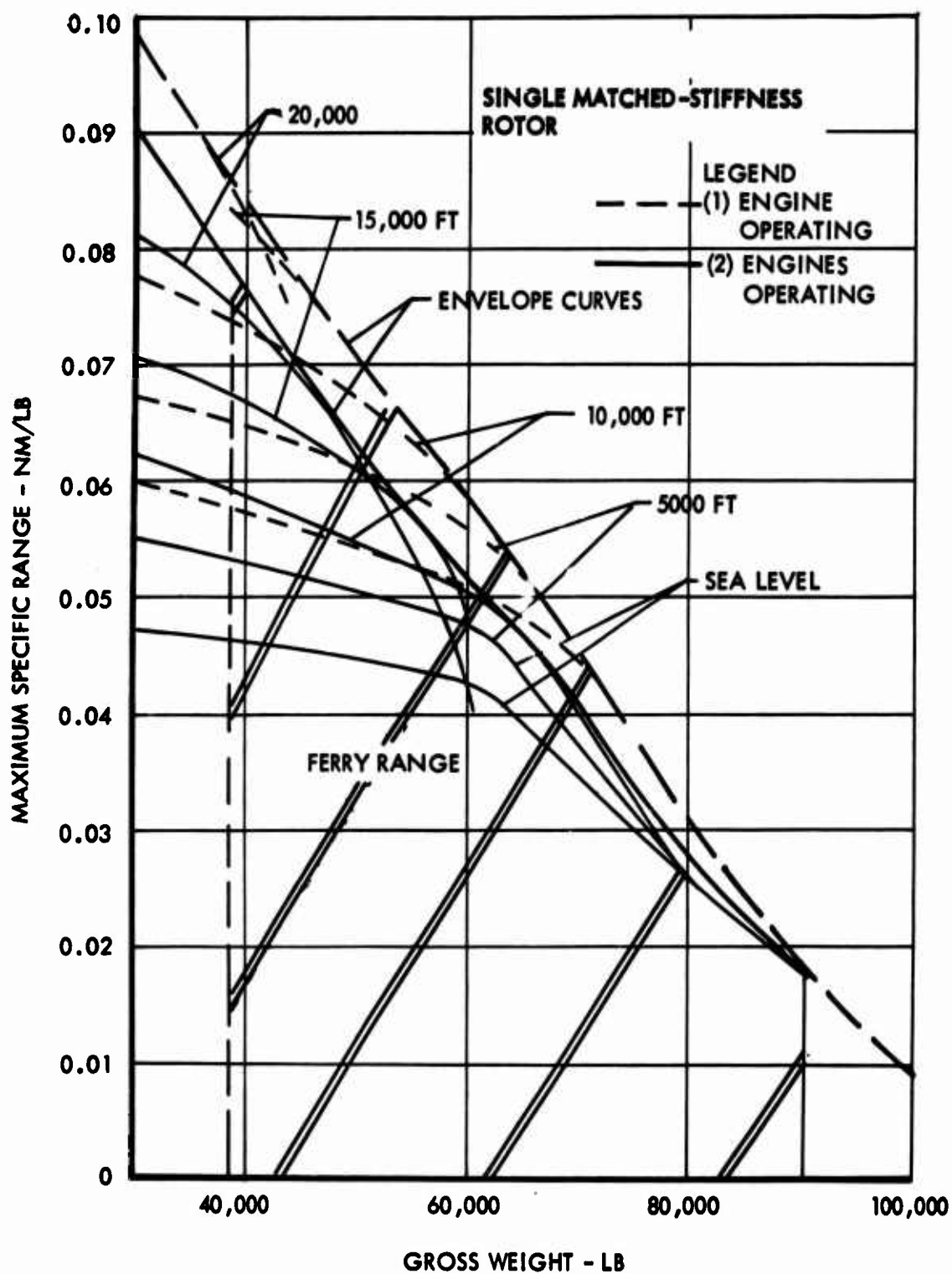


Figure 34. Ferry Range, Two 501-M26 Engines, Standard Day

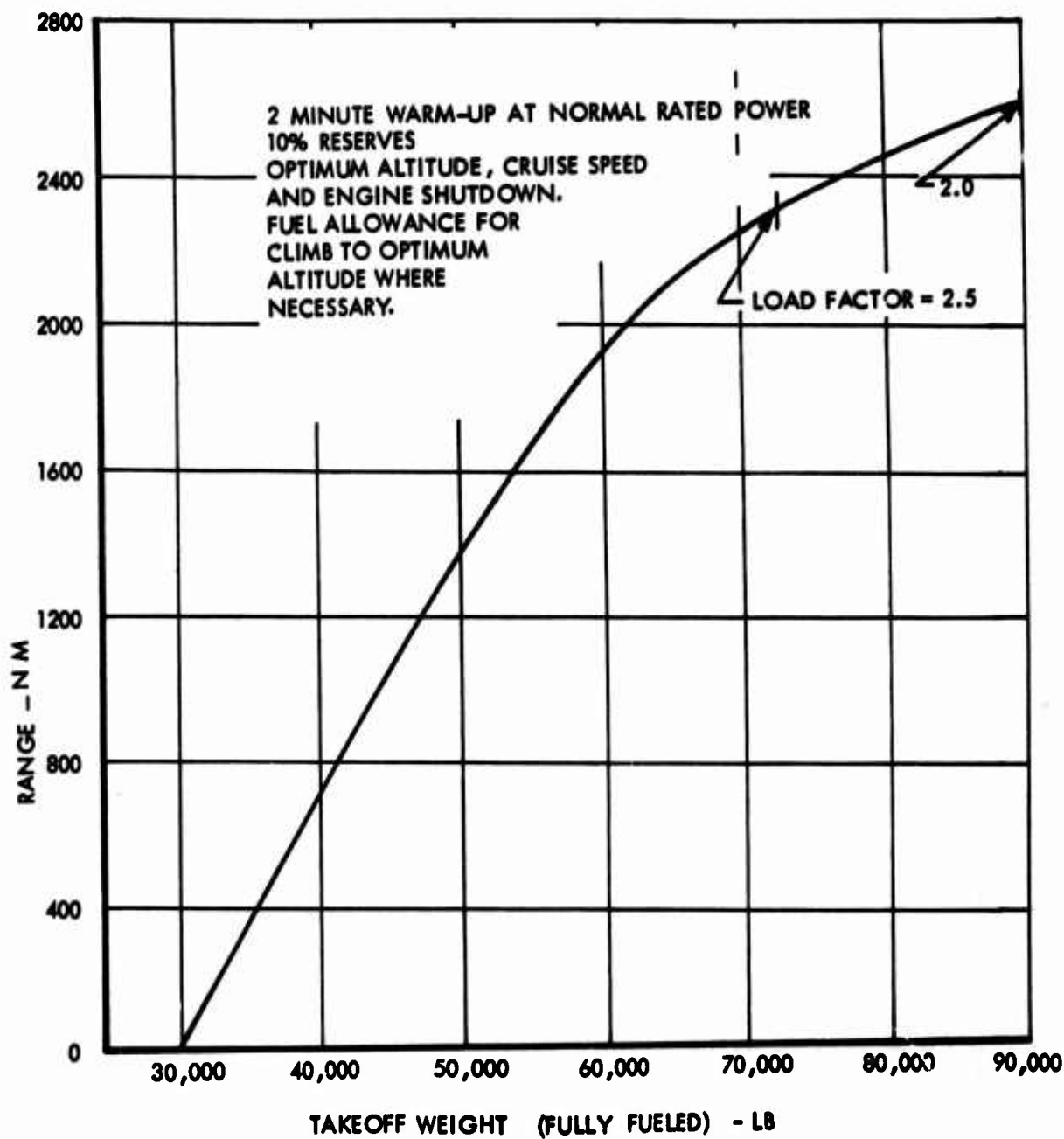


Figure 35. Takeoff Weight vs Range for Matched-Stiffness Single-Rotor System, Standard Day,  $f_0 = 80$  Square Feet

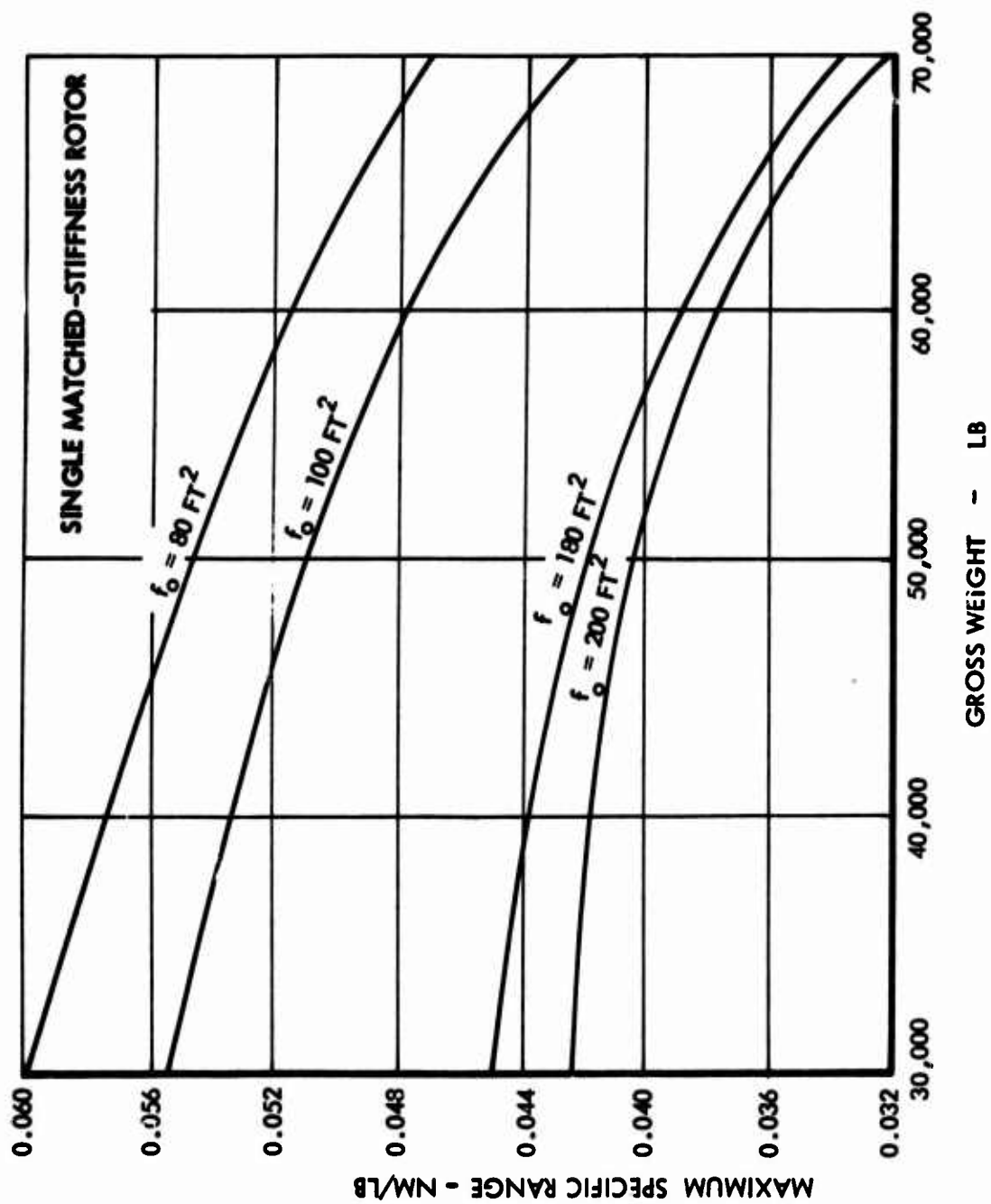


Figure 36. Weight - Maximum Specific Range Relationships - One 501-M26 Engine, Sea Level Standard Day

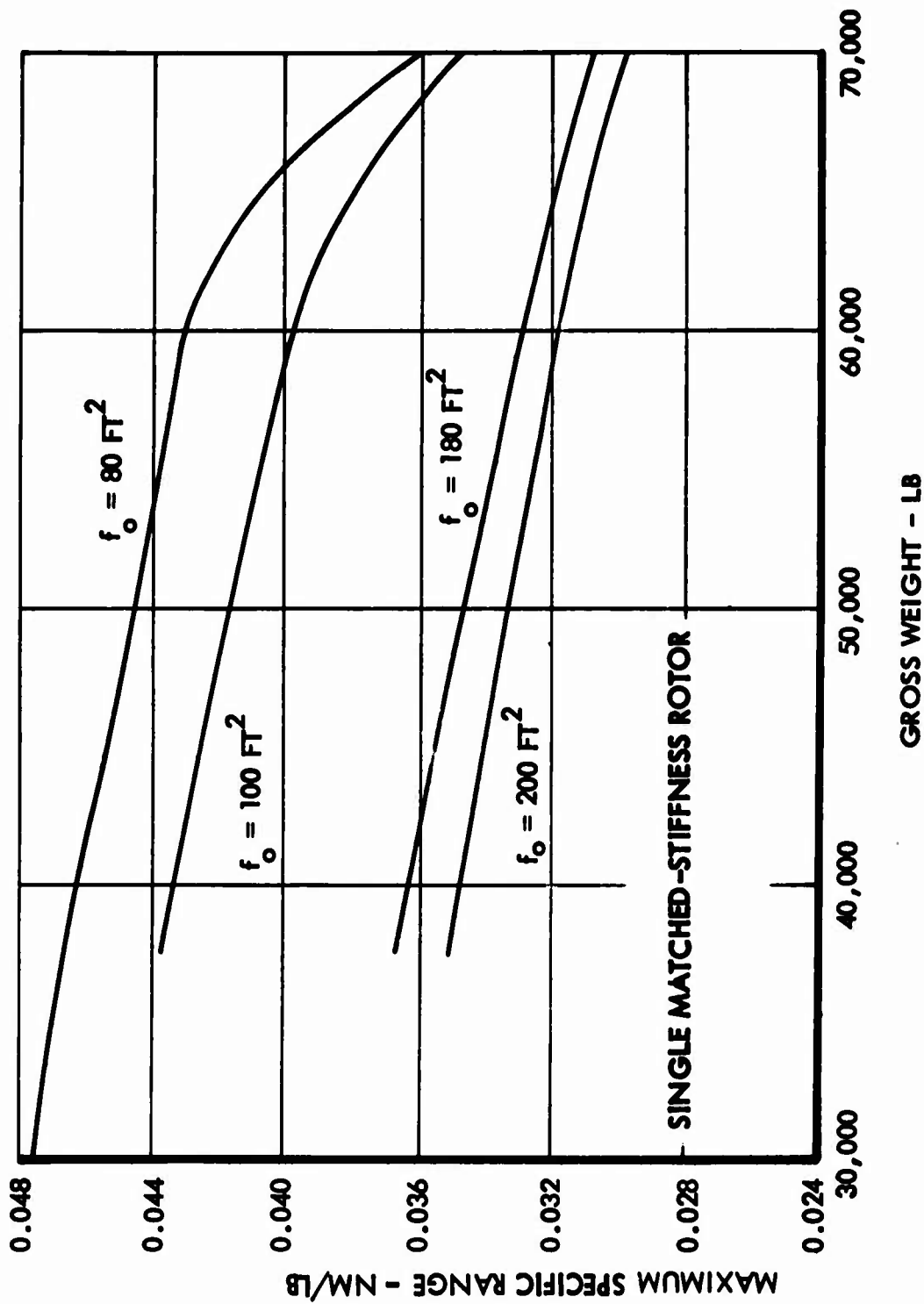


Figure 37. Weight - Maximum Specific Range Relationships - Two 501-M26 Engines, Sea Level Standard Day

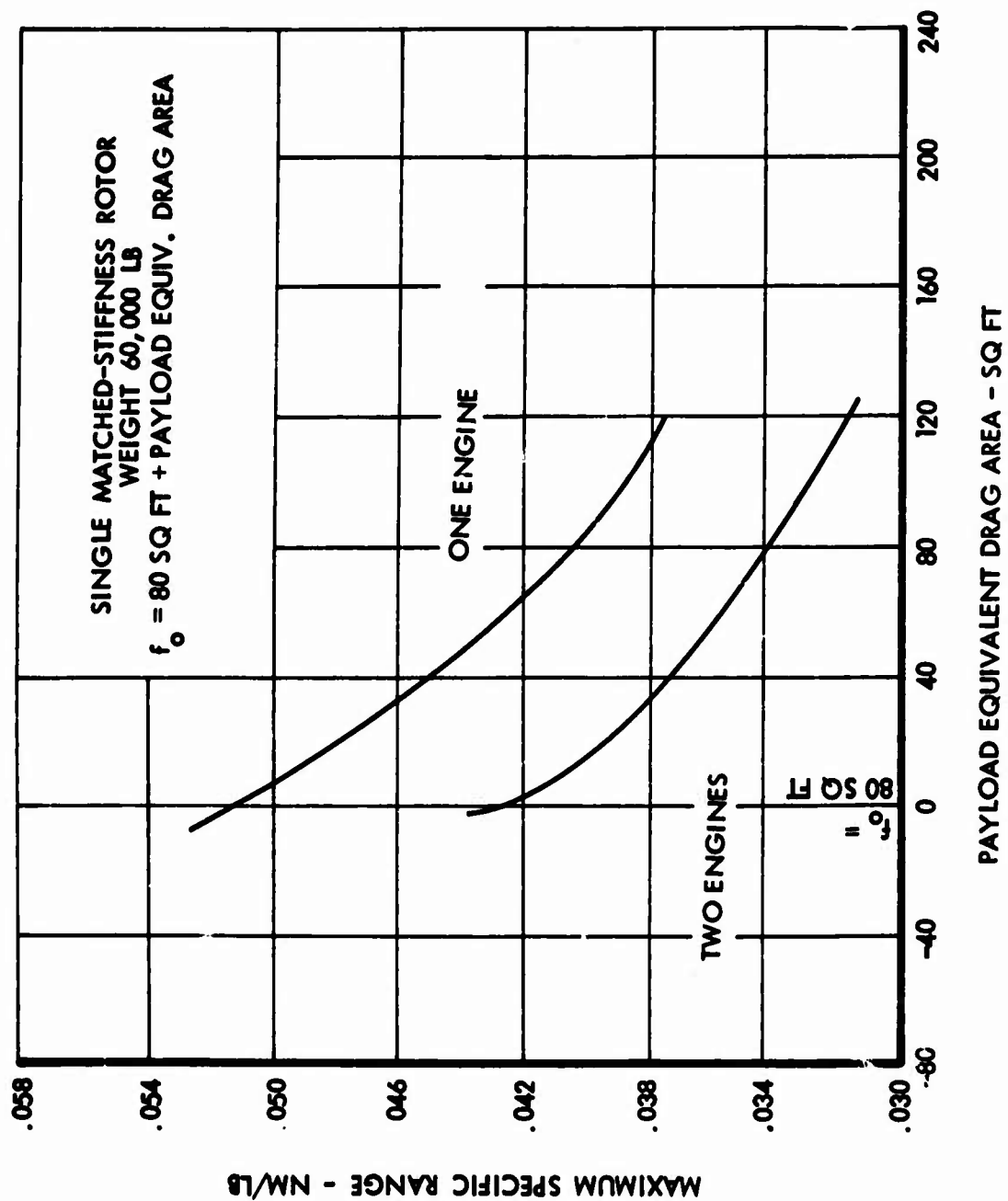


Figure 38. Maximum Specific Range - Payload Equivalent Flat Plate Area, 501-M26 Engine, Sea Level Standard Day

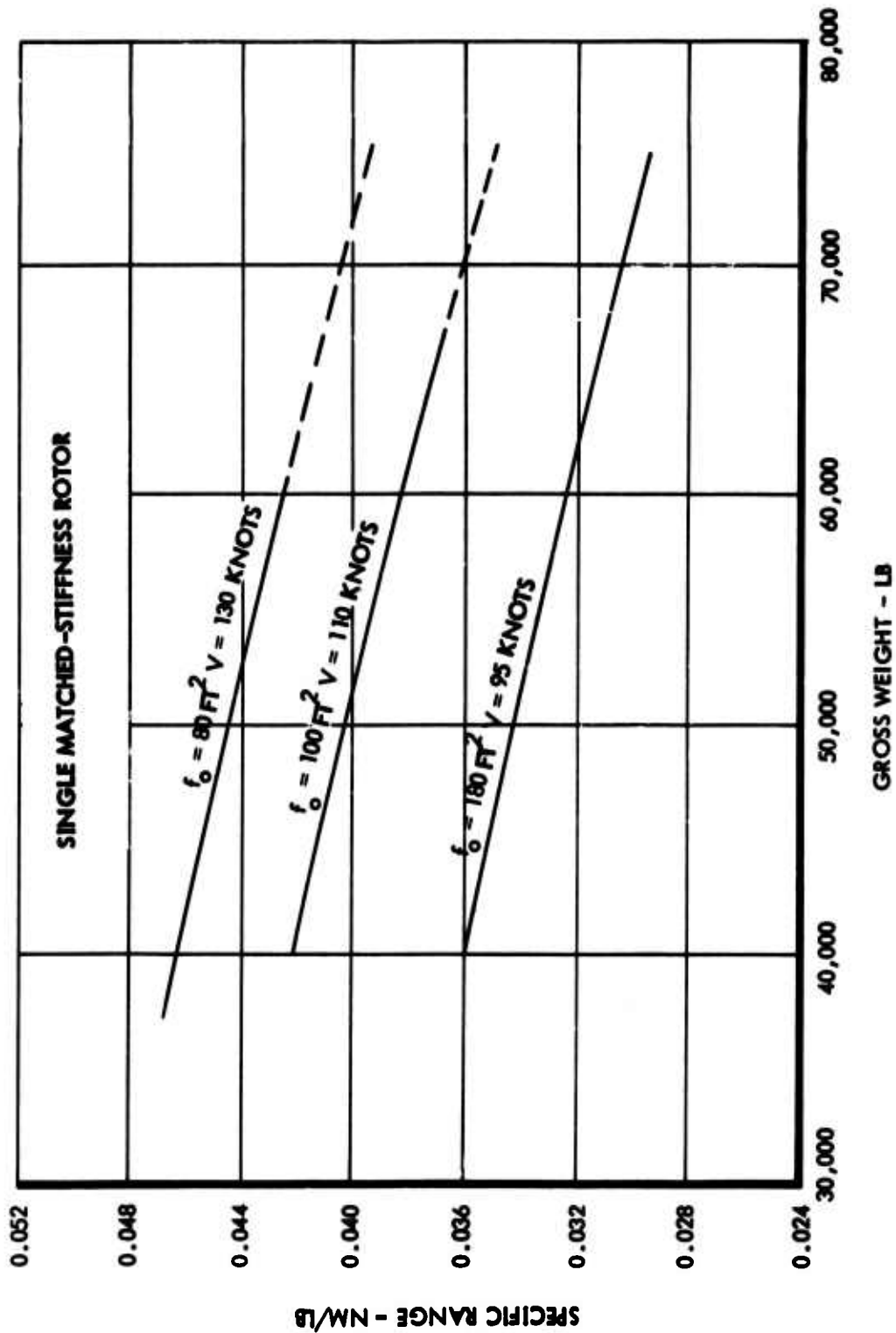


Figure 39. Specific Range for Standard Mission Conditions - Two 501-M26 Engines,  $\Theta_1 = -5$  Degrees



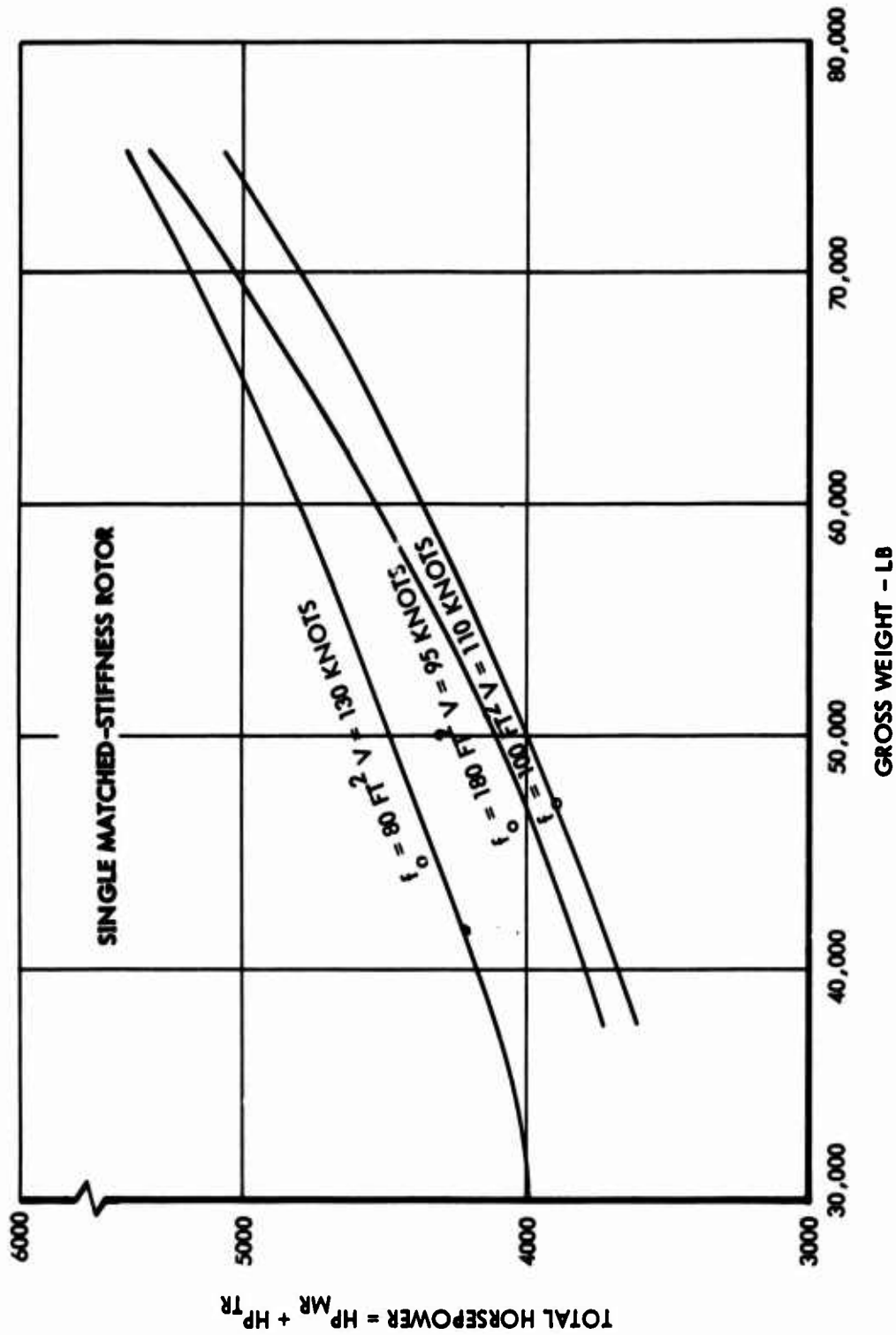


Figure 40. Power Requirements for Standard Mission Forward Flight Conditions,  $\Theta_1 = -5$  Degrees

The fuel flow rates thus obtained were combined with the corresponding velocities to determine the equation for the mission radius, RM. This RM, with a given amount of fuel, can be derived from the following relationship:

$$\left(\frac{RM}{\frac{NM}{LB}}\right)_{out} + \left(\frac{RM}{\frac{NM}{LB}}\right)_{in} = W_{F3} + W_{F5}$$

Solving for RM gives:

$$RM = \frac{\left(\frac{NM}{LB}\right)_{out} \left(\frac{NM}{LB}\right)_{in} (W_{F3} + W_{F5})}{\left(\frac{NM}{LB}\right)_{out} + \left(\frac{NM}{LB}\right)_{in}}$$

where

$W_{F3}$  = fuel weight for a standard mission outbound leg

and

$W_{F5}$  = fuel weight for a standard mission inbound leg

The results of using this equation are shown in Figure 41 which gives mission range for several outbound and inbound speeds, and two values of flat plate area for the outbound and inbound legs.

To determine the effect of speed and flat plate area on the payload that can be carried on standard transport and heavy-lift missions, an expression relating the change in payload to the change in fuel weight and accounting for reserves and tankage was used:

$$\Delta PL = - \frac{(\Delta W_{F out} + \Delta W_{F in})}{0.90} \quad (1.075).$$

The change in fuel,  $\Delta W_{F out}$  and  $\Delta W_{F in}$ , from the standard mission fuel weights, was determined from specific range curves for the weights, speeds and flat plate areas studied. The results are shown in Figure 42 which gives payload for several outbound and inbound speeds and for two values of flat plate area for the outbound and inbound legs.

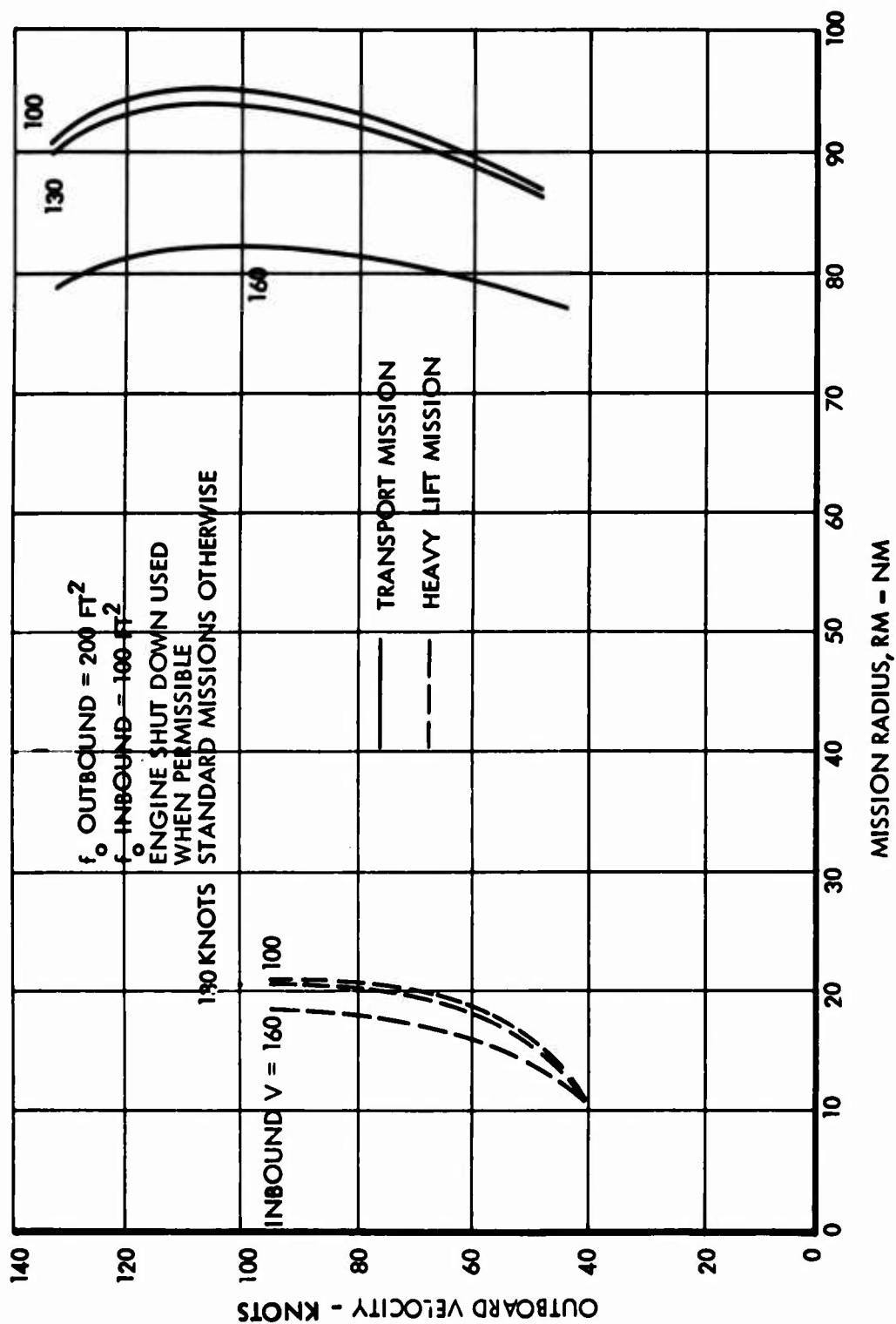


Figure 41. Effect of Cruise Speed On Mission Radius

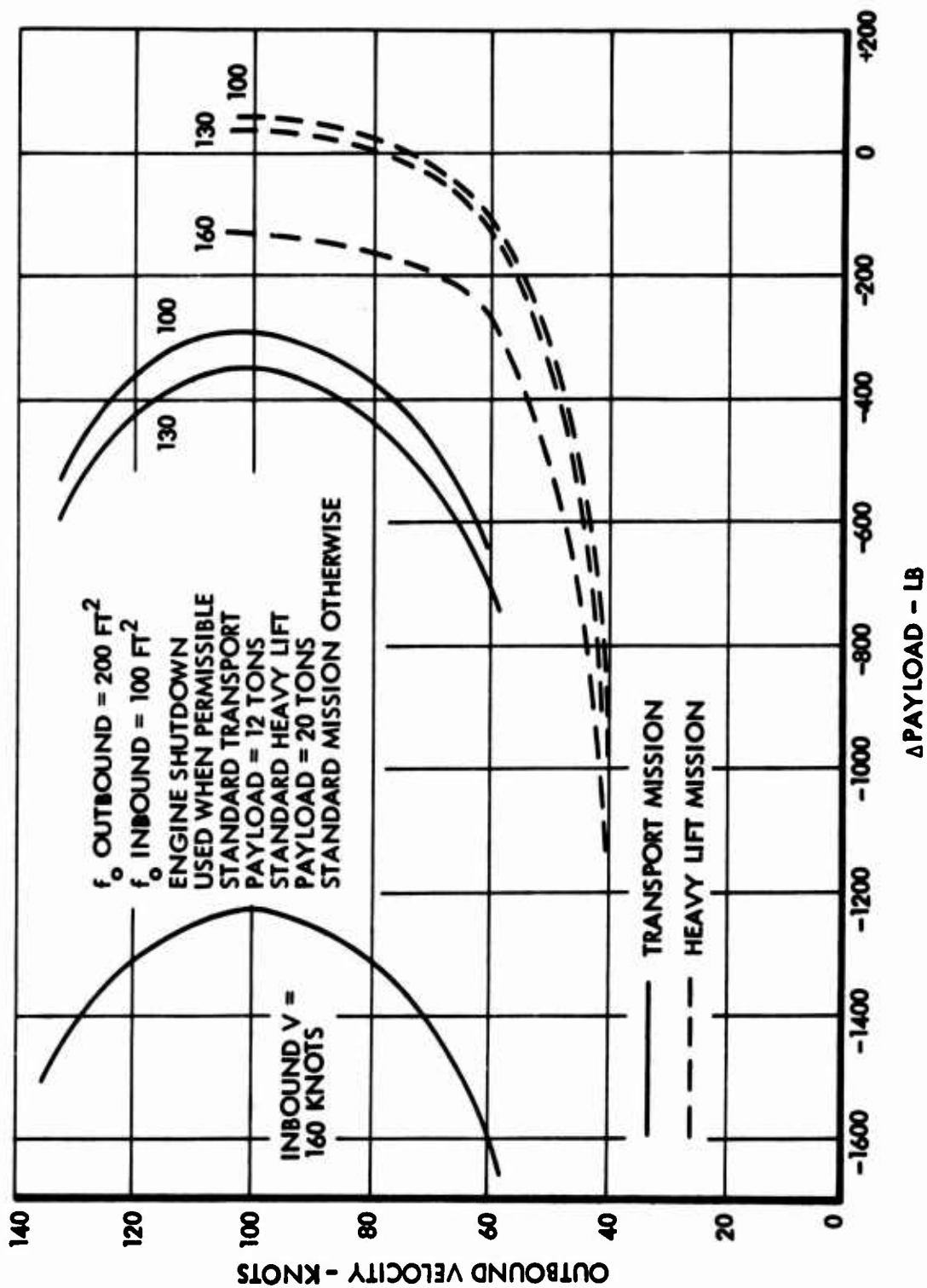


Figure 42. Effect of Cruise Speed On Payload

### Maximum Speed Limits

The maximum speed as affected by the equivalent drag area of the payload was determined and is shown in Figure 43. The maximum speed is limited by power available, retreating blade stall, or blade loading limit, whichever comes first. The power limits and requirements are shown in Figures 44 and 45.

### Hover Performance

The hovering ceiling as a function of gross weight is shown in Figure 46 for both standard day and 95°F day conditions. Both out-of-ground-effect and in-ground-effect hovering performance at the military rating of the two 501-M26 engines are shown. The in-ground-effect performance is based on a wheel height of 10 feet and uses the ground effect relationships plotted in Figure 5-13 of Reference 12. The power available from the engines as a function of altitude and temperature is shown in Figure 47.

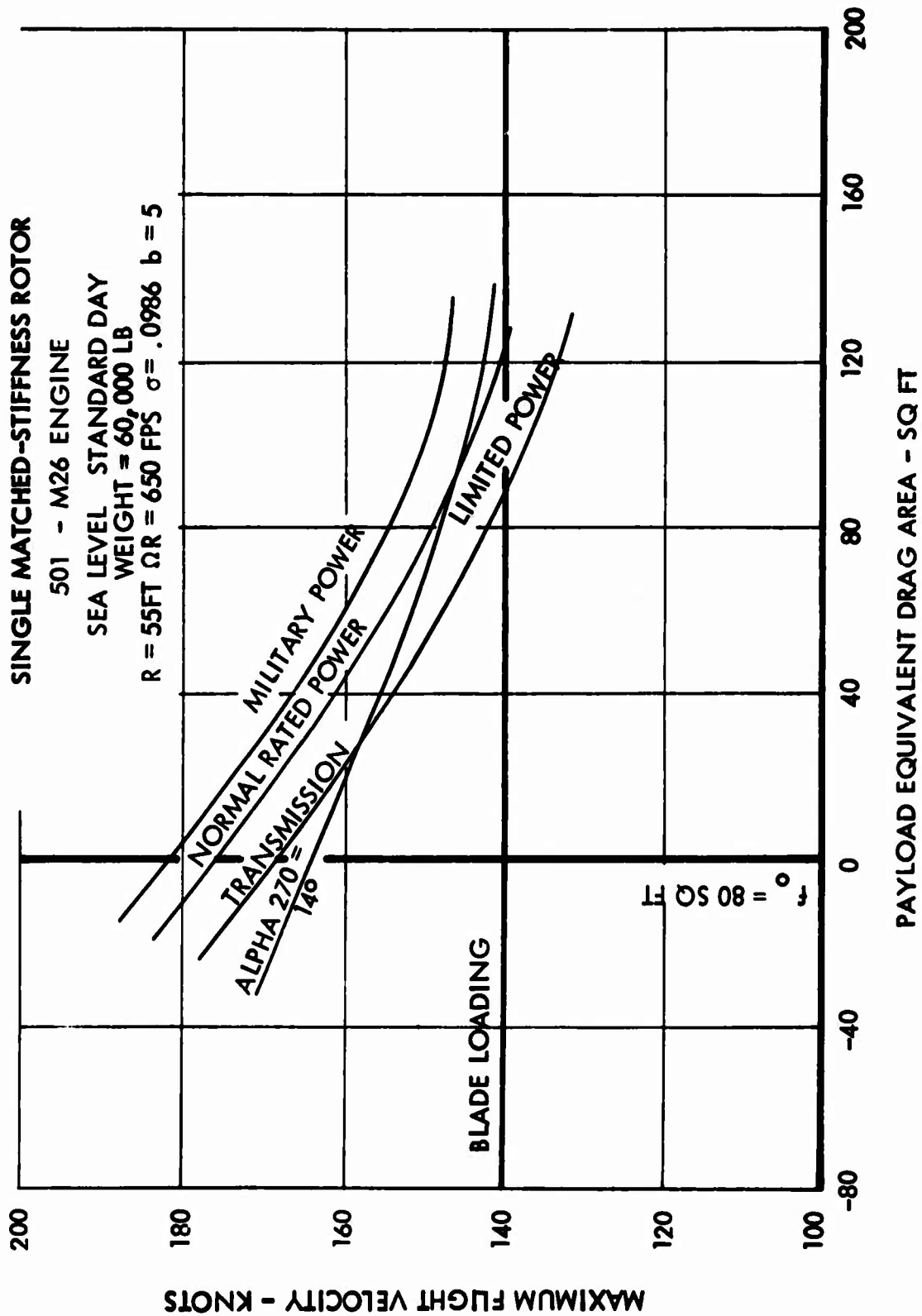


**Figure 43. Effects of Power Limits, Stall Limits, and Payload Equivalent Drag Area on Maximum Speed - Maximum Speed vs Payload Equivalent Drag Area**

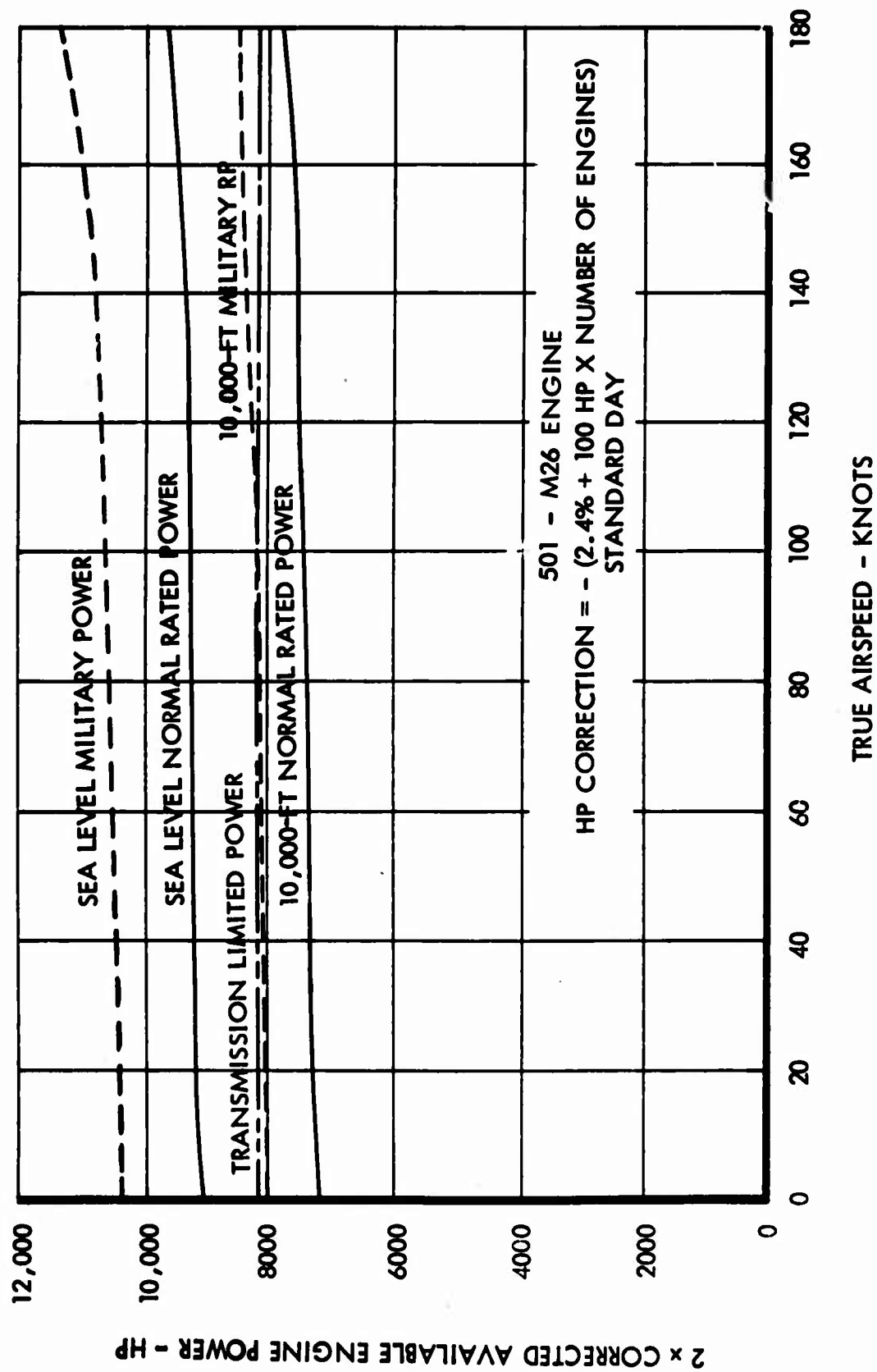


Figure 44. Corrected Available Engine Horsepower vs True Airspeed

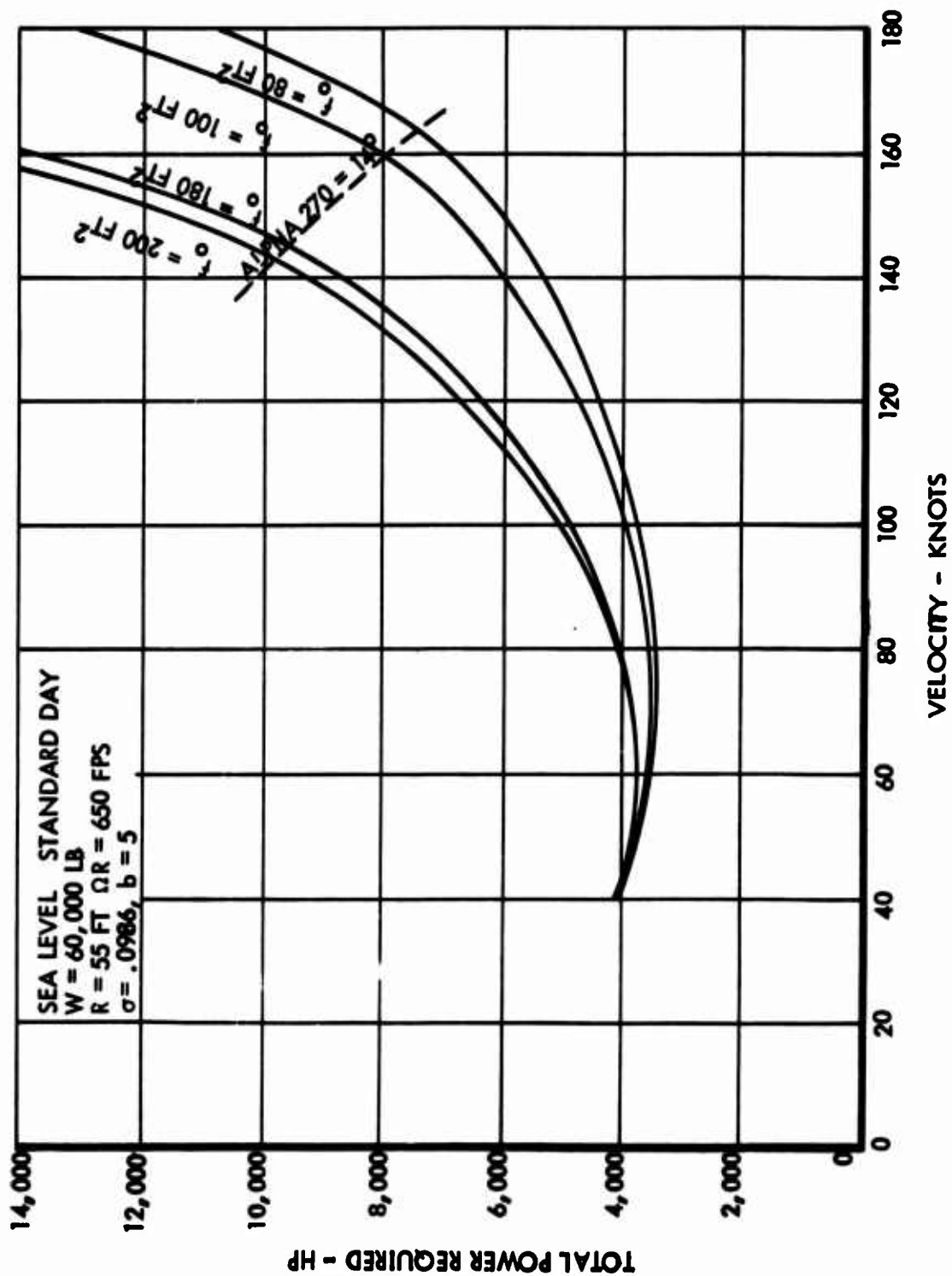


Figure 45. Effects of Power Limits, Stall Limits, and Payload Equivalent Drag Area On Maximum Speed - Velocity vs Total Horsepower Required



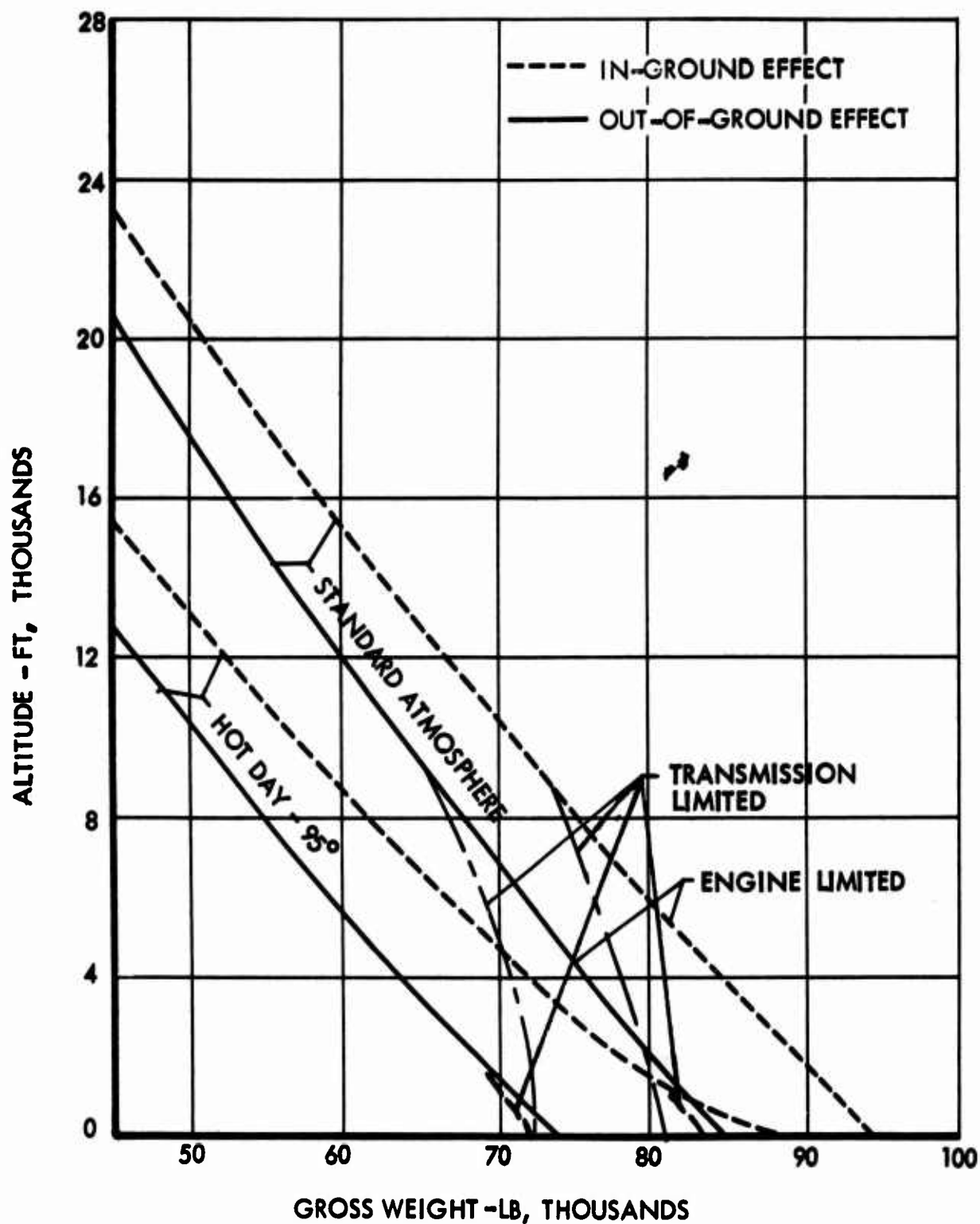


Figure 46. Hover Limits for Matched-Stiffness Single-Rotor Helicopter -  $\Theta_1 = -5$  Degrees

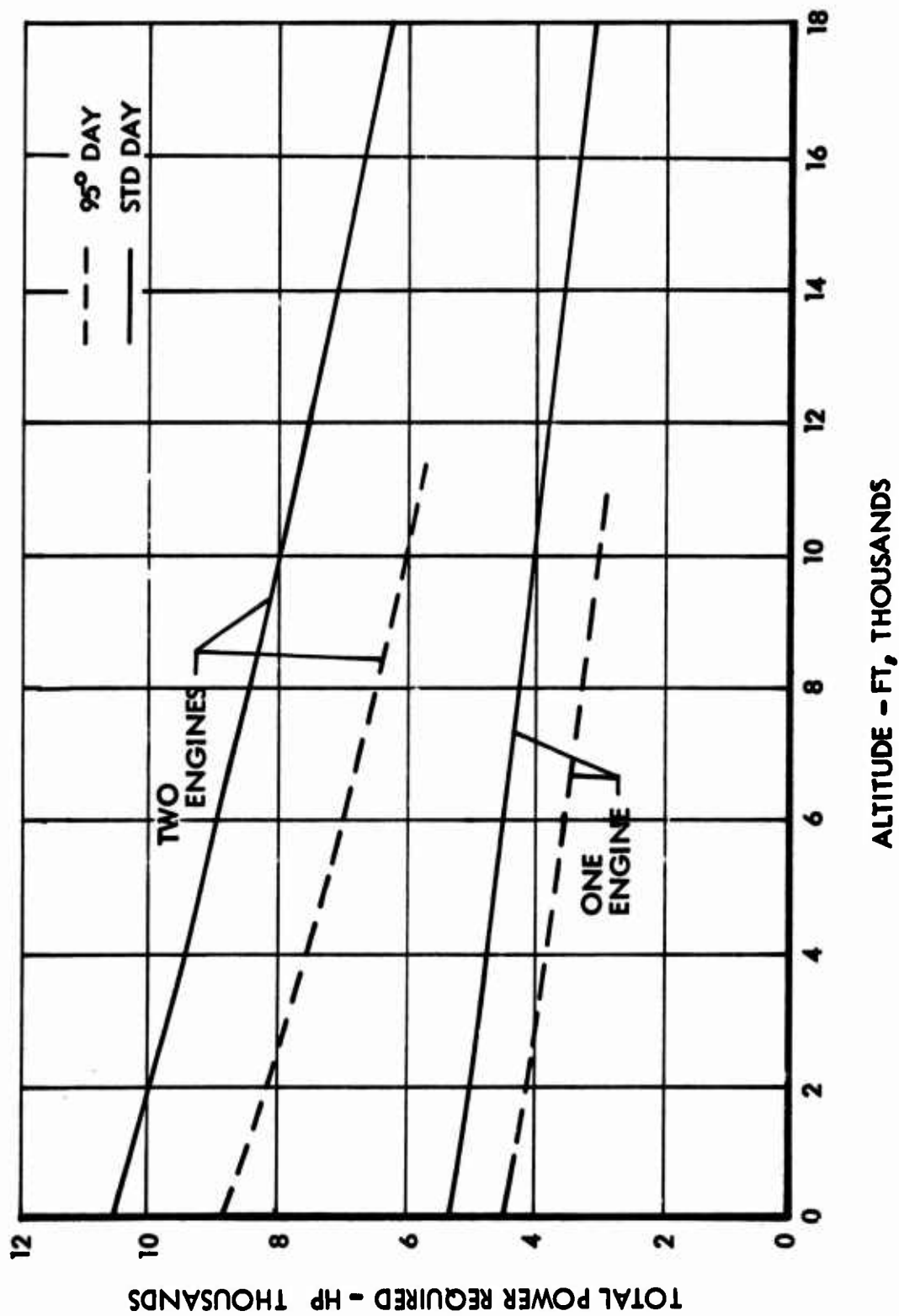


Figure 47. Maximum Hover Power - 501-M26 Engine

## SECTION 2

### DESIGN LAYOUT

#### INTRODUCTION

The design study, based on the rotor system characteristics resulting from the parametric study of Section 1, covers the design for:

- Blade and hub geometry
- Blade retention configuration
- Flight control configuration
- Rotor/propulsion system general arrangement
- Helicopter general arrangement

The configuration selected is a single-rotor with a matched-stiffness, flexure-hub-type rigid rotor. Various types of flexure, hub, and blade designs were studied and layouts were made. Detailed descriptions of these designs are presented in the following sections.

#### DESIGN CRITERIA

The preliminary design of the heavy-lift helicopter rotor system was based on the design criteria set forth in the following paragraphs.

##### Basic Characteristics

The vehicle and rotor design characteristics used for the design study are:

Design gross weight, lb	72,300
Disc loading, psf	7.62
Tip speed, fps	700

Rotor diameter, ft	110
Rotor solidity	0.0986
Rotor blade loading, psf	77
Number of blades	5
Blade airfoil	NACA 0012 or NACA 63015
Blade chord, in.	41
Blade twist	-5°

The design study utilized a tip speed of 700 fps although the parametric study resulted in a tip speed of 650 fps. Figure 12 indicates that there would not be a gross weight difference between these two tip speeds. The tip speed change did not affect the other rotor parameters because they were established by the blade-loading limit rather than the aerodynamic optimum. This relationship can be seen in Figure 11. Since the rotor weight decreases with increased tip speed, it was felt that it would be more economical to reduce the rotor system weight at the expense of adding the equivalent weight into the propulsion system.

#### Operational Considerations

The heavy-lift helicopter, hovering in close quarters to pick up or to place an external cargo load, has a need for both the high-damping and the high-control power in pitch and roll that are inherent in the Lockheed rigid-rotor concept. These qualities must not be compromised to ease the design requirements of a very large rigid rotor. One way to ensure that the heavy-lift helicopter will have the same handling qualities demonstrated by the XH-51 is to set the required rotor stiffness on the shaft at least as high as it would be if the XH-51 were scaled up from a 35-foot-diameter to a 110-foot-diameter rotor.

The rotor stiffness,  $K_B$  (foot-pounds/radian), would scale with the cube of the scale factor  $(110/35)^3 = 31.0$ . The XH-51 rotor stiffness is approximately 90,000 foot-pounds/radian. Therefore, HLH rotor stiffness should be not less than  $2.79 \times 10^6$  foot-pounds/radian.

The productivity in ton-miles per hour of a short-range vehicle like the HLH is highly dependent on loading and unloading speed. Allowable center-of-gravity range is not a problem if the load is suspended externally from a single point at the heavy-lift helicopter center of gravity. However, if the cargo is attached at multiple points or placed inside the fuselage or in a cargo pod, the center-of-gravity range must be sufficiently wide to prevent losing loading time because of a

requirement for very careful positioning of the cargo center of gravity. For the design study, a total vehicle center-of-gravity range of 5 feet was selected. This is approximately three times the loading tolerance of a C-130 airplane which has a forward center-of-gravity limit between 16 and 20 percent of the mean aerodynamic chord (MAC = 164.5 inches) and an aft center-of-gravity limit between 26 and 30 percent of MAC, depending on gross weight conditions. With the 5-foot center-of-gravity range, transport payload center of gravity can be located anywhere within a 15-foot range.

### Size Considerations

If the 35-foot-diameter XH-51 rotor were scaled up to a 110-foot-diameter rotor, the lift per blade would increase directly with the blade area or as the square of the scale factor. The centrifugal force per blade for a constant tip speed would increase as the ratio of blade weight to rotor radius  $\frac{W_b}{R}$ . Thus

$$CF = \frac{W_b}{g} R \omega^2 = \frac{V_T^2}{g} \frac{W_b}{R}$$

If the blade design were an exact scale-up of the XH-51, the blade weight would increase with the cube of the scale factor. Centrifugal force would then increase with the ratio of blade weight to rotor radius or the square of the scale factor. Thus the ratio of blade lift to centrifugal force (a function of coning angle) would remain constant as would all blade flapping excursions. The rotor weight fraction or weight-to-lift ratio would increase linearly with the scale factor, and the rotor weight as a percent of gross weight would be 3.14 times greater in the HLH than in the XH-51. Any attempt to design a large lightweight rotor would automatically involve a relative reduction in blade centrifugal force and an increase in coning angle. The coning angle is expressed by the following:

$$\text{Coning angle} = \frac{W}{b \times CF} = \frac{R}{b \frac{V_T^2}{g} \left( \frac{W_b}{W} \right)}$$

Therefore

$$\frac{\text{Coning angle}}{R} = \frac{1}{b \frac{V_T^2}{g} \left( \frac{W_b}{W} \right)}$$

If the blade weight to gross weight fraction  $\left( \frac{W_b}{W} \right)$  is held constant as the blade radius (R) is increased (constant tip speed and number of blades), the coning angle increases linearly with the radius. Scaling from the

XH-51 to the HLH would show a coning angle of 9.4 degrees ( $3.14 \times 3^\circ$ ) for the HLH. However, in the preliminary design of the HLH rotor system, the coning angle was determined to be 7 degrees. This indicates that the blade weight fraction increases as radius increases. This is substantiated by the statistical rotor weight trend equation shown on page 264. This equation indicates that rotor weight increases with the 1.576 power of the radius as opposed to the third power of the radius indicated by direct geometric scaling.

The relatively high rotor stiffness and the large built-in coning angle would greatly alleviate the static droop deflection problem that is characteristic of very large articulated rotors.

Based on the parametric analysis, each blade assembly will be 55 feet long and will weigh approximately 1000 pounds. Blade replacement under field conditions will not be a simple operation. It would be advantageous if the external portions of the blade were removable segments which could be replaced in the field and would cover and protect the primary blade structure from environmental damage.

#### Additional Design Goals

Minimum rotor weight for the selected rotor aerodynamic configuration is the criterion for measuring the relative effectiveness of various solutions to the rotor design problems posed in the preliminary design study.

Consideration must also be given to development, tooling and production costs. For a vehicle of the type and size of the heavy-lift helicopter, the development and tooling costs could be a substantial part of the total cost per vehicle.

Because structural joints are a major source of trouble in rotor development, the number of joints in the primary load path of the blade, flexure, and hub should be held to a minimum. For safety, the primary structural load path should be redundant, so that a crack through any one piece will not be catastrophic.

#### Matched-Stiffness Concept

The matched-stiffness rotor concept was developed by the Lockheed-California Company from a continuing program of rigid-rotor research and development. The principal feature of this concept is that a matched-stiffness flexure hub replaces the hub spindle and feathering bearings associated with the original Lockheed rigid-rotor design. The matched-stiffness flexure hub is a torsionally soft flexure element. The flapping and in-plane stiffness of this flexure are matched. This stiffness-matching results in a fundamental improvement in the servo feed-back characteristics of the Lockheed gyro control system.

In 1962 and 1963, a dynamic model wind tunnel program was funded by USATRECOM\* to explore rigid rotor dynamics in general, and the matched-stiffness concept in particular. This program is reported in TRECOM Technical Report 63-75, "Investigation of Elastic Coupling Phenomena of High-Speed Rigid Rotor Systems," June 1964 (Reference 13).

In December 1962, seven rotor configurations were tested in the Langley Full Scale Wind Tunnel up to the 127-mph maximum simulated speed available in that tunnel. In May 1963, two of these configurations were tested in the controlled atmosphere of the Langley Transonic Dynamics Tunnel to simulated speeds of 250 mph. Full-scale Reynolds and Mach numbers were obtained. Thus, the model was properly scaled aerodynamically as well as dynamically for small helicopters; however, the Reynolds number was considerably smaller than that for a rotor of the size of the HLH. These tests showed the matched-stiffness type of rotor to be stable with extremely small values of gyro inertia, just as the theory had indicated. In addition, the in-plane oscillating loads at the blade root were reduced by from 70 to 90 percent from those of the stiff in-plane rotor configurations tested.

The rigid-rotor design eliminates lag and flapping hinges in the rotor but requires blade-feathering bearings. It is desirable to remove the last of the hub bearings, i.e., the blade-feathering bearing. The matched-blade type of rotor with its low in-plane stiffness requirements is ideally suited to the design of a torsionally flexible blade root member, which eliminates the need for feathering bearings.

Figure 48 shows the rotor design system which has evolved from the integration of the flexure-hub and stiffness-matching concepts. A slender spar is designed to provide the desired flapping stiffness and identical in-plane stiffness. It has an open cross section of minimum torsional stiffness. The inboard end of the spar is attached solidly to the rotor shaft. This spar becomes part of the blade "D" spar at from 20 to 30 percent of the rotor radius. A tube enclosing this spar or flexure functions as an aerodynamic fairing in addition to serving as the control torque tube for the transmission of feathering moments and blade pitch angles. The outboard end of the torque tube attaches to the blade "D" spar through a flexible coupling which transmits only torsional moments. The root end of the torque tube is supported by a bearing attached to the hub and incorporates a pitch horn with an attachment for the pitch link from the gyro swash plate.

In 1963 and 1964, with the support of USAAVLABS and the cooperation of NASA, a second wind tunnel program was undertaken to examine the dynamics of an optimized matched-stiffness rotor. This program is reported in USATRECOM Technical Report 64-56, "Wind Tunnel Tests of an Optimized, Matched-Stiffness Rigid Rotor," November 1964 (Reference 11).

---

\*Changed to USAAVLABS in June 1965.





Testing was conducted in the controlled atmosphere of the Langley Transonic Dynamics Tunnel in both helicopter and unloaded-rotor flight regimes to simulated speeds as high as 263 mph.

In general, the tests were successful in confirming the feasibility of the matched-stiffness type of rotor. The rotor and control system functioned very much as predicted by theory.

The cyclic in-plane stresses at the root of any blade that does not have lead-lag freedom are a crucial design consideration. The principal oscillating load is the 1/rev differential blade drag load caused by forward velocity of the rotor. One of the basic advantages of the matched-stiffness design is that considerable attenuation of 1/rev in-plane loads is achieved because the first in-plane natural frequency is substantially below the 1/rev forcing frequency.

If the flexure fairing torque tube is considered to be part of the control system, the rotor itself has no bearings, requires no lubrication, has no rubbing surfaces (thereby eliminating wear or fretting corrosion), and has only one structural joint per blade. This single joint which attaches the blade flexure to the shaft can be designed to accomplish blade folding, if required.

Simplifications possible from use of this type of rotor extend to other systems. The elimination of feathering-bearing friction and the gross reduction in gyro size indicate that much larger rigid-rotor helicopters can now be built without resorting to boosting for cyclic controls. Friction in the rotor and control systems results in damping which is undesirable in a gyro control system. However, a spring force or spring stiffness is desirable to tune the feathering natural frequency to 1/rev for best operation of the gyro control system. As such, the elastic torsional stiffness of the flexure is an advantage. Scaling of the control forces from the 10-foot model indicates that it may be feasible in an emergency to fly manually a 100-foot-diameter rotor of this type. Thus, dual-boost system requirements would be eliminated.

Elimination of hub articulation mechanisms allows a drastic reduction in hub size and a corresponding reduction in hub drag. A typical hub fairing radius would be 4 percent of the rotor radius while the rotor maintains a stiffness equal to an articulated rotor with a 12-percent radius flapping hinge offset.

Production cost estimates indicate that to manufacture this new type of rotor will cost approximately one third less than to manufacture previous rigid rotors.

#### DESIGN EVOLUTION

From the functional standpoint, the rotor system can be divided into four component areas, as follows:

- Blade
- Flexure
- Hub
- Torque tube

Basically, the blade configuration evolves from aerodynamic requirements; the blade attachment, hub, and torque tube design evolve from the requirements of the flexure and conform to present design configurations.

### Flexure Evolution

The flexure is by far the most difficult part of this type of rotor to design. The real challenge in this design study was to meet the design requirements without having either high-flexure stress levels or high-flexure weight.

The stiffness of the rotor on the shaft ( $K_B$ ) is

$$K_B = \frac{b}{2} \times CF \times \text{effective flapping hinge offset}$$

where

$b$  = number of blades

$CF$  = centrifugal force/blade

The effective flapping hinge offset dimension is the sum of the hub radial dimension plus a portion of the radial length of the flexure. The portion of the flexure that is effective is a function of the flap bending stiffness of the flexure. In the case where the flexure flap bending deflection curve is a constant radius arc, the effective flapping hinge offset is

$$\text{Offset} = \text{hub radius} + 0.707 \sqrt{\frac{EI_a}{CF}}$$

where

$EI_a$  = flexure flap bending stiffness at the point where the flexure joins the hub.

The centrifugal force is determined by the blade design. Thus, the flexure stiffness ( $EI$ ) level and distribution are the only variables available with which to obtain the desired rotor stiffness. With the selection of a flexure material, the modulus of elasticity ( $E$ ) is fixed.

The radius of curvature ( $R_c$ ) of the flapping deflection shape of the flexure is

$$R_c = \frac{EI}{M}$$

The bending moment ( $M$ ) which the flexure must carry is determined by the gross weight, center-of-gravity travel, and the rotor stiffness. The 1/rev flapwise bending stress ( $f$ ) in the flexure is

$$f = \frac{MC}{I}$$

A constant radius of curvature along the length of the flexure can be obtained by matching the stiffness distribution to the moment distribution. With a constant radius of curvature, bending stress is solely a function of flexure thickness, and a constant thickness flexure will have constant 1/rev bending stress along its length. This is a very efficient arrangement because it works the full length of the flexure material to the same stress level to obtain a given flapping deflection.

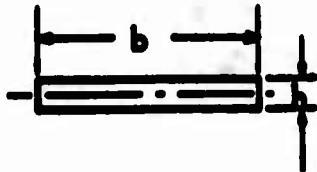
The problem with a constant thickness flexure is that the maximum thickness is determined by the blade thickness where the flexure joins the blade. This thickness usually yields an efficient section at the blade junction where the bending moment, and therefore the moment of inertia ( $I$ ) required, is small. However, the same thickness of flexure adjacent to the hub can result in an impossible situation if the moment of inertia required is greater than can be obtained with a flat plate. Even if the flap plate is possible, it is not efficient from the weight standpoint.

The condition for holding constant bending stress along the beam is that the flexure thickness ( $h$ ) to radius of curvature ( $R$ ) ratio must be constant and, therefore, the stress is a function of  $\frac{h}{R}$ . This says that the flexure thickness can vary along the length of the flexure if the deflection radius is varied in the same way. The radius of curvature can be varied by adjusting the moment of inertia distribution to make the inboard portion of the flexure stiffer and the outboard portion softer. Thus, less of the flapping deflection will occur inboard and more outboard. The weight efficiency is improved because the flange material is still uniformly stressed while the inboard flexure cross section can be more efficient section than a flat plate because of its increased depth. The taper in depth of the flexure also reduces shear in the webs.

#### Flexure Weight Efficiency

In a flapping sense, the flexure is a spring designed to give a desired rotor stiffness while transmitting blade loads to the shaft at reasonable stress levels. It is usually a rather soft spring carrying

large loads and/or large deflections. Because of this, the hub flapping flexure has usually evolved into a flat plate cross-sectional shape as shown.



The weight of this type of section in pounds per inch of length will be derived in terms of the material properties (E), allowable stress (S), and density ( $\rho$ ).

It is assumed that a flapping stiffness (EI) has been determined and must be held constant and that the flap bending moment (M) will remain constant since the flapping stiffness is constant and hence, the bending stress is constant. Therefore

$$EI = K,$$

$$\text{from } S = \frac{MC}{I} \text{ and } C = \frac{h}{2}$$

$$I = \frac{MC}{S}; \quad K = \frac{EMh}{2S}; \quad h = \frac{2SK}{EM}$$

$$\text{from: } I = \frac{bh^3}{12} = \frac{K}{E}$$

$$b = \frac{12K}{Eh^3}$$

$$\text{Weight in lb/in.} = b \times h \times \rho$$

$$\text{Wt/in.} = \frac{12K\rho}{Eh^3} = \frac{12K\rho E^2 M^2}{E^4 S^2 K^2} = \frac{3\rho E M^2}{S^2 K}$$

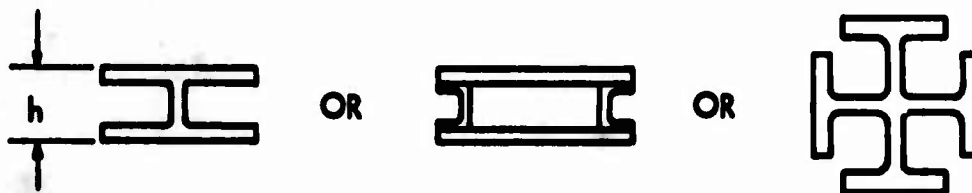
Since  $3$ ,  $K$  and  $M$  are constants,

$$\text{Weight in lb/in.} = f \left( \frac{\rho E}{S^2} \right)$$

Thus, the best flexure material is one with a low density ( $\rho$ ), low modulus of elasticity (E), and high allowable stress (S). The allowable stress is particularly important, as it is a squared term in the equation.

Basic flat plate shapes are inefficient for carrying bending loads. Since  $h = f \left( \frac{S}{E} \right)$ , the use of low modulus of elasticity materials and/or

higher allowables would permit the height to increase and allow the use of more efficient flexure shapes, such as the following:



Since the allowable stress ( $S$ ) in the above equation is the average stress in bending, the form factor weight efficiency of a flat plate is:

$$\frac{(S_{max})^2}{\left(\frac{S_{max}}{2}\right)^2}$$

or only 25 percent. In contrast, an "I" beam with a flange thickness to section depth ratio of 1/10 has a form factor weight efficiency of approximately 80 percent.

#### Flexure Weight Tradeoffs

If the varying radius deflection shape stiffness distribution is used, it is possible to use an efficient cruciform cross section over the whole length of the flexure. This section is also matched in stiffness and torsionally soft over its whole length. Stiffness distribution was developed to give the required rotor stiffness, and five flexure designs were developed. Two designs are in titanium alloy and three are in stainless steel. Each design has a different cross-sectional height and therefore a different bending stress level. This bending stress level was held constant for each design between station 40 and station 133.

The weight of each design is represented by a horizontal line in Figure 49. Each design represents a variety of stress levels corresponding to a variety of center-of-gravity offset values for the vehicle. Therefore, lines of constant stress level versus center-of-gravity offset are shown.

The stress shown is the total alternating flapping stress in the flexure. The flight condition is 95 knots at a heavy-lift mission gross weight of 72,300 pounds.

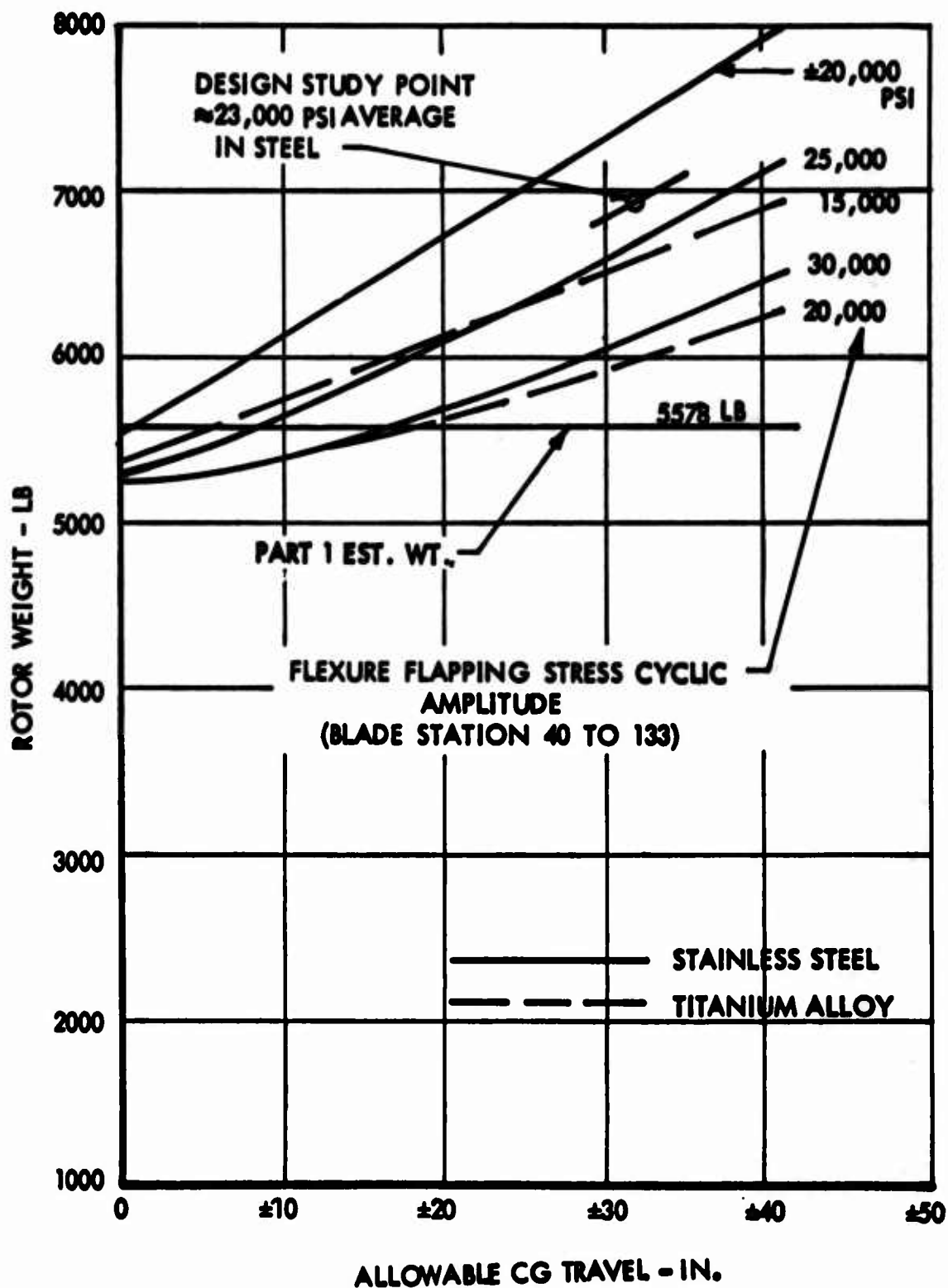


Figure 49. Rotor Weight vs Center-of-Gravity Travel and Flexure Stress

This family of stress curves covers approximately the whole area for which the cruciform cross section is applicable to the HLH. Thus, it is not possible to extrapolate the data presented to substantially higher or lower stress levels. At lower stress levels, the cruciform must be abandoned in favor of the flat plate, and flexure weight will increase rapidly. At higher stresses, the flexure depth becomes awkwardly large, too much material goes into shear webs, and flange stability becomes a problem.

### DESIGN DESCRIPTION

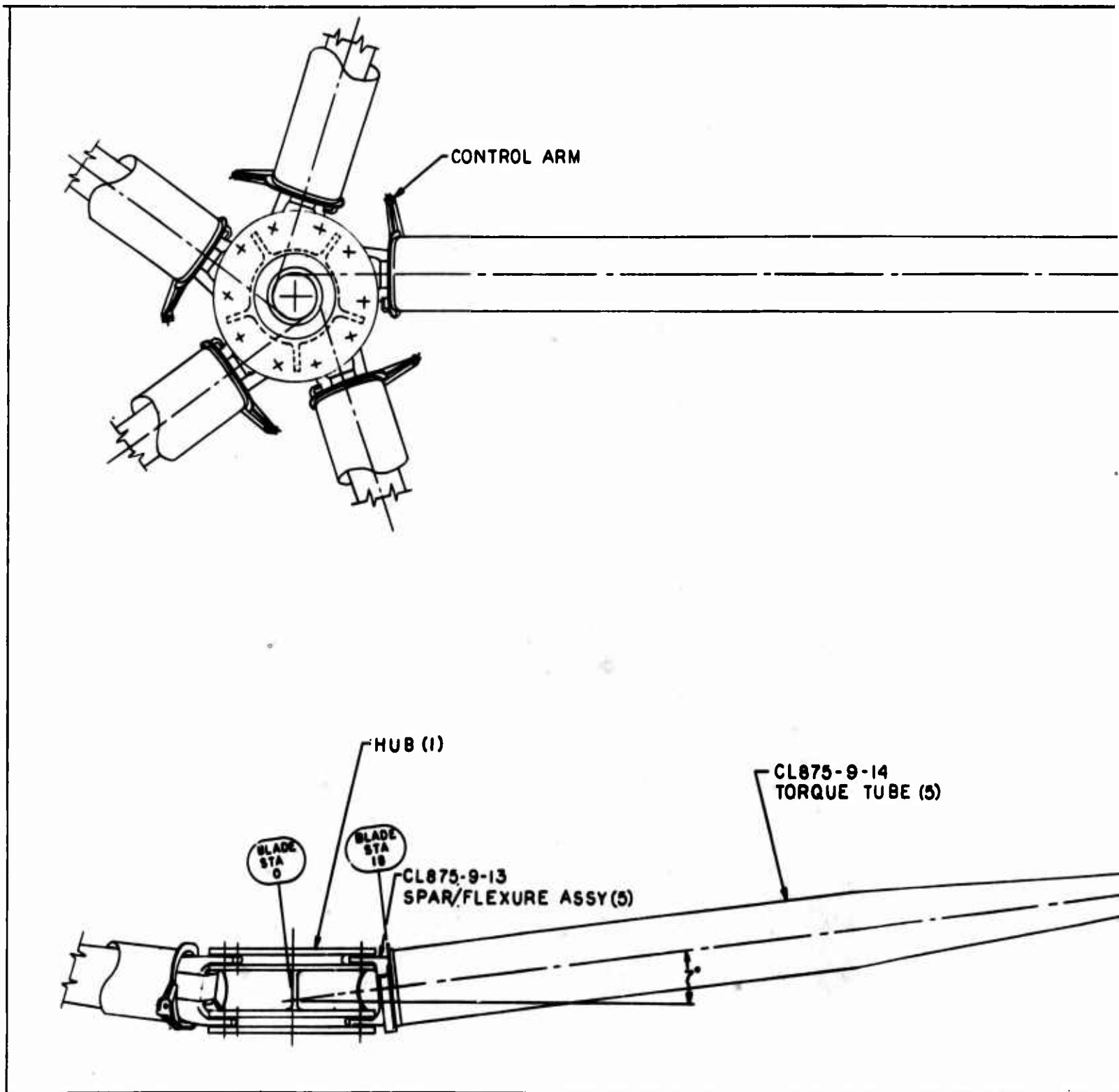
A detail description of the components of the matched-stiffness rotor configuration is presented in the following paragraphs and is shown in Figure 50.

#### Blade

The primary rotor blade construction as shown in Figure 51 is a segmented type (nose and trailing-edge integral unit) installed around a square tabular spar extending from 25 to 100 percent of the rotor radius. The segmented construction is slightly heavier than the continuous type of blade construction frequently used on smaller blades. The weight penalty of approximately 300 pounds per helicopter is justified by the ease with which repairs can be made in the field by replacing individual segments rather than removing and/or scrapping an entire blade assembly as in the case of a continuous stressed skin blade. Twelve segments are required per blade. Each segment is 41.1 inches long. Each segment can be removed from the spar without disturbing the adjacent segments. The replacement procedure, as shown in Figure 51, is to remove the single line of flush screws which clamp the segment around the spar, spring the upper flap up and the trailing edge down, and pull the segment forward and down off of the spar. The deflection of the 0.060 epoxy fiber glass skins required to remove the segment from the spar results in flexure bending stresses in the fiber glass of 15,000 psi compared with a flexural strength ultimate of 76,000 psi for this type of material.

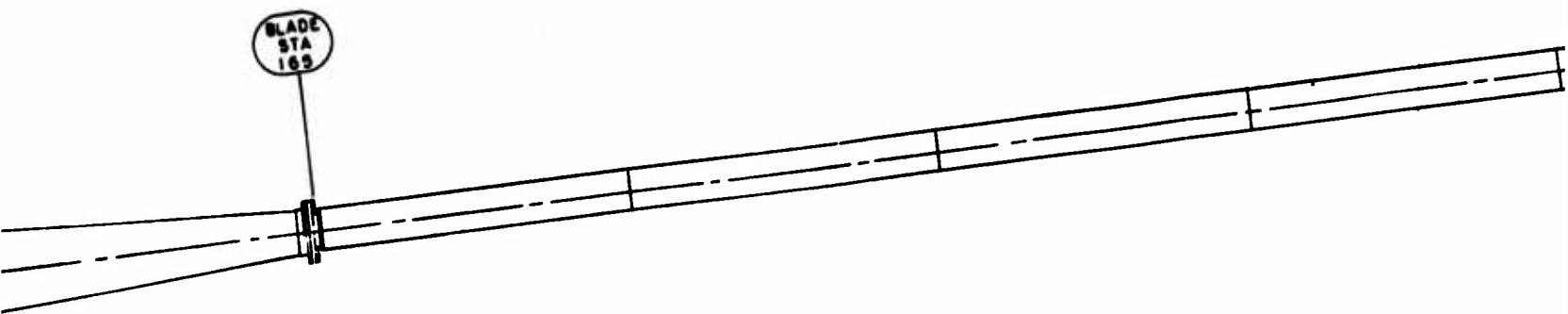
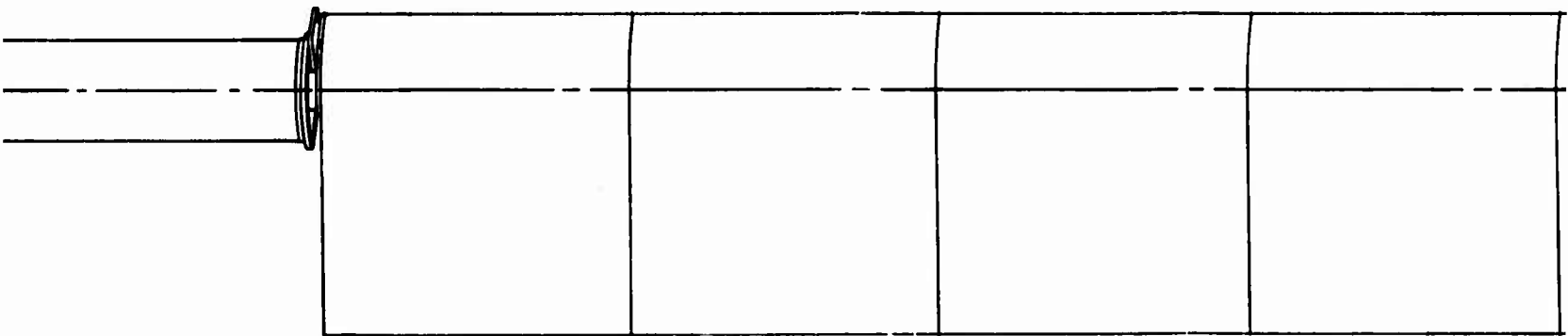
The segment trailing-edge outer skins could be either aluminum alloy or epoxy fiber glass. The 6-pound/cubic foot density polyurethane foam in the leading edge is the lowest foam density that has been found to be practical in rotor blades. The fiber glass cylinders are simply elongated lightening holes to reduce the weight of the leading edge.



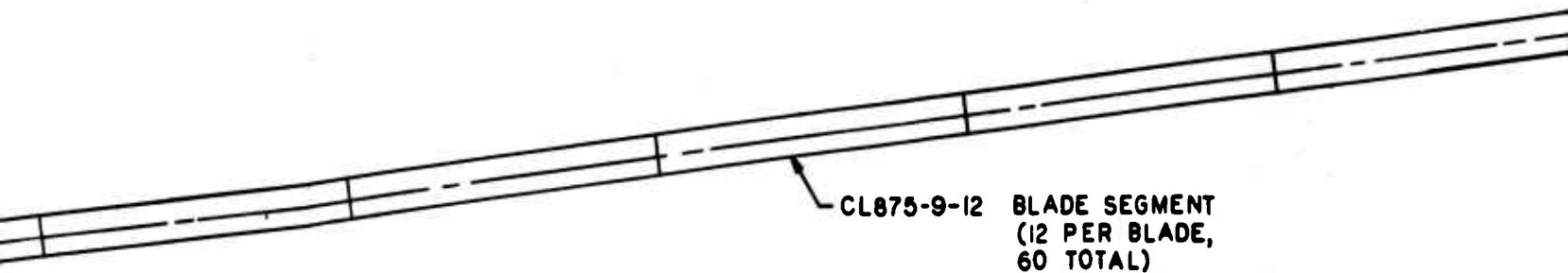


**Figure 50. Rotor Assembly, Heavy-Lift Helicopter**

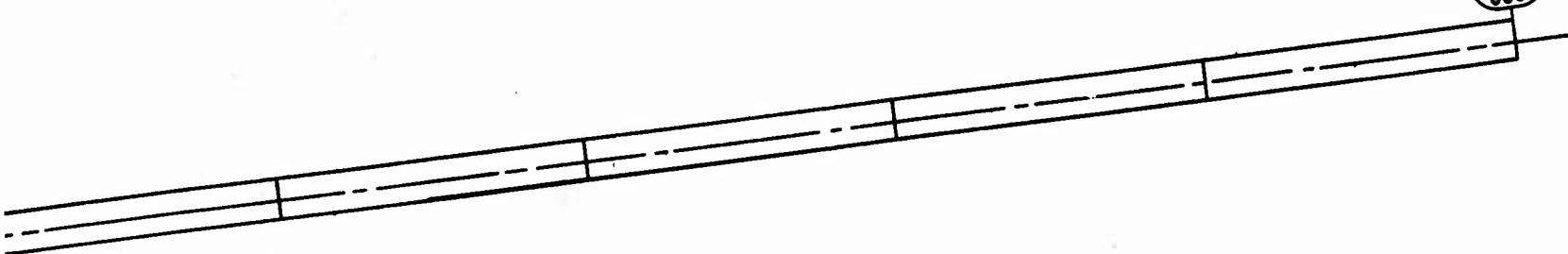




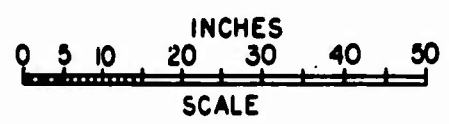
BLADE  
STA  
169


BLADE  
STA  
660



BLADE SEGMENT  
(12 PER BLADE,  
60 TOTAL)



APPROVED DESIGN		REVISION
ROTOR ASSY		
CL875-9	CL875-9	CL875-9

C

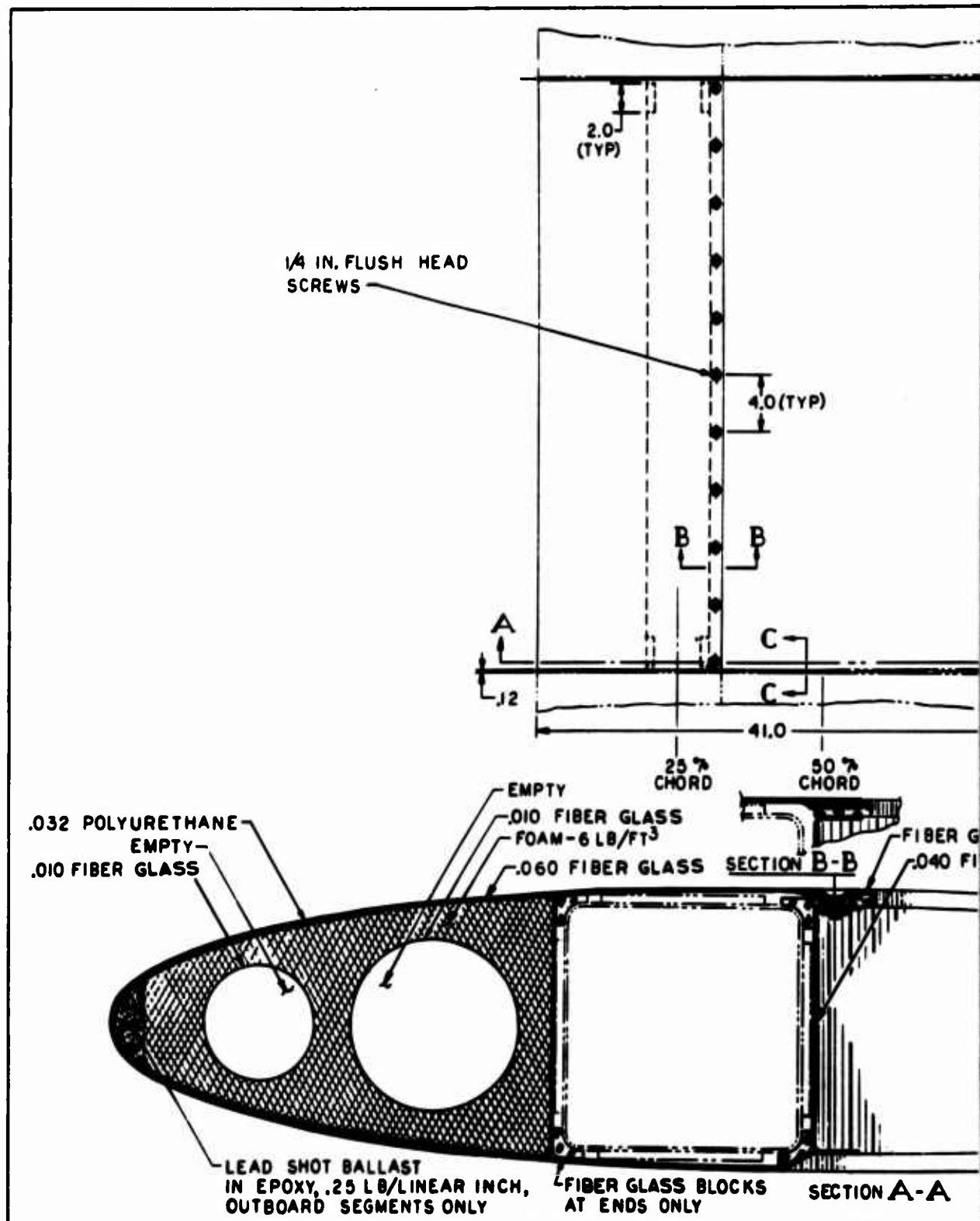
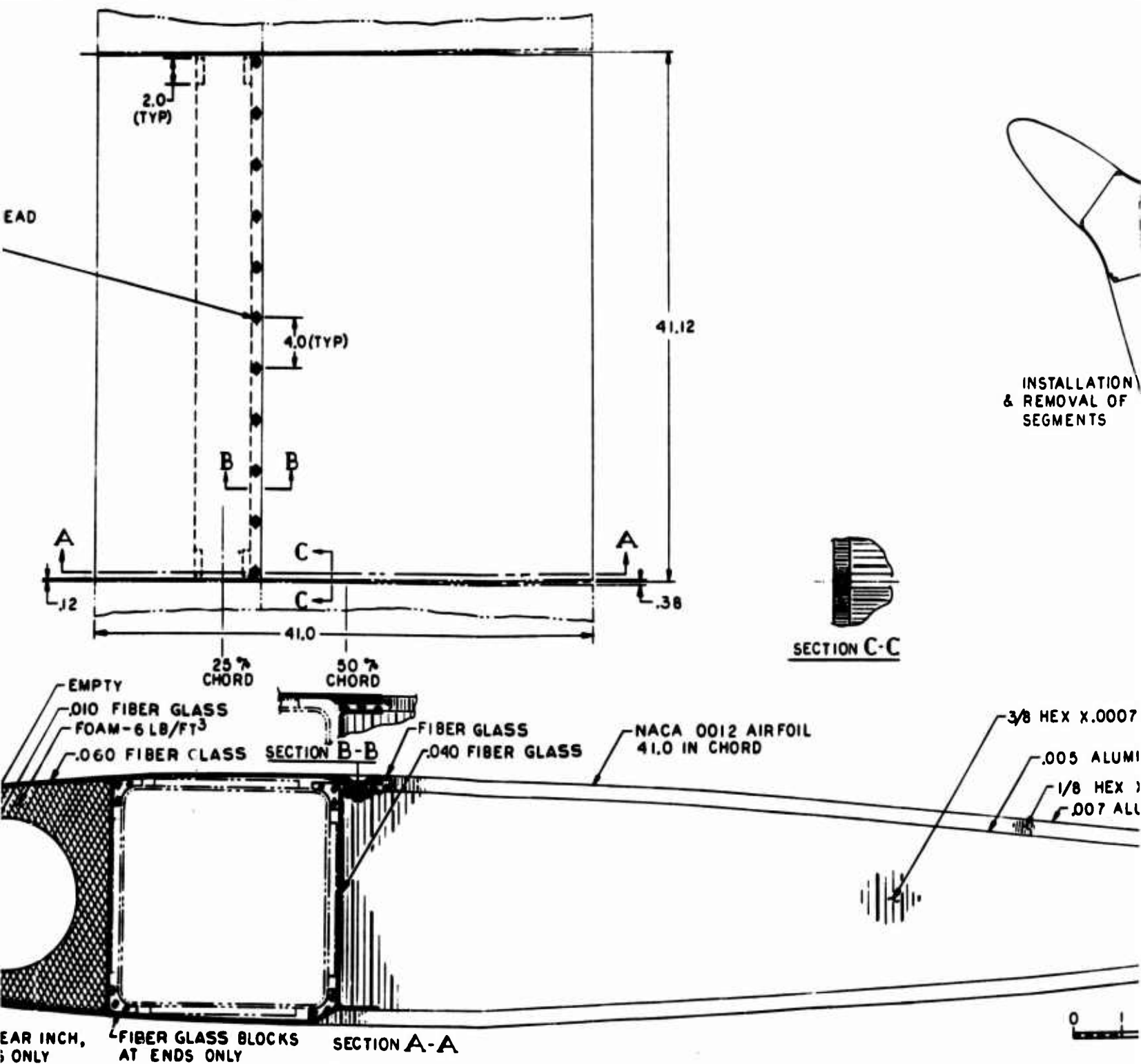
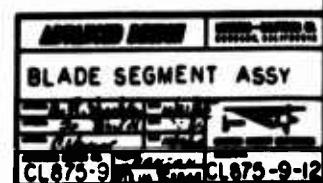
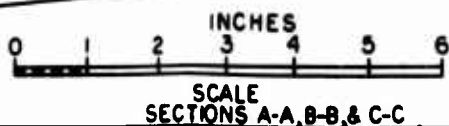
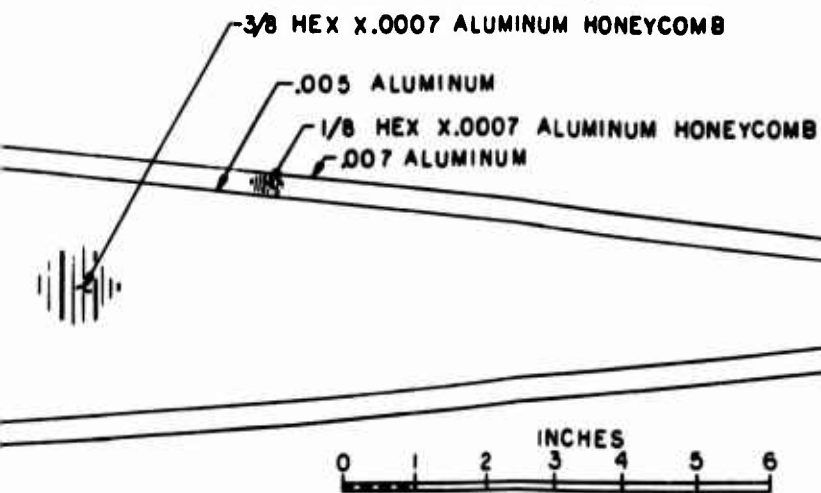
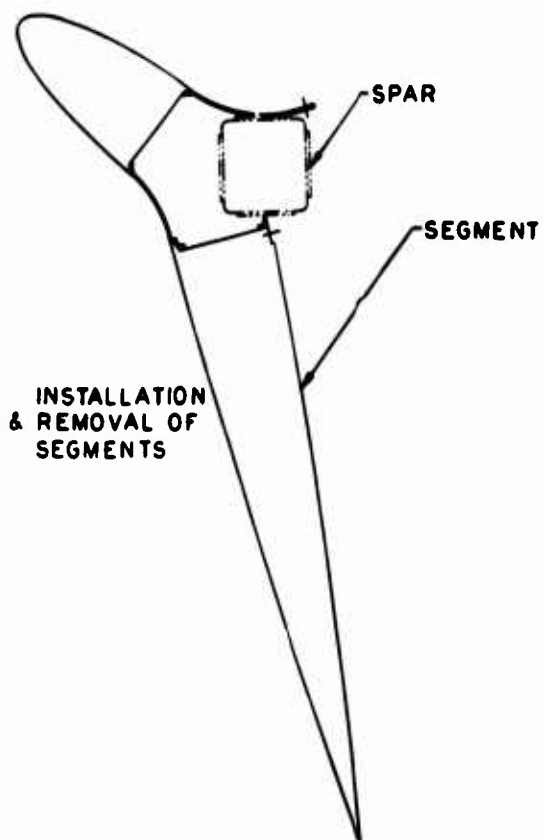


Figure 51. Main Rotor Blade Segment, Heavy-Lift Helicopter



Segment, Heavy-Lift Helicopter



The inboard segments differ from the outboard segments only in the deletion of the chordwise balance weight from the leading edge. The only contact between the segment and the spar is through the corner blocks at each end of each segment. The centrifugal force generated in each segment is carried into the spar where the inboard set of corner block bear on the corner blocks bonded to the spar.

The blade segments are the source of most of the rotor system centrifugal and inertia forces since the centroid of the segment weight is further outboard than the centroid of the spar weight. Their mass and the stiffness of the spar primarily determine the blade frequencies and mode shapes except for the first or cantilever mode.

Although the airfoil section shown is an NACA 0012, the use of any 12- to 15-percent-thick airfoil would not appreciably affect the construction, rotor frequencies, or rotor weight shown for the 0012 section.

#### Spar/Flexure

The blade spar and the root flexure are constructed as a complete bonded assembly to avoid the weight and structural problems of a mechanical joint. Figure 52 shows the spar/flexure assembly.

The flexure connects the hub to the blade and extends from about 3 to 25 percent of the radius for this design. It is torsionally soft to allow blade pitch changes through a range of 24 degrees. The in-plane stiffness is matched to the flapping stiffness. These stiffnesses, in conjunction with the blade mass and centrifugal force, determine the first, or cantilever, mode frequencies, and in-plane blade motions are accommodated by elastic bending of the flexure.

The blade spar is a square tubular section and is sized to stiffness requirements for blade frequencies and centrifugal force. The spar incorporates an antinodal weight to control the second mode flap frequency.

#### Hub

The hub as shown in Figure 53 is the central fitting to which the inboard ends of the five flexures attach. The hub transmits the blade forces through bearings to the nonrotating rotor mount spindle. The hub as shown is a titanium alloy forging. The hub could also be built of steel in which case the flanges and walls could be thinner and the weight would not be appreciably greater than for titanium. The flanges to which the flexure root fittings attach are positioned to back up and stiffen the radially loaded rotor bearings.

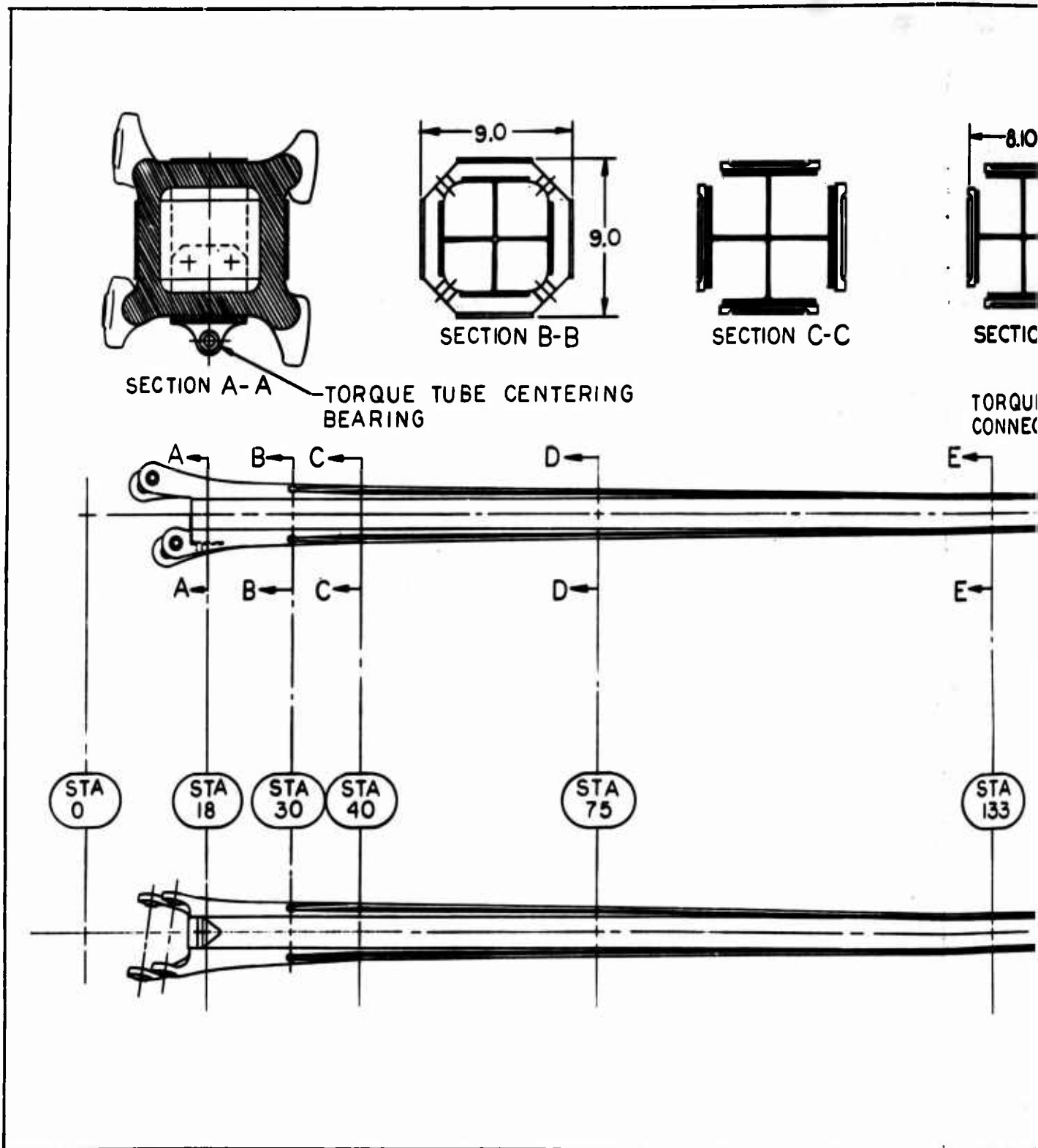
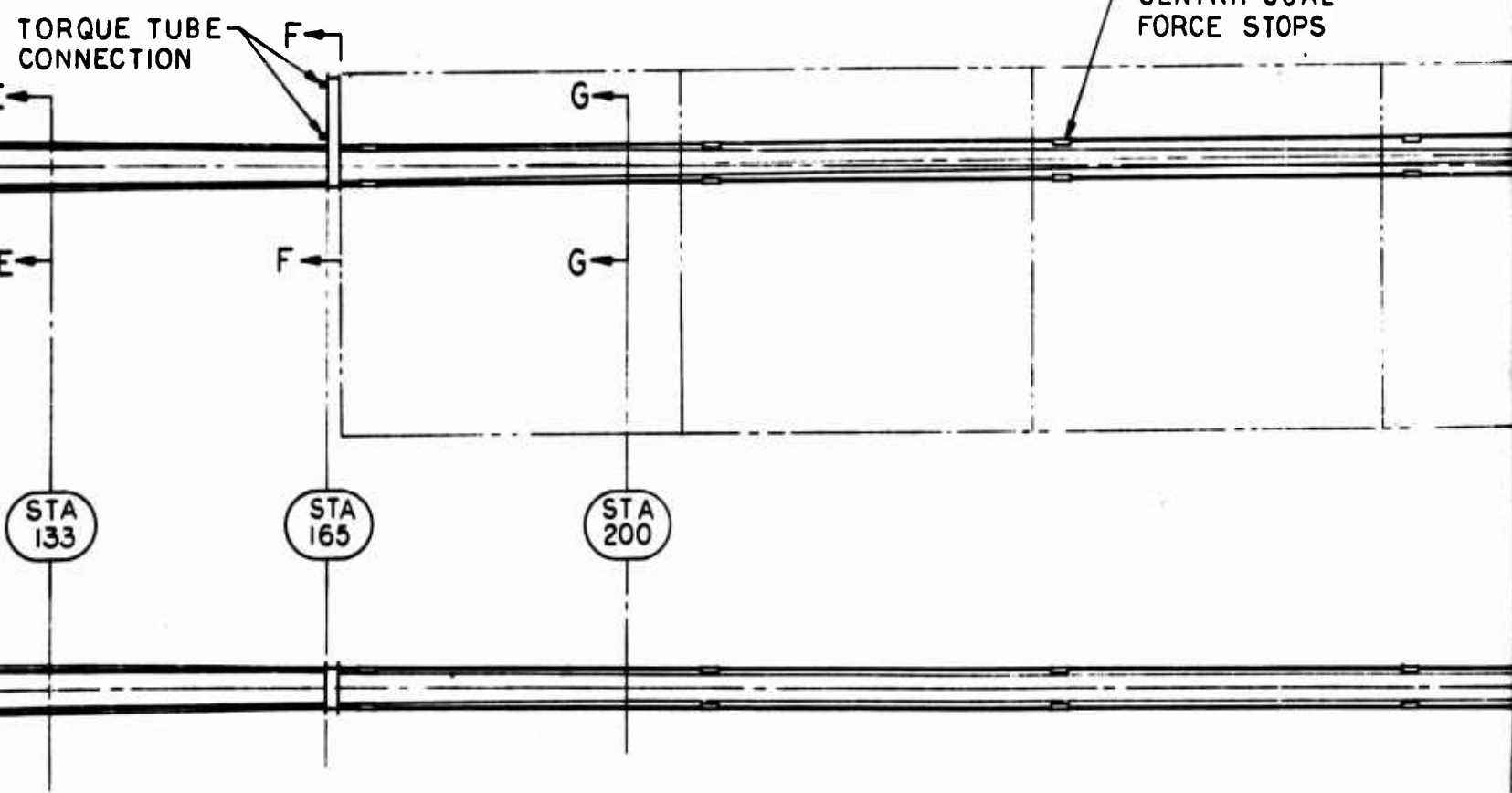
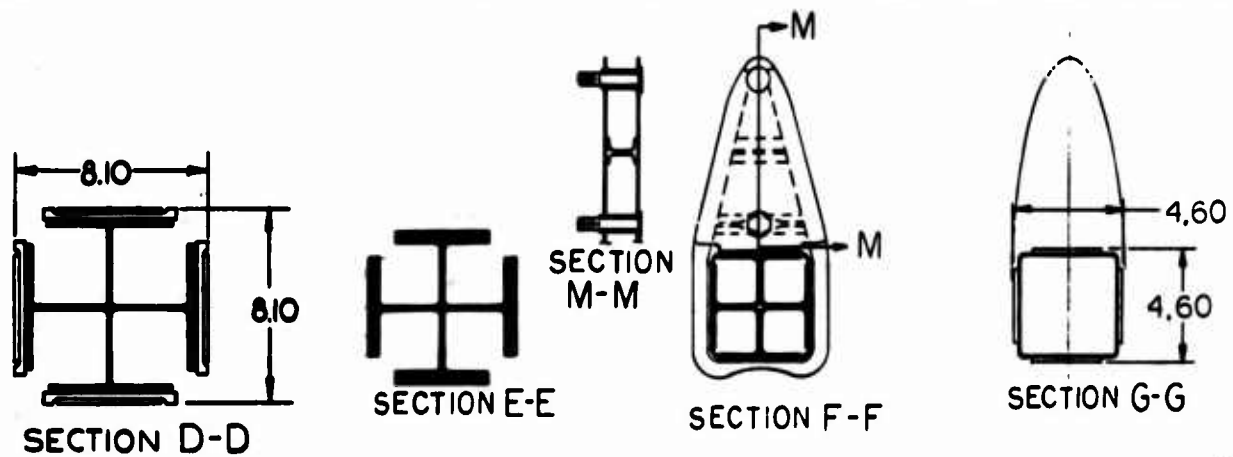


**Figure 52. Spar/Flexure Assembly, Heavy-Lift Helicopter**

A

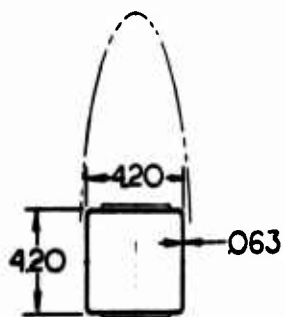




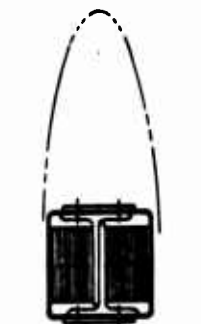
BOND STRAPS TOGETHER  
THIS AREA ONLY



SECTION N-N



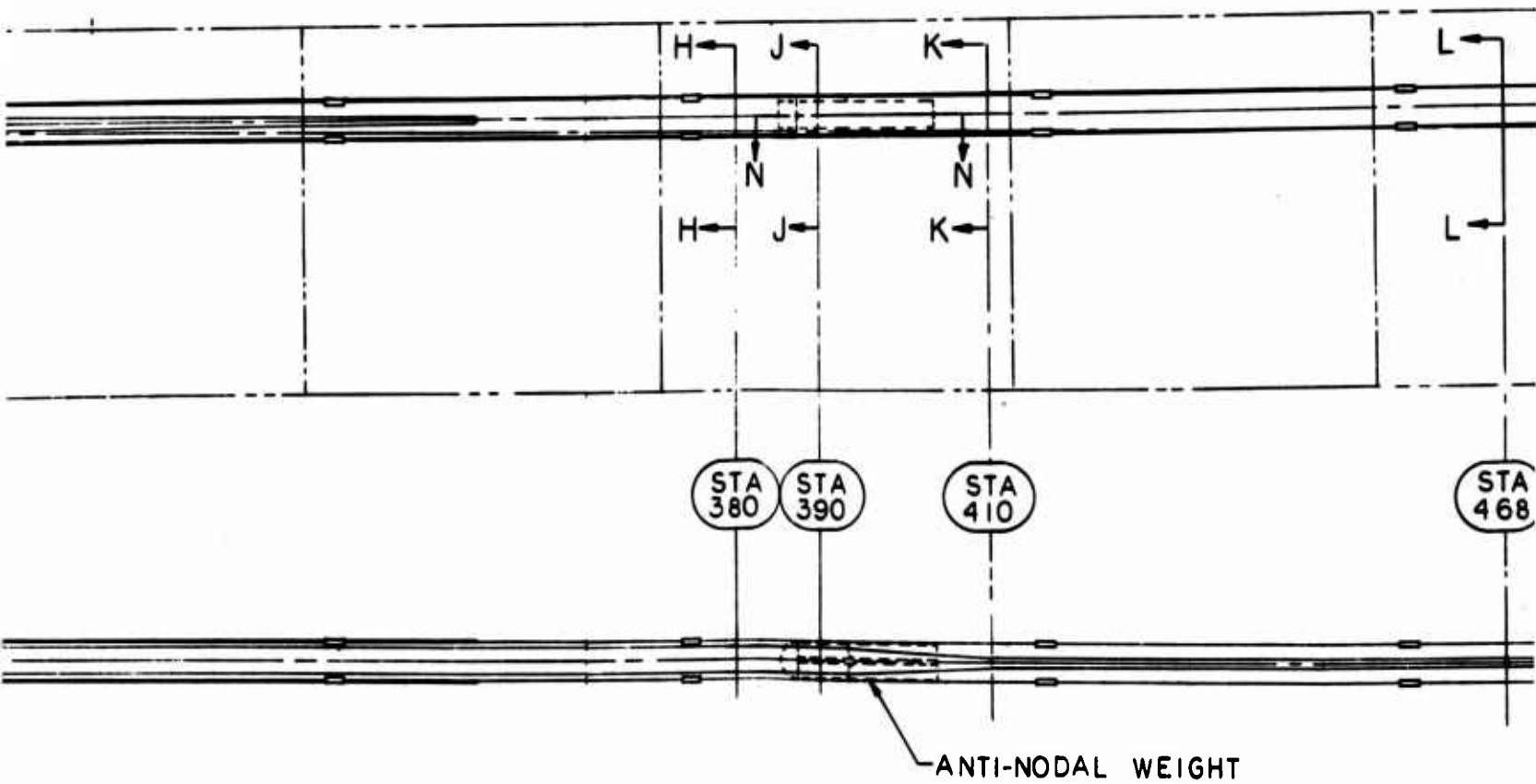
SECTION H-H  
(TYP SPAR DIMEN.)

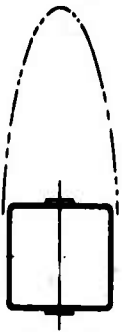


SECTION J-J

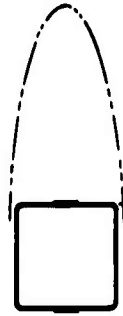


SECTION K-K



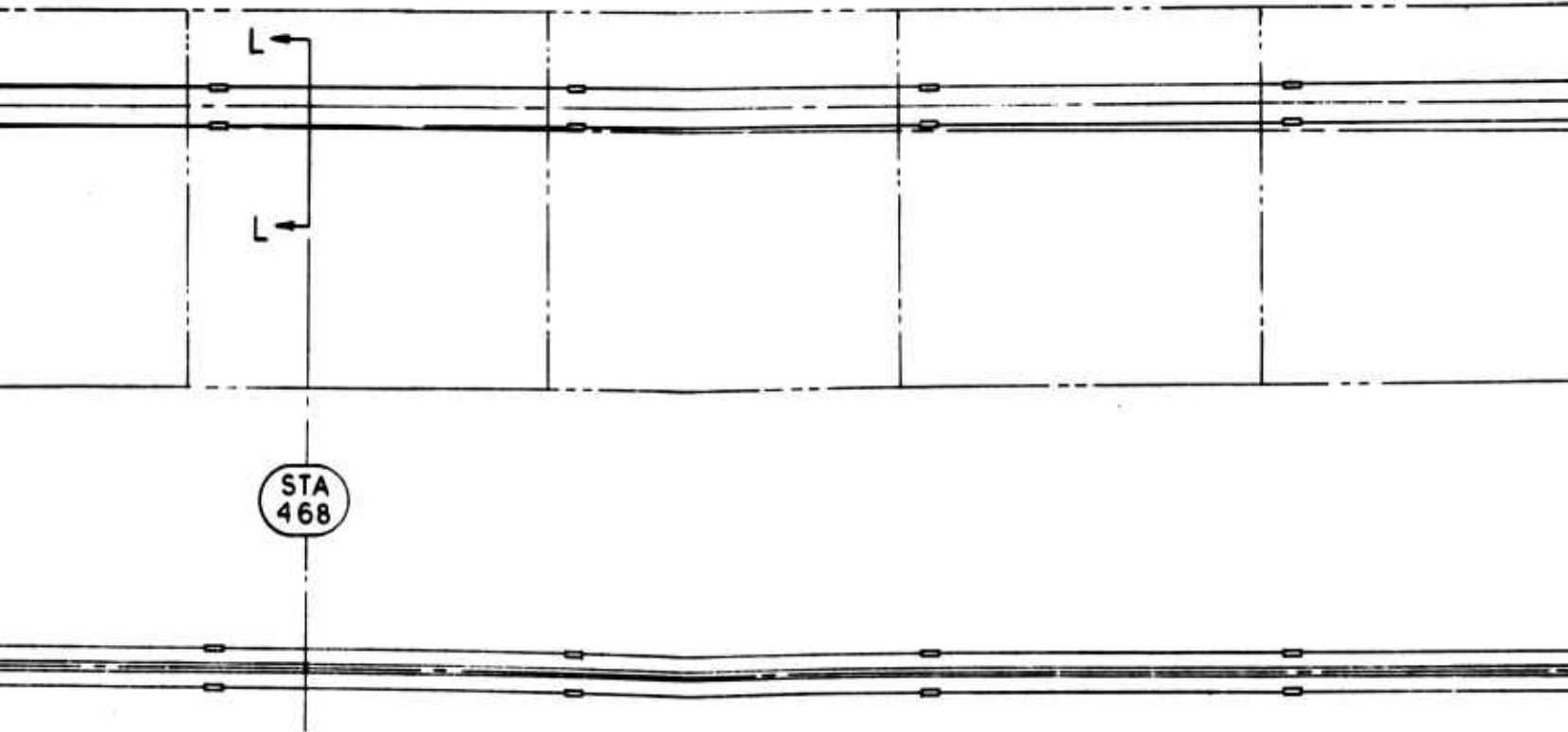


SECTION K-K



SECTION L-L  
TYP FROM STA  
468 TO STA 660

0 1 2

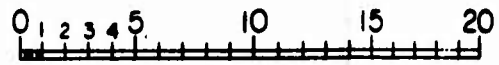


STA  
468

SHT

MATERIAL - AM - 350  
STAINLESS STEEL

C



SCALE  
CROSS SECTIONS

SECTION L-L  
TYP FROM STA  
468 TO STA 660

BLADE SWEEP

3.4

STA  
660

MATERIAL - AM - 350  
STAINLESS STEEL

ADVANCED DESIGN

DESIGNED - CONSTRUCTION CO.  
STOCKTON, CALIFORNIA

SPAR/FLEXURE ASSY

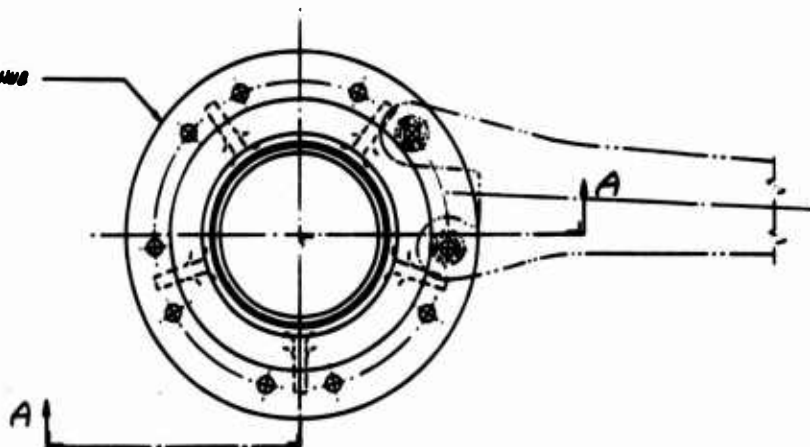
CL 875-9

CL 875-9-13

Q



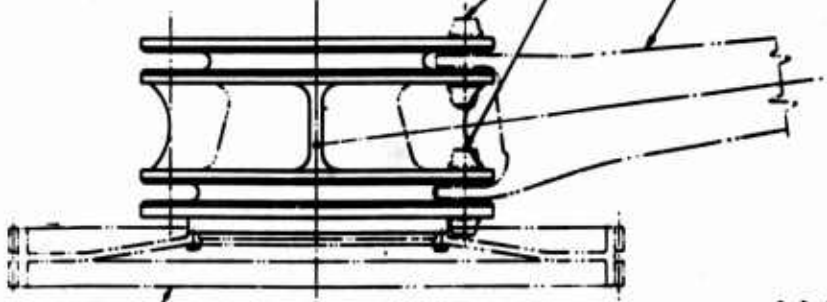
MAIN ROTOR HUB



A

BOLT-TYPE S-9 (SPECIAL) 1.375 DIA  
NUT-SELF-LOCKING-DOMINANT 1/4" (TYP) 1.375 DIA.  
(TYPICAL - 10 PLACES)

SPAC (FLANGE) 1/4" CL 815-9-13 (REF)  
(TYPICAL - 5 PLACES)



TRANSMISSION BULL GEAR  
(REF)



SCALE - INCHES

MATERIAL: T1-6AL-4V TITANIUM ALLOY

ADVANCED DESIGN		DESIGNER: [Signature]
MAIN ROTOR HUB HEAVY LIFT HELICOPTER		
CL 815-9	CL 815-9-15	CL 815-9-15

This type of rotor design is not dependent on the use of an integrated hub and transmission as shown. This same type of hub could be installed on top of a conventional rotating rotor shaft. The hub would be internally splined to fit the shaft, and the hub weight would be practically the same as that shown for the integrated hub. While this rotor is not designed for blade folding, the four-bolt lug-type of joint used to attach the blades to the hub would be easily adaptable to folding.

#### Control Torque Tube

Functionally, the torque tube is not a structural part of the rotor as it transmits only control forces and motions. It extends generally parallel to the flexure from the hub to the blade and is very stiff torsionally. The outer end of the torque tube is attached to the blade rigidly in a feathering sense through a flexible coupling which will not transmit appreciable in-plane or flapwise bending moments from the blade into the tube. The inboard end of the torque tube is attached to the hub through a bearing which is free to rotate in a feathering sense and to the swash plate through a pitch horn and pitch link. Thus, cyclic and collective pitch changes are fed to the blade by the torque tube, and feathering moments generated in the blade are carried by the torque tube back to be reacted in the flight control system.

The torque tube torsional stiffness requirement is such that the torque tube diameter must be in the order of 10 to 12 inches to achieve a light torque tube design, as shown in Figure 54. The torque tube encloses the flexure and serves as a protective covering. With proper contouring, the torque tube also serves as an aerodynamic fairing over the flexure.

To allow inspection of the flexure and replacement of the torque tube without removal of the entire blade, the torque tube is split lengthwise. A Thomas-type flexible coupling is used to attach the torque tube to the blade.

#### Gyro/Swash Plate

A gyro/swash plate installation above the rotor hub is shown in Figure 55 to illustrate that the rotor design presented in this report is compatible with reasonable control systems. No weight or stress analysis data are presented for the gyro/swash plate, as it is not considered as part of the rotor.

A nonrotating control pylon is mounted inside the nonrotating rotor mount spindle. The gyro/swash plate is mounted on a nonrotating gimbal on top of the pylon. An arm extends from the nonrotating center part of the gyro/swash plate down through the control pylon. Cyclic control moments are applied to the gyro as horizontal forces on the lower end of

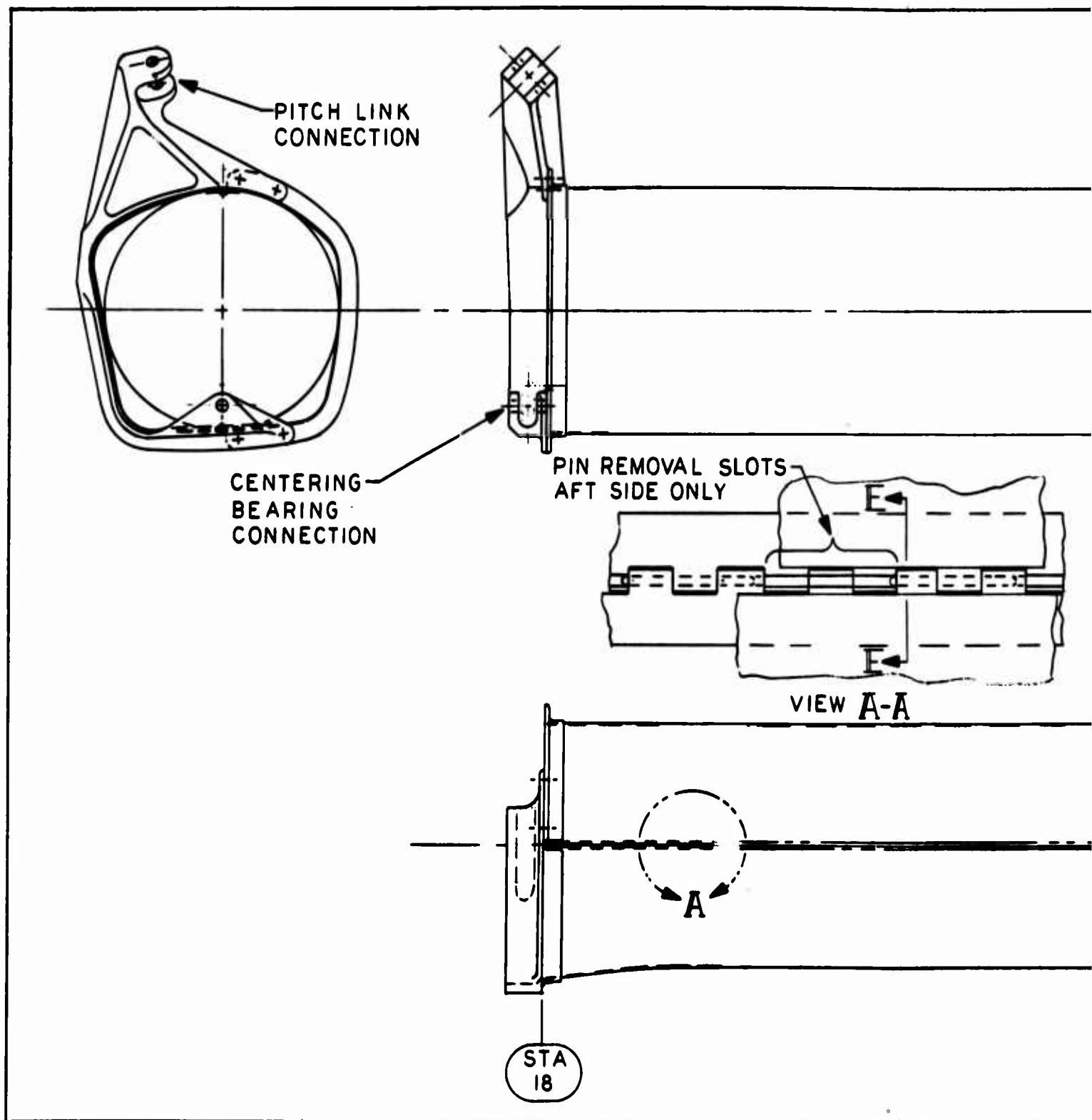
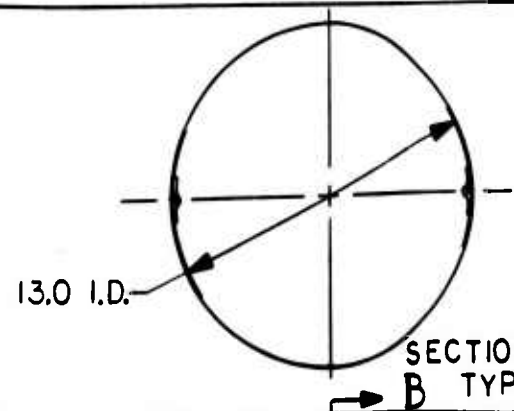
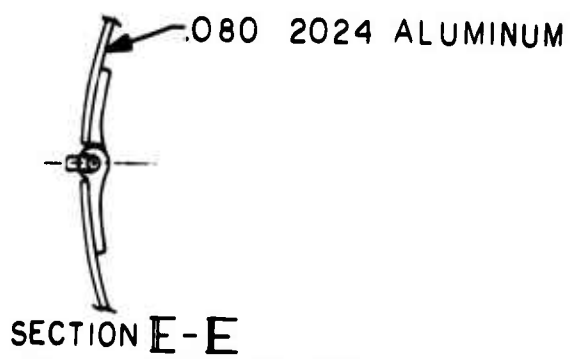
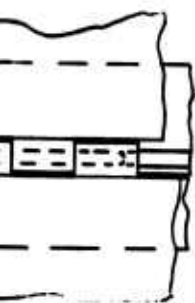
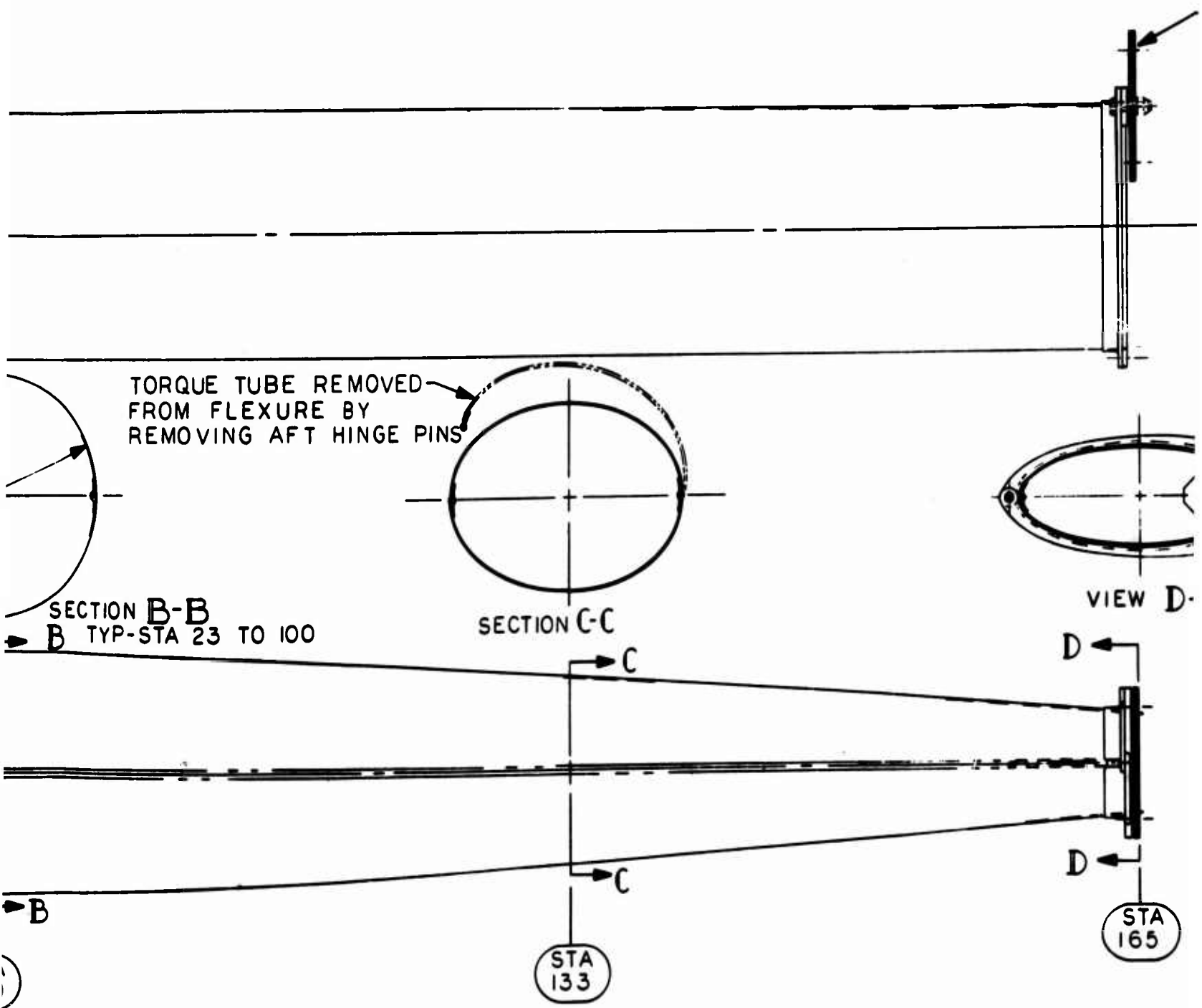


Figure 54. Control Torque Tube Assembly, Heavy-Lift Helicopter



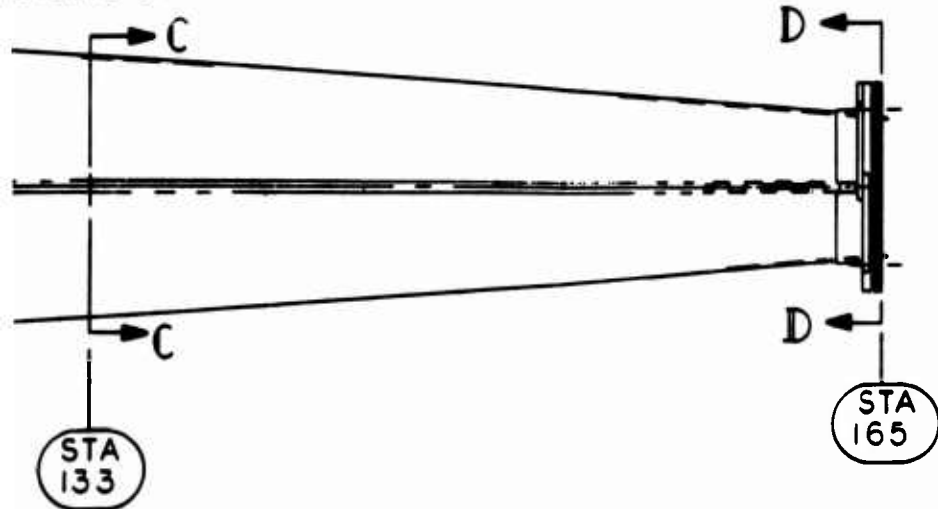
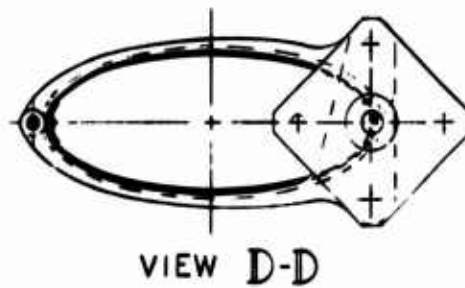
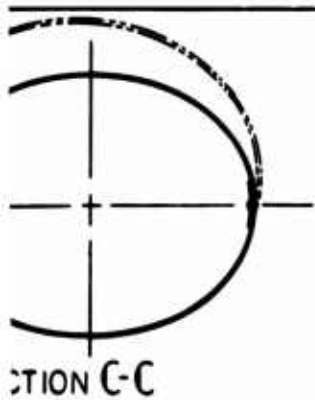



STA  
100



C

FLEXIBLE COUPLING  
301 1/2H STEEL  
10 PIECES .025 THK



<b>ADVANCED DESIGN</b>		LOCKHEED - CALIFORNIA CO. BURBANK, CALIFORNIA	
<b>CONTROL TORQUE TUBE ASSY</b>			
DESIGNED BY <i>[Signature]</i>	DATE <i>5/1/68</i>		LOCKHEED SECURITY REQUIREMENTS
CHECKED BY <i>[Signature]</i>	DATE <i>5/1/68</i>		
APPROVED BY <i>[Signature]</i>	DATE <i>5/1/68</i>		
CL875-9	72	CL875-9-14	72

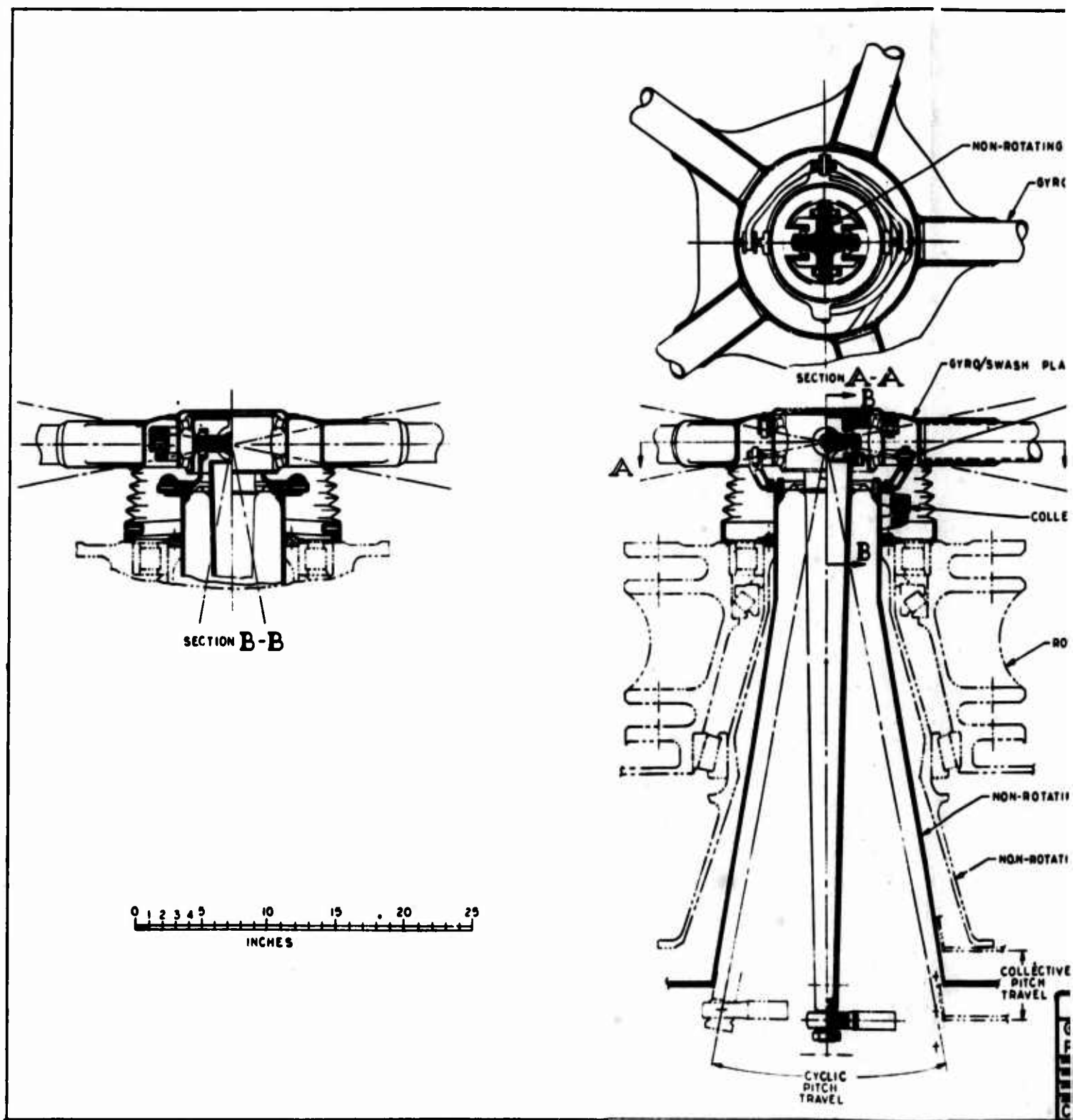
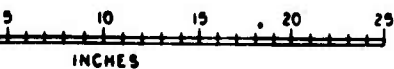
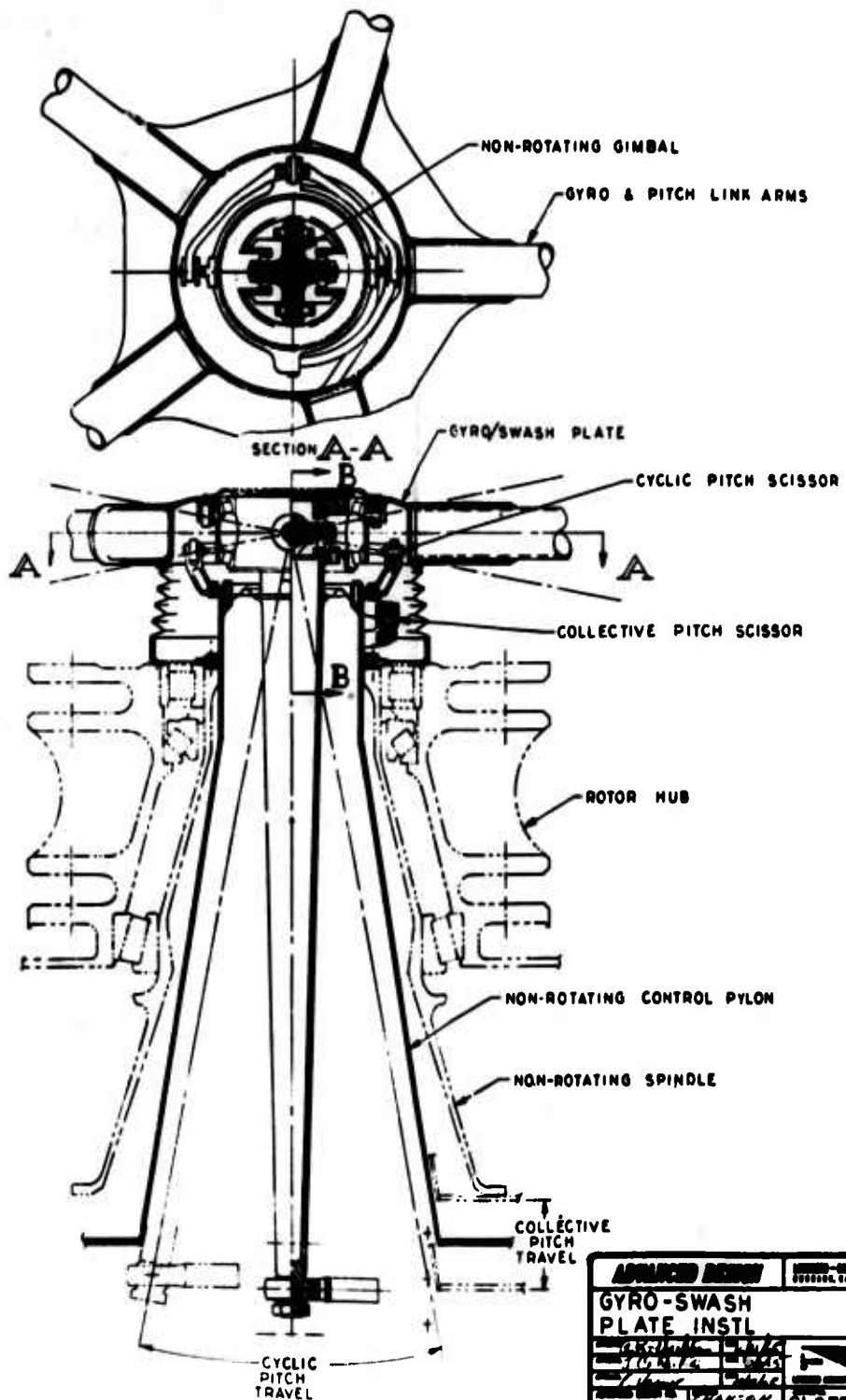
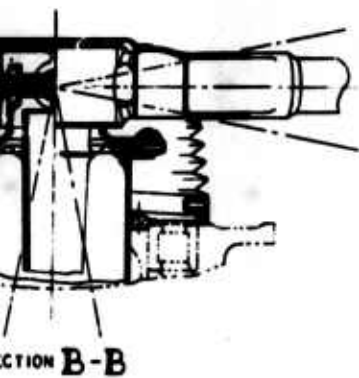


**Figure 55. Gyro/Swash Plate Installation, Heavy-Lift Helicopter**



<b>ADVANCED DESIGN</b>		<b>UNITED STATES OF AMERICA</b>	
<b>GYRO-SWASH PLATE INSTL</b>		<b>CL875-9-6</b>	
APPROVED	DATE	BY	CHKD
10/1/68	10/1/68	J. M. G.	J. M. G.
CL875-9	CL875-9-6		

Gyro/Swash Plate Installation, Heavy-Lift Helicopter

this arm. Collective pitch is applied by moving the entire control pylon and gyro/swash plate vertically. With this arrangement there is only one major rotating piece, which is both the gyro and swash plate. Five arms extend from the gyro hub. A pitch link attaches each arm to a blade torque tube pitch horn. Weights at the ends of the arms create the necessary gyro moment of inertia.

#### Rotor/Propulsion System General Arrangement

The general arrangement of the rotor/propulsion system is shown in Figure 56. The transmission is mounted directly below the rotor with vertically mounted engines. The use of engines mounted vertically eliminates the need for bevel gearing in the gear train between the engines and the main rotor. The power and rotational speed requirements of the HLH transmission would stretch the present state of the art in bevel gear technology. On the other hand, conventional, parallel shaft gearing is commonly used to run at far higher speeds and powers than is required for the HLH.

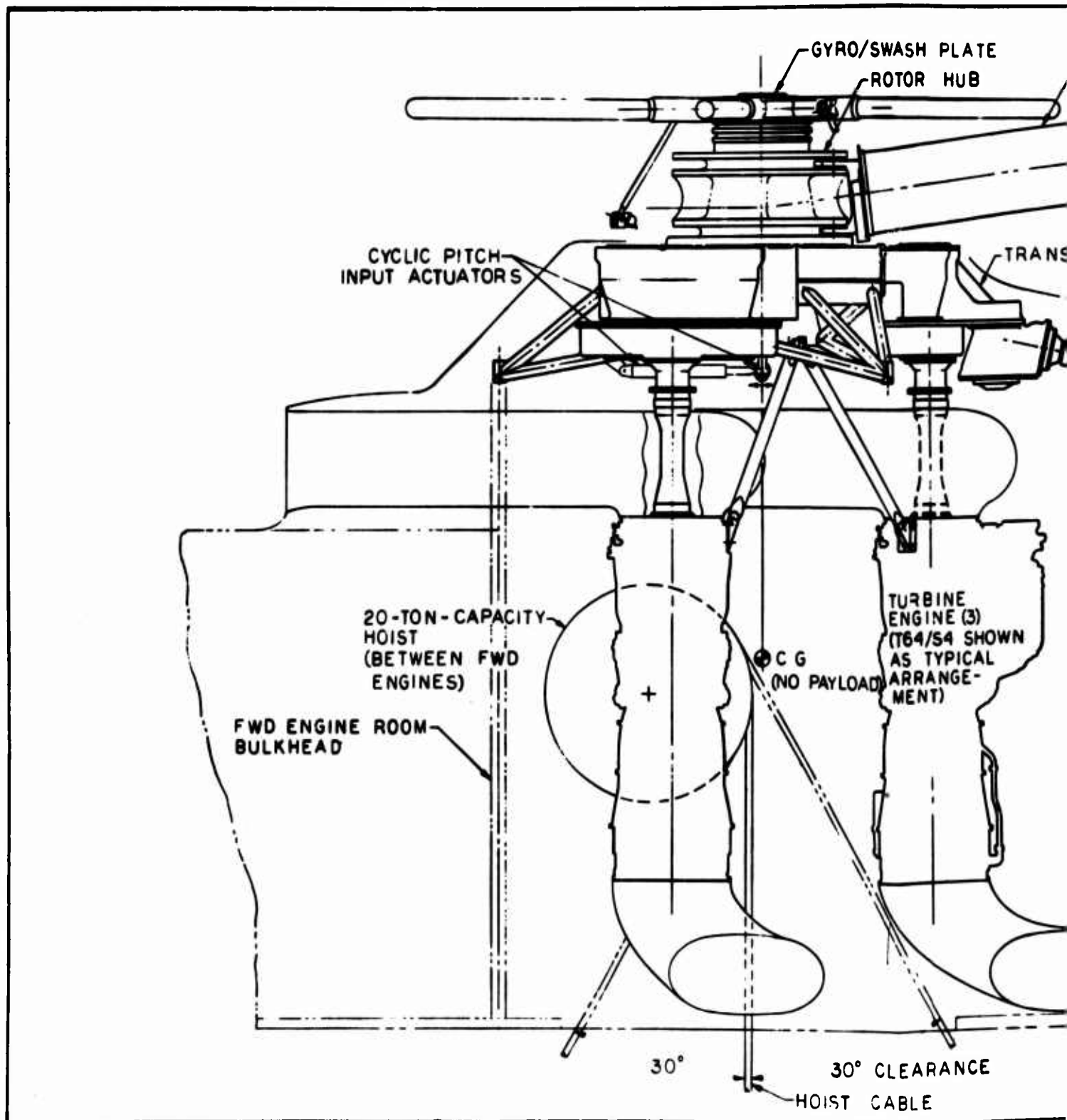
Three T64/S4 engines were used only for configuration purposes to show the vertical engine concept. Other arrangements or combinations of engines could be incorporated.

Figure 56 shows the space available with this transmission design to mount a 20-ton-capacity cargo hoist directly below the center of the rotor and at the center of gravity of the vehicle. If the hoist had to be mounted below the center of gravity because of the transmission arrangements, it is possible that the vehicle/cargo dynamics could create a problem. The hoist has clearance for a 30-degree cable angle with respect to the rotor axis.

The size of this vehicle and the height of most of the components from the ground suggest that maintenance could be more simply accomplished if access were provided from inside rather than from outside the fuselage. Thus, the vehicle arrangement shown in Figure 56 is such that all systems are placed inside the body insofar as possible, and internal passage ways are provided to reach them. This feature allows in-flight inspection of systems where trouble is suspected. It also allows repair work at night with no light showing externally. The possibility even exists of extending this concept to the point where it would be possible to effect an in-flight engine change during an overseas ferry flight.

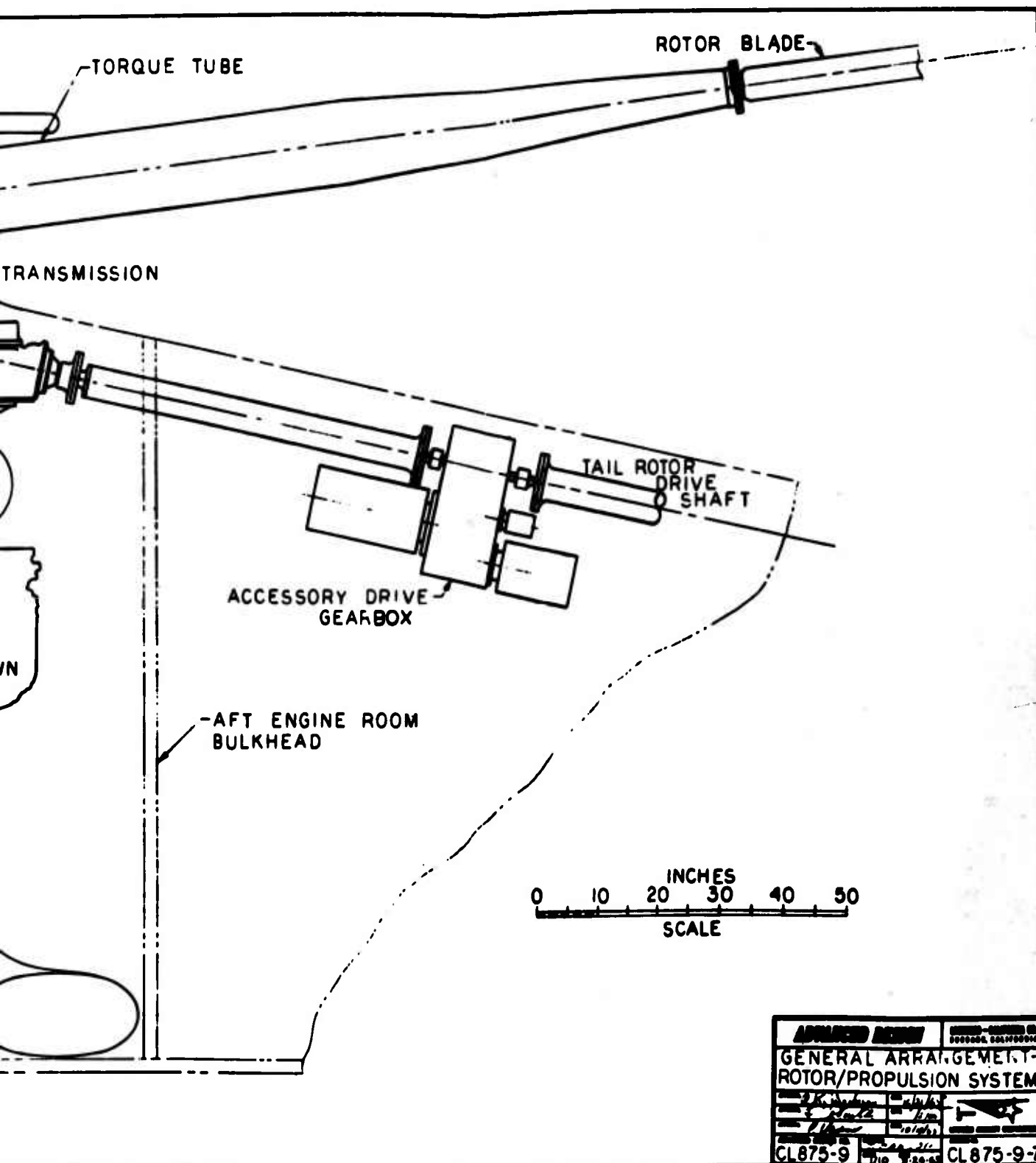
The engine room directly below the rotor provides access to:

- All three engines and related systems
- Most of the transmission
- The separate accessory drive gearbox and all accessories including the APU



**Figure 56. General Arrangement - Rotor/Propulsion System,  
Heavy-Lift Helicopter**

A





- The cargo hoist
- The cyclic and collective nonrotating parts of the flight control system
- Transmission lube system

The fuel system tanks would be located in the general area of the transmission/engine compartment with tanks both forward and aft. It is anticipated that crash-resistant-type fuel cells would be used.

The fuselage size is sufficient to accommodate necessary fuel tanks internally for the fuel requirements of the ferry mission.

#### Alternate Design

Alternate studies were conducted for the design of the blade segment and the flexure member. The primary purpose of this alternate study was to provide backup configurations for weight study purposes and to evaluate differences in design with respect to manufacturing techniques. The alternate designs are presented for conceptual comparison only, as no detailed weight or stress analysis is presented in this report.

#### Blade Segment

The rotor blade segment design, as shown in Figure 57, presents a configuration that is compatible with the spar/flexure configuration previously discussed. This blade segment design study was conducted as an alternate to the segment configuration of Figure 51. The configurations differ primarily in the detailed buildup of the leading edge and in the fact that the segment is a two-piece section. A tradeoff study would be required to establish the optimum detailed configuration.

#### Flexure

An alternate flexure configuration was studied. The configuration, as shown in Figure 58, is a matched-stiffness flexure and differs from the configuration of Figure 52 in that a tie rod is incorporated to preload the flexure in compression for increased fatigue life and in the method of manufacturing. This flexure is machined from a steel section instead of from a built-up bonded section. This configuration will require further design study and refinement.

The hub configuration of Figure 58 is a tension-type multiple-bolt pattern flexure attachment instead of a lug attachment. It is felt that either configuration will satisfy the requirements of the design and will weigh approximately the same. A tradeoff study would be required to establish the optimum configuration.

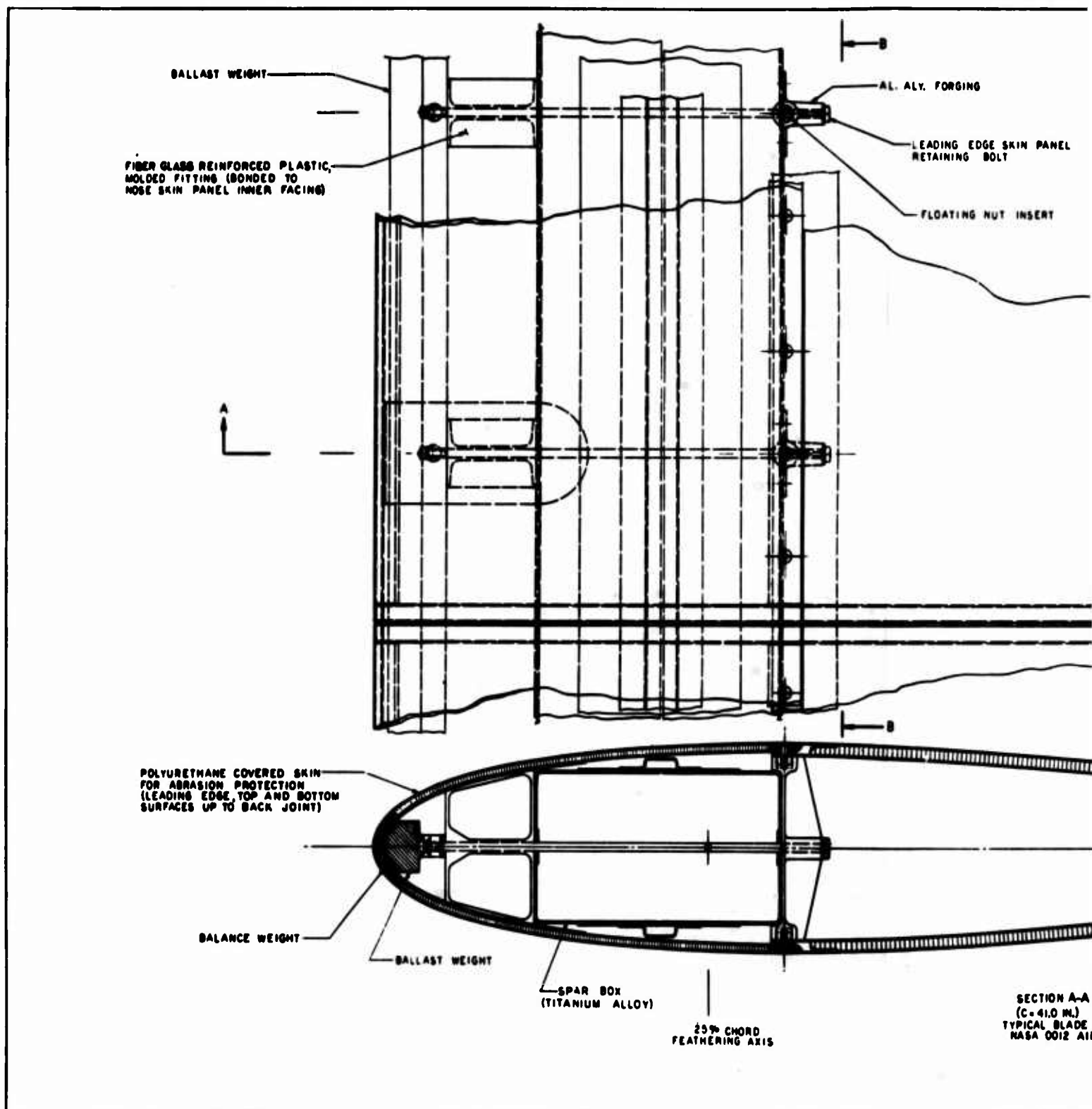
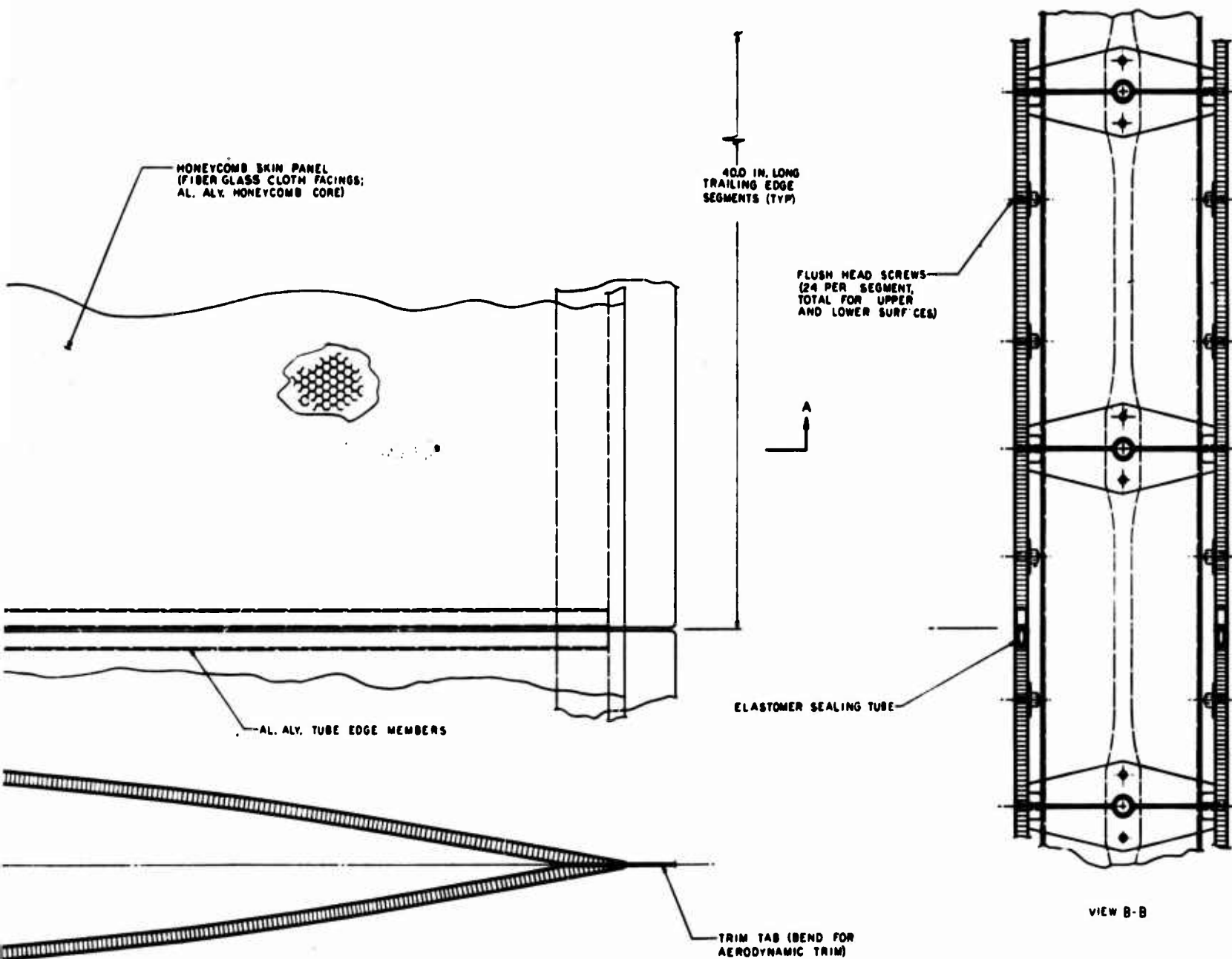


Figure 57. Main Rotor Blade Segment, Alternate Design



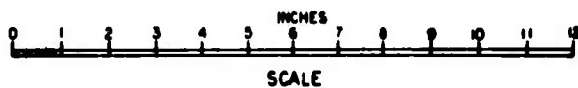
400 IN. LONG  
TRAILING EDGE  
SEGMENTS (TYP)

FLUSH HEAD SCREWS  
(24 PER SEGMENT,  
TOTAL FOR UPPER  
AND LOWER SURFACES)

ELASTOMER SEALING TUBE

TRIM TAB (BEND FOR  
AERODYNAMIC TRIM)

VIEW B-B



<b>ARMED AIR</b>		<b>NAVY-NAVY &amp; AIR FORCE</b>	
<b>MAIN ROTOR BLADE - STRUCTURE (ALTERNATE)</b>			
DESIGNED BY	DESIGNED BY	DESIGNED BY	DESIGNED BY
CL 875-0	CL 875-0	CL 875-0	CL 875-0
CL 875-0	CL 875-0	CL 875-0	CL 875-0

B

C

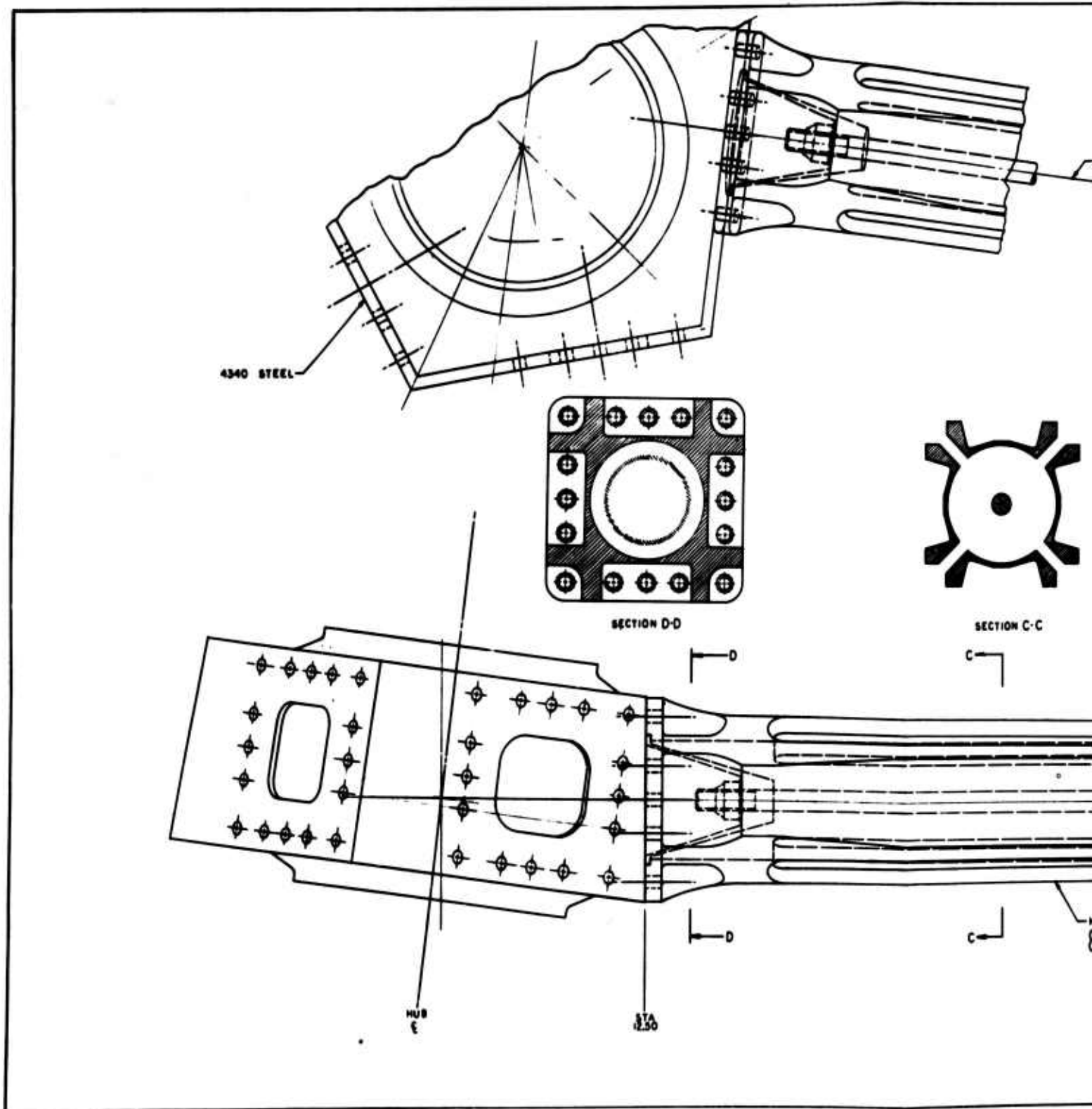
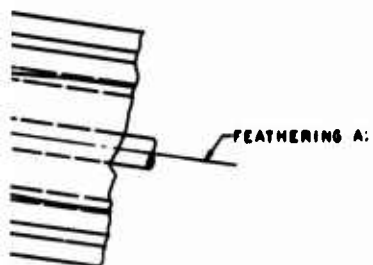


Figure 58. Flexure Assembly, Alternate Design



SECTION C-C



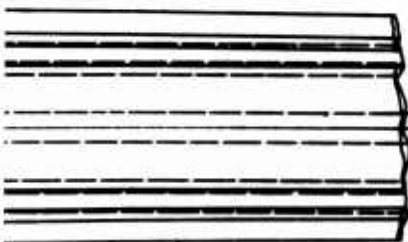
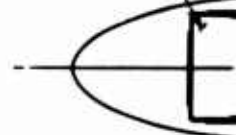
HIGH STRENGTH STEEL TIE ROD PRELOADING TO INDUCE INITIAL COMPRESSION OF THE HUB ARMS (PRESTRESSING FOR IMPROVED FATIGUE LIFE WITHOUT INCREASING STIFFNESS CHARACTERISTICS)  
(BONDED ELASTOMER PADS NOT SHOWN KEEP TIE ROD CENTERED AND RESTRAIN HUB ARM CAPS FROM BUCKLING AND VIBRATING)



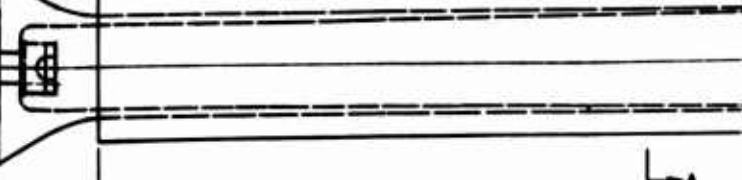
SECTION B-B

FIBER GLASS FILLER

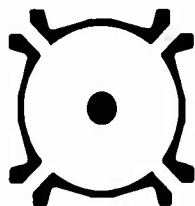
BLADE SPAR BOX



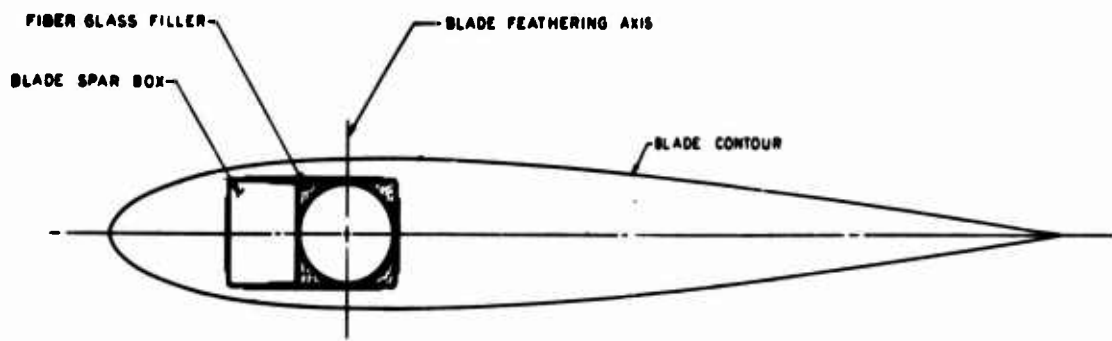
HUB ARM (FLEXURE)  
(TYP 3 PLACES)  
(4340 STEEL)



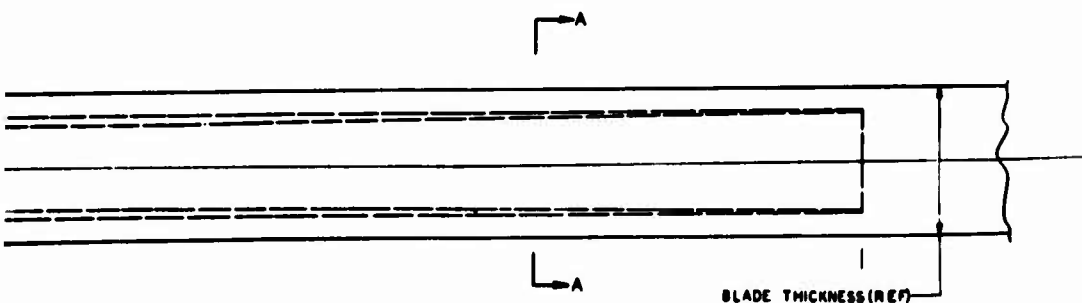
STA 165.0



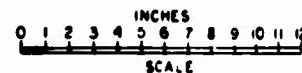
SECTION B-B



DETAIL OF JOINT OF HUB ARM TO  
BLADE SPAR (FIBER GLASS FILLED POCKETS  
-MOLDED IN PLACE)  
SECTION A-A



STA  
203.0



<b>APPROVED DESIGN</b>		<b>DESIGN - DRAWING NO.</b> 00000000000000000000	
<b>FLEXURE ASSY-ALTERNATE</b>			
DESIGNED BY C.E.75-9	CHECKED BY [Signature]	DATE [Date]	PROJECT NO. CL-875-9-10

## OPERATIONAL FEATURES

If the requirement for safe autorotation is intended to restrict disc loading to values at which autorotation is possible, the 7.6 psf disc loading of this rotor should be quite satisfactory. Rate of descent, power off, at heavy-lift gross weight will be quite rapid, and the flare and touchdown will require a skilled pilot. The energy storage capacity of this rotor is probably not quite high enough to allow a zero forward speed landing with power off. However, completely power-off landings in a multiengine machine such as this should be rare and do not appear to justify a weight penalty in the rotor to increase the rotor energy further. The flare capability should be comparable to most large operational helicopters in use today.

During flying-crane-type operation, when an external cargo hook is used, it will probably be necessary for ground personnel to be beneath the hovering helicopter to hook and unhook the load. The cargo would be resting on the ground and the rotor-induced velocities would correspond to the operational empty weight disc loading of approximately 3.5 psf. Disturbances due to the induced velocities at such a low disc loading should not be dangerous to ground personnel.

Rotor blade tip lg static droop is 53 inches. The built-in cone is 82 inches at the blade tip.

Because the rotor static droop is not large, it is not necessary to resort to a fixed tilt of the rotor shaft forward with respect to the static ground line. This is advantageous to a crane-type helicopter as there is then no tendency to roll or slide along the ground as lift is increased at takeoff.

The flexure structure is redundant in that each flange is composed of several pieces. A crack in one piece should not progress into the other pieces with catastrophic rapidity. The flexure is fail-safe with respect to the largest loads which are the first, or cantilever, mode flapping (rotor moment) and the first mode in-plane (drag variation due to forward velocity). The ability of the flexure to transmit a flap-wise bending moment is a function of its stiffness. If a crack should progress through one of the flanges of the cruciform flexure cross section, the flexure stiffness would decrease substantially. The blade would move toward the articulated blade situation where no moment can be transmitted because no stiffness is present. Sufficient material would remain to carry centrifugal force and to prevent blade separation. The rotor would probably become quite rough in operation with one soft blade out of track with the other four. This should warn the pilot to make an emergency landing.



Because its first in-plane natural frequency is below 1/rev, the flexure is similiary fail-safe with respect to first-mode in-plane loads. As the in-plane stiffness decreases with the damage to the flexure, the first in-plane natural frequency is reduced further below 1/rev and the dynamic magnification factor decreases very rapidly. Thus, as the damage progresses, the loads causing the damage decrease.

Repair and inspection on this rotor are simplified by the ability to remove the torque tube and blade segments individually without removing the entire blade assembly from the vehicle. The blade can be stripped down to the spar/flexure for inspection and replacement of damaged segments.

#### FABRICATION CONSIDERATIONS

The hub is a one-piece forging in titanium alloy or steel. It is 30 inches in diameter and about 16 inches high. Fabrication does not appear to offer any particular problems.

The flexure/spar assembly requires bonding facilities capable of handling a 54-foot length.

Strip stock in the thicknesses and lengths required for the flexure/spar is currently available in stainless steel but not in titanium alloy. According to titanium suppliers, the mill facilities capable of rolling the material required in this design are being constructed and should be in operation by the end of this year (1965).

The formed sections in titanium alloy would require hot forming. This is feasible but considerably more expensive than cold forming in stainless steel.

The flexure/spar root fitting is a machined forging in either titanium alloy or steel. While its machining is complicated because it accommodates the blade built-in coning angle and an average blade angle of attack, it is no more difficult than many current rotor articulation fittings.

Fairly sophisticated tooling can be justified for the molded fiber glass blade segments because of the large number required. Sixty segments are required per helicopter.

#### HELICOPTER GENERAL ARRANGEMENT

The helicopter general arrangements presented in this report were developed for analysis purposes and are not intended to reflect a recommended configuration.

The general arrangement configuration shown in Figure 59 was developed during the preliminary design phase of this program. The primary differences between this configuration and the configuration of Figure 2 are:

- Landing gear arrangement
- Passenger carrier in crane configuration
- Engine arrangement

The landing gear was changed from a main and tail type to a tandem straddle type. The tandem straddle-type gear has the following advantages.

- Helicopter can taxi forward off a cargo load, which eliminates hovering release or takeoff after load is released.
- Cockpit height from ground is greatly reduced during landing flares
- Ground height can be varied through use of landing gear oleo struts

The fuselage was sized to accommodate passengers, which eliminated the need of the pod as a passenger carrier.

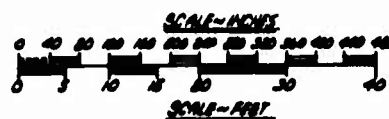
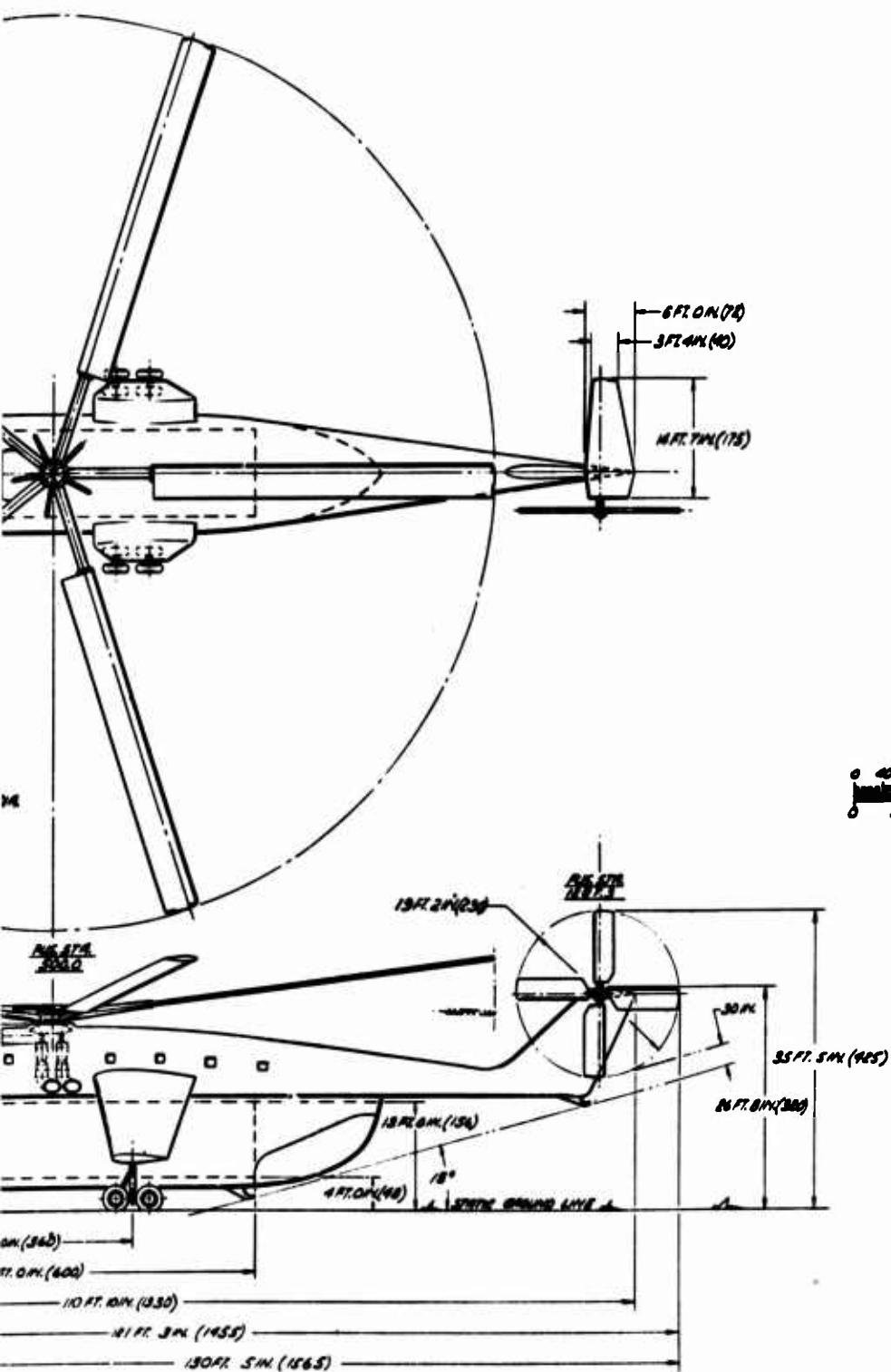
The engine arrangement was changed from two horizontally mounted to three vertically mounted engines.

The external cargo pod configuration as shown has an advantage over the internal cargo configuration in that the side area is greatly reduced for the transport configuration. A more detailed design and tradeoff study would be required to determine the optimum configuration.

The cargo compartment size for the external pod configuration shown is 50 feet long, 9 feet high, and 10 feet 5 inches wide, which is equivalent to that of a C-130 airplane.

The rotor/propulsion system resulting from this study would be applicable to either an external or an internal cargo configuration.





<b>ADVANCED DESIGN</b>		DESIGNED - CALIFORNIA
GENERAL ARRANGEMENT - H.L.H.		DESIGNED - CALIFORNIA
SINGLE MOTOR-CARGO POD		
CL 875-9	CL 875-9	CL 875-9

### SECTION 3

## STATIC AND DYNAMIC ANALYSES

### INTRODUCTION

Analyses were conducted to determine the static and dynamic loads, and the dynamic and aeroelastic characteristics of the rotor system. The fatigue loading spectra of the rotor system are included in this section.

Although this study is concerned only with a shaft-driven rotor system, suitable assumptions are made to define those vehicle parameters necessary for an adequate analysis of the rotor system, such as center-of-gravity limits, main landing gear tread, etc.

The criteria for structural design and the methods for determining the elastic response and the resulting loads on the rotor for the various flight conditions are consistent with the Lockheed gyro controlled-rigid-rotor concept. Helicopters using such a system (e.g., the Model XH-51) have been shown, both in wind tunnel tests and in extensive flight testing, to achieve the goals initially established for this rotor concept.

### STRUCTURAL DESIGN CRITERIA

The structural design criteria adopted for this heavy-lift rotor study are guided by the requirements of MIL-S-8698(ASG) and are presented in the following paragraphs.

#### Mission Profiles

Three missions are considered in defining the required strength level of the rotor system. The parameters which are pertinent to the structural design of the rotor system and are dependent on the mission are given in Table I.

#### Design Weights

The design weights vary with the mission as indicated in Table IX.

TABLE IX DESIGN WEIGHTS			
	TRANSPORT (1b)	HEAVY-LIFT (1b)	FERRY (1b)
Weight Empty	29,105	29,105	32,944
Crew	600	600	600
Operating Weight Empty	29,705	29,705	33,544
Fuel	5,620	2,620	56,800
Gross Weight Less Payload	35,325	32,325	90,344
Payload	24,000	40,000	0
Design Gross Weight (Outbound)	59,325	72,325	90,344
Design Gross Weight (No Payload)	35,325	32,325	

#### Design Center-of-Gravity Range

The range of center-of-gravity travel considered for structural design is

Forward	32 in.
Aft	28 in.
Lateral	0 in.

These distances are measured from the centerline of the main rotor shaft and represent the maximum center-of-gravity travel. For the fatigue life determination, rational intermediate centers of gravity are considered together with appropriate percentages of total flight time at each selected location.

## Design Speeds

### Design Vehicle Speeds:

	<u>Transport</u>	<u>Heavy-Lift</u>	<u>Ferry</u>
V Cruise (knots)			
With payload	110	95	
No payload	130	130	130
V <sub>D</sub> (knots)			
With payload	132	114	
No payload	156	156	156

### Design Rotor Speeds (Power-On):

	<u>rpm</u>	<u>Angular Velocity (radian/sec)</u>	<u>Tip Speed (ft/sec)</u>
Normal	121	12.65	700
Design minimum	109	11.48	627
Design maximum	133	13.90	765

### Design Rotor Speeds (Power-Off):

	<u>rpm</u>	<u>Angular Velocity (radian/sec)</u>	<u>Tip Speed (ft/sec)</u>
Normal	121	12.65	700
Design minimum	105	11.00	605
Design maximum	137	14.33	790

## Design Load Factors

Maneuver Load Factors - The design maneuver load factors for the three missions considered are specified in the Statement of Work. These are repeated below, the values shown being at the design gross weight.

<u>Load Factor</u>	<u>Transport</u>	<u>Heavy-Lift</u>	<u>Ferry</u>
+ n	2.5	2.5	2.0
- n	-0.5	-0.5	-0.5

The expression which describes the load factor capability of a rotor as a function of the maximum mean rotor lift coefficient,  $\bar{C}_{L_{\max}}$ , is given in NACA TN 2990 (Reference 14) as:

$$n_{\max} = \left( \frac{\bar{C}_{L_{\max}}}{\bar{C}_{L_t}} \right) \left( \frac{B^3 + \frac{3}{2}B\mu_n^2 - \frac{4}{3\pi}\mu_n^3}{B^3 + \frac{3}{2}B\mu_t^2 - \frac{4}{3\pi}\mu_t^3} \right) \left( \frac{\Omega_n}{\Omega_t} \right)^2 \left( \frac{\cos \alpha_{on}}{\cos \alpha_{ot}} \right)^3$$

where

$\bar{C}_{L_{\max}}$  = maximum mean rotor lift coefficient

$$\bar{C}_{L_t} = \text{trim lg lift coefficient} = \frac{6 C_{T_t}}{\sigma} \left[ \frac{1}{B^3 + \frac{3}{2}B\mu_t^2 - \frac{4}{3\pi}\mu_t^3} \right]$$

$B$  = tip loss factor = 0.97

$\Omega$  = rotor speed, radians/sec

$\mu$  = advance ratio =  $\frac{V \cos \alpha}{\Omega R}$

$V$  = forward velocity, fps

$\alpha$  = rotor angle of attack

$R$  = rotor radius, 55 ft

$$C_{T_t} = \text{thrust coefficient} = \frac{T_t}{\pi R^2 \rho (\Omega_t R)^2}$$

$\rho$  = air mass density

$T_t$  = trim lg rotor thrust =  $W$

$\sigma$  = rotor solidity =  $\frac{bC}{\pi R}$

$b$  = number of blades = 5

$C$  = blade chord = 3.41 ft



### Subscripts

t = trimmed lg flight

n = value at maximum load factor

Substituting the expressions for  $\bar{C}_{L_t}$  and  $C_{T_t}$  into the equation for  $n_{\max}$  and letting

$$v = B^3 + \frac{3}{2} B \mu_n^2 - \frac{4}{3\pi} \mu_n^3$$

yields

$$n_{\max} = \frac{b C_R \rho \bar{C}_{L_{\max}} v (\Omega R)_n^2}{6 W} \left( \frac{\cos a_{On}}{\cos a_{Ot}} \right)^3$$

Introducing the constants above and conservatively assuming

$\left( \frac{\cos a_{On}}{\cos a_{Ot}} \right)^3 = 1$  results in the following solution for this vehicle at sea level.

$$n_{\max} = (0.372) \frac{\bar{C}_{L_{\max}} v (\Omega R)_n^2}{W}$$

The maximum attainable mean rotor lift coefficient,  $\bar{C}_{L_{\max}}$ , for a given rotor speed and forward speed is obtained by conservatively assuming that all blade sections are operating at  $C_{L_{\max}}$  as a function of local Mach number. When the reverse flow region is considered, the following equality describes  $\bar{C}_{L_{\max}}$ :

$$\begin{aligned} \bar{C}_{L_{\max}} \frac{b}{2\pi} \rho C \left\{ \int_0^B \int_0^{2\pi} \frac{U^2}{2} dx d\psi - \int_0^{\mu \sin \psi} \int_{\pi}^{2\pi} U^2 dx d\psi \right\} \\ = \frac{b}{2\pi} \rho C \left\{ \int_0^B \int_0^{2\pi} C_{L_{\max}} \frac{U^2}{2} dx d\psi - \int_0^{\mu \sin \psi} \int_{\pi}^{2\pi} C_{L_{\max}} U^2 dx d\psi \right\} \end{aligned}$$

where

$$U = \Omega R (X + \mu \sin \psi)$$

= blade section local velocity, fps

$X$  = spanwise blade section location, nondimensional

$\psi$  = rotor blade azimuth position

$C_{L_{\max}}$  = Two-dimensional section maximum lift coefficient  
as a function of local Mach number

$$= A_0 + A_1 M_x + A_2 M_x^2 + A_3 M_x^3 + A_4 M_x^4$$

$A_0, A_1, A_2, A_3, A_4$  = coefficients which describe the curve for  $C_{L_{\max}}$  as a function of local Mach number

$M_x$  = local Mach number

$$= M_t (X + \mu \sin \psi)$$

$M_t$  = rotational tip Mach number

$$= \frac{\Omega R}{1116.89} \text{ (sea level)}$$

Substituting the expressions for  $U$  and  $C_{L_{\max}}$  in the above equality yields the following, when  $B = 0.97$ :

$$\bar{C}_{L_{\max}} = \left[ \frac{1}{0.9127 + 1.455\mu^2 - 0.4244\mu^3} \right] \left\{ \begin{aligned} &0.9127 A_0 + 0.6640 A_1 M_t + 0.5152 A_2 M_t^2 + 0.4165 A_3 M_t^3 + 0.3463 A_4 M_t^4 \\ &+ \left[ 1.455 A_0 + 2.1170 A_1 M_t + 2.7380 A_2 M_t^2 + 3.3198 A_3 M_t^3 + 3.8643 A_4 M_t^4 \right] \mu^2 \\ &+ \left[ 0.2812 A_1 M_t + 1.0912 A_2 M_t^2 + 2.6463 A_3 M_t^3 + 5.1338 A_4 M_t^4 \right] \mu^4 \\ &+ \left[ 0.1562 A_3 M_t^3 + 0.9094 A_4 M_t^4 \right] \mu^6 \\ &- 0.4244 A_0 \mu^3 - 0.2037 A_2 M_t^2 \mu^5 - 0.1247 \mu^7 \end{aligned} \right\}$$

Figure 60 shows the maximum two-dimensional lift coefficient versus Mach number as given in Figure 33 of ARC R and M No. 2678 (Reference 15). The expression for  $C_{L_{\max}}$  and the resulting curve which fits the reference points are also included.

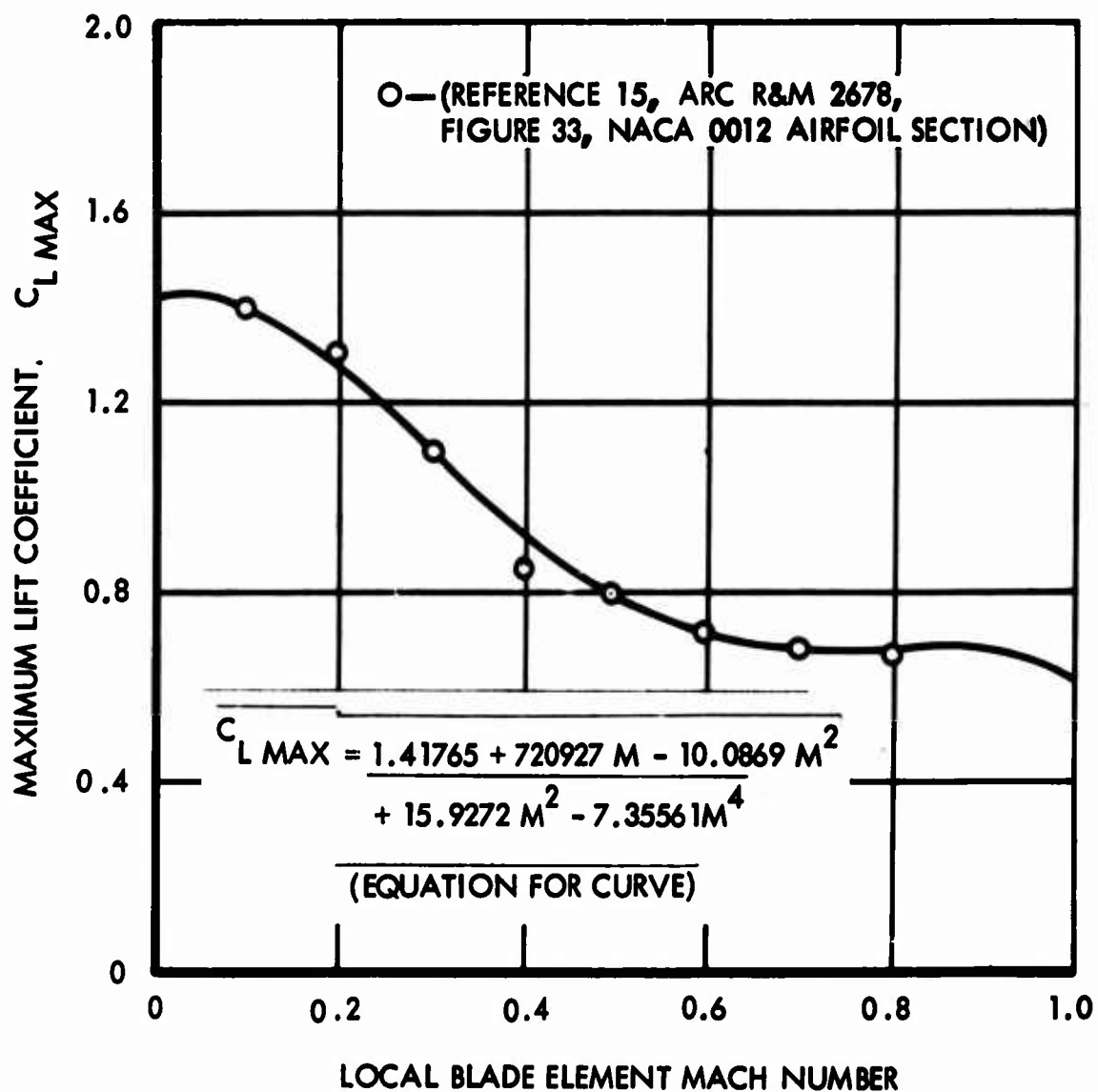


Figure 60. Variation of Two Dimensional Section  $C_{L \text{ max}}$  with Mach Number

Figure 61 shows the maximum mean rotor lift coefficient,  $\bar{C}_{L_{\max}}$ , versus advance ratio,  $\mu$ , for various mean rotor tip Mach numbers,  $M_t$ . This figure was constructed by substituting the coefficients which describe Figure 60 into the above expression for  $\bar{C}_{L_{\max}}$  and by evaluating for various combinations of  $\mu$  and  $M_t$ .

An example calculation for the rotor load factor capability is shown below.

$$\text{rpm} = 121 \quad (\Omega R = 700 \text{ fps})$$

$$W = 72,325 \text{ lb}$$

$$\mu = 0.2$$

$$V = 140 \text{ fps (82.9 knots)}$$

$$M_t = \frac{700}{1116.89} = 0.627$$

$$\bar{C}_{L_{\max}} = 0.848 \text{ (Figure 61)}$$

$$\nu = 0.965 \text{ (Figure 61)}$$

$$n_{\max} = 0.372 \quad \frac{C_{L_{\max}} (\Omega R)^2 \nu}{W}$$

$$n_{\max} = \frac{(0.372) (0.848) (700)^2 (0.965)}{72,325} = 2.06$$

Figure 62 shows calculated values of  $n_{\max}$  and the structural design envelopes for the design weights at sea level conditions. Load factors at higher altitudes are less than those for sea level.

Gust Load Factor - The rotor system is designed to a 30-fps vertical gust in combination with 1.0g flight. No alleviation factor is considered. Only at low gross weights does the incremental load factor exceed 1.5g. Although, at these gross weights, the total load factor would increase the design loads on fuselage dead weight items, the associated rotor loads based on  $nW$  will be less than those resulting from maneuvering flight.

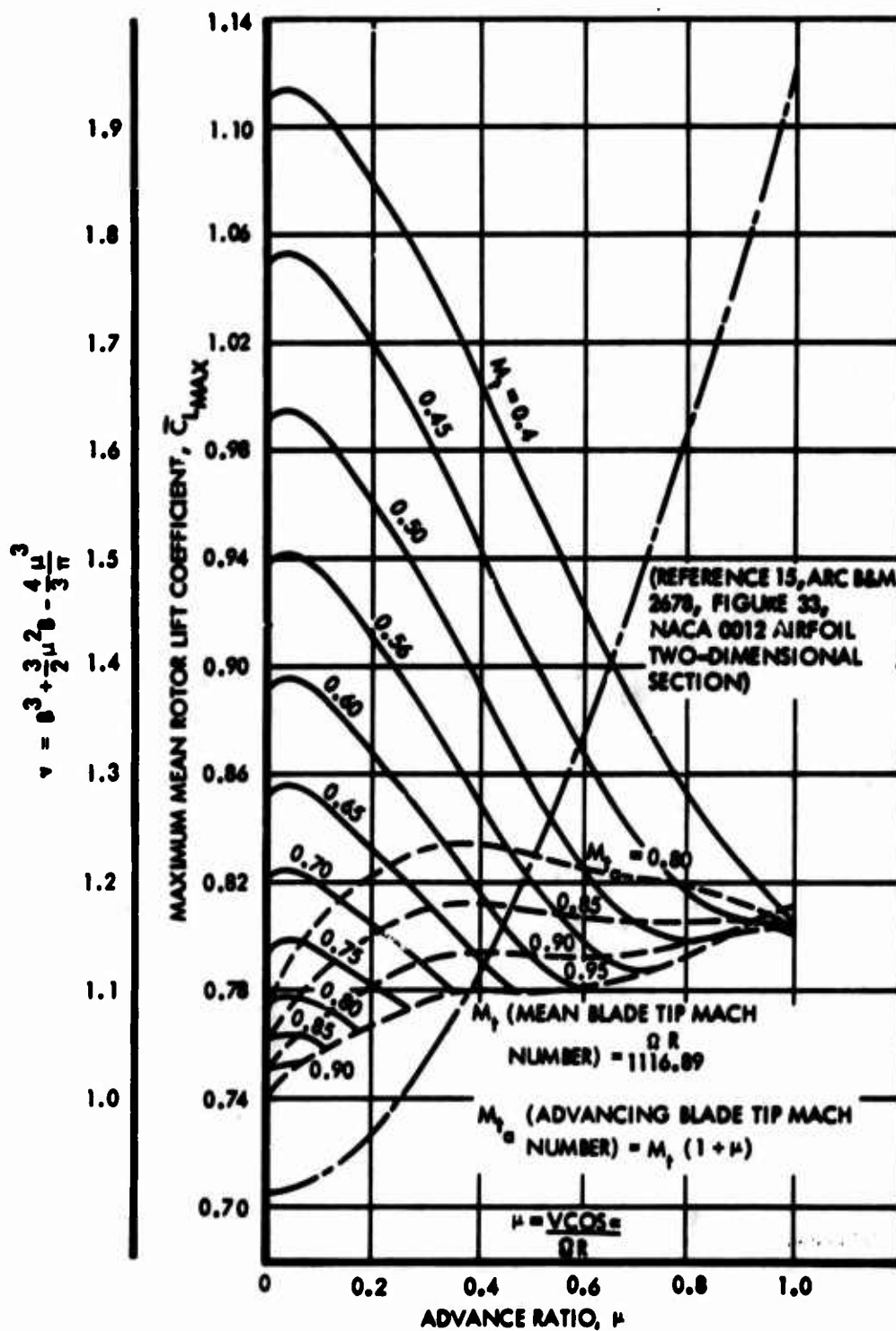


Figure 61. Maximum Mean Rotor Lift Coefficient vs Advance Ratio

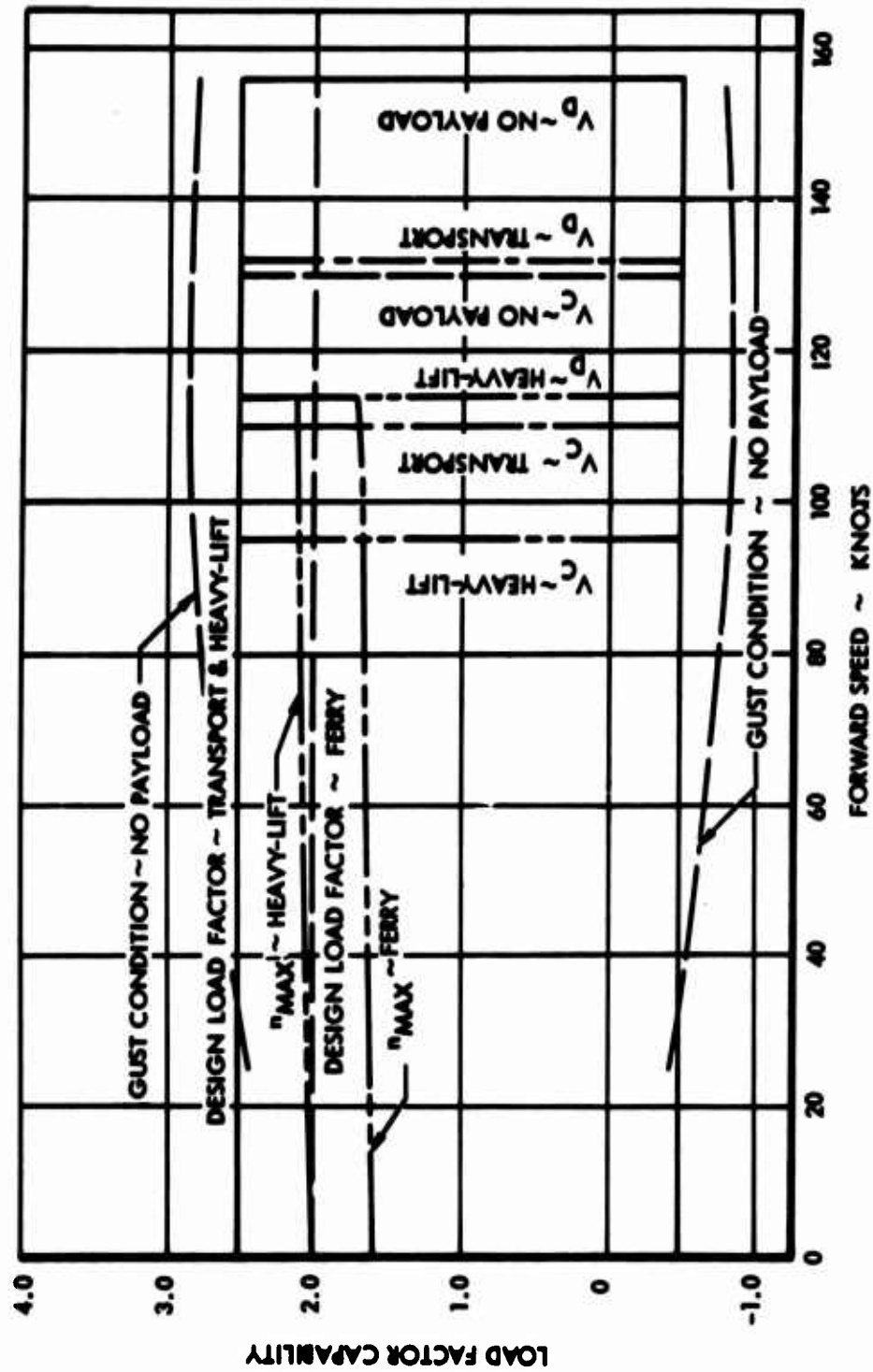


Figure 62. V-n Diagram

### Design Flight Conditions

To evaluate the feasibility of the heavy-lift rotor system, strength level loads and fatigue spectra are determined for a number of points on the V-n diagrams. These include forward speeds from hover to 1.2 cruise speed and load factors from -0.5g to the maximum design value for the given mission. At each of the selected combinations of velocity and load factors, an appropriate range of center-of-gravity travel is assumed. Since this is a feasibility study, rotor rpm excursions are not considered.

- Symmetrical Flight

Unaccelerated Flight - Rotor loads are obtained in the 1.0g balanced flight conditions at a range of significant forward speeds for the three missions.

Symmetrical Dive and Pull-Out - These maneuvers are performed for the same speeds as those considered for the unaccelerated flight conditions.

### Design Ground Loading Conditions

- Design Landing Conditions

The design landing conditions do not result in critical rotor loads and are not considered in this study.

- Design Takeoff conditions

The Lockheed gyro controlled-rigid-rotor system permits take-off from sloping terrain without the pendulum action associated with the articulated rotor system. The placard operation sequence for takeoff from such a terrain consists of first applying collective pitch to attain a rotor lift of at least  $1/3 W$  followed by cyclic control to right the vehicle. Upon reaching a horizontal attitude, further collective pitch is applied with appropriate reduction of cyclic pitch as the vehicle lifts off. The maximum rotor hub moment occurs at the instant the downhill gear leaves the ground. The heavy-lift rotor system is designed for takeoff from a 10-degree slope.

### Main Rotor Structural Requirements

The main rotor is designed to the following specific requirements:

- The main rotor structure is designed to withstand the critical flight and ground loading conditions, the criteria for which are presented in paragraphs "Design Flight Conditions" and "Design Ground Loading Conditions."
- The hub, blades, blade attachments, and blade controls which are subject to alternating stresses are designed to the requirements presented in this section under "Fatigue Evaluation."
- The rotor assembly is designed to withstand, at all speeds including zero, a design limit torque of 1.25 times the mean torque for maximum continuous power.
- The requirements for rotor acceleration are those of paragraph 3.3.1 of MIL-S-8698. The rotor acceleration loads are those developed by application of 1.5 times the torque developed at the military power rating of the engine in 0.1 second. These loads are equally distributed to all blades of the rotor.

### METHOD OF ANALYSIS - BASIC LOADS PROGRAM

Whereas the dynamic stability and forced response of the vehicle are examined by considering the coupling between the flapwise bending, chordwise bending, and the torsional characteristics of the rotor, the rotor blade loads analysis considers only the structural coupling between flapwise and chordwise bending. The inclusion of torsional characteristics in any rotor blade coupled loads analysis is primarily to gain an insight to blade torsion and associated control loads and does not materially affect the amplitude or character of the flapwise and chordwise bending. The coupled flapwise-chordwise response program described here, therefore, is adequate for rotor blade parametric studies.

### Digital Program for Coupled Helicopter Blade Loads

This program consists of a performance/trim program and a coupled dynamic response analysis for the individual blades. An iterative procedure is used to obtain the performance and trimmed attitude of the vehicle consistent with blade flexibility and loads. In an added option, this program is capable of considering the rotor isolated from the vehicle body when the rotor angle of attack, thrust and hub moments are assigned. The advantage of the isolated rotor capability is that the rotor performance conditions can be obtained from any source to determine the blade loads.



The rotor aerodynamic output determines the radial distribution of aerodynamic loads at preselected azimuth positions and the azimuthal distributions, in harmonic form, at preselected radial stations. The blade loading at any radial station and azimuth position is obtained by use of local  $C_L$  and  $C_D$  data versus angle of attack and Mach number. The inflow velocity includes components which reflect the damping in the system resulting from the elastic motion of the blade.

The coupled dynamic response analysis of the blade considers the structural coupling between flapwise and chordwise bending due to the collective and blade twist angle. For the rigid rotor, the coupling effect of cyclic pitch, with built-in cone and sweep angles, on the first harmonic response is also considered. The coupled response of the blade is computed for the first six harmonics of the airload distribution obtained in the aerodynamic analysis, the total response being the summation of these. The spanwise variation of bending moment on the elastic blade is calculated by successively evaluating the moment, slopes, displacements, and inertia shears, along the blade, in terms of the unknown conditions at the blade root. The boundary conditions at the blade tip are that the moments and inertia shears must be zero. The solution of the simultaneous equations representing the flapwise and chordwise moments and inertia shears at the tip yields the root moments and inertia shears. The blade loads presented in this report are developed by using both options of this program, i.e., the trimmed vehicle and the isolated rotor.

#### Feathering Control Moments

Blade-feathering control moments are estimated by considering the results from the coupled flapwise-chordwise bending response program, the torsional stiffness of the blade flexure, and the centrifugal restoring moment.

The flapwise and chordwise bending moments are resolved into components parallel to and perpendicular to the blade-feathering axis, the blade-feathering moment being the sum of the components along the feathering axis. This resolution is accomplished at blade station 165, at which point the outboard end of the control torque tube is attached, by considering the steady and first two harmonics of blade bending. The inboard end of the torque tube is attached at station 29. The torque tube is capable of carrying torsion and shear loads only. The blade bending moments are resolved into a control moment by multiplying the flapwise bending moment by the blade sweep angle and the chordwise bending moment by the relative blade flapping outboard of the torque tube with respect to the torque tube.

This relationship may be expressed as:

$$M_{fb} = M_{b165} \psi' + Q_{b165} B_{f165}$$

where

$M_{fb}$  = feathering control moment due to blade bending moments

$M_{b165}$  = flapwise bending at station 165

$Q_{b165}$  = chordwise bending at station 165

$\psi'$  = blade sweep angle

$B_{f165}$  = relative blade flapping with respect to the torque tube as a function of the vertical blade displacement (discussed in the following paragraph) and the blade azimuth position

$$= a_0 + a_1 \cos \psi + a_2 \sin \psi + a_3 \cos 2\psi + a_4 \sin 2\psi$$

The relative flapping coefficients  $a_n$  are determined by considering the vertical blade displacement at the end points of the torque tube and the three-quarter point of the blade radius (blade station 495) as follows:

$$a_n = \left[ \frac{\delta_{495n} - \delta_{165n}}{495 - 165} - \frac{\delta_{165n} - \delta_{29n}}{165 - 29} \right]$$

$$= 0.088224 \delta_{29n} - 0.124584 \delta_{165n} + 0.036360 \delta_{495n}$$

where  $\delta_{29n}$ ,  $\delta_{165n}$ , and  $\delta_{495n}$  are vertical blade displacements measured in feet at blade stations 29, 165 and 495, respectively.

The feathering control moment required to overcome the torsional spring rate at the blade flexure is:

$$M_{fK} = K (A_0 - \theta_{165} + \theta_{1c} \cos \psi + \theta_{1s} \sin \psi)$$

where

$K$  = torsional spring rate of the flexure, in.-lb/radian

$A_0$  = static angular position of the flexure, radians

$\theta_{165}$  = mean blade pitch angle at station 165, radians

$\theta_{1c}$  = longitudinal cyclic pitch angle, radians

$\theta_{1s}$  = lateral cyclic pitch angle, radians

The centrifugal restoring moment is determined by the standard method of analysis, and when cyclic pitch is considered, the following expression results:

$$M_{f_{cf}} = -A_1 \sin^2 (\theta_1 + \theta_{0.75}) + 2 A_1 \theta_{1c} \cos \psi + 2 A_1 \theta_{1s} \sin \psi$$

where

$A_1$  = maximum centrifugal restoring moment possible, in.-lb

$\theta_1$  = angle for zero centrifugal restoring moment, radians

$\theta_{0.75}$  = mean blade pitch angle at the three-quarter blade radius, radians

The feathering control moment,  $M_f$ , is

$$M_f = M_{f_b} + M_{f_K} + M_{f_{cf}}$$

### STRUCTURAL DESIGN LOADS

The rotor blade loads for this program were developed for the five different loading conditions shown in Table X.

TABLE X					
STRUCTURAL DESIGN LOAD CONDITIONS					
ITEM	CONDITIONS				
	POWER-ON FLIGHT			POWER-OFF FLIGHT	TAKE-OFF
	COND. 1	COND. 2	COND. 3		
Mission Weight					
Heavy-Lift, 72,325 lb	X			X	X
Transport, 59,325 lb		X			
Minimum Flying, 29,705 lb			X		
Design Cruise Speed					
130 knots			X		
110 knots		X			
95 knots				X	
49 knots	X				
Rotor Speed					
Normal, 121 rpm	X	X	X	X	X
Center of Gravity					
Forward, 32 in.	X	X	X		X
Aft, 28 in.	X	X	X	X	
Zero	X	X	X		
Load Factor - Maneuver					
2.5g to -0.5g	X	X	X		
1g				X	X
Terrain Slope					
10°	-	-	-	-	X

#### Forward Flight

The rotor blade loads as developed by the coupled blade response method described in "Method of Analysis" are given in Figures 63 through 78. Figures 63 and 64 show the variation of flapwise and chordwise bending moment with rotor azimuth position with the steady moment indicated. Figures 65 and 66 show the flap and chord bending moment distribution for cyclic and steady moments along the span of the blade. Figures 67 through 78 show the variation of steady and cyclic blade moments with load factors at selected blade stations for power-on flight conditions of Table X. Figure 79 presents the rotor blade centrifugal force distribution at the normal rotor rpm. Table XI shows blade loads for the power-off flight conditions.

RPM = 121  
C G = 28 IN. AFT OF ROTOR SHAFT

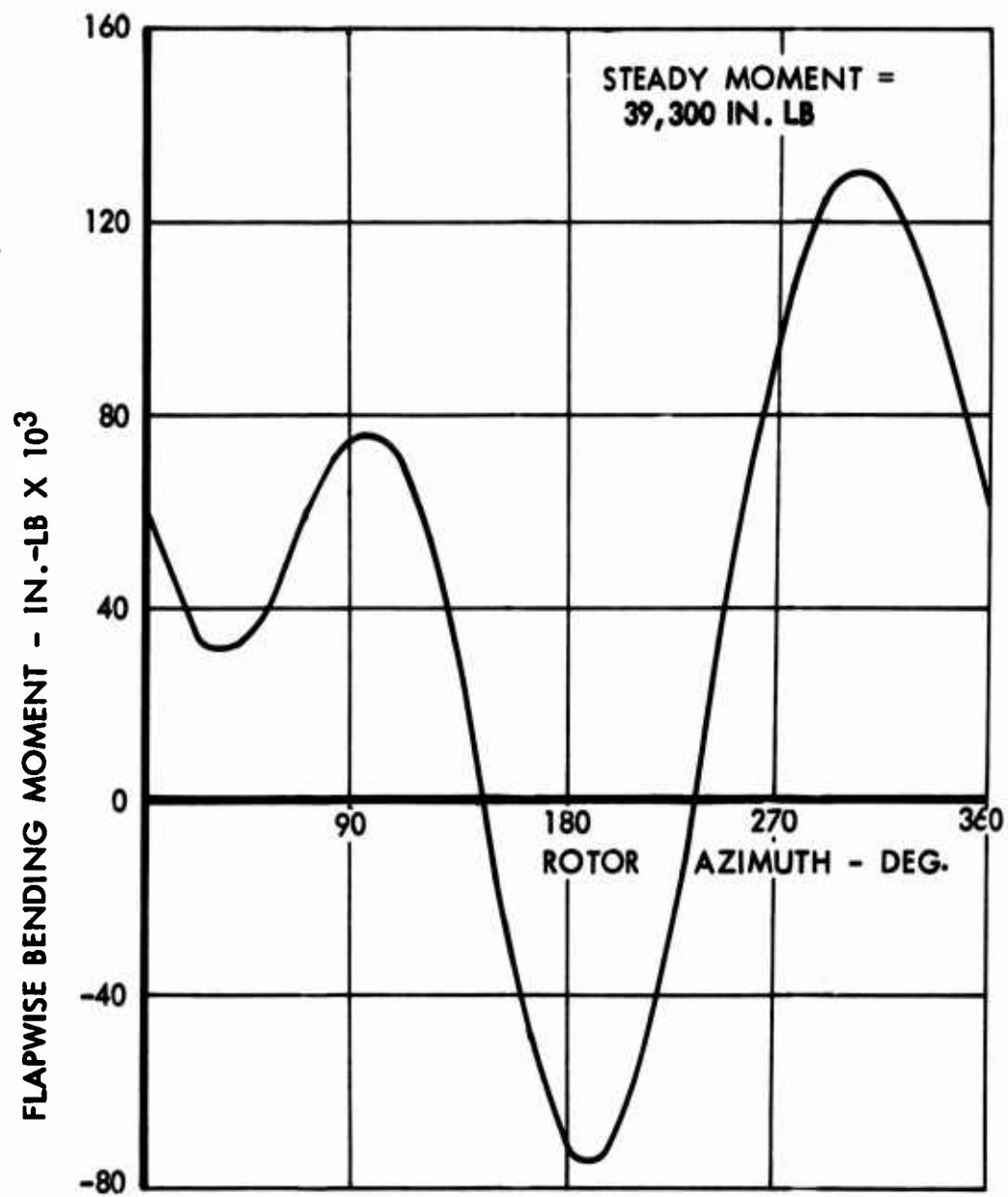


Figure 63. Flapwise Bending Moment vs Rotor Azimuth - Heavy-Lift Mission, 72,325 Pounds, 95 Knots, Rotor Station 165

RPM = 121  
C G = 28 IN. AFT OF ROTOR SHAFT

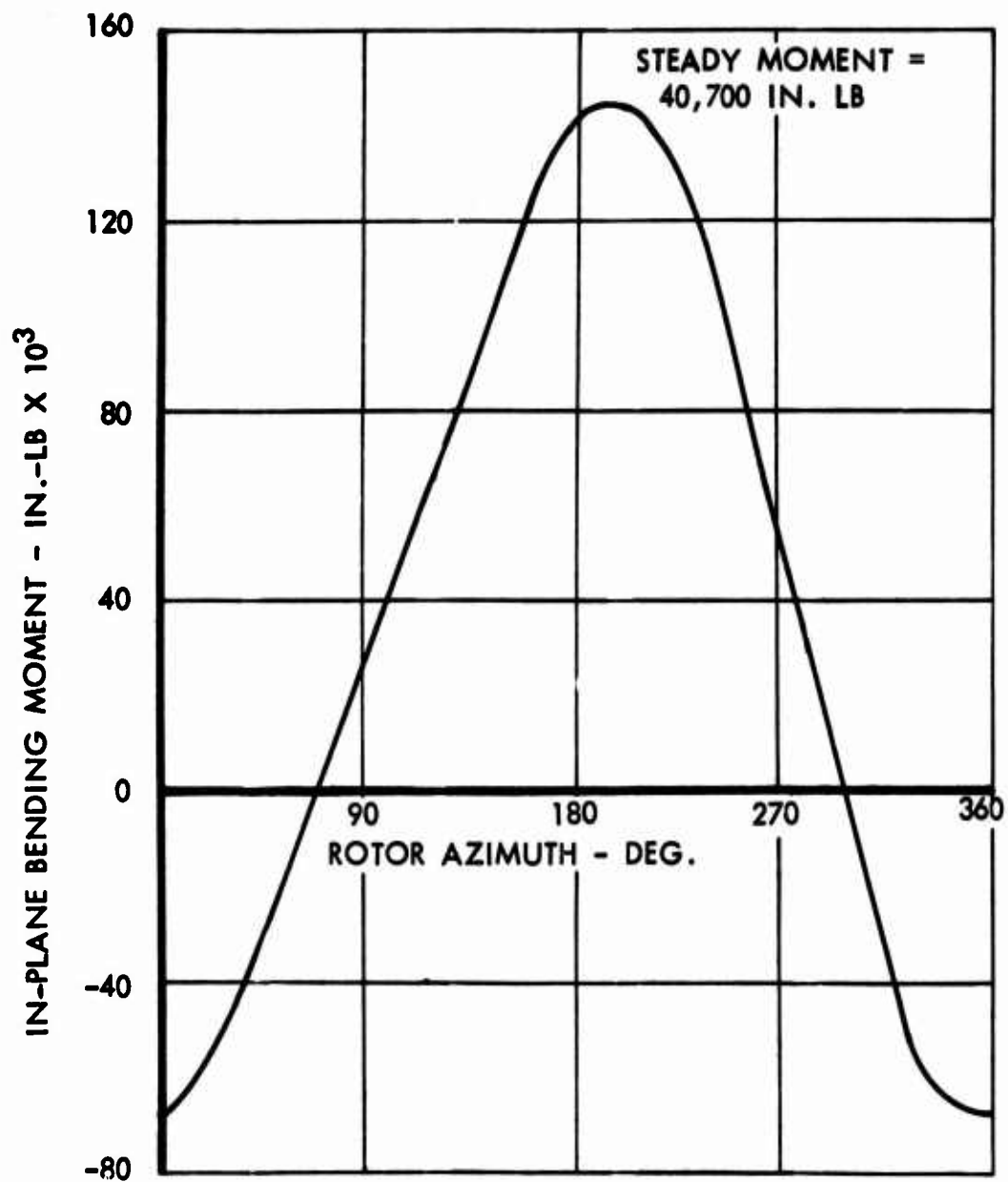


Figure 64. Chordwise Bending Moment vs Rotor Azimuth - Heavy-Lift Mission, 72,325 Pounds, 95 Knots, Rotor Station 165

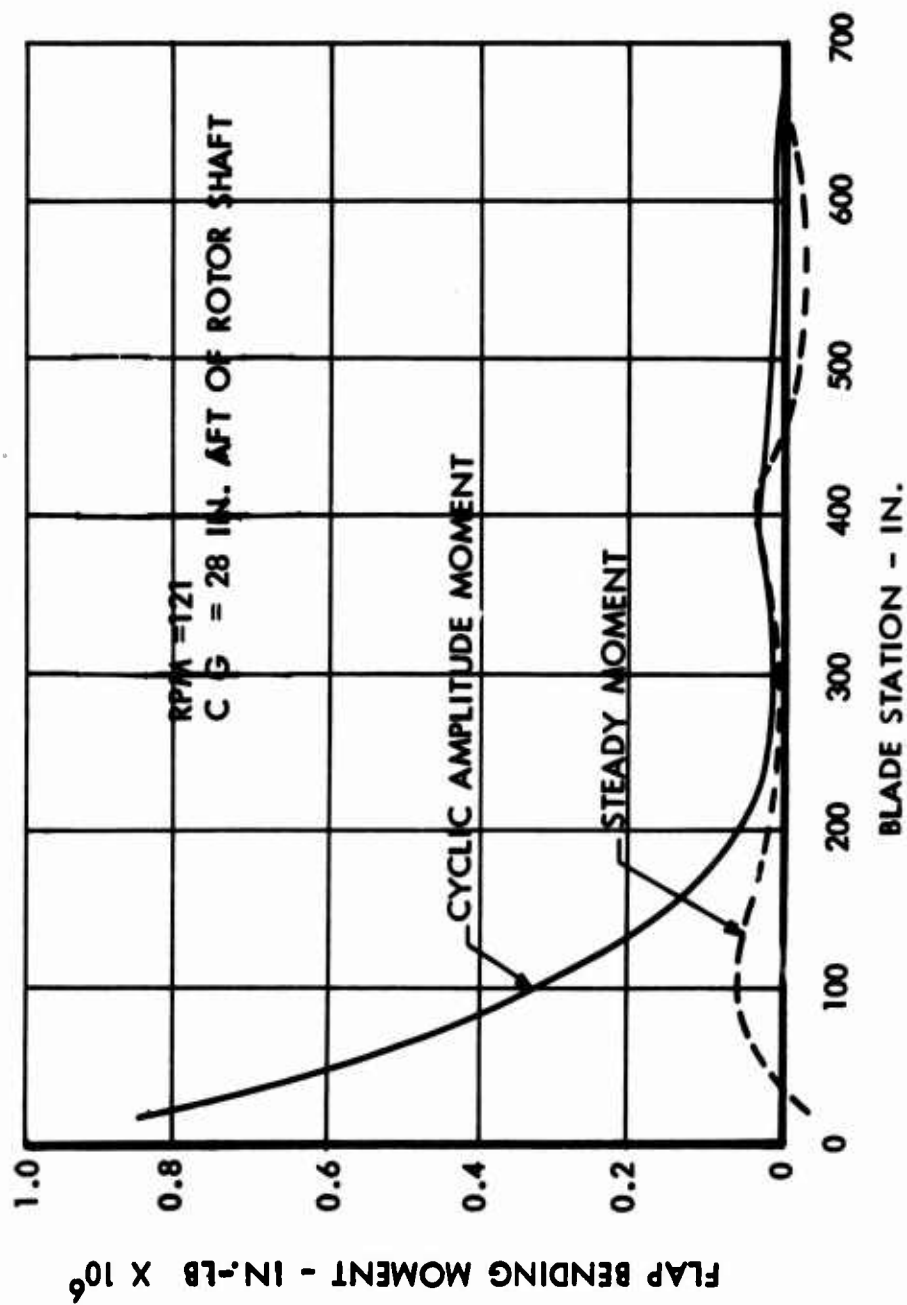


Figure 65. Flap Bending Moment vs Blade Station - Heavy-Lift Mission, 72,325 Pounds, 95 Knots

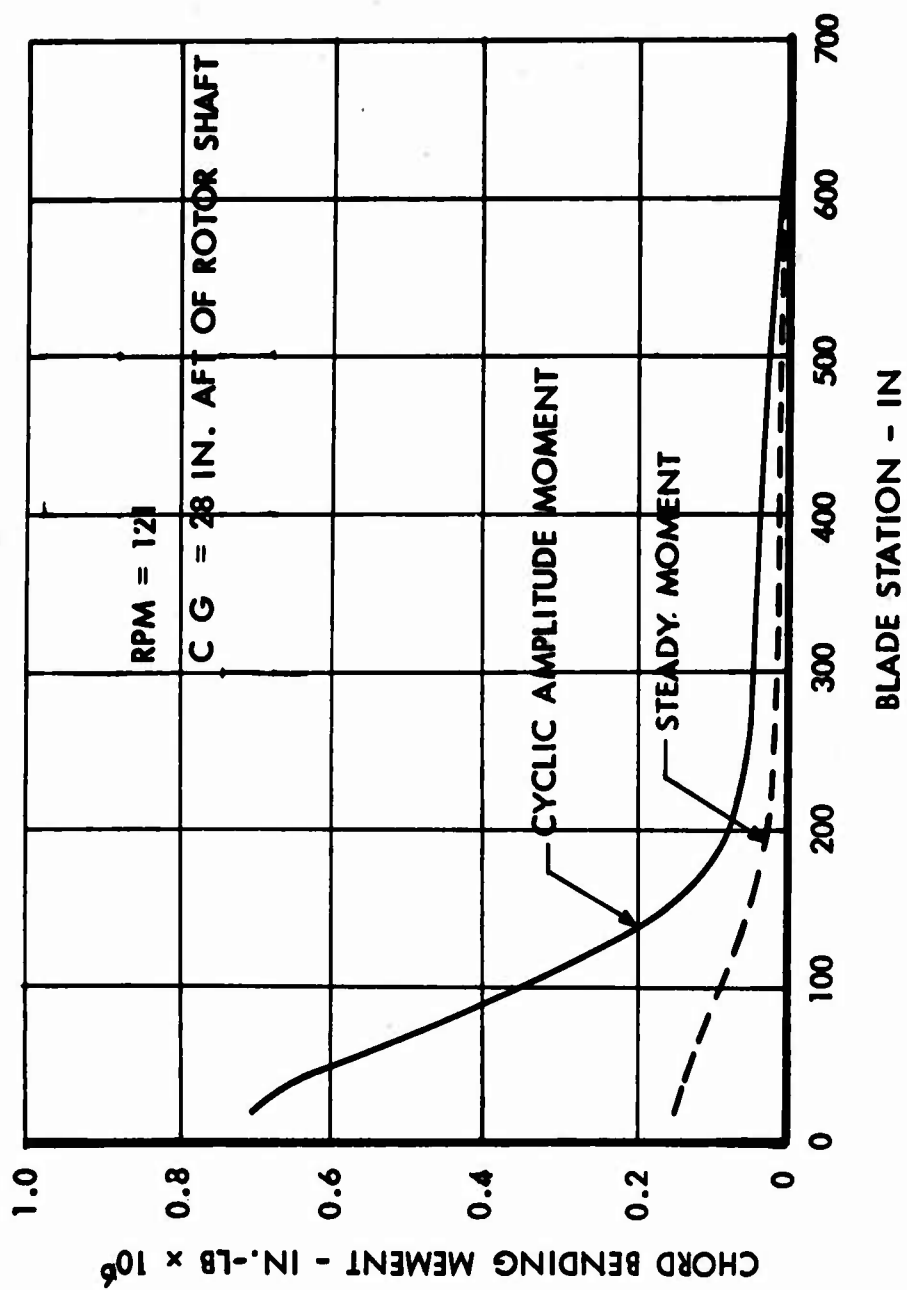


Figure 66. Chord Bending Moment vs Blade Station - Heavy-Lift Mission, 72,325 Pounds, 95 Knots



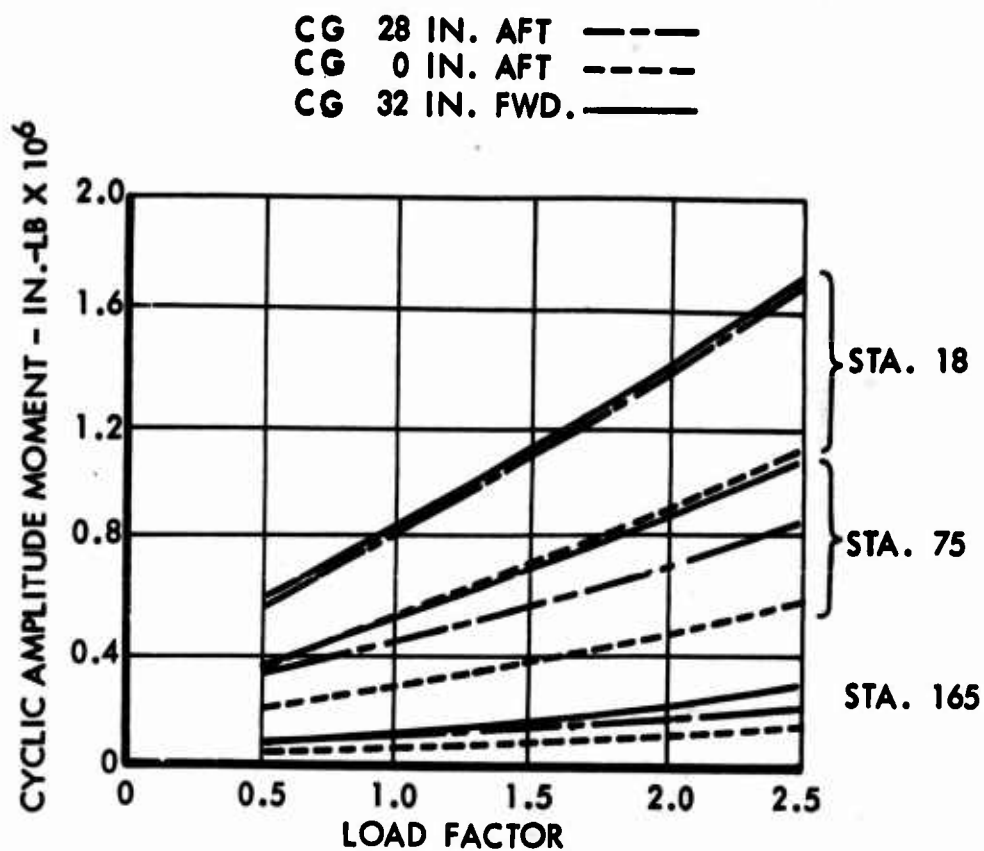


Figure 67. Cyclic Flap Bending Moment vs Load Factor - Heavy-Lift Mission, 72,325 Pounds, 95 Knots

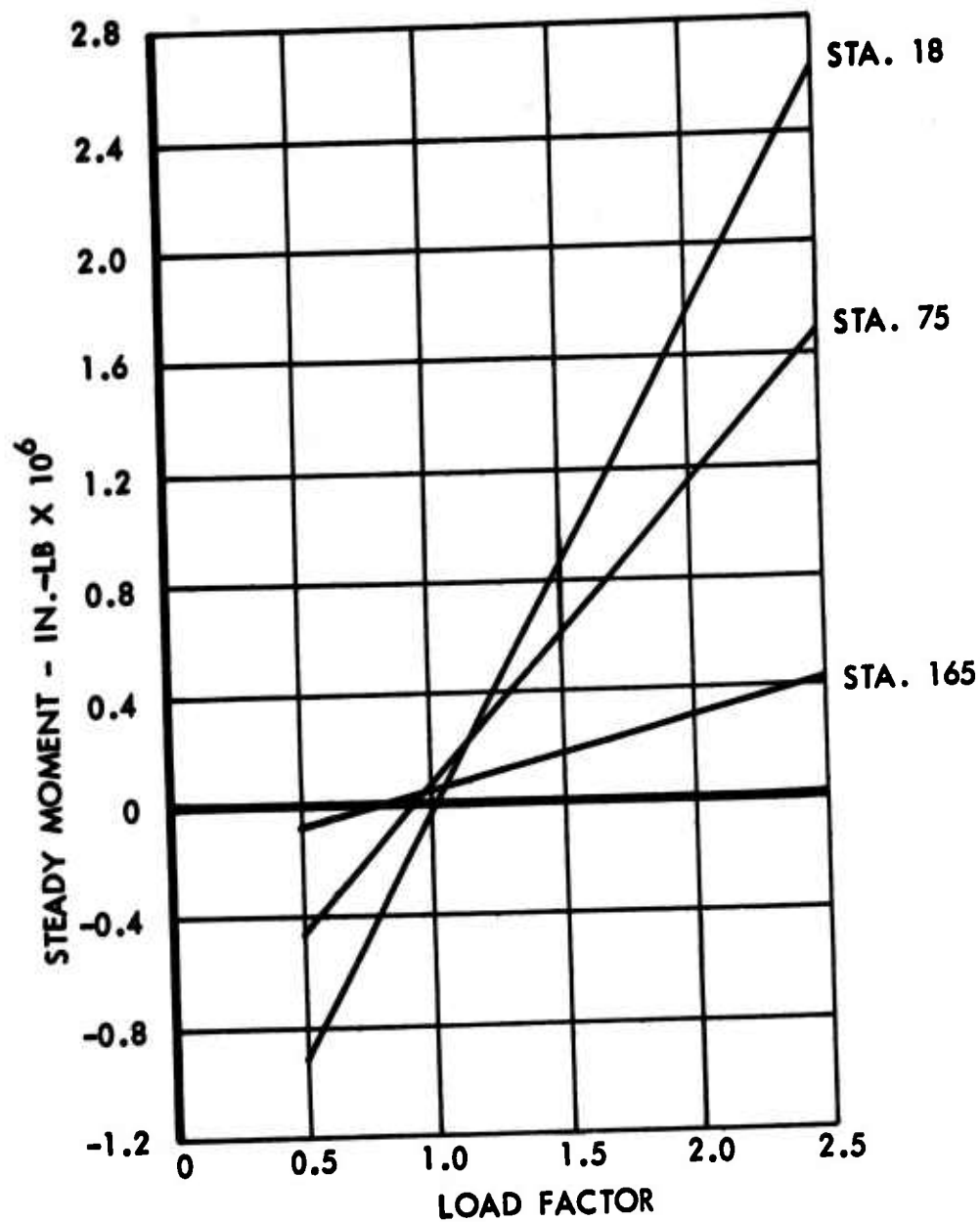


Figure 68. Steady Flap Bending Moment vs Load Factor - Heavy-Lift Mission, 72,325 Pounds, 95 Knots

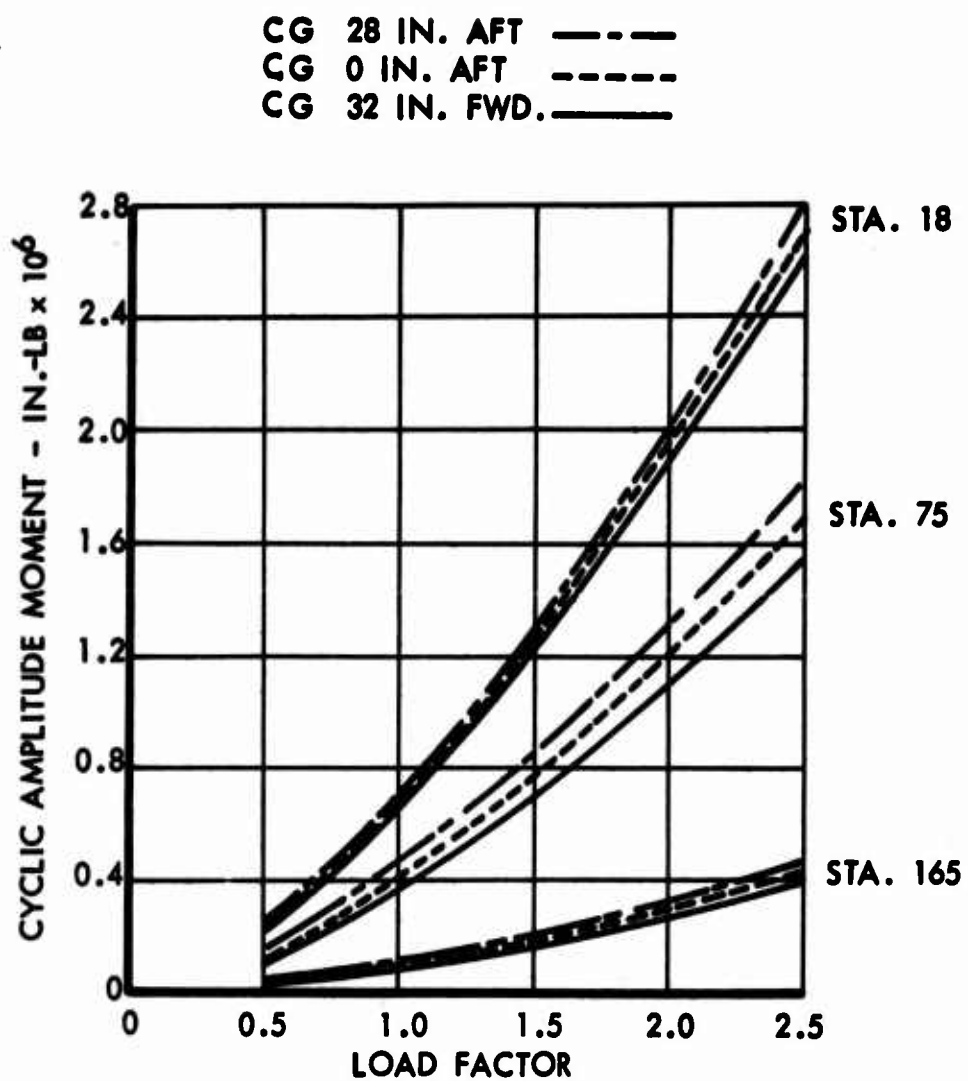


Figure 69. Cyclic Chord Bending Moment vs Load Factor - Heavy-Lift Mission, 72,325 Pounds, 95 Knots

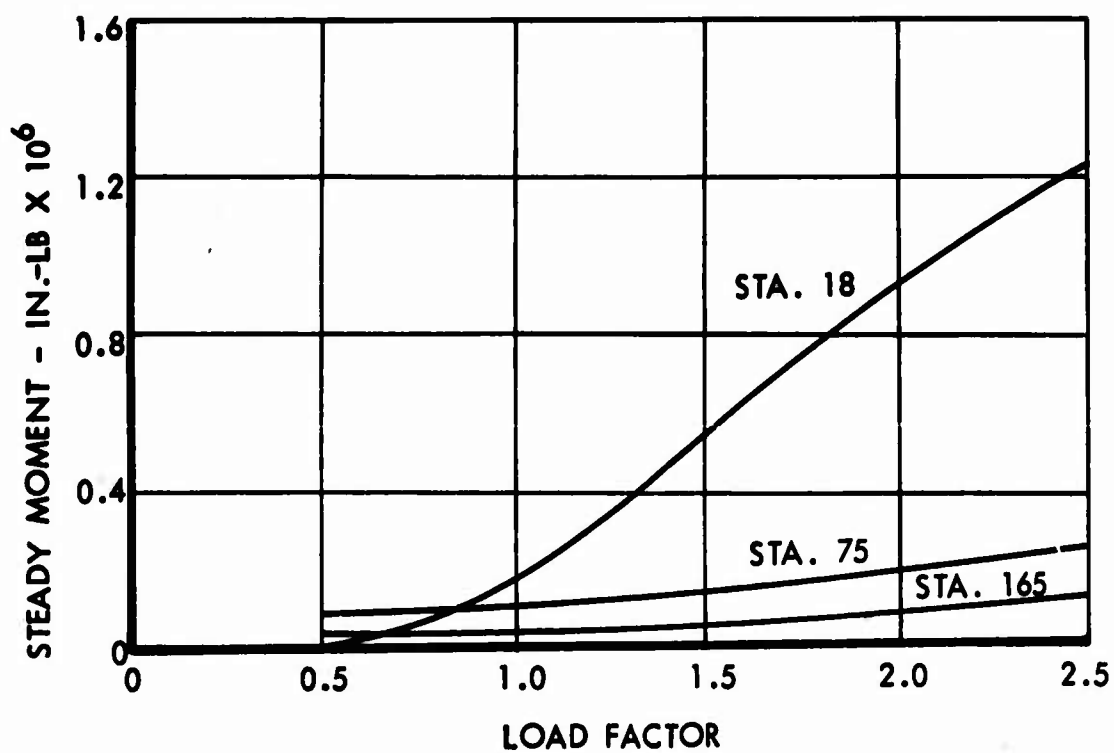


Figure 70. Steady Chord Bending Moment vs Load Facotr - Heavy-Lift Mission, 72,325 Pounds, 95 Knots

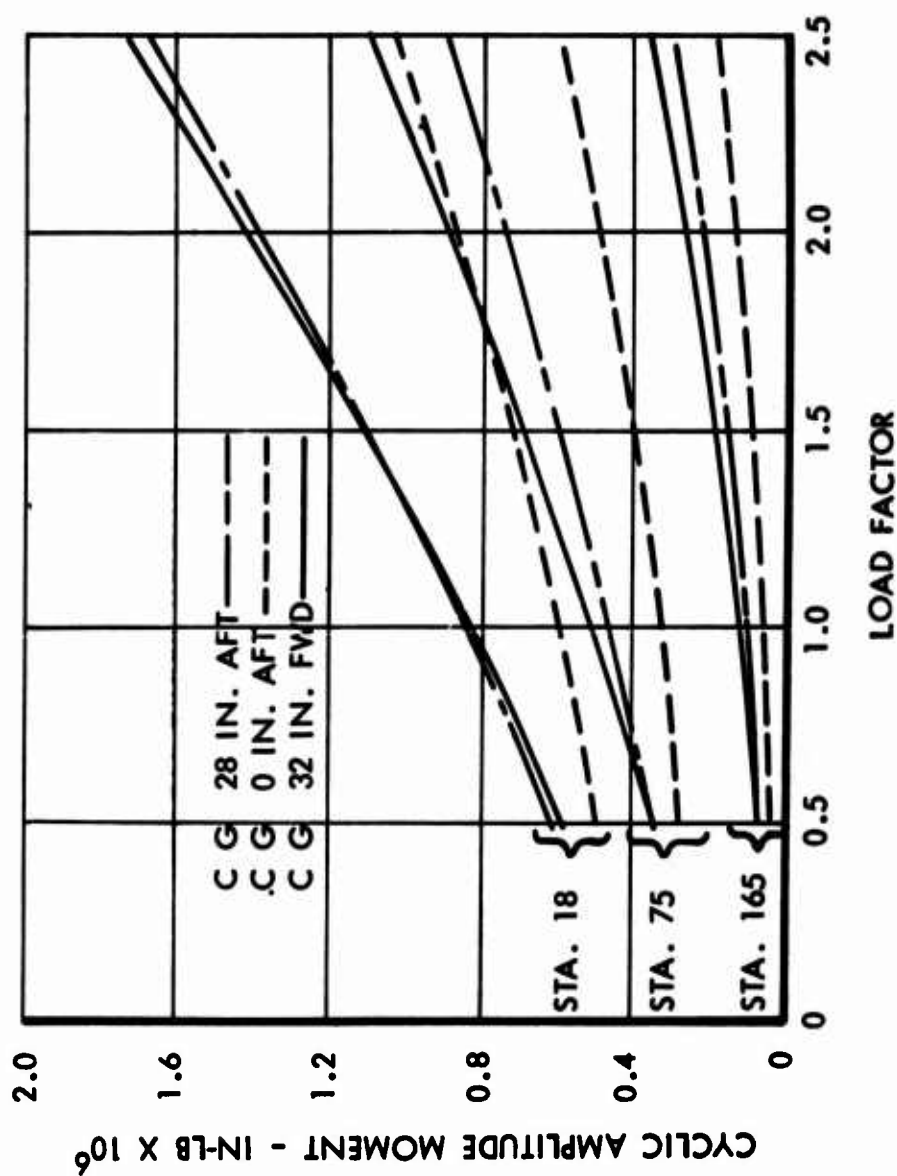


Figure 71. Cyclic Flap Bending Moment vs Load Factor - Transport Mission, 59,325 Pounds, 110 Knots

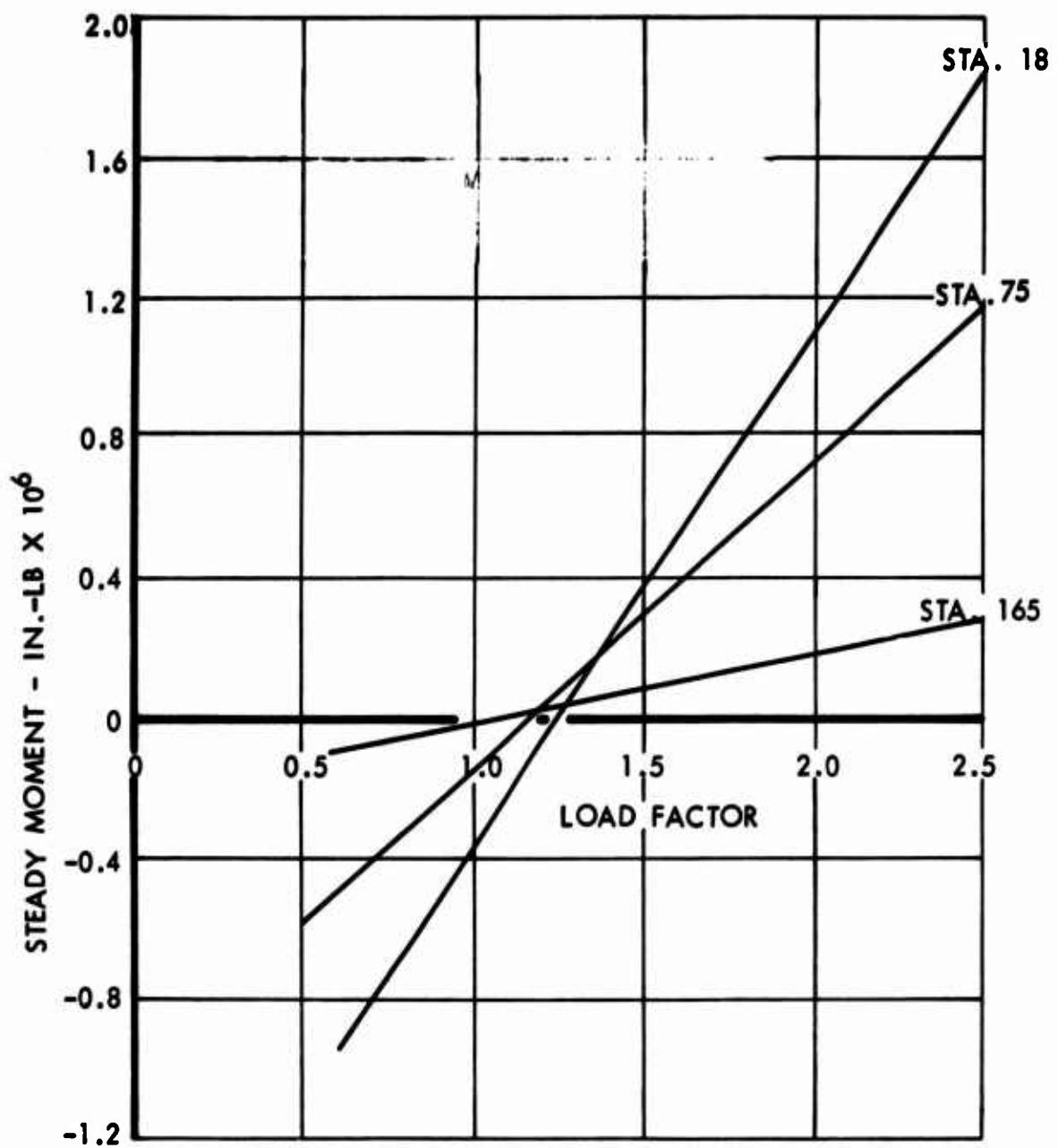


Figure 72. Steady Flap Bending Moment vs Load Factor - Transport Mission, 59,325 Pounds, 110 Knots

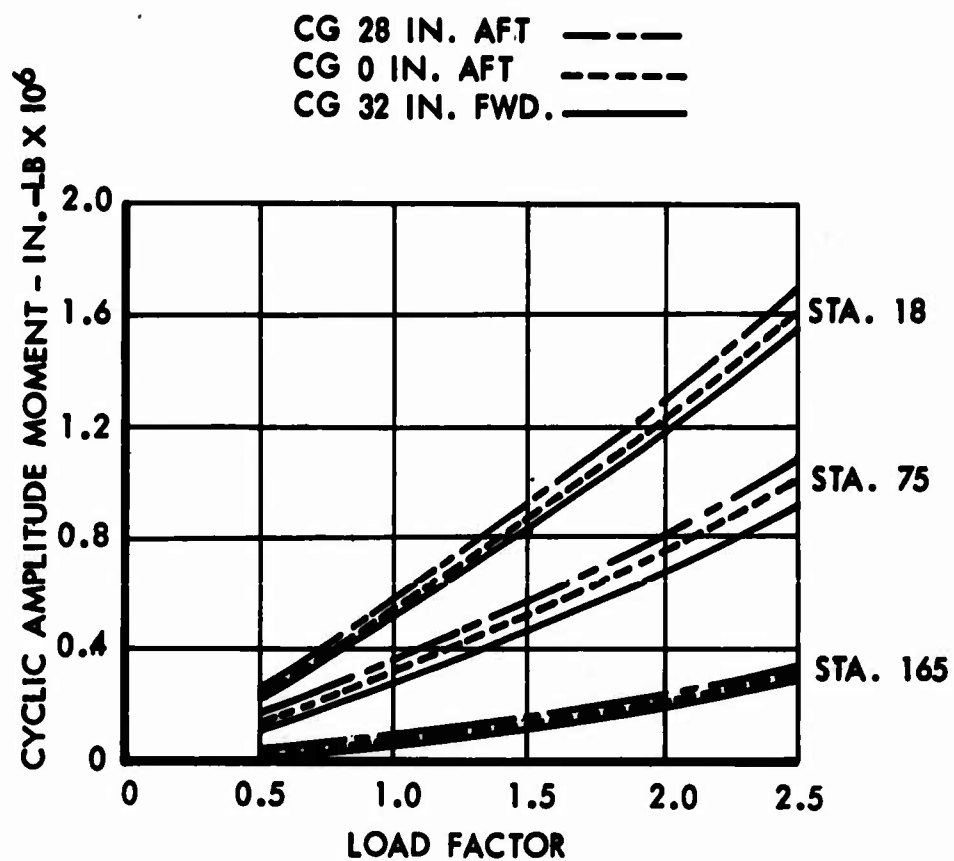


Figure 73. Cyclic Chord Bending Moment vs Load Factor -  
Transport Mission, 59,325 Pounds, 110 Knots

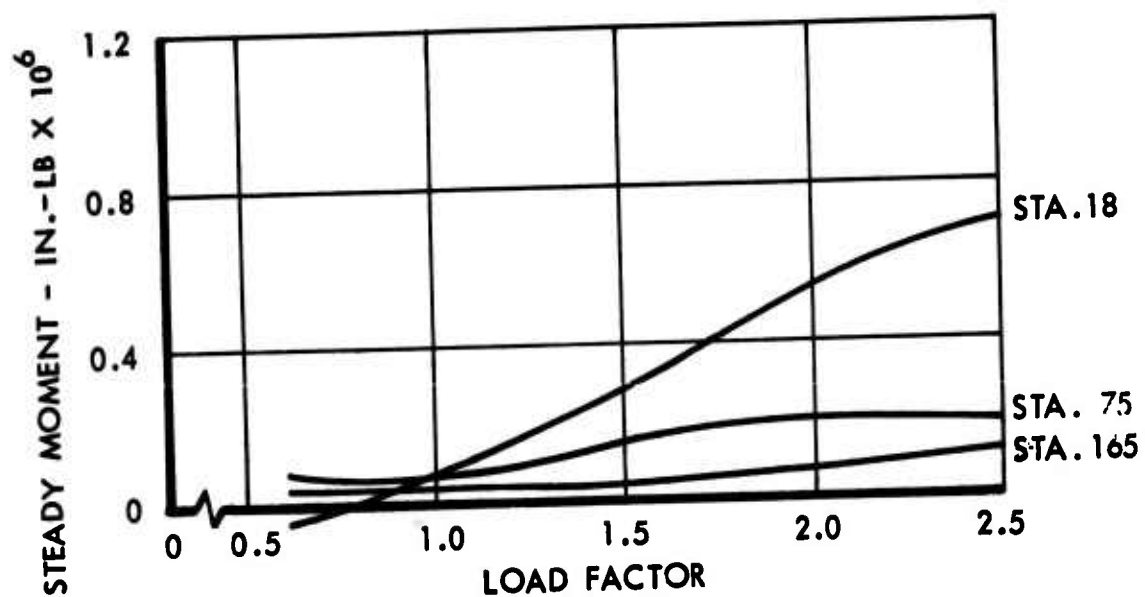


Figure 74. Steady Chord Bending Moment vs Load Factor - Transport Mission, 59,325 Pounds, 110 Knots



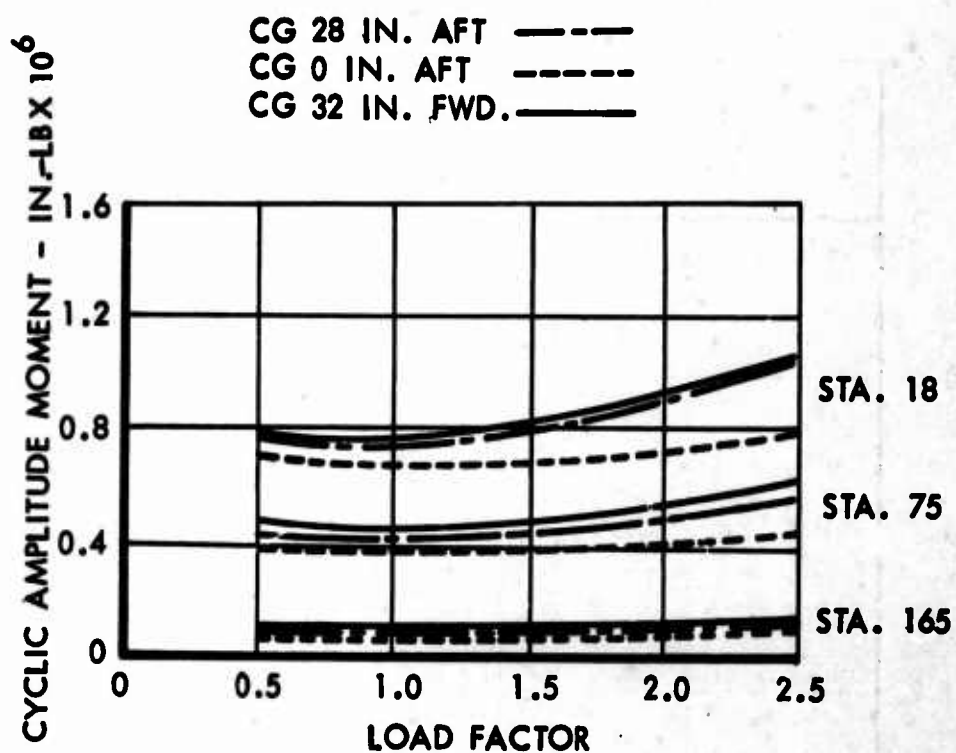


Figure 75. Cyclic Flap Bending Moment vs Load Factor-  
 29,705 Pounds, 130 Knots

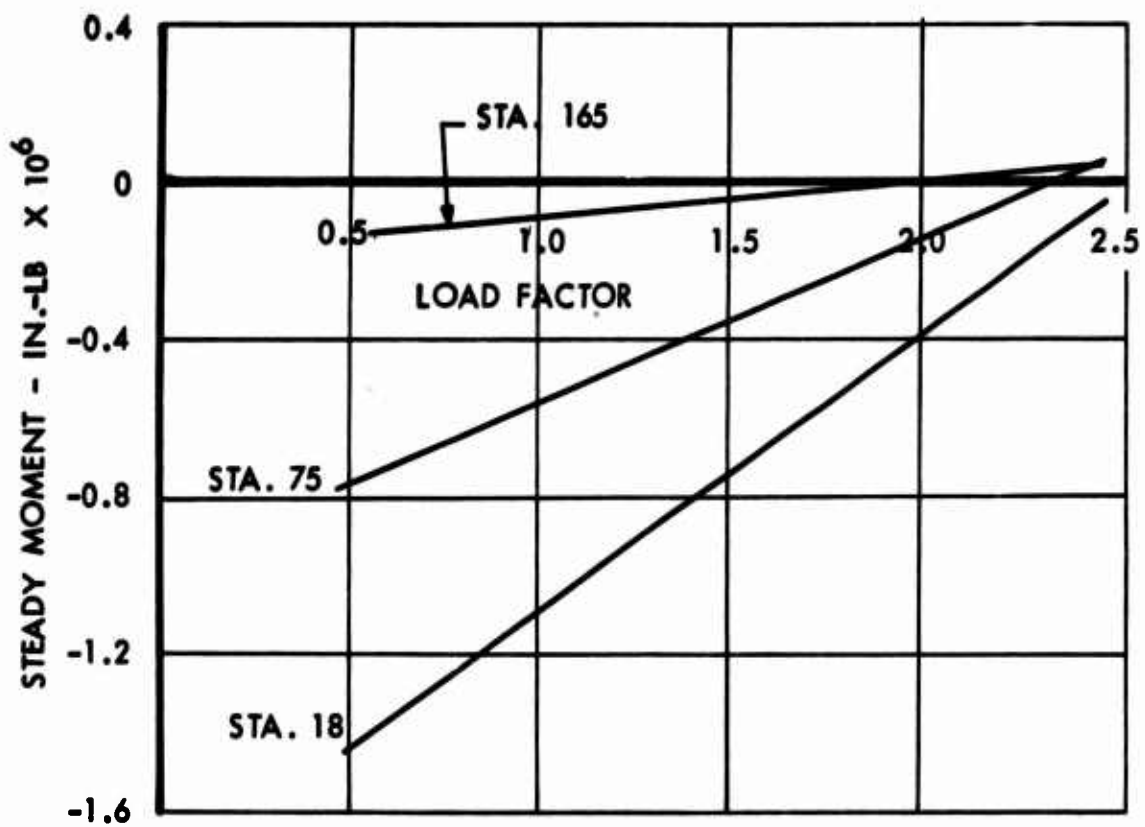


Figure 76. Steady Flap Bending Moment vs Load Factor -  
29,705 Pounds, 130 Knots

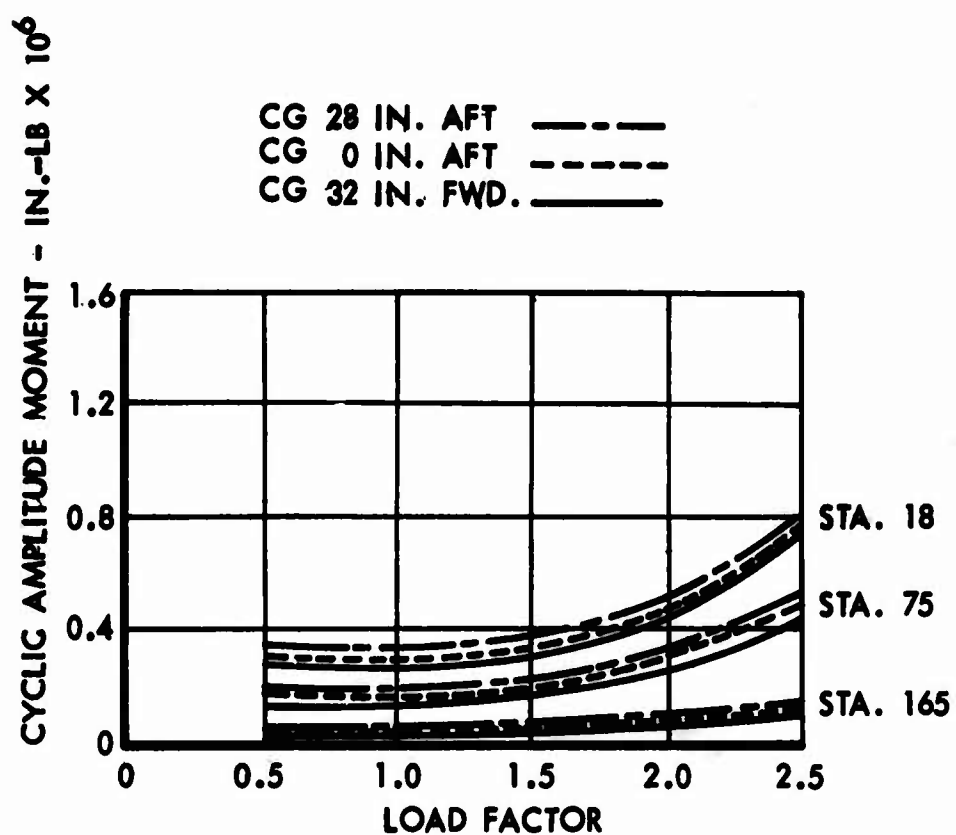


Figure 77. Cyclic Chord Bending Moment vs Load Factor -  
29,705 Pounds, 130 Knots

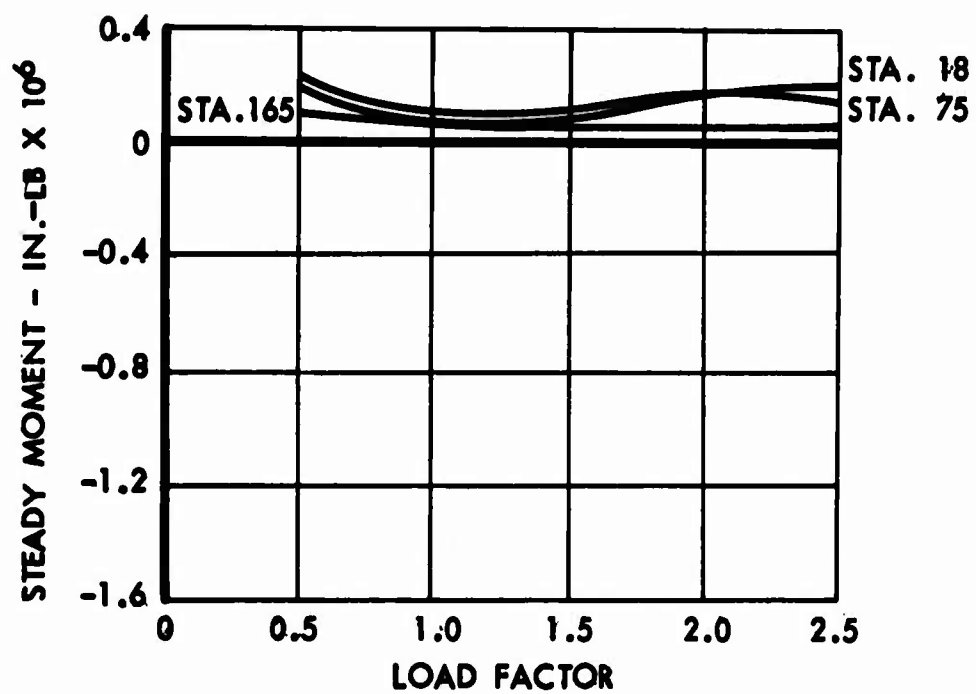


Figure 78. Steady Chord Bending Moment vs Load Factor -  
29,705 Pounds, 130 Knots

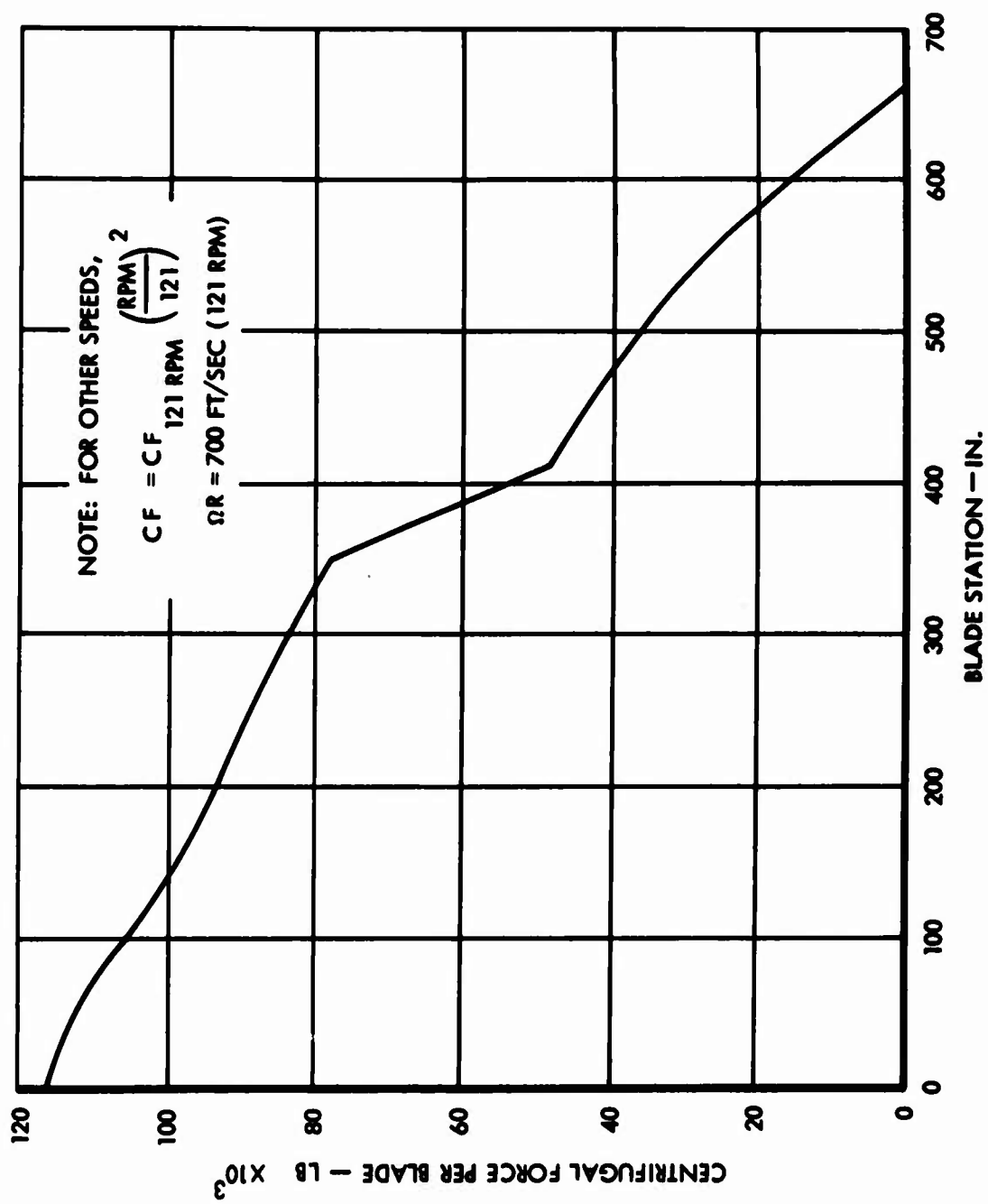


Figure 79. Centrifugal Force Per Blade vs Blade Station

TABLE XI				
POWER-OFF FLIGHT HEAVY-LIFT MISSION AUTOROTATION AT 1G				
Conditions: Weight = 72,325 lb Velocity = 95 knots rpm = 121 CG = 28 inches aft of rotor shaft				
BLADE STATION (in.)	FLAP BENDING MOMENTS (in.-lb)		CHORD BENDING MOMENT (in.-lb)	
	STEADY	CYCLIC AMPLITUDE	STEADY	CYCLIC AMPLITUDE
18	-93,973	495,052	-363,968	418,944
75	-19,308	293,527	-190,893	254,708
165	13,439	74,852	- 27,603	66,041

The determination of the blade-feathering control moment for 1g flight at the heavy-lift mission weight of 72,325 pounds and 95-knot cruise speed is presented below using the method outlined under "Feathering Control Moments." The center of gravity is located 28 inches aft of the rotor shaft. The output from the computer program for this condition yields the following results for the steady and first two harmonics of blade bending loads and vertical displacements:

$$M_{b_{165}} = 39,333 + 61,955 \cos \psi - 10,490 \sin \psi - 43,266 \cos 2\psi - 36,936 \sin 2\psi \text{ (in.-lb)}$$

$$Q_{b_{165}} = 40,700 - 113,143 \cos \psi - 15,616 \sin \psi - 1351 \cos 2\psi + 13,295 \sin 2\psi \text{ (in.-lb)}$$

$$\delta_{29} = 0.16571 + 0.00151 \cos \psi + 0.00004 \sin \psi - 0.00092 \cos 2\psi - 0.00083 \sin 2\psi \text{ (ft)}$$

$$\delta_{165} = 1.68468 + 0.14427 \cos \psi + 0.00136 \sin \psi - 0.08831 \cos 2\psi - 0.07880 \sin 2\psi \text{ (ft)}$$

$$\delta_{495} = 6.17762 + 1.79120 \cos \psi - 0.68120 \sin \psi - 0.68470 \cos 2\psi - 0.65149 \sin 2\psi \text{ (ft)}$$

The relative flapping coefficients  $a_n$  (see page 154) are determined from the expression  $0.088224 \delta_{29n} - 0.124584 \delta_{165n} + 0.036360 \delta_{455n}$  and result in the following flapping expression:

$$B_{f165} = 0.02935 + 0.04729 \cos \psi - 0.02493 \sin \psi - 0.01397 \cos 2\psi - 0.01394 \sin 2\psi$$

Substituting  $B_{f165}$ ,  $M_{b165}$ ,  $Q_{b165}$  and the blade sweep angle,  $\psi$ , equal to 0.005 radians into the expression

$$M_{g_b} = M_{b165} \psi' + Q_{b165} B_{g165}$$

yields the feathering control moment due to blade bending moments.

$$M_{f_b} = -1222 - 385 \cos \psi - 330 \sin \psi - 3694 \cos 2\psi + 679 \sin 2\psi$$

The expression which describes control moment required to overcome the torsional spring characteristics of the flexure is given as:

$$M_{f_K} = K (A_0 - \theta_{165} + \theta_{1c} \cos \psi + \theta_{1s} \sin \psi)$$

The torsional spring rate of the flexure,  $K$ , is 25,000 inch-pounds per radian, and the static angular position of the flexure,  $A_0$ , at blade station 165 is 0.1396 radians. The required mean blade pitch angle,  $\theta_{165}$ , is 0.170648 radians, and the required cyclic pitch is -0.0889 radians for  $\theta_{1c}$  and 0.0765 radians for  $\theta_{1s}$ .

Substituting the values of  $K$ ,  $\theta_{165}$ ,  $\theta_{1c}$ , and  $\theta_{1s}$  into the expression for  $M_{f_K}$  yields

$$M_{f_K} = -776 - 2220 \cos \psi + 1910 \sin \psi$$

The centrifugal restoring moment is given as

$$M_{f_{cf}} = -A_1 \sin Z (\theta_1 + \theta_{0.75}) + 2A_1 \theta_{1c} \cos \psi + 2A_1 \theta_{1s} \sin \psi$$

For the rotor blade under consideration,  $A_1$  is equal to 20,935 inch-pounds and  $\theta_1$  is equal to 0.01097 radians, which reduces the equation for centrifugal restoring moment to

$$M_{f_{cf}} = -20,935 \sin (0.02194 + \theta_{0.75}) + 41,870 \theta_{1c} \cos \psi + 41,870 \theta_{1s} \sin \psi$$

The cyclic pitch is that given above and  $\theta_{0.75}$  is 0.1270 radians. The centrifugal restoring moment for this condition is

$$M_{f_{cf}} = -5705 - 3720 \cos \psi + 3200 \sin \psi$$

The net blade feathering control moment is the sum of  $M_{f_b}$ ,  $M_{f_k}$ , and  $M_{f_{cf}}$ .

$$M_f = -7703 - 6325 \cos \psi + 4780 \sin \psi - 3694 \cos 2\psi + 679 \sin 2\psi$$

#### Slope Terrain Takeoff

Rotor hub moments during takeoff are based on the requirement of takeoffs from a 10-degree slope. When the side hill takeoff is considered, the maximum rotor hub moment developed occurs at the instant the down-hill landing gear just clears the ground. The expression which describes the magnitude of this hub moment as a function of rotor thrust, landing gear characteristics and center-of-gravity offsets is as follows:

$$R_H = L_H + M_H$$



$$R_H = \frac{12}{\left[1 + \frac{T}{K_\theta} (h+h_r)\right]} \left[ hW \sin (\theta_s + \theta) + \left( \frac{l_g}{2} + \eta \right) W \cos (\theta_s + \theta) - \frac{l_g}{2} T \right]$$

$\rightarrow * W \text{ (in.-lb)}$

where

$L_H$  = rolling moment on hub

$M_H$  = pitching moment on hub

$R_H$  = vector sum, or resultant, of  $L_H$  and  $M_H$

$T$  = rotor lift, 24,100 lb

$K_\theta$  = rotor stiffness (3,280,000 ft-lb/radian)

$W$  = gross weight (72,325 lb)

$h$  = distance between W.L through CG and ground line at the uphill main landing gear (14.9 ft)

$h_r$  = distance between CG and rotor hub (9.25 ft)

$l_g$  = landing gear tread (20 ft)

$\eta$  = lateral CG offset with respect to the rotor shaft (0.0 ft)

$\theta_s$  = angle of ground lines with horizontal (10 deg)

$\theta$  = angle formed by the attitude of the vehicle with the ground plane when the downhill main landing gear just clears the ground (-2.43 deg)

$*$  = longitudinal CG offset with respect to the rotor shaft  
32 in. forward)

Take-offs from sloping terrain are in accordance with an operation sequence in which the pilot first applies collective pitch to attain a rotor lift of at least one-third of the vehicle weight, followed by cyclic control to right the vehicle. Applying a rotor lift of 24,100 pounds to the above expression yields a rotor hub moment of 7,710,000 inch-pounds. The spanwise distribution of this hub moment into the blades is shown in Figure 80. The spanwise distribution is

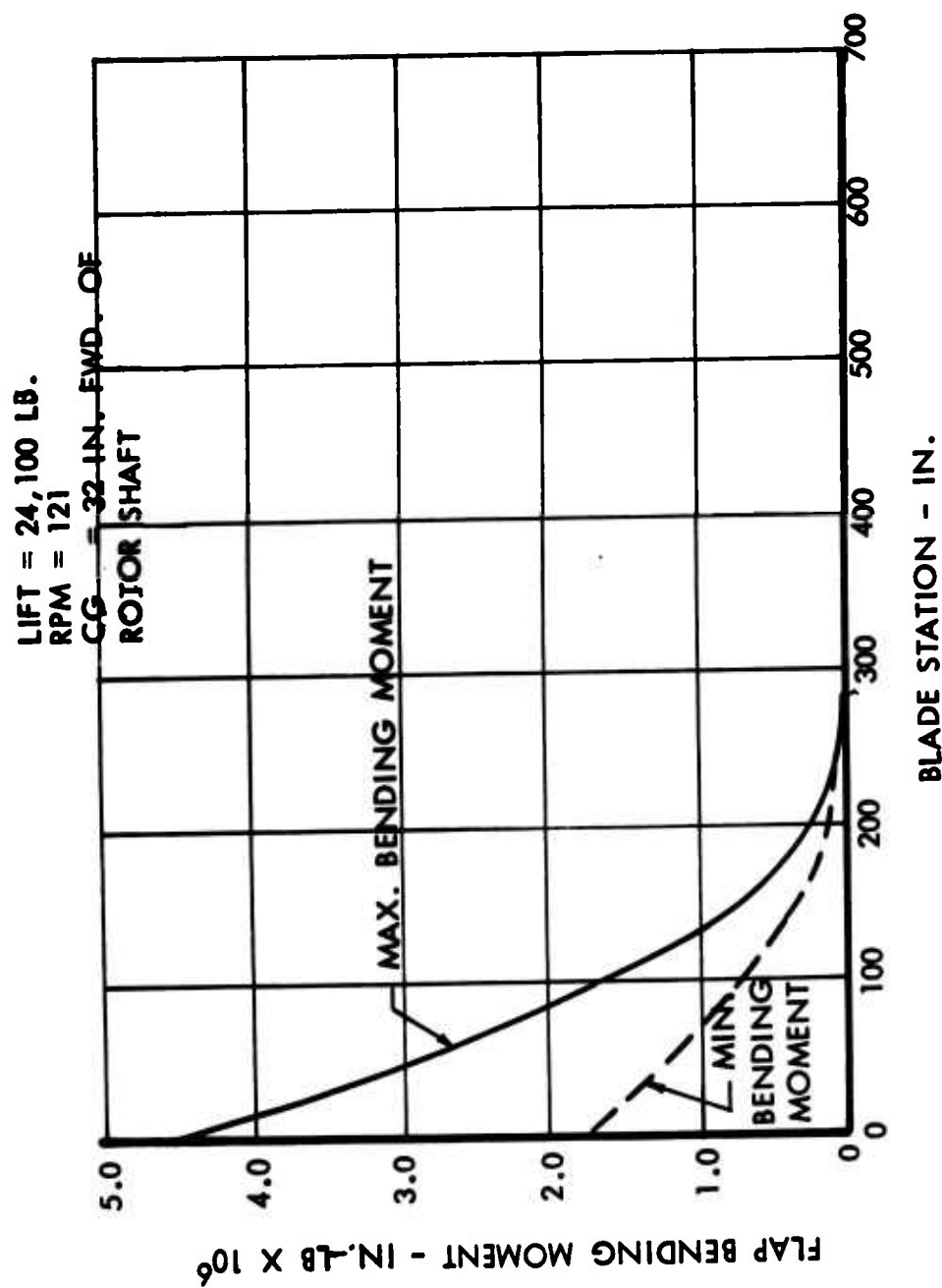


Figure 80. Flap Bending Moment vs Blade Station - Takeoff From 10-Degree Slope, 72,325 Pounds

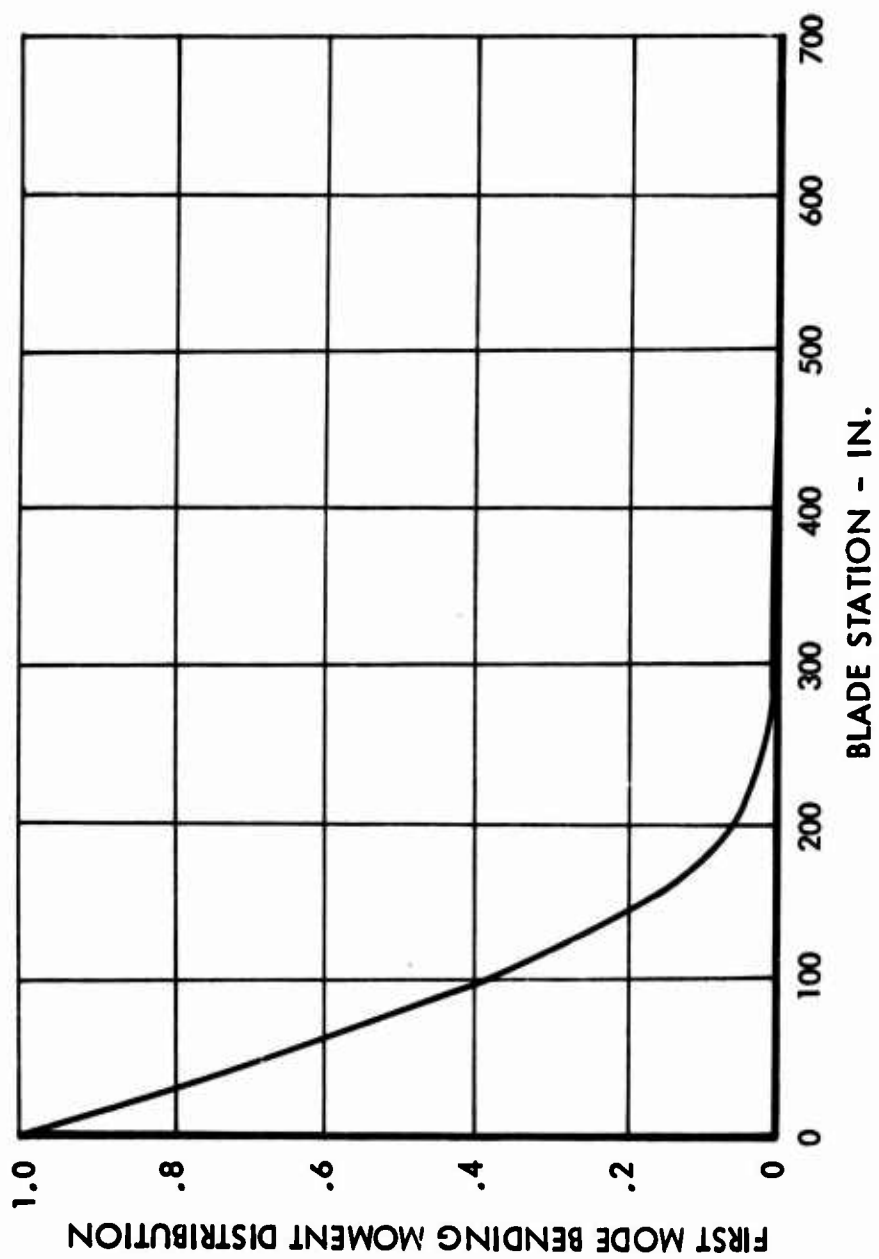


Figure 81. First Mode Flapping Bending Moment Distribution

$A_1, B_1$  = cyclic pitch, radians

$C$  = blade chord, ft

$\frac{CQ_0}{\sigma}$  = rotor profile torque coefficient

$I_b$  = blade mass inertia, slug-ft<sup>2</sup>

$K_\theta$  = rotor stiffness, ft-lb/radian

$L_H$  = rotor hub roll moment, in.-lb

$M_H$  = rotor hub pitch moment, in.-lb

$R$  = blade radius, ft

$T$  = rotor thrust, lb

$b$  = number of blades

$f_1$  = first mode amplification factor

$r_{0.75}$  = 3/4 blade radius, ft

$\beta_0$  = effective fixed cone angle, radians

$\lambda$  = inflow ratio

$\mu$  = tip speed ratio

$\Omega$  = rotor speed, radians/sec

The input values for the slope terrain takeoff are as follows:

$A_1$  = 3.380 deg (0.059 radian)

$B_1$  = 1.071 deg (0.187 radian)

$C$  = 41 in. (3.4167 ft)

$I_b$  = 23.144 slug-ft<sup>2</sup>

$K_\theta$  = 3,280,000 ft-lb/radian

$L_H$  = 613,200 ft-lb

$M_H$  = 192,800 ft-lb

$$R = 55 \text{ ft}$$

$$T = 24,100 \text{ lb}$$

$$b = 5 \text{ blades}$$

$$f_1 = 0.815$$

$$r_{0.75} = 41.25 \text{ ft}$$

$$\beta_0 = 7.6 \text{ deg (0.132645 radian)}$$

$$\mu = 0$$

$$\psi_0 = \tan^{-1} \frac{1.071}{3.380} = 72.5 \text{ deg, } \sin \psi_0 = 0.9537, \cos \psi_0 = 0.3007$$

$$\Omega = 12.7273 \text{ radians/sec}$$

By substituting the above values in the appropriate equations, the results are:

$$\alpha_{re} = -0.196 \text{ radians}$$

$$\psi_q = 25.86 \text{ deg}$$

$$Q_q = 179,170 \text{ ft-lb (2,150,000 in.-lb)}$$

$$q_c = 2,150,000 \cos (\psi - 25.86), \text{ in.-lb}$$

The distribution of the root in-plane moment along the span of the blade is accomplished by the spanwise distribution factor curve shown in Figure 82.

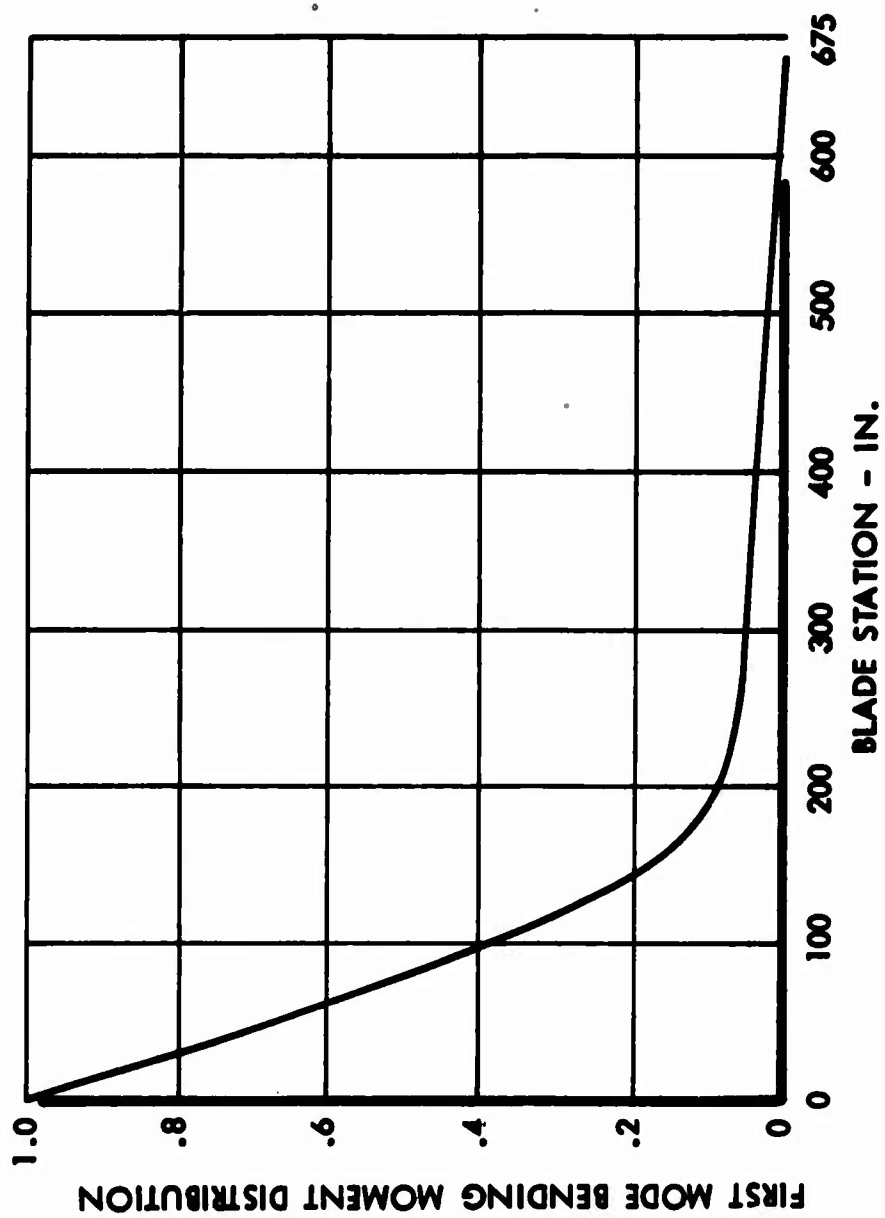


Figure 82. First Mode In-Plane Bending Moment Distribution

## FATIGUE EVALUATION

The analytical evaluation of the service life of structural components requires a description of the anticipated service use of the complete vehicle. This description provides the basis for the definition of the loading history anticipated in service. It must cover a variety of utilizations of the vehicle in a long service life. From this description, the loading history of the main rotor system can be established and the potential life evaluated by fatigue analysis and tests.

The description of service use is most conveniently presented in the form of mission outlines together with a selection of the percentage of the total service time spent in each type of mission. Each mission outline must adequately and conservatively represent the wide range of parameters associated with the mission. The selection of the distribution of missions must represent the worst probable composite use of the vehicle under varying operational conditions over its maximum useful life.

The definition of these missions as developed for the heavy-lift program is given in Table XII. Four basic missions are included in the definition. These are the transport, heavy-lift, and ferry missions specified in the Statement of Work, and a training mission which is an essential part of the operational use of the vehicle.

### Mission Loading Spectra

The local loading history is calculated for each of the missions for 3600 hours of service life. Subsequently, various percentages of these separate loading spectra are combined to provide several composite loading spectra for 3600 hours. The effects of these composites on service life are discussed later under "Fatigue Life Prediction."

Two stations of the main rotor are selected for fatigue analysis. Station 75 represents the flexure section of the main rotor system. Station 165 is typical of the blade section structure. The details of these sections are discussed in Sections 2 and 4.

The spectra of bending moments at these stations for 3600 hours of utilization of each mission, including the effects of rotor on-off cycles, are shown in Figures 83 through 86. These spectra are based upon the matched-stiffness rotor response over a range of load factors up to 2.5g at normal (121 rpm) rotor speed and center-of-gravity offsets from -32 inches forward to 28 inches aft of the centerline of rotor for the distribution of the mission velocities in Table XII.

**TABLE XII**  
**DEFINITION OF MISSIONS**

Item	Time Per Event (sec)	Mission					
		Transport		Heavy-Lift		Ferry	Training
		Out	Return	Out	Return		
Mission Time, min		52	38	11	9	1207	60
Cruise Altitude		G.L.	G.L.	G.L.	G.L.	10,000 ft	G.L.
Takeoff Weight, lb		59,000	32,000	72,000	31,000	50,000	44,000
Landing Weight, lb		56,000	30,000	71,000	30,000	52,000	44,000
Steady Flight							
Hover, min		1	1	1	0	0	4
45 knots, min		3	2	3	0	1	6
95 knots, min		3	2	3	0	2	24
110 knots, min		12	5	2	0	600	24
130 knots, min		33	20	2	9	600	0
156 knots, min		0	9	0	0	0	2
-----							
NUMBER OF EVENTS PER MISSION							
-----							
Climb	40	1	1	1	1	2	6
Descent	15	1	1	1	1	2	5
Transitions							
Low Speed	3	1	1	1	1	1	6
To Autorotation	1	0.1	0.1	0	0	0	1
From Autorotation	2	0.1	0.1	0	0	0	1
Maneuvers							
Flare	8	0.9	0.9	0	0	0	5
Pull-up	8	0.2	0.2	0.2	0	0	1
Turn	20	6	6	2	2	2	10
Reversal	2	2	2	1	0	0	4
Autorotation Flight							
Descent	15	0.1	0.1	0	0	0	1
Flare	8	0.1	0.1	0	0	0	1
Pull-up	6	0.1	0.1	0	0	0	1
Turn	15	0.1	2	0	0	0	1
Reversal	2	0	0	0	0	0	1
Takeoffs & Landings	-	1	1	1	1	1	6
Ground Conditions							
Rotor On-Off	10	1	1	1	1	1	2
Power-On Landing	8	0.9	0.9	1	1	1	5.5
Autorotation Landing	8	0.1	0.1	0	0	0	.5
Level Takeoff & Landing	8	.73	.73	1	1	1	5.5
5-Degree Takeoff & Landing	8	.25	.25	0	0	0	.5
10-Degree Takeoff & Landing	8	.02	.02	0	0	0	0



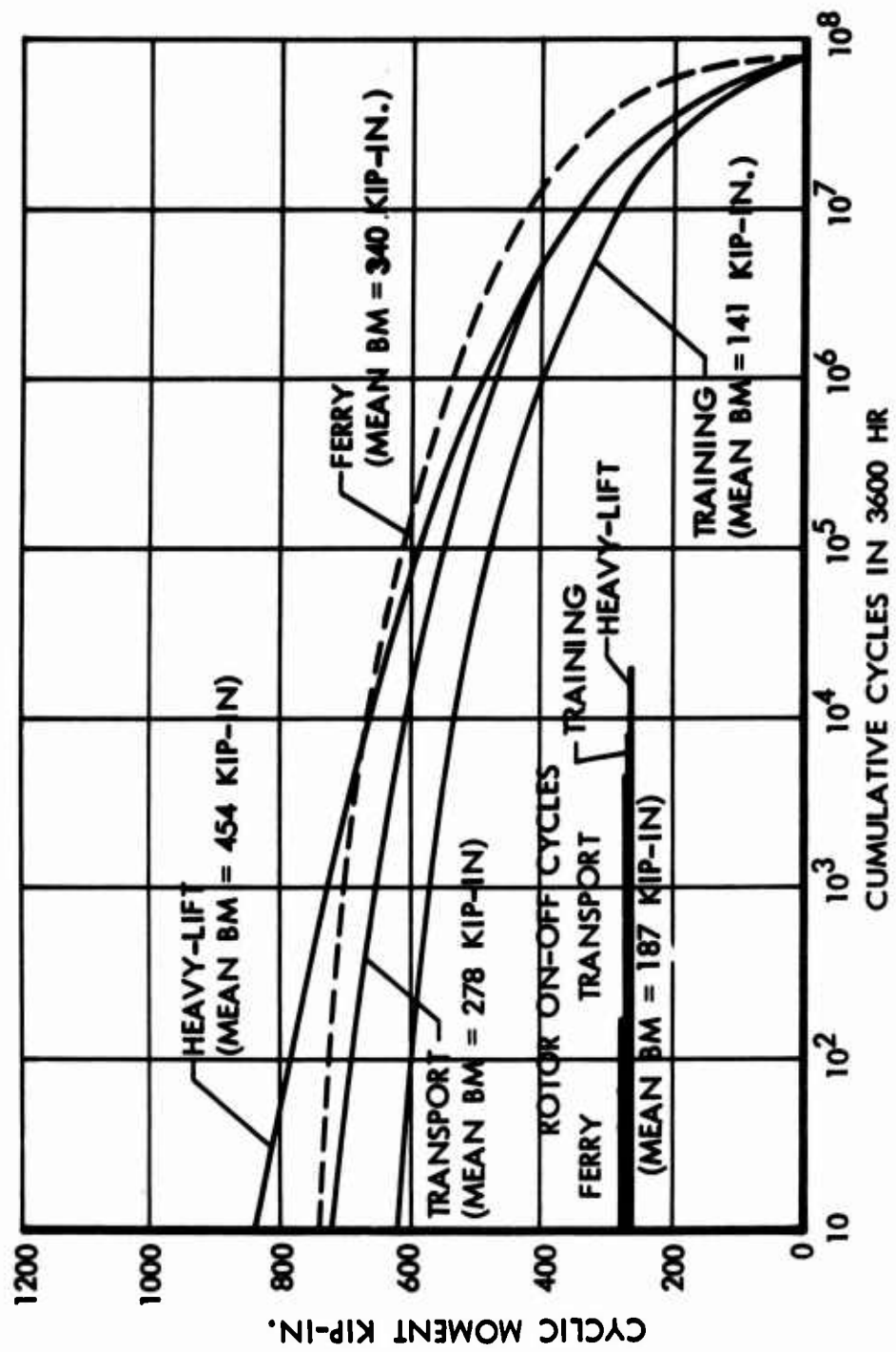


Figure 83. Flap Bending Moment Spectra at Main Rotor Blade Station 75

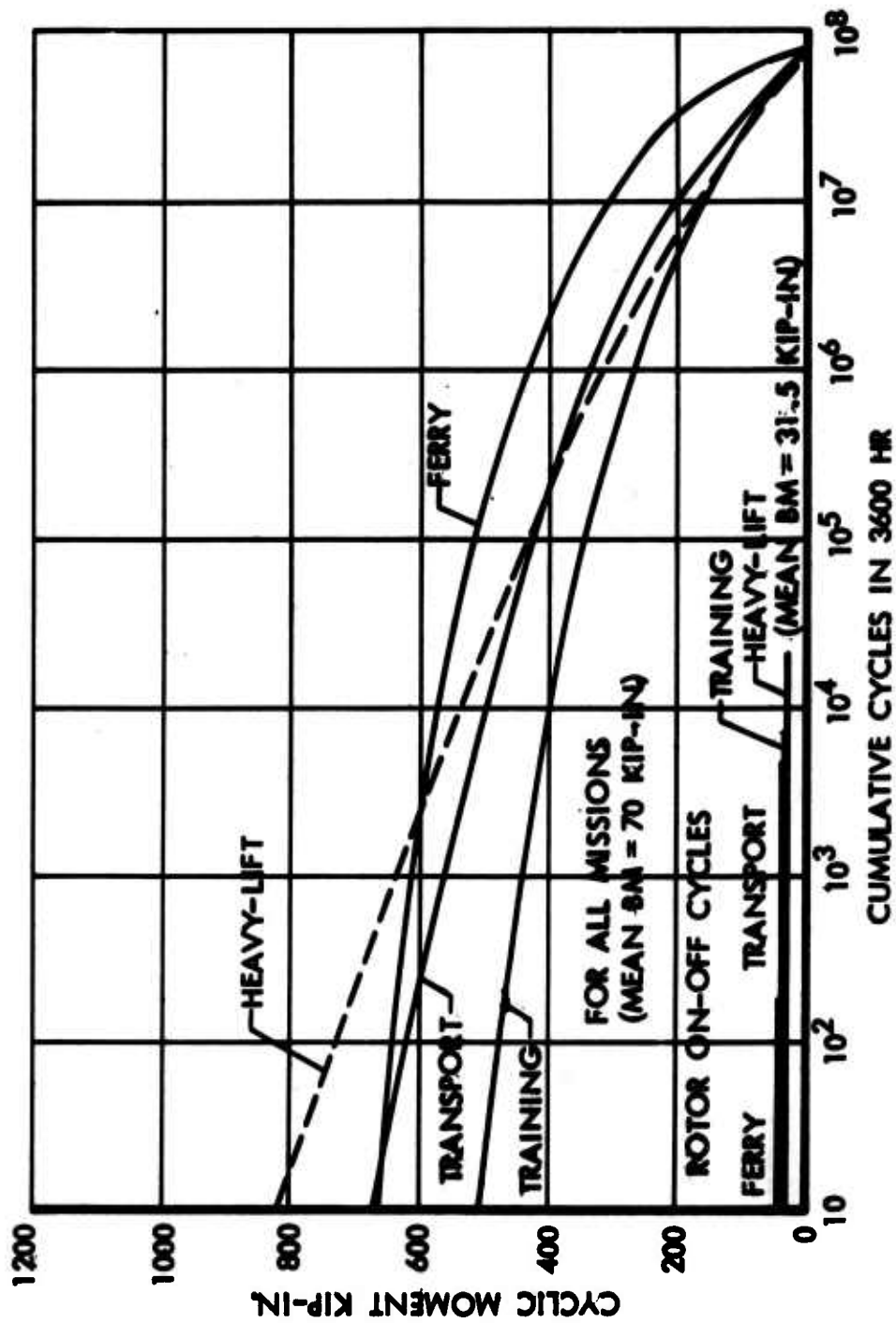


Figure 84. Chord Bending Moment Spectra at Main Rotor Blade Station 75

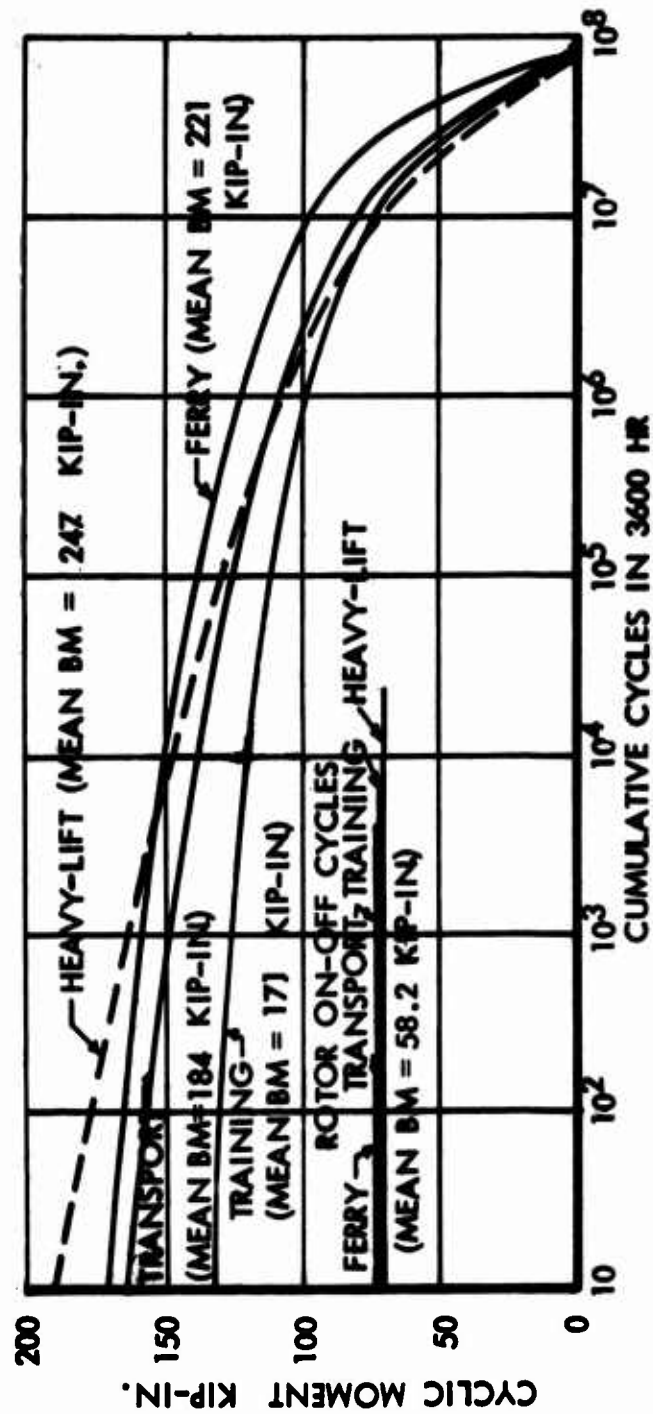


Figure 85. Flap Bending Moment Spectra at Main Rotor Blade Station 165

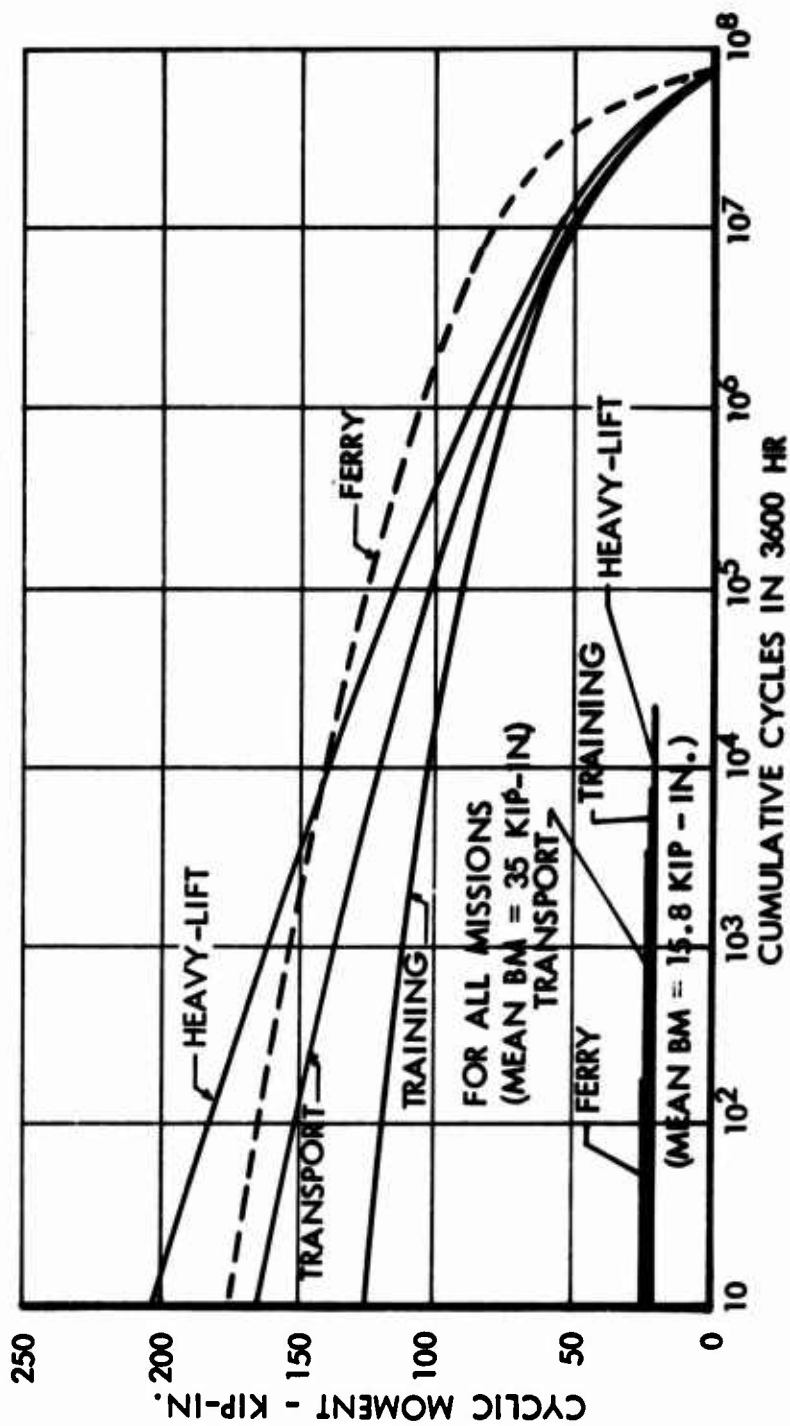


Figure 86. Chord Bending Moment Spectra at Main Rotor Blade Station 165

## DYNAMIC AND AEROELASTIC INVESTIGATIONS

### Introduction

The basic dynamics of the Lockheed rigid-rotor system for a helicopter are describable in terms of the rotor as a flexible gyroscope, connected to a fuselage and slaved to a control gyroscope which receives feedback information from the rotor and fuselage as well as command signals from the pilot. The primary design variables for obtaining satisfactory and stable operation of the system are the blade sweep forward relative to the feathering axis and the lead angle between control gyro tilt and blade feathering.

The possibility of high-frequency blade flutter has been eliminated by positioning the blade mass centroids on or ahead of the blade quarter chord over the outboard two-thirds of the blade. The high-frequency control gyro nutation occurring at a frequency of twice per revolution is well stabilized by relatively light damping at the control gyro swash plate.

The feedback information to the control gyroscope from the rotor and fuselage, as affected by rotor design characteristics, has been extensively examined both experimentally and analytically. These studies show that in the case of a cantilevered rotor blade with sweep,  $\lambda$ , and overcone,  $\Delta\beta$ , angles built into the blade outboard of the feathering bearing, the feathering moment from Equation (24) of Reference 13, with a term added for overcone, is

$$M_{\theta} = K_{\beta_0} \lambda \bar{\beta}_0 - E \bar{\beta}_0 (K_{\beta_0} - K_{\epsilon}) - B_0 \bar{\epsilon} (K_{\beta_0} - K_{\epsilon}) + K_{\epsilon} \Delta\beta \bar{\epsilon}$$

where

$M_{\theta}$  = feathering moment, positive nose up

$\lambda$  = blade sweepforward, positive forward

$\bar{\beta}_0$  = flapping displacement due to perturbational load, positive up

$E$  = in-plane displacement due to static load, positive aft

$K_{\beta_0}$  = flapping stiffness of blade outboard of feathering bearing

$K_{\epsilon}$  = in-plane stiffness of blade outboard of feathering bearing

$B_0$  = flapping displacement due to static load, positive up

$\bar{\epsilon}$  = in-plane displacement due to perturbational load, positive aft

$\Delta\beta$  = blade overcone angle outboard of feathering bearing angle, positive up

This indicates that feathering moments based on deflections  $E$  and  $B_0$  due to steady loads are eliminated when stiffnesses are matched,  $K_{\beta_0} = K_{\epsilon}$ . These couplings are undesirable in that the vehicle dynamic characteristics are somewhat affected by power loading, gross weight, and maneuvering load factor.

The Lockheed Model CL 875 heavy-lift helicopter is a matched-stiffness/flexure hub rigid-rotor system incorporating the principle of designing  $K_{\beta_0} = K_{\epsilon}$  which eliminates these undesirable couplings in its basic design. The bending distortion in the first-flap and first-in-plane modes takes place predominately in the flexure, where  $K_{\beta_0} = K_{\epsilon}$ , and sufficiently decouples the fundamental modes of the rotor system. Although the stiffnesses are presently matched only in the flexure, the blade portion of the span is designed as soft as possible in the chordwise direction to obtain as high a degree of matching as possible for the higher order modes. An additional feature of eliminating the control system feathering bearings is accomplished by designing the blade-matched flexure to have low torsional stiffness. Blade feathering is accomplished by bridging the flexure in the control system design to the outboard end of the matched flexure, approximately 0.25 of the radius. The reduction of rotor weight, reduction of control gyro size, and elimination of feathering bearings are the primary advantages. However, the combination of structural elements which satisfies these combined requirements results in a rotor configuration with a subcritical in-plane bending frequency which introduces the possibility of mechanical instability.

Whirl tower tests of a subcritical three-blade, 32-foot-diameter rigid-rotor system, as well as dynamic model tests of subcritical matched-stiffness rigid-rotor systems which incorporated gimbal-mounted as well as spring-supported fuselage inertia frames, indicated that, when ground resonance was induced, it was slow in building up and would be eliminated by landing gear spring-damper elements.

Existence of a mechanical air resonance (free flight) is a theoretical possibility (Reference 13) in that the effective rotor stiffness, as seen by the body motions due to rotor structural, centrifugal and aerodynamic moments, permits the free-flight body pitch and roll frequencies to be sufficiently high to warrant consideration of their location relative to the chord bending frequency,  $\Omega - \omega_{1p}$ , viewed in stationary coordinates. A universally mounted rotor, or a rotor with a small effective offset hinge, would completely eliminate the possibility of air resonance, but the attendant reduction in vehicle handling qualities is highly undesirable.

The analytical study of the free-flight dynamics of a gyro-controlled matched-stiffness rigid rotor, wherein the in-plane bending frequency is subcritical, is the principal focus of the investigation reported herein.

The analytical methods utilized in the course of these investigations have been previously applied in the study of a 35-foot-diameter, four-blade, matched-stiffness/flexure root blade rotor system (Reference 16). The initial phase of this work included correlation of the stability characteristics predicted by analysis with the results obtained from the matched-stiffness dynamic model tests conducted in the NASA-Langley Transonic Dynamics Tunnel (Reference 11).

Fabrication of this 35-foot-diameter rotor is now being completed, and whirl tower tests are planned to begin in early 1966. Flight test of this rotor system on the model XH-51A helicopter is scheduled following completion of this whirl tower program.

#### Discussion of Air/Ground Resonance

Air/ground resonance is basically a form of mechanical instability involving any body mode which includes in-plane hub motion and the first in-plane blade motion, and it occurs at rotor rpm less first in-plane frequency when this difference matches, or is in close proximity to, the body mode frequency. Both the body mode and the in-plane mode frequencies are functions of rpm; they increase somewhat with rotational speed owing to centrifugal stiffening of the rotor. This instability is almost entirely mechanical; drive is not obtained from rotor aerodynamics but energy is obtained from the power turning the rotor or from the stored energy in the rotor in the case of autorotation. However, the air may furnish some damping to the motion; and by proper selection of rotor parameters, e.g., sweep and droop, the air may be caused to furnish considerable damping.

For an explanation of the physics of this mechanical instability, consider the following example: A four-bladed rotor has opposite blades 1 and 3 vibrating in the first in-plane mode at the natural frequency of the mode and has blades 2 and 4 also vibrating in the

same motion; but timewise, blade 2 is moving a quarter of a cycle later than blade 1. The forward displacement of each blade appears to indicate a steady displacement running around the rotor at speed  $\omega_{ip} - \Omega$  in a sense opposite to the normal rotation of the rotor. When the rotor is started and gradually brought up to speed, the spinning of the blade deflection mode is regressive but appears to slow down until  $\Omega = \omega_{ip}$ . At this speed, the blade deflection mode appears to stand still, the blades standing in a permanently deflected shape; but they oscillate structurally at their natural frequencies as it is increased by centrifugal stiffening.

At higher rotor speeds, the blade deflection mode appears to advance with the rotor but the advance is slower than rotor rpm, the rate being  $\Omega - \omega_{ip}$ . In this speed regime, if the hub whirls about an eccentric point or oscillates through such a point at a low frequency, the rotor eccentricity is able to absorb energy from the rotation. This is principally seen as increased amplitudes of blade chord bending and body motions. This occurs when Coriolis forces are induced because the hub has a velocity relative to the instantaneous center of rotation of the rotor.

When the rotor rpm reaches a value such that the apparent rotation of the blade deflection matches the frequency of the hub oscillation, the blade bending mode can then couple with the hub oscillation mode, and an energy input circuit is established for taking energy from shaft rotation to drive a body oscillation mode. If this frequency coincidence can be avoided or if the body mode or the blade in-plane mode can be sufficiently damped, the mechanical instability can be avoided.

This simplified discussion applies to any rotor which has three or more blades. In the case of a subcritical two-bladed rotor, the mechanical instability phenomenon is still possible. The physical mechanism is similar to the polar symmetric system, but the time dependency effects of the anisotropic body and rotor system adds additional complications.

The use of lead-lag dampers and specialized landing gear spring-damper systems represents the current state-of-the-art method of controlling the mechanical instability of articulated rotor systems. Experimental and analytical results indicate that the ability of a rigid-rotor system with gyro control to sense body moments and to transmit rotor moments to the shaft to damp hub motions as well as in-plane bending motions provides sufficient aerodynamic damping to relieve this problem area greatly.

In the course of the experimental programs conducted by the Lockheed-California Company wherein full-scale or dynamic model subcritical rigid rotors with gyro control were investigated, no lead-lag dampers nor dampers in the support system were utilized. Only that



damping present was that which was associated with friction and material hysteresis, neither of which could be completely eliminated.

The classical analytical studies of ground resonance by Coleman (Reference 17) and Brooks (Reference 18) do not include blade flapping or rotor aerodynamic effects, since the associated hub moments for a teetering or universally-mounted rotor are zero; and for the articulated rotor with small offset flapping hinge, they are small. Unexplained instabilities which occurred during ground operation prompted these early studies. Since the characteristics of these analyses and the vehicle being analyzed precluded air resonance, the origin of the term "ground resonance" to describe this form of mechanical instability is clear.

Later studies by Bielawa (Reference 19) show analysis for a system with several body modes and experimental confirmation of the ground resonance instabilities including range of rotor rpm over which the instability persists.

This study included an experimental examination of two- and three-bladed subcritical rotor systems. The correlation of these experimental results with the analytical work due to Brooks (Reference 18) was the principal focus of this work. The observation of distinct ranges of rpm over which these instabilities occur, as well as the modes involved are significant contributions in furthering a physical understanding of the phenomena. The models tested provided spring-supported rigid body motions, as well as motions of the main rotor shaft relative to the body. Motion pictures of these tests show that in all cases where instability occurred, the motions were in an advancing phase as suggested by both physical and theoretical considerations.

#### Analytical Methods

The analytical studies of the dynamics of the Lockheed heavy-lift helicopter rotor system design were conducted on digital computer equipment; the Lockheed FAMAS System (Flutter and Matrix Algebra System) and special FORTRAN programs, previously developed for helicopter blade analysis, were utilized.

An analytical model was developed that utilized lumped parameter techniques. This system described a complete elastic rotor including the control gyro and a flexible shaft and transmission support system. The flexible rotor blade contains 11 lumped stations, each having 3 degrees of freedom, vertical translation, in-plane translation, and pitching angle. Coupling of vertical bending, in-plane bending and torsion due to sweep, coning, collective angle, and blade twist are included in the structural description. This type of system description also permits a complete description of the gyro control system which includes flexibility

of components. The total coupled system contains 80 degrees of freedom. These degrees of freedom are listed in Table XIII. To reduce the time required to solve the eigen-value problem, this eightieth order system is reduced in size to twenty-second order; natural cantilever blade modes are used. The final 22 degrees of freedom used are shown in Table XIV.

Due to the anisotropic nature of the fuselage, the rotor system is transformed from a rotating coordinate system to a stationary coordinate system, and hovering cyclic stability solutions are obtained in the stationary coordinate system.

The motion of all 80 coordinates is obtained by utilization of the eigenvectors from the twenty-second order solutions and their associated normal mode shapes.

In the course of the matched-stiffness/flexure hub rotor system analytical studies (Reference 16), a simplified analysis utilizing 10 degrees of freedom was developed to permit more rapid parametric investigations. This analysis improved the physical understanding of the solutions obtained, and it provided an additional cross-check with the larger order system. This system basically described the first flapping, first in-plane bending, and feathering modes (includes gyro control system) of each blade in combination with the four rigid-body motions of the vehicle. These basic equations are shown in matrix format in Table XV with symbols identified in Table XVI.

### Analytical Investigation

The analytical model used in the dynamic analysis of the Lockheed heavy-lift helicopter was previously applied to the study of a full-scale 35-foot-diameter, four-bladed, matched-stiffness/flexure root blade rotor system (Reference 16). Correlation of the stability characteristics predicted by analysis with the results obtained from the matched-stiffness dynamic model tests conducted in the NASA Langley Transonic Dynamics Tunnel was an important part of this earlier work and is included in the above reference.

Results of dynamic analysis conducted on the matched-stiffness rotor system indicate that two modes of operation are possible for the free-flight conditions.

The first mode of operation places the body roll and pitch natural frequencies below the nominal operating rpm minus the first in-plane bending frequency. The second mode of operation places the body roll frequency coincident with the rotating rpm minus the first in-plane bending frequency well above the operating rpm.

TABLE XIII			
SUMMARY OF 80-DEGREE-OF-FREEDOM SYSTEM			
NUMBER OF COORDINATE		DESCRIPTION OF COORDINATE	
1	$X_o$	Hub Fore and Aft Translation	
2	$Y_o$	Hub Lateral Translation	
3	$\phi_o$	Hub Roll	
4	$\theta_o$	Hub Pitch	
Blade No. 1	Blade No. 2		
5	39	Z 18	Vertical Deflection at Rotor Station 18
6	40	Z 66	Vertical Deflection at Rotor Station 66
7	41	Z132	Vertical Deflection at Rotor Station 132
8	42	Z198	Vertical Deflection at Rotor Station 198
9	43	Z264	Vertical Deflection at Rotor Station 264
10	44	Z330	Vertical Deflection at Rotor Station 330
11	45	Z396	Vertical Deflection at Rotor Station 396
12	46	Z462	Vertical Deflection at Rotor Station 462
13	47	Z528	Vertical Deflection at Rotor Station 528
14	48	Z594	Vertical Deflection at Rotor Station 594
15	49	Z660	Vertical Deflection at Rotor Station 660
16	50	X 18	Chordwise Deflection at Rotor Station 18
17	51	X 66	Chordwise Deflection at Rotor Station 66
18	52	X132	Chordwise Deflection at Rotor Station 132
19	53	X198	Chordwise Deflection at Rotor Station 198
20	54	X264	Chordwise Deflection at Rotor Station 264
21	55	X330	Chordwise Deflection at Rotor Station 330
22	56	X396	Chordwise Deflection at Rotor Station 396
23	57	X462	Chordwise Deflection at Rotor Station 462
24	58	X528	Chordwise Deflection at Rotor Station 528
25	59	X594	Chordwise Deflection at Rotor Station 594
26	60	X660	Chordwise Deflection at Rotor Station 660

TABLE XIII (CONTINUED)

Blade No. 1	Blade No. 2		
27	61	$\theta$ 18	Torsional Deflection at Rotor Station 18
28	62	$\theta$ 66	Torsional Deflection at Rotor Station 66
29	63	$\theta$ 132	Torsional Deflection at Rotor Station 132
30	64	$\theta$ 198	Torsional Deflection at Rotor Station 198
31	65	$\theta$ 264	Torsional Deflection at Rotor Station 264
32	66	$\theta$ 330	Torsional Deflection at Rotor Station 330
33	67	$\theta$ 396	Torsional Deflection at Rotor Station 396
34	68	$\theta$ 462	Torsional Deflection at Rotor Station 462
35	69	$\theta$ 528	Torsional Deflection at Rotor Station 528
36	70	$\theta$ 594	Torsional Deflection at Rotor Station 594
37	71	$\theta$ 660	Torsional Deflection at Rotor Station 660
38		$\phi$ G	Gyro Roll
	72	$\theta$ G	Gyro Pitch
73	$X_T$	Transmission Fore and Aft Translation	
74	$Y_T$	Transmission Lateral Translation	
75	$\phi_T$	Transmission Roll	
76	$\theta_T$	Transmission Pitch	
77	$X_F$	Fuselage Fore and Aft Translation	
78	$Y_F$	Fuselage Lateral Translation	
79	$\phi_F$	Fuselage Roll	
80	$\theta_F$	Fuselage Pitch	

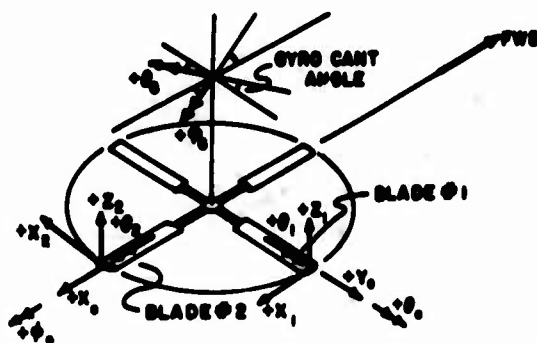


**TABLE XIV**  
**SUMMARY OF 22-DEGREE-OF-FREEDOM SYSTEM**

NUMBER OF COORDINATE		DESCRIPTION OF COORDINATE
1	$X_0$	Rotor Fore and Aft Translation
2	$Y_0$	Rotor Lateral Translation
3	$\phi_0$	Rotor Roll
4	$\theta_0$	Rotor Pitch
5	$X_{11}$	First In-Plane Bending
6	$Z_{11}$	First Flap Bending
7	$\theta_{11}$	Feathering
8	$Z_{12}$	Second Flap Bending
9	$X_{12}$	Second In-Plane Bending
10	$X_{21}$	First In-Plane Bending
11	$Z_{21}$	First Flap Bending
12	$\theta_{21}$	Feathering
13	$Z_{22}$	Second Flap Bending
14	$X_{22}$	Second In-Plane Bending
15	$X_T$	Transmission Fore and Aft Translation
16	$Y_T$	Transmission Lateral Translation
17	$\phi_T$	Transmission Roll
18	$\theta_T$	Transmission Pitch
19	$X_F$	Fuselage Fore and Aft Translation
20	$Y_F$	Fuselage Lateral Translation
21	$\phi_F$	Fuselage Roll
22	$\theta_F$	Fuselage Pitch

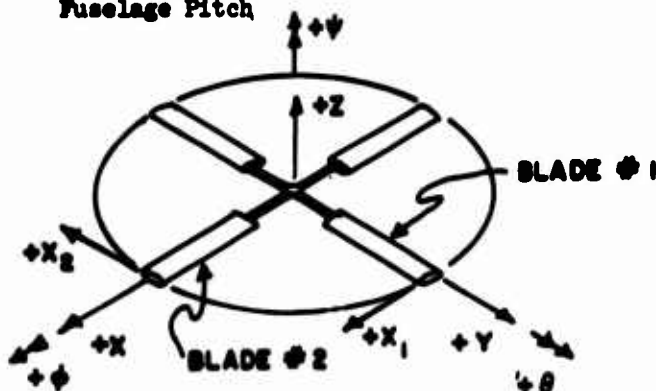


TABLE XV

DYNAMIC EQUATIONS OF EQUILIBRIUM FOR MATCHED-S

$F_x$	$-(M_R + M_F)P^2$				
$F_y$	$-(M_R + M_F)P^2$				
$M_{\theta_R}$		$-I_R P^2$ $+M_F P$ $-2K\beta$	$-J_R \Omega P$ $-M_A$ $-I_R P^2$	$+M_A \frac{\cos \psi_2}{K}$ $+M_A \frac{\sin \psi_2}{K}$	
$M_{\phi_R}$		$+J_R \Omega P$ $+M_A$	$+M_F P$ $-2K\beta$	$-M_A \frac{\sin \psi_2}{K}$ $+M_A \frac{\cos \psi_2}{K}$	
$M_{\theta_G}$		$+e_m 2K\beta \frac{\cos \psi_2}{K} \lambda$	$-e_m 2K\beta \frac{\sin \psi_2}{K} \lambda$	$-I_G P^2$ $-M_F P$ $-J_G \Omega P$	
$M_{\phi_G}$		$+e_m 2K\beta \frac{\sin \psi_2}{K} \lambda$	$+e_m 2K\beta \frac{\cos \psi_2}{K} \lambda$	$+J_G \Omega P$ $-M_F P$ $-I_G P^2$	
$M_{\theta_F}$	$(M_F h_F)P^2$			$+M_F P$ $+K_G$	
$M_{\phi_F}$		$(M_F h_F)P^2$		$+2K\beta$	$+M_F P$ $+K_G$
$M_{e_x}$	$-2S_{e_x} P^2$		$+2K\beta$		
$M_{e_y}$	$-2S_{e_y} P^2$				

TABLE XV

UM FOR MATCHED-STIFFNESS/FLEXURE HUB ROTOR

		$(M_r h_r) p^2$	$-2S_{00} p^2$	
		$(M_r h_r) p^2$	$-2S_{00} p^2$	X
				Y
				$\theta_R$
$\frac{\sin \psi_2}{K}$	$+M_A \frac{\sin \psi_2}{K}$	$+2K_B - M_A \frac{\cos \psi_2}{K}$	$+M_A \left(1 - \frac{\sin \psi_2}{K}\right)$	$\phi_R$
$\frac{\sin \psi_2}{K}$	$+M_A \frac{\cos \psi_2}{K}$	$-M_A \left(1 - \frac{\sin \psi_2}{K}\right)$	$+2K_B - M_A \frac{\cos \psi_2}{K}$	$\theta_0$
$\frac{1}{p}$	$-J_0 \Omega p$	$+M_0 p$	$+c_m 2K_B \frac{\sin \psi_2}{K} \lambda$	$\phi_0$
$\frac{1}{p}$	$-I_0 p^2$	$+K_0 - c_m 2K_B \frac{\cos \psi_2}{K} \lambda$	$+c_m 2K_B \frac{\sin \psi_2}{K} \lambda$	$\theta_f$
$\Omega p$	$-M_0 p$		$+M_0 p$	$\phi_f$
$\frac{1}{p}$	$-K_0$	$-c_m 2K_B \frac{\sin \psi_2}{K} \lambda$	$+K_0 - c_m 2K_B \frac{\cos \psi_2}{K} \lambda$	$\theta_r$
$\frac{1}{p}$		$-(I_{0r} + M_r h_r^2) p^2$		$\phi_r$
$\frac{1}{p}$		$-M_0 p$	$-(I_{0r} + M_r h_r^2) p^2$	$\epsilon_x$
$\frac{1}{p}$		$-2K_B - K_0$	$-2K_B - K_0$	$\epsilon_y$
	$+M_0 p$		$-2I_{00} p^2$	
	$+K_0$		$-2K_0 + 2\Omega^2 [I_{00} - S_{00}]$	
			$-4\Omega I_{00} p$	
			$-2I_{00} p^2$	
			$-4\Omega I_{00} p$	
			$-2K_0 + 2\Omega^2 [I_{00} - S_{00}]$	

TABLE XVI

## SYMBOLS FOR 10 X 10 EQUATIONS

$X$	Fore and aft translation of entire system, positive forward
$Y$	Lateral translation of entire system, positive right
$\theta_R$	Pitch attitude of rotor plane relative to horizontal, positive nose up; the rotor plane is defined by the plane joining the 0.75R stations
$\phi_R$	Roll attitude of rotor plane, positive right side down
$\theta_G$	Pitch attitude of control gyro, positive nose up
$\phi_G$	Roll attitude of control gyro, positive right side down
$\theta_F$	Pitch attitude of fuselage and shaft, positive nose up
$\phi_F$	Roll attitude of fuselage and shaft, positive right side down
$\epsilon_X$	Angular deflection component of all blades toward front of rotor
$\epsilon_Y$	Angular deflection component of all blades toward right side of rotor
$M_R$	Mass of rotor
$M_F$	Mass of fuselage, transmission and shaft system
$J_R, J_G$	Polar moment of inertia of rotor or gyro
$I_R, I_G$	Diametral moment of inertia of rotor or gyro
$e$	Distance of effective in-plane pivot location from center line of hub
$I_{eb}$	Moment of inertia of one blade about effective pivot location
$S_{eb}$	Blade static unbalance about effective pivot location



TABLE XVI (CONTINUED)

$S_\beta$	Blade static unbalance in flapping
$W_F$	Weight of fuselage, transmission and shaft system
$I_{\theta_F}, I_{\phi_F}$	Pitch or roll moment of inertia of fuselage, transmission, and shaft system about its center of gravity
$K_\beta$	Stiffness of rotor plane relative to shaft
$K_\epsilon$	In-plane structural stiffness about effective pivot location
$M_A$	Aerodynamic effectiveness of cyclic feathering in producing moment
$M_{\dot{\theta}}, M_{\dot{\phi}}$	Rotor aerodynamic damping in pitch and roll
$K_G$	Control spring stiffness as seen by control gyro swash plate
$M_{\dot{G}}$	Swash plate damper
$h_F$	Distance of fuselage, transmission, shaft system center of gravity from hub
$\beta_0$	Blade precone angle
$\psi_0$	Control gyro cant angle to blade
$K$	Control gyro mechanical advantage (gyro angle/blade angle)
$\lambda$	Blade sweep forward, net angle between blade quarter chord and feathering axis as seen in plane view
$C_m$	Moment coefficient to account for spanwise location of sweep angle
$\Omega$	Rotational speed of rotor, counterclockwise as viewed from above
$P$	Laplace operator

The selection of the mode of operation for any vehicle depends upon the basic design requirements: i.e., the type of mission for which the vehicle is being designed and the basic configuration of the rotor-fuselage combination. The location of the fundamental body frequencies in the preliminary design phase will generally dictate the mode of operation which will be most desirable. The rotor and gyro control system parameters are then adjusted to meet the stability requirements for the system.

In the case of the heavy-lift helicopter design, the fuselage has a very high fineness ratio. This results in a relatively low roll inertia and consequently yields a relatively high body roll frequency. This suggests that the desired mode of operation will be the second one in which the body roll frequency crosses the  $\Omega-\omega_{ip}$  line above the operating rpm. The structural design requirements on the flexure also result in a high rotor stiffness which contributes to a high body roll frequency.

The analytical results obtained for the minimum and maximum gross weight configurations of the Lockheed heavy-lift helicopter, which utilizes the second mode of operation, are shown on Figures 87 and 88. These results are conservative in that the rotor structural damping has been assumed to be zero in these calculations. It is important to recognize that the body pitch mode, which is indicated by this analysis to be marginally unstable, is basically a regressive mode. This is extremely unfavorable in that the principal energy source is due to the advancing component of this mode. The figures also show that there is a considerable frequency separation between the  $\Omega-\omega_{ip}$  line and body roll mode. This is extremely significant in that the roll mode is basically an advancing mode and therefore susceptible to a high degree of coupling, which results in a potentially large mechanical instability. The modes for which solutions are shown are those potentially associated with mechanical instability; all other modes (not shown) were stable with satisfactory margins.

The free-flight parametric study reported in the matched stiffness/flexure root blade analytical study (Reference 16) shows that the body frequencies, i.e., both the pitch and roll modes, can be significantly altered by use of gyro mechanical advantage. During the prototype design phase, the pitch and roll inertias are more accurately determined and/or the rotor stiffness is modified to provide a final selection of the gyro mechanical advantage. The possible use of control system couplings and blade droop or overcone will also be determined.

The rotor parameters utilized in this analysis were: blade sweep angle  $\lambda = 1.5^\circ$  (forward blade sweep),  $\Delta\beta = 0$ , gyro mechanical advantage = 1.40 (gyro angle/blade angle), and gyro control lead angle =  $45^\circ$ .

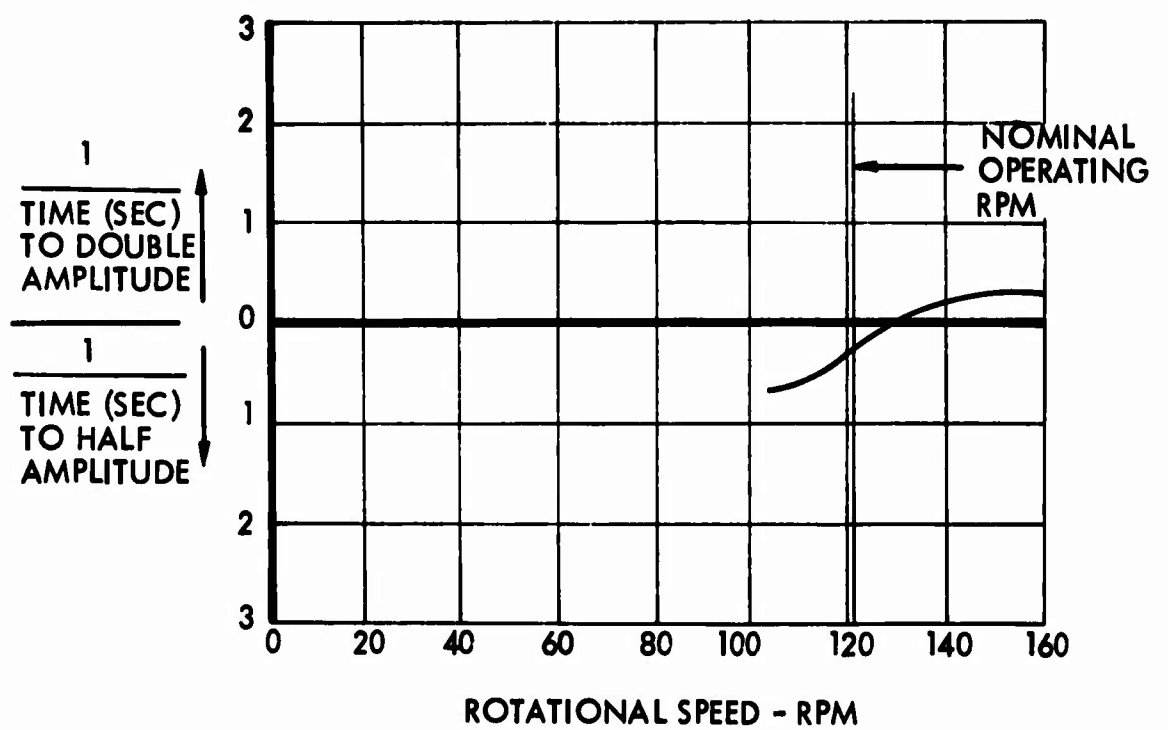
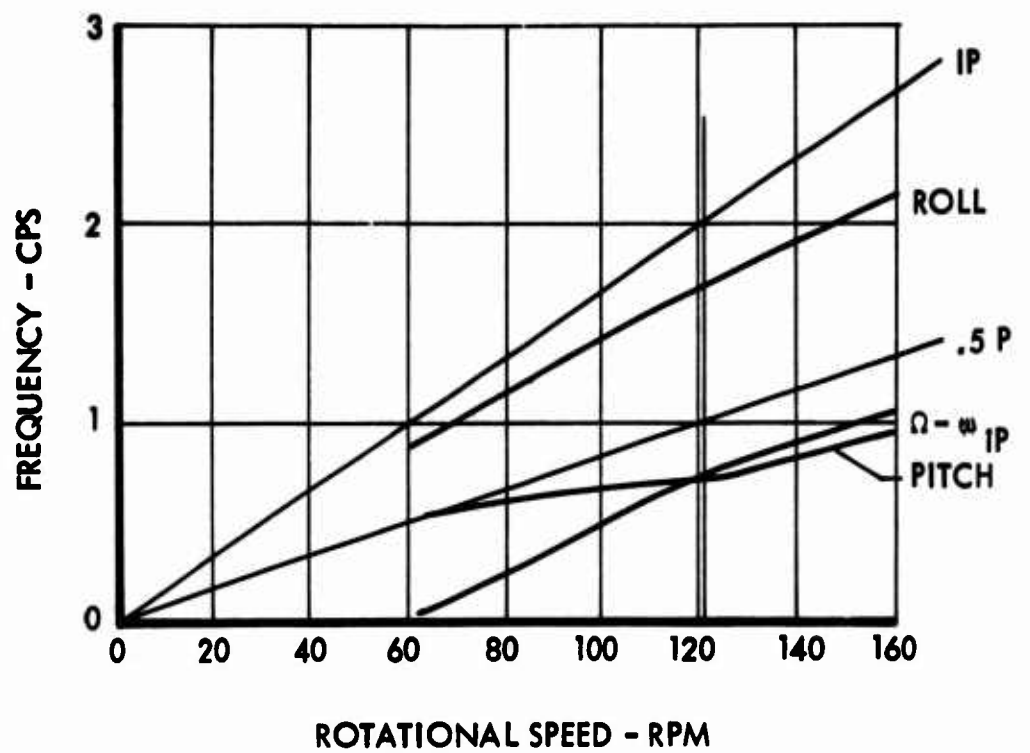


Figure 87. Flight Resonance Analysis of Heavy-Lift Helicopter - Minimum Gross Weight

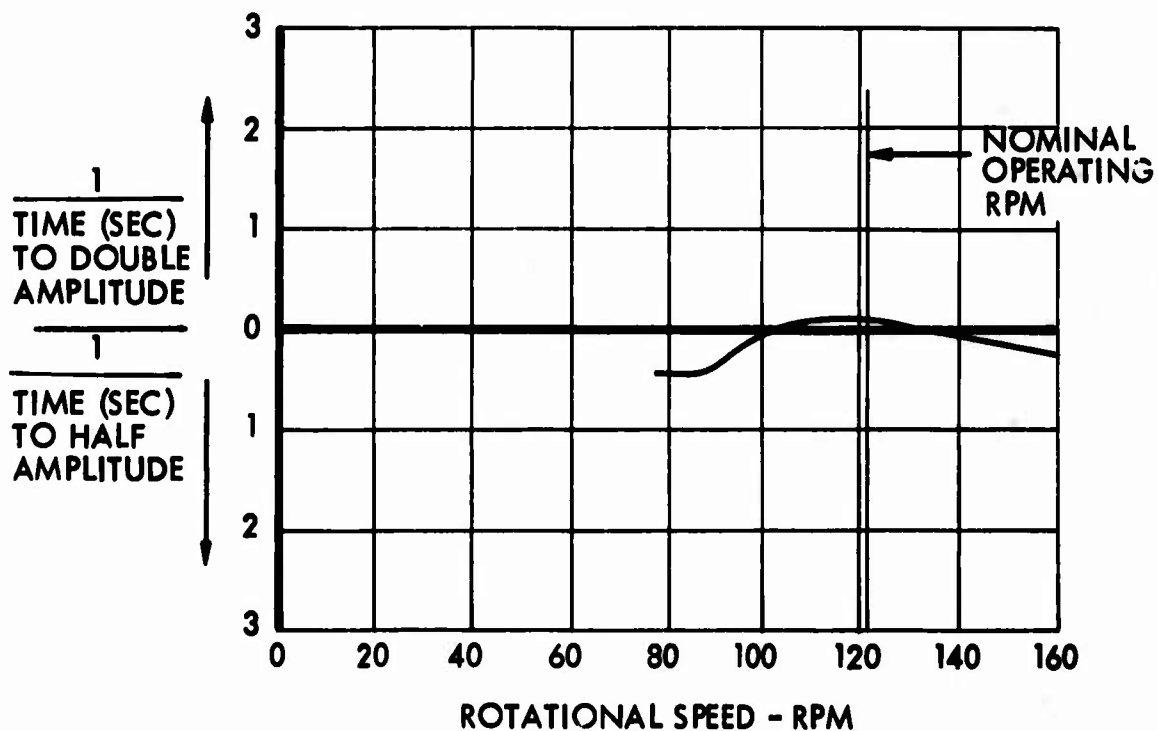
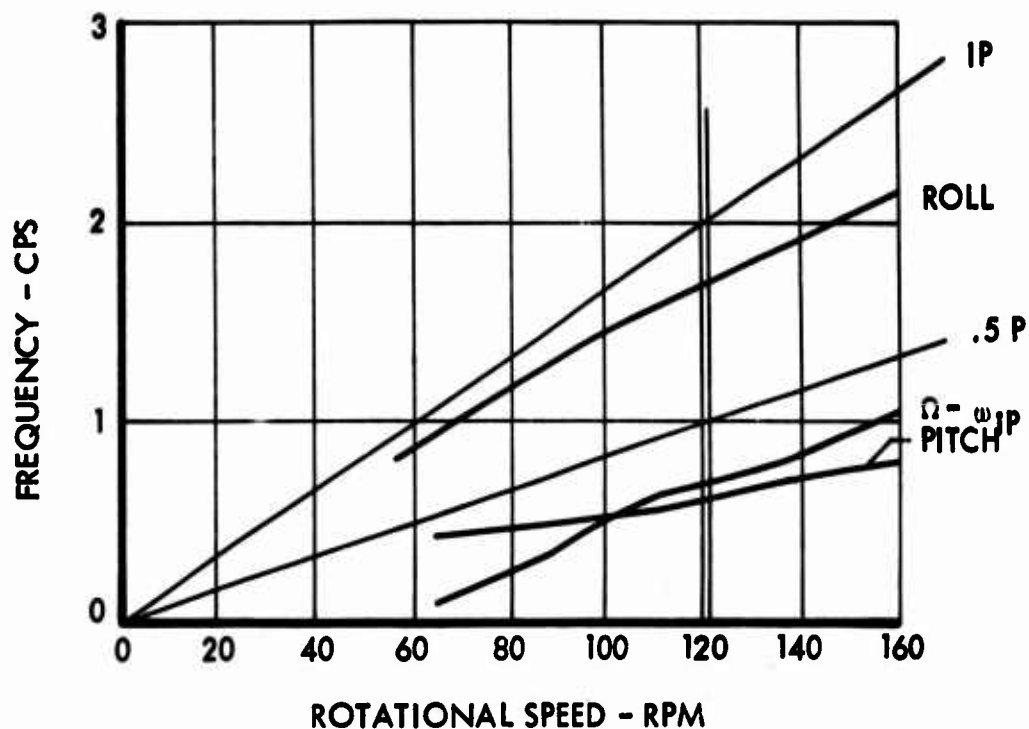


Figure 88. Flight Resonance Analysis of Heavy-Lift Helicopter - Maximum Gross Weight

The first in-plane bending frequency is 0.66P with a rotor stiffness of 3 million foot-pounds per radian at nominal operating rpm.

The torsional stiffness of the flexure is relatively low owing to its length and low stiffness design. This characteristic has been assumed in the analysis for which solutions are shown.

Should the final prototype design result in an increased torsional stiffness, the use of negative cyclic control spring rates on the swash plate will be incorporated in the design.

The possibility of ground resonance is extremely remote since any reasonable gear stiffness and damping will further increase the body frequencies and add additional damping to the system.

The landing gear stiffness and damping characteristics will be added to the analytical description in the study of the prototype vehicle. The possibility of bottoming the dampers, as well as spring rate characteristics for various attitudes of the vehicle relative to the ground, will be carefully examined.

#### Main Rotor Blade Frequency Analysis

As has been demonstrated by experimental programs and correlated with analysis, it is necessary to design blades within acceptable rotating blade natural frequencies for reasons of optimal vibration levels and fatigue life.

The determination of the rotating blade natural frequencies was performed on a computer program developed and extensively used at Lockheed. A lumped parameter system capable of accommodating 30 mass elements is used to describe in detail the inertial and stiffness characteristics of the blade in the flapping, in-plane, and torsional directions. The results are comprised of the coupled flapping, in-plane, torsional frequencies, and the corresponding mode shapes as well as the shear and moment distributions on each of the three axes for nonuniform, twisted blade at any specified collective angle setting.

The coupled frequencies were determined for three collective angles (5, 10, and 15 degrees) and for five rpm's (0, 75, 100, 121, and 150). The frequency results are plotted in Figures 89, 90 and 91 and mode shapes are shown on Figures 92 and 93.

In the case of a five-bladed rotor system the vibratory response of the cabin will principally occur at a frequency of 5P owing to main rotor aerodynamic excitations at 4P, 5P, and 6P in the rotating system. The rotating blade frequency spectra versus rpm for various collective

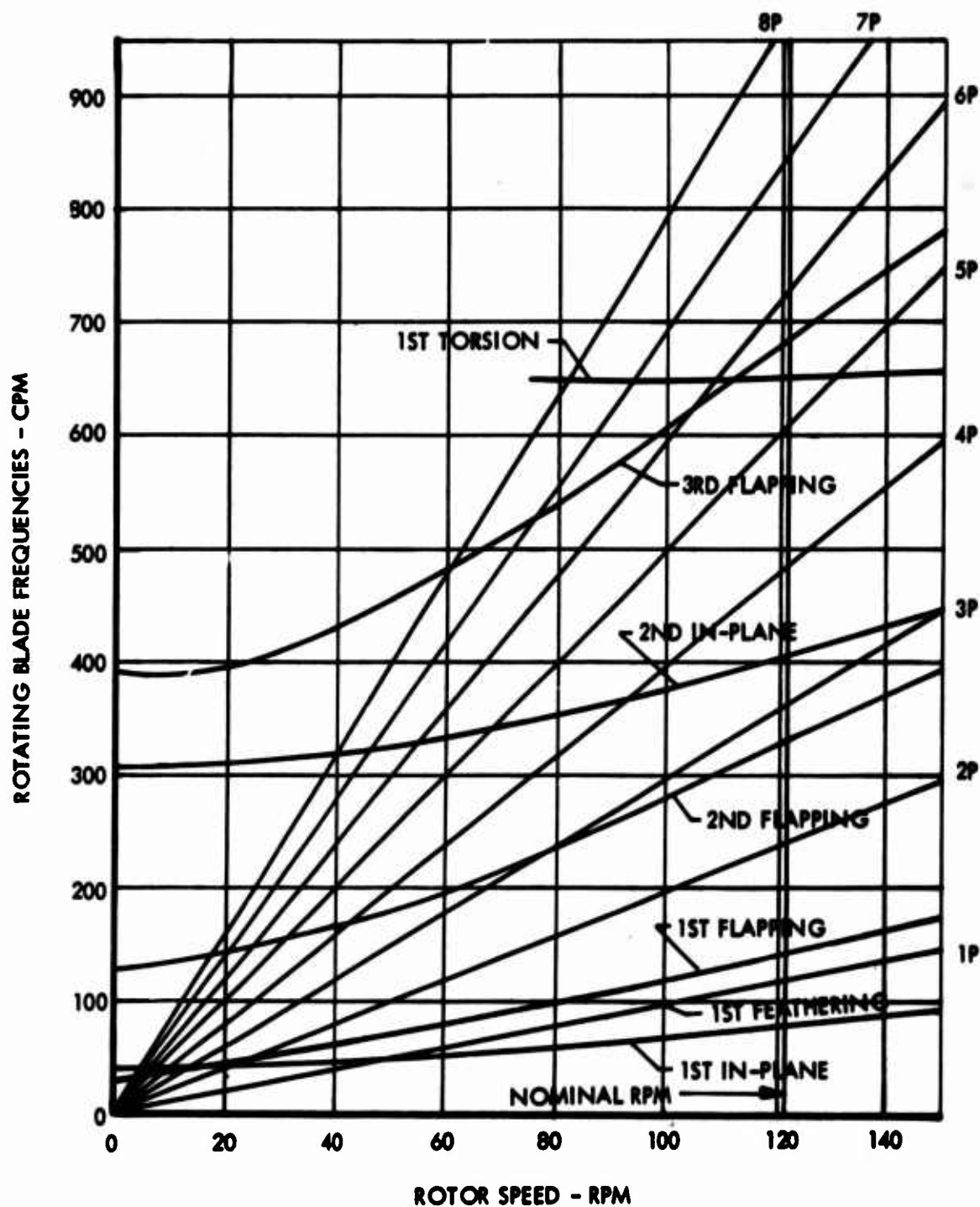


Figure 89. Main Rotor Frequency Spectrum, Heavy-Lift Helicopter - Collective Angle = 5 Degrees,  $\theta_1 = -5$  Degrees

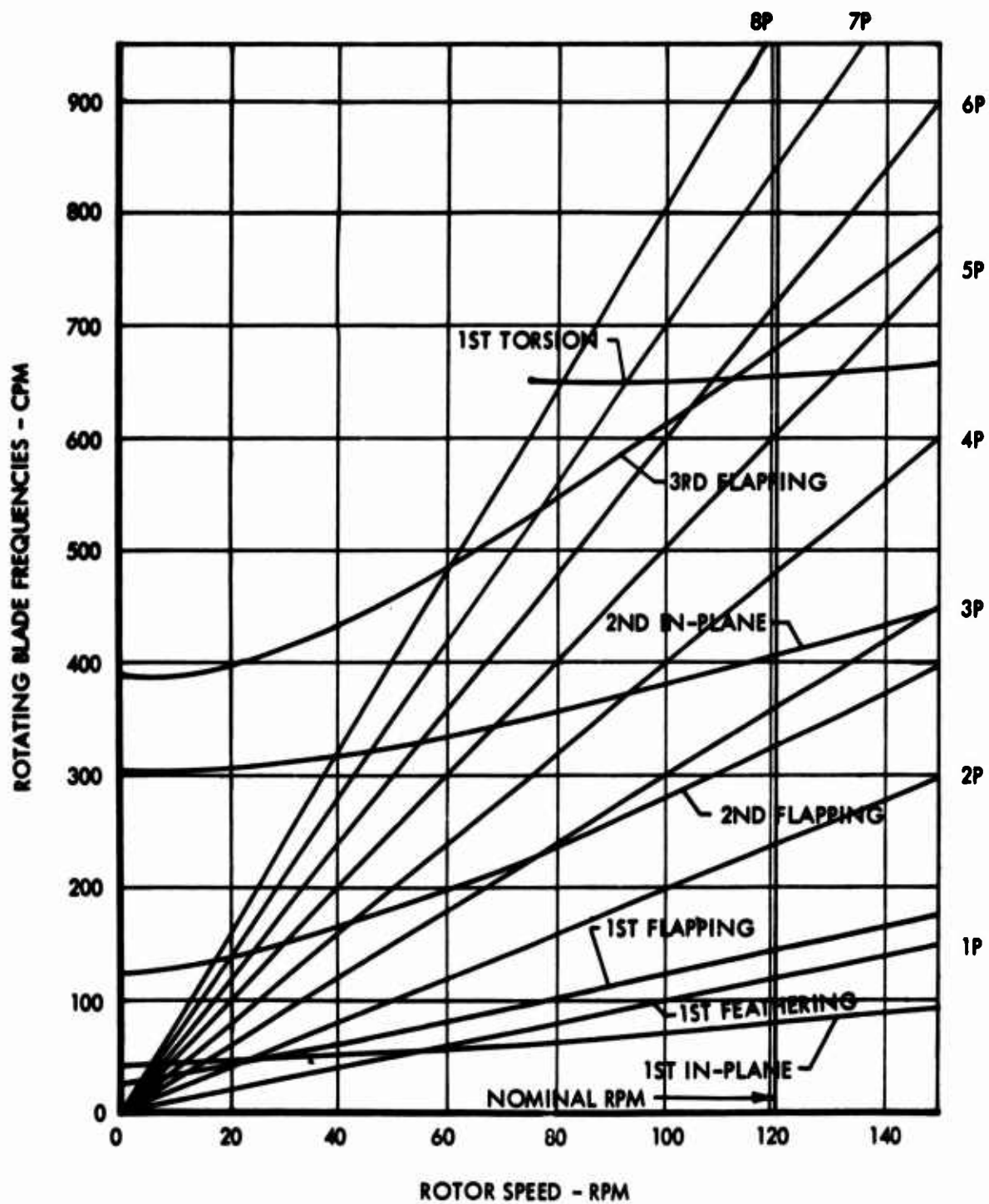


Figure 90. Main Rotor Frequency Spectrum, Heavy-Lift Helicopter -  
Collective Angle = 10 Degrees,  $\theta_1 = -5$  Degrees

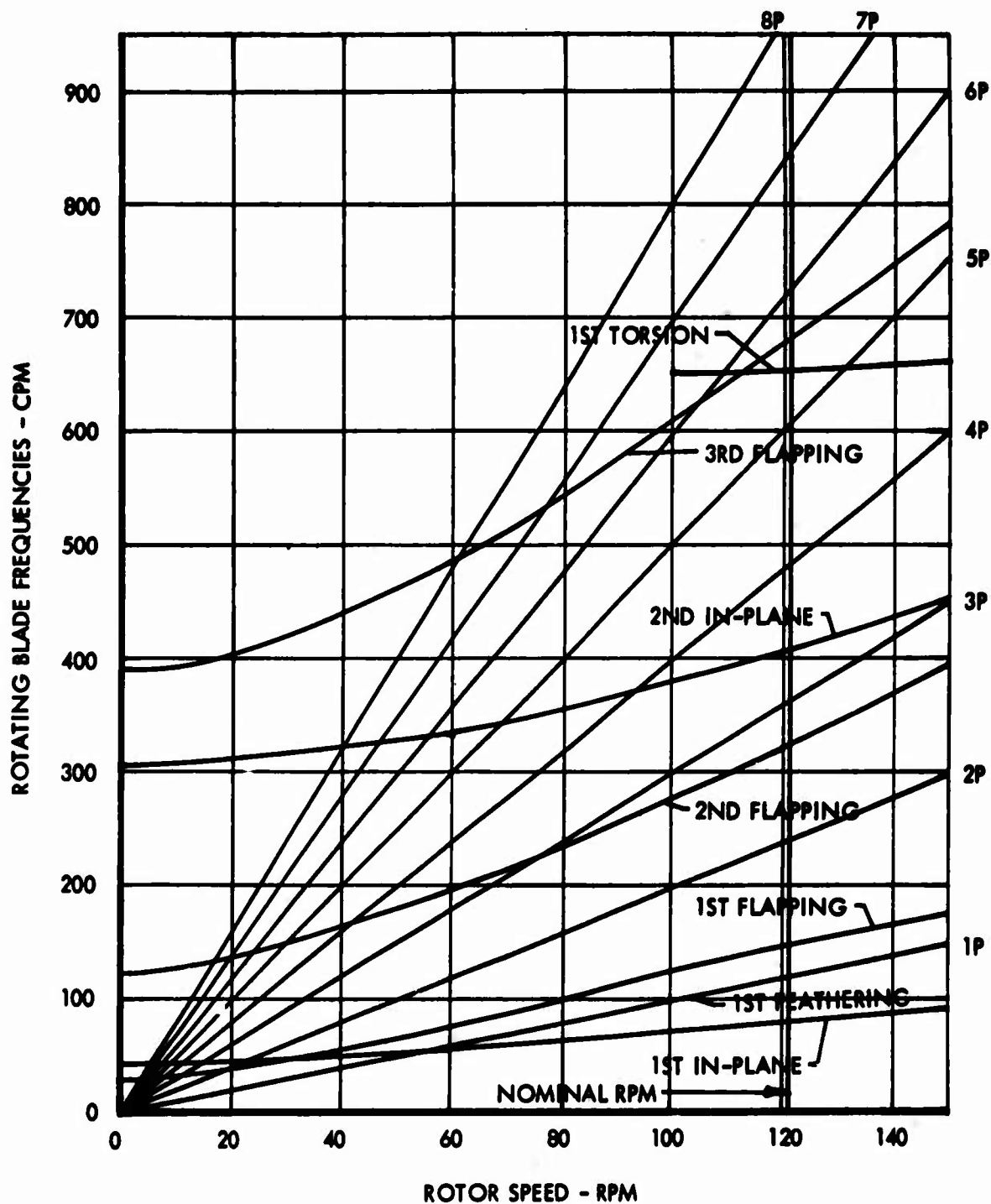


Figure 91. Main Rotor Frequency Spectrum, Heavy-Lift Helicopter -  
Collective Angle = 15 Degrees,  $\theta_1 = -5$  Degrees



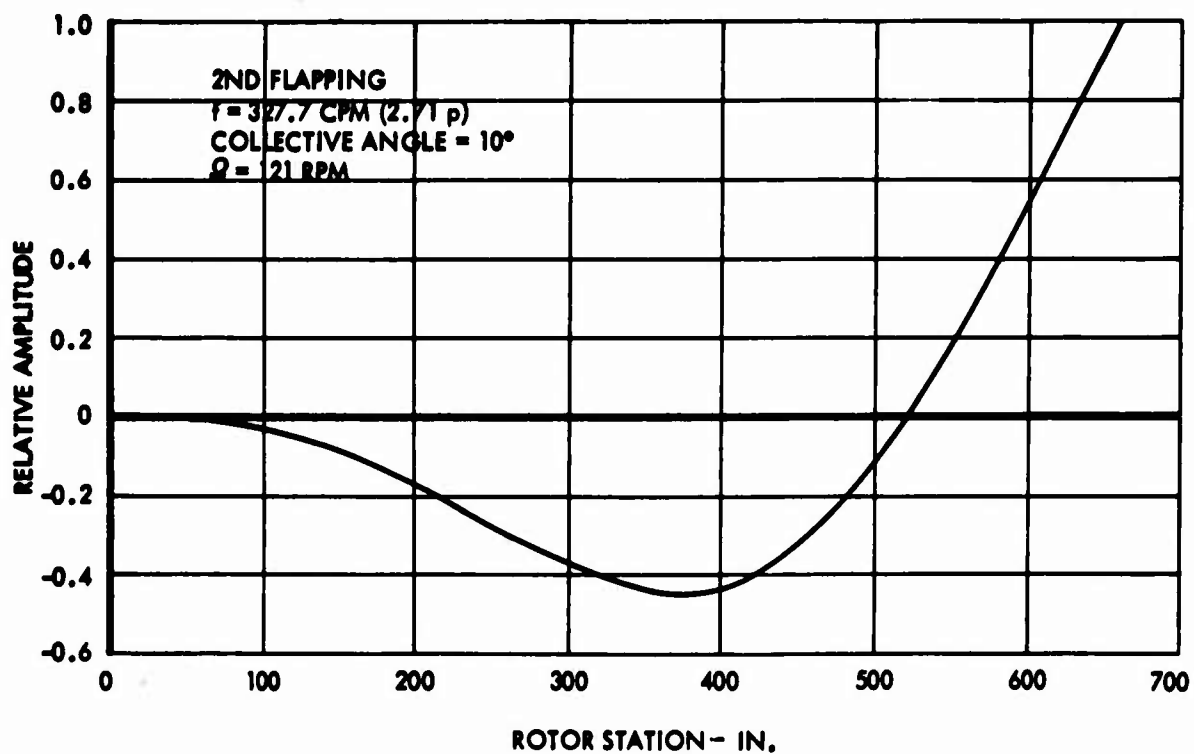
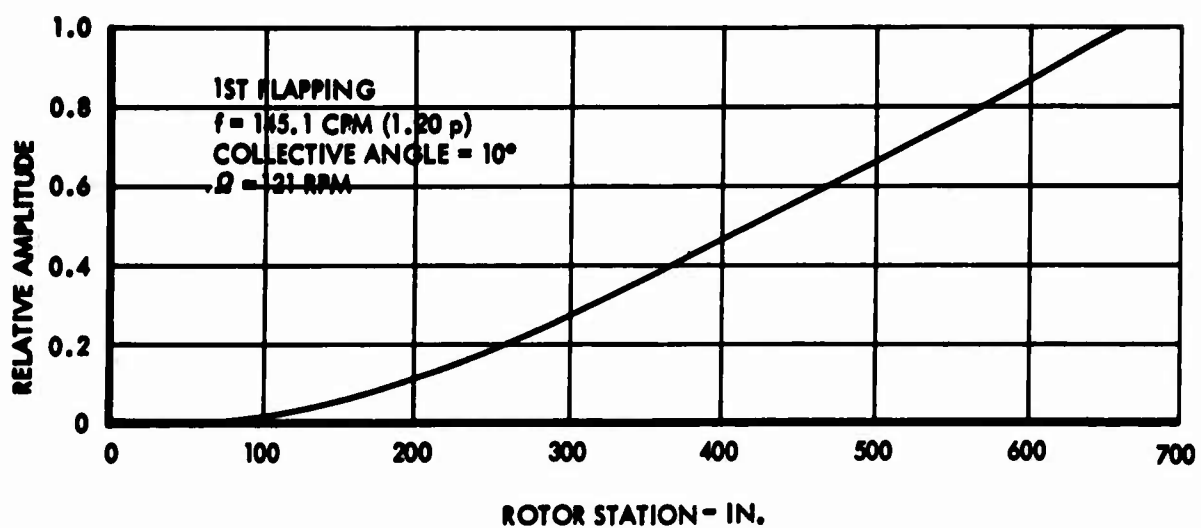


Figure 92. Blade Cantilever Flapping Mode Shapes

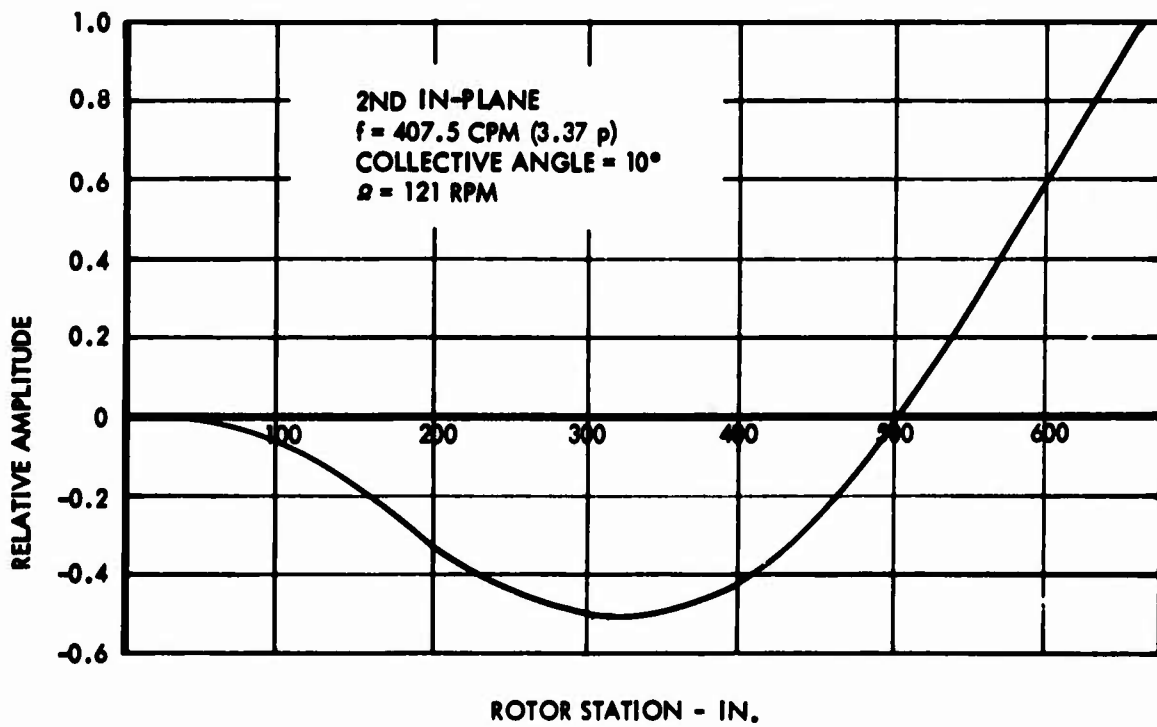
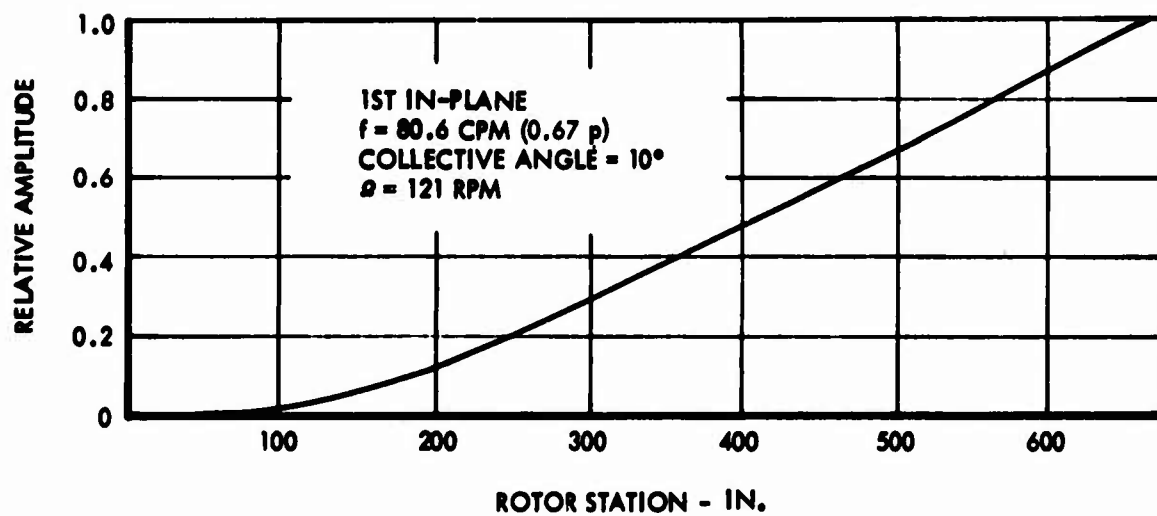


Figure 93. Blade Cantilever In-Plane Mode Shapes

angles indicates that a good frequency separation relative to these harmonic aerodynamic excitations has been achieved. These results indicate that low cabin vibration levels can be expected, providing the fuselage natural frequencies are properly located. This is a detailed design consideration which will be carefully examined in the design of the prototype vehicle.

The response of the rotor to other harmonic aerodynamic excitations must be considered to ensure long rotor life. This is principally associated with the 2P and 3P excitation frequencies. The two modes which are of primary interest are the second flapping and second in-plane bending frequencies relative to 3P excitation. In both cases the computed frequencies of these modes vs rpm and collective angle show good separation relative to this harmonic excitation.

The inertia, stiffness, and geometry of the main rotor used in the determination of these natural frequencies are presented in Figures 113 and 114 (Section 4).

## SECTION 4

### STRUCTURAL DESIGN AND WEIGHT ANALYSES

#### INTRODUCTION

Structural and weight analyses were prepared to substantiate the preliminary design of the main rotor system for the heavy-lift helicopter. The analyses for the selected configuration including a fatigue analysis are presented in this section for the blade spar and flexure, blade segment, rotor hub, and control torque tube, as defined in Figures 50 through 54.

The structural design criteria, development of rotor loads, and fatigue loading spectra are covered in Section 3.

#### STRUCTURAL ANALYSIS

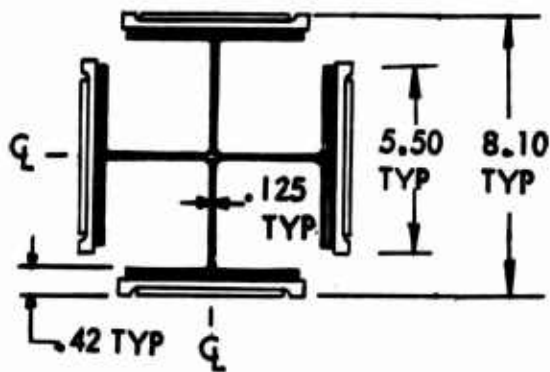
The structural analysis for the listed components was conducted for the critical static and dynamic conditions. The static loading conditions were obtained from the basic loads presented in Section 3, and material allowables were obtained from MIL-HDBK-5. For the dynamic condition, unit stresses were determined for use in the fatigue analysis to determine cyclic and steady stresses for a spectrum of loading conditions. Fatigue allowables were determined and are discussed in "Fatigue Analysis" of this section.

#### Blade Spar and Flexure

The blade spar and flexure consists of two built-up sections joined at the blade root section by bonding (Figure 52). Inherent in this design of wide, flat, tapered plates is the large margin of safety obtainable on the shear bonding stresses. Calculated cyclic shear stresses are less than 5 percent of the minimum shear bonding test values listed in Lockheed Bonding Specification No. 355M. This safe-life concept eliminates the necessity of introducing the notch factors associated with redundant fasteners.

Flexure - The flexure consists of a bonded AM-350 stainless steel crossed "I" section. Spanwise taper is utilized to provide the proper stiffness distribution within allowable stress limits. The attachment of the flexure is accomplished through a built-up fitting at the end of the flexure, picking up a Bolted connection to the hub. Since the flexure material is steel and the hub is titanium, the lug design is critical in the hub; the analysis is presented under "Rotor Hub" in this section.

The analysis of a typical section of the flexure for cyclic flapping and in-plane bending stresses and centrifugal force tension stresses at rotor station 75 for the cross section, as shown, is as follows.



Section Properties:

$$I_{x-x} = 97.9 \text{ in.}^4$$

$$I_{y-y} = 97.9 \text{ in.}^4$$

$$A = 11.04 \text{ in.}^2$$

### Unit Stresses:

The unit stresses at the flexure corner for in-plane and flapping moments of 100,000 inch-pounds based on

$$f = \frac{Mc}{I}$$

are

$$f_b \text{ (flapping)} = 4140 \text{ psi}$$

$$f_b \text{ (in-plane)} = 2810 \text{ psi}$$

The unit stress for a centrifugal force of 100,000 pounds based on

$$f = \frac{P}{A}$$

is

$$f_t \text{ (centrifugal force)} = 9050 \text{ psi}$$

### Flexure Stability (Ground Flapping):

The lateral instability flapwise buckling stress ( $F_{bu}$ ) of the flexure, based on an average value of  $M'$  from Table XV, Formula 18, Reference 20, is calculated to be

$$F_{bu} = 120,000 \text{ psi}$$

The 1.0g (deadweight) flapwise bending moment (nonrotating) at rotor station 75 is integrated from Figure 113 and is

$$M = 232,600 \text{ in.-lb}$$

or a stress of

$$\begin{aligned} f_b &= \frac{232,600}{100,000} \times 4140 \\ &= 9,600 \text{ psi} \end{aligned}$$

If a ground-handling ultimate load factor of 3 is used, the margin of safety is as follows:

$$M.S. = \frac{120,000}{3 \times 9,600} - 1 = \underline{\underline{3.16}}$$

#### Flexure Torsional Stress:

The cyclic torsional shear stress imposed on the bond of the flexure during non-maneuvering flight conditions is based on the average torsional rigidity of the flexure between rotor stations 75 and 165 with an average blade pitch excursion of  $\pm 4^\circ$ .

$$KG_{ave} = 9.6 \times 10^5 \text{ lb-in.}^2 \text{ (Table IX, Formula 4, Reference 20)}$$

where  $G = 11.5 \times 10^6$  (Modulus of rigidity)

$$\begin{aligned} \text{and } Q &= \frac{KG\theta}{l} = \frac{9.6 \times 10^5 \times 4}{90 \times 57.3} \\ &= 745 \text{ in.-lb} \end{aligned}$$

Station 75:

$$f_s = \frac{745 \times 0.42}{0.115} = 2,720 \text{ psi}$$

where  $K = 0.115 \text{ in.}^4$  and  $t = 0.42 \text{ in.}$

Station 165:

$$f_s = \frac{745 \times 0.38}{0.051} = 5,550 \text{ psi}$$

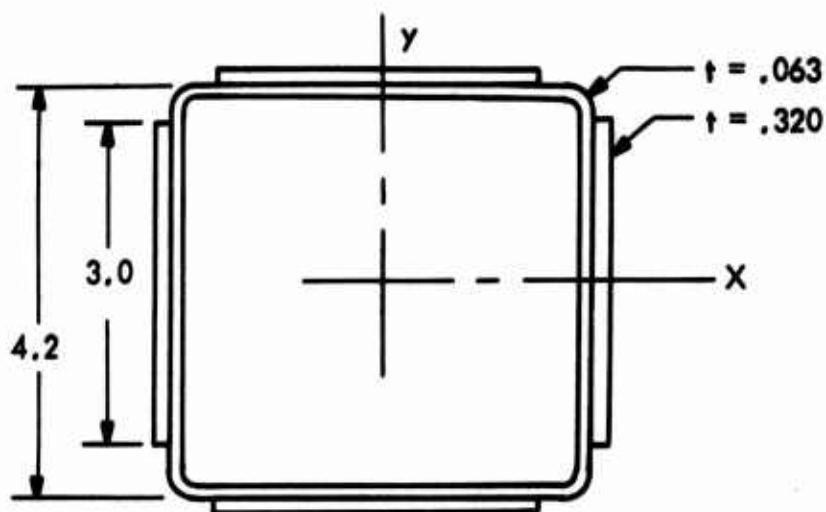
where  $K = 0.051 \text{ in.}^4$  and  $t = 0.38 \text{ in.}$

Because these stresses are peak bond stresses and are averaged in an indeterminate manner, fatigue testing will be required to substantiate this detail of the design configuration.

Blade Spar - The blade spar is a square AM-350 stainless steel tube of constant cross section and wall thickness. Tapered steel plates bonded to the spar at the inboard end provide increased strength and moment of inertia. These plates are continuous with, and form part of, the blade flexure.

The analysis of a typical section of the spar for cyclic flapping and in-plane bending stresses and centrifugal force tension stresses at rotor station 165 for the cross section, as shown, is as follows:

Rotor Station 165



Section Properties:

$$I_{x-x} = 16.5 \text{ in.}^4$$

$$I_{y-y} = 16.5 \text{ in.}^4$$

$$A = 4.86 \text{ in.}^2$$

Unit Stresses:

The unit stresses at the spar corners for in-plane and flapping moments of 10,000 inch-pounds and for a centrifugal force of 100,000 pounds are as follows

$$f_b \text{ (flapping)} = 1,270 \text{ psi}$$

$$f_b \text{ (in-plane)} = 1,270 \text{ psi}$$

$$f_t \text{ (centrifugal force)} = 20,600 \text{ psi}$$

These unit stresses are used to obtain fatigue stresses based on the calculated load spectrum shown in "Fatigue Analysis" of this section.

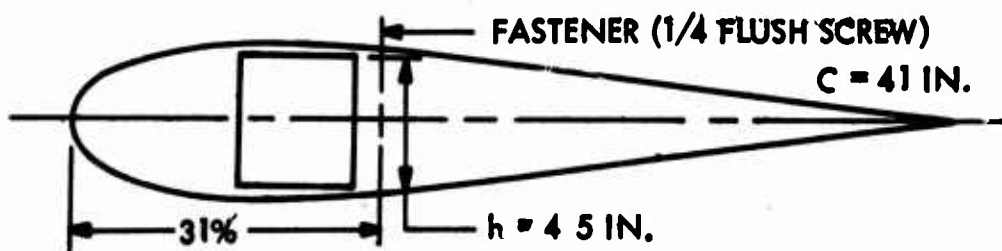


### Blade Segments

The blade structure utilizes 12 spanwise segments, 41 inches long, attached to the spar in such a manner as to transfer airloads, inertia loads, and centrifugal force without imposing large stress concentrations in the spar. The segments at  $r/R = 0.9$  sustain the highest centrifugal force in conjunction with steady and cyclic air loads. Structural analysis is made of the attachment of the most highly loaded segment fastener (4-inch spacing) for the 2.5g condition.

#### Blade Segment

(Reference Figure 51)



#### Fastener Attachment:

Airload/ft span (2.5g, 95 knots)

$$W = 950 \pm 450 \text{ lb (r/R = 0.9)}$$

Twenty-eight percent of the airload is used in a triangular distribution aft of the section (31 percent) of fastener attachment.

$$\begin{aligned} M_f &= \frac{0.28 (950 \pm 450)}{3} \times (1 - 0.31) \times 49 \\ &= 3000 \pm 1420 \text{ in.-lb/ft span} \end{aligned}$$

The moment due to centrifugal force is:

$$M_{CF} = \frac{w^2 R}{g} \times W \times R = \frac{12.7^2 \times 49.5 \times 8.4 \times 13.1}{32.2}$$

$$= 27,300 \text{ in.-lb/segment}$$

Fatigue load on fastener:

$$P = 1/3 \frac{3000 \pm 1420}{4.5} + 1/2 \frac{27,300 \times 20}{1760}$$

$$= 377 \pm 105 \text{ lb}$$

$$P_{ALLOW.} = 0.20 \times 3680 = 736 \text{ lb}$$

$$M.S. = \frac{736}{105} - 1 = \underline{\underline{6.02}}$$

Ultimate load on fastener:

$$P = 1.5 \times (377 \pm 105)$$

$$= 722 \text{ lb}$$

$$P_{ALLOW.} = 3,680 \text{ (Reference MIL-HDBK-5)}$$

$$M.S. = \frac{3680}{722} - 1 = \underline{\underline{4.10}}$$

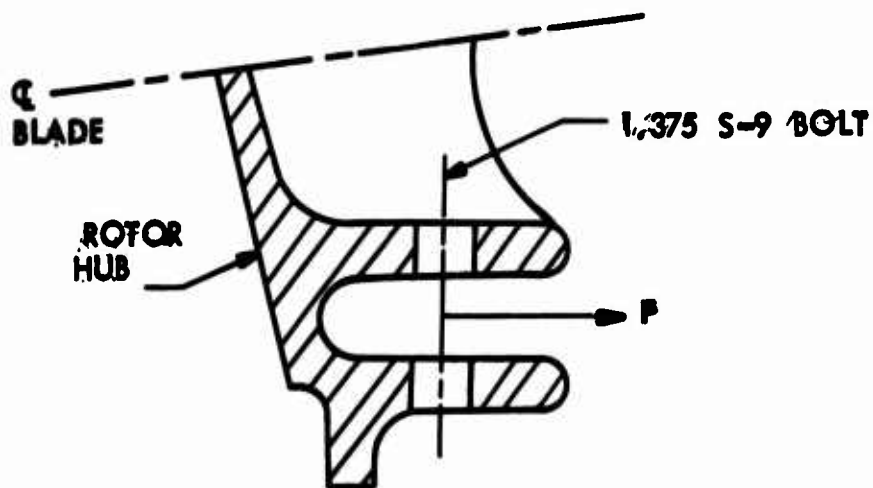
### Rotor Hub

The rotor hub is made from a single titanium ring forging. Attachment of each blade root fitting to the hub is by means of four 1-3/8-inch bolts in double shear. Redistribution of blade root loads by the upper and lower ring elements of the hub produces steady and cyclic bending stresses in these ring elements. Shears, lift, and bending moments are transferred to the nonrotating mast by the upper and lower bearings (Figure 53).

Analysis is made of the bolt attachment for the ultimate condition of takeoff from a 10-degree slope. (Reference page 177)

The mating lug of the spar flexure fitting is 1.50 inches thick and by comparison is of comparable strength to the two 1-inch-thick titanium lugs of the rotor hub.

Hub Bolt Lug



Lug Shear:

$$M_F = 4,350,000 \text{ in.-lb (ultimate) (Reference page 177)}$$

$$M_C = 3,225,000 \text{ in.-lb (ultimate)}$$

$$CF = 159,000 \text{ lb (ultimate)}$$

$$P (\text{lug}) = \frac{4,350,000}{10.5 \times 2} + \frac{3,225,000}{9.25 \times 2} + \frac{159,000}{4}$$

$$= 421,000 \text{ lb (ultimate)}$$

Lug Shear-out:

$$P = \frac{421,000}{2} = 210,500 \text{ lb/lug (ultimate)}$$

$$P_{\text{ALLOW}} = A \times F_s = 2 \times 1.8 \times 1 \times 76,000 \\ = 274,000 \text{ lb (ultimate)}$$

$$\text{M.S.} = \frac{274,000}{210,500} - 1 = \underline{\underline{0.30}}$$

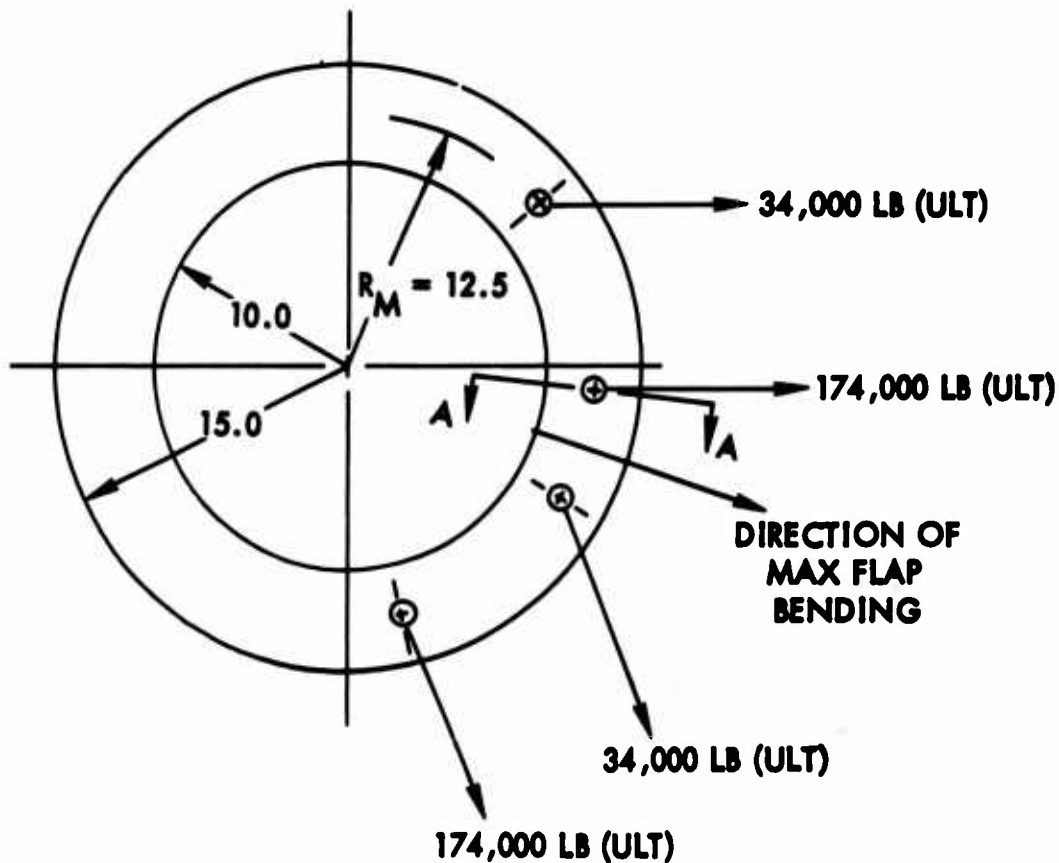
Bolt Shear:

The attaching bolts are Type S-9 (Special) 1.375-diameter with a double-shear allowable of

$$P_{\text{ALLOW}} = 463,000 \text{ lb (Reference MIL-HDBD-5, Page 8.1.2(a))}$$

$$\text{M.S.} = \frac{463,000}{423,000} - 1 = \underline{\underline{0.10}}$$

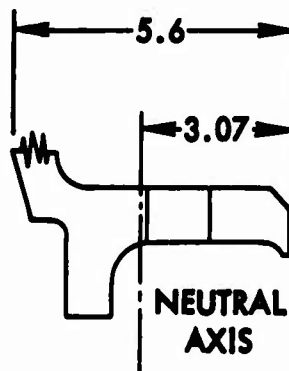
Hub Lower Flange:



The loads shown adjacent to Section A-A are a conservative combination of ultimate flapping and in-plane bending moments and centrifugal force. The maximum bending moment at Section A-A is determined by means of influence coefficients.

$$\begin{aligned} M_{a-a} &= 34,000 \times 12.5 (0.05) + 174,000 \times 12.5 (-0.2387) \\ &\quad + 34,000 \times 12.5 (-0.046) + 174,000 \times 12.5 (0.103) \\ &= -293,300 \text{ in.-lb (ultimate)} \end{aligned}$$

$$\begin{aligned} N_{a-a} \text{ (axial load)} &= \frac{5(34,000 + 174,000)}{2\pi R_M} \times R_M \\ &= 83,000 \text{ lb (ultimate)} \end{aligned}$$



**SECTION A-A**

Section Properties:

$$I_{x-x} = 17.3 \text{ in.}^4$$

$$A = 4.25 \text{ in.}^2$$

The material is T1-6AL-4V forging (annealed)

$$F_{tu} = 130,000 \text{ psi (Reference MIL-HDBK-5)}$$

$$f_b = \frac{293,300 \times 3.07}{17.3} = 52,000 \text{ psi (ultimate)}$$

$$f_t = \frac{83,000}{4.25} = 19,500 \text{ psi (ultimate)}$$

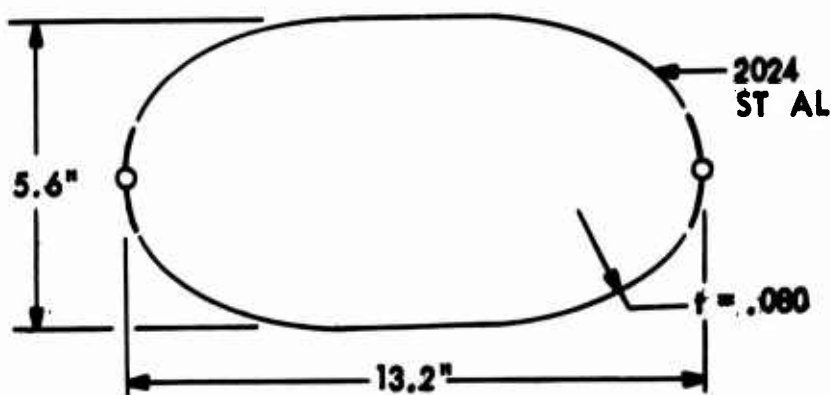
$$M.S. = \frac{130,000}{71,500} - 1 = \underline{\underline{0.82}}$$

The remaining three hub flanges all have greater radial depth and their margins of safety are considered high by comparison.

#### Control Torque Tube

Blade feathering, or pitch control, is transmitted to the blade from the gyro by means of the torque tube shown in Figure 54. The rigidity requirement of the control system is the governing parameter in the design of the torque tube. As such, the stress level is considerably below the endurance limit. The stresses, based on the section properties required for control system stiffness, were determined for the maximum expected operating cyclic feathering moments.

Torque Tube at Station 165



#### Torque Tube Area:

$$A = \pi \times a \times b = \pi \times \frac{13.2}{2} \times \frac{5.6}{2} = 58.1 \text{ sq in.}$$

#### Maximum cyclic feathering moment:

$$M = \pm 20,000 \text{ in.-lb}$$

$$f_{s-a} = \frac{T}{2At} = \frac{\pm 20,000}{2 \times 58.1 \times 0.080}$$

$$= \pm 2,150 \text{ psi (alternating shear stress)}$$

$$F_{se} = 0.6 \times 7,000 \text{ (Reference MIL-HDBK-5)}$$

$$= 4,200 \text{ psi (shear endurance stress)}$$

$$M.S. = \frac{4,200}{2,150} - 1 = \underline{\underline{0.99}}$$

### FATIGUE ANALYSIS

A fatigue analysis of the heavy-lift rotor system at rotor stations 75 and 165 was prepared to assure that the preliminary design configuration would be capable of meeting the required 3600-hour service life.

The extreme range of operational conditions of the heavy-lift helicopter demands careful consideration of detail design, loading history, and selection of design stresses which are compatible with a useful service life for the structure. The fatigue analysis makes use of all available information to provide a design guide to achieve this objective. In the final stages of design development, verification of loading spectra and realistic full-scale testing are required to substantiate service life.

#### Method of Analysis

The method of fatigue analysis used is based upon the anticipated spectra of loadings and linear cumulative damage analysis. In this analysis, the spectra of loadings for the two sections of the rotor system selected are shown in Figures 83 through 86. AM-350 stainless steel,  $F_{tu} = 230$  ksi, is the material proposed for the flexure and blade structures. The basic S-N diagrams for this material appear in Figures 94 through 97.

The interpretation of cumulative damage calculations, as used by the Lockheed-California Company, is based upon a comparison of calculated lives with known test data. Figure 98 is an example of this comparison, which shows the cumulative percentage of test specimens that equal or exceed a given ratio of test life to calculated life with and without reduction in S-N data. These curves are based on a substantial number of tests in which realistic fatigue loading sequences were used on specimens for which S-N data were available. The figure gives an indication of the reduction required in the varying stress scale of the S-N data to obtain predictions of test life potential with test-to-calculated-life ratio of one or more for various degrees of assurance. For this fatigue analysis, a 40-percent

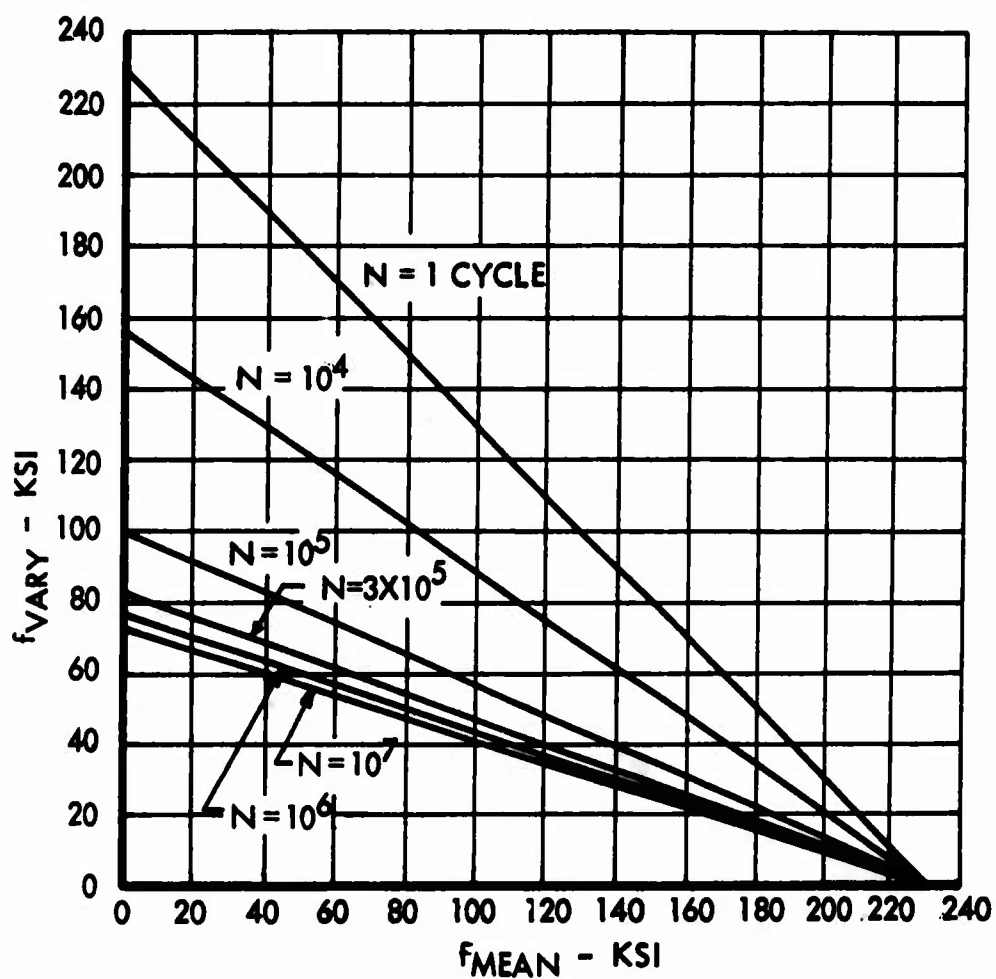


Figure 94. S-N Diagram - AM-350 Stainless Steel,  $K_T = 1.0$



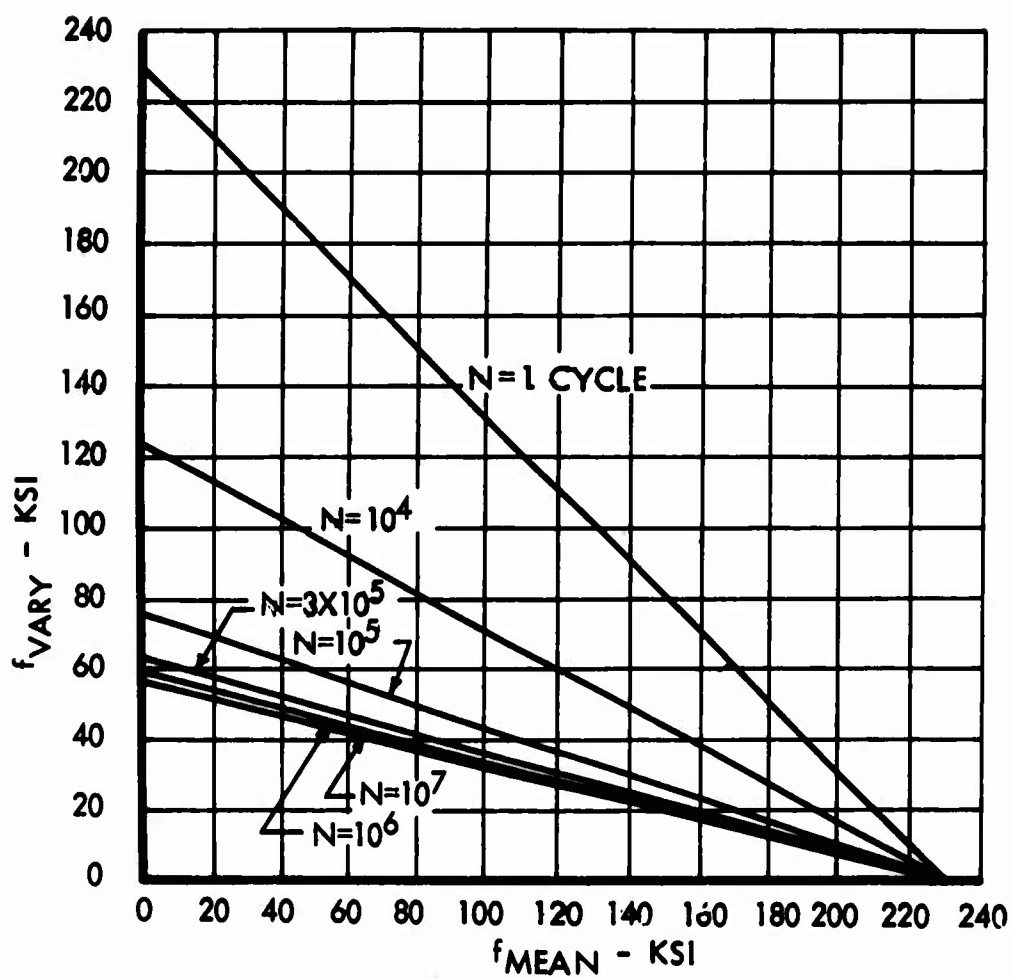


Figure 95. S-N Diagram - AM-350 Stainless Steel,  $K_T = 2.0$

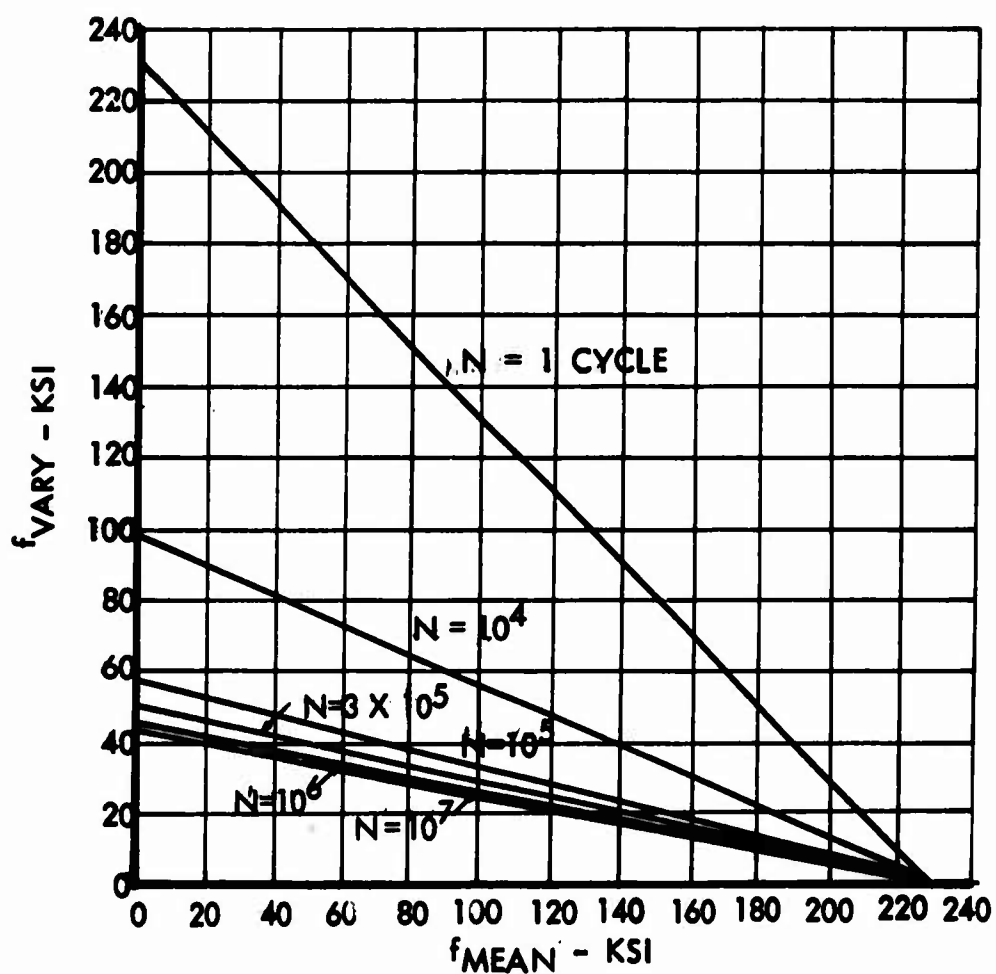


Figure 96. S-N Diagram - AM-350 Stainless Steel,  $K_T = 3.0$

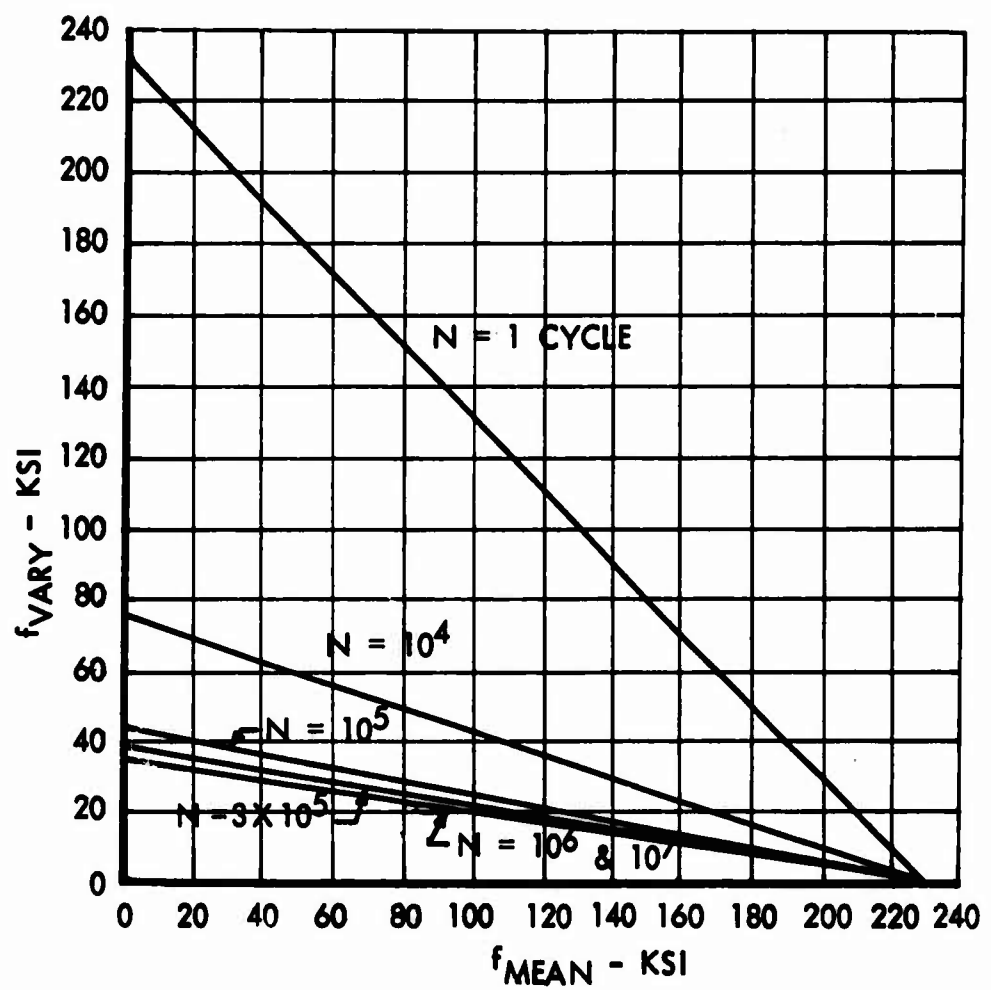


Figure 97. S-N Diagram - AM-350 Stainless Steel,  $K_T = 4.0$

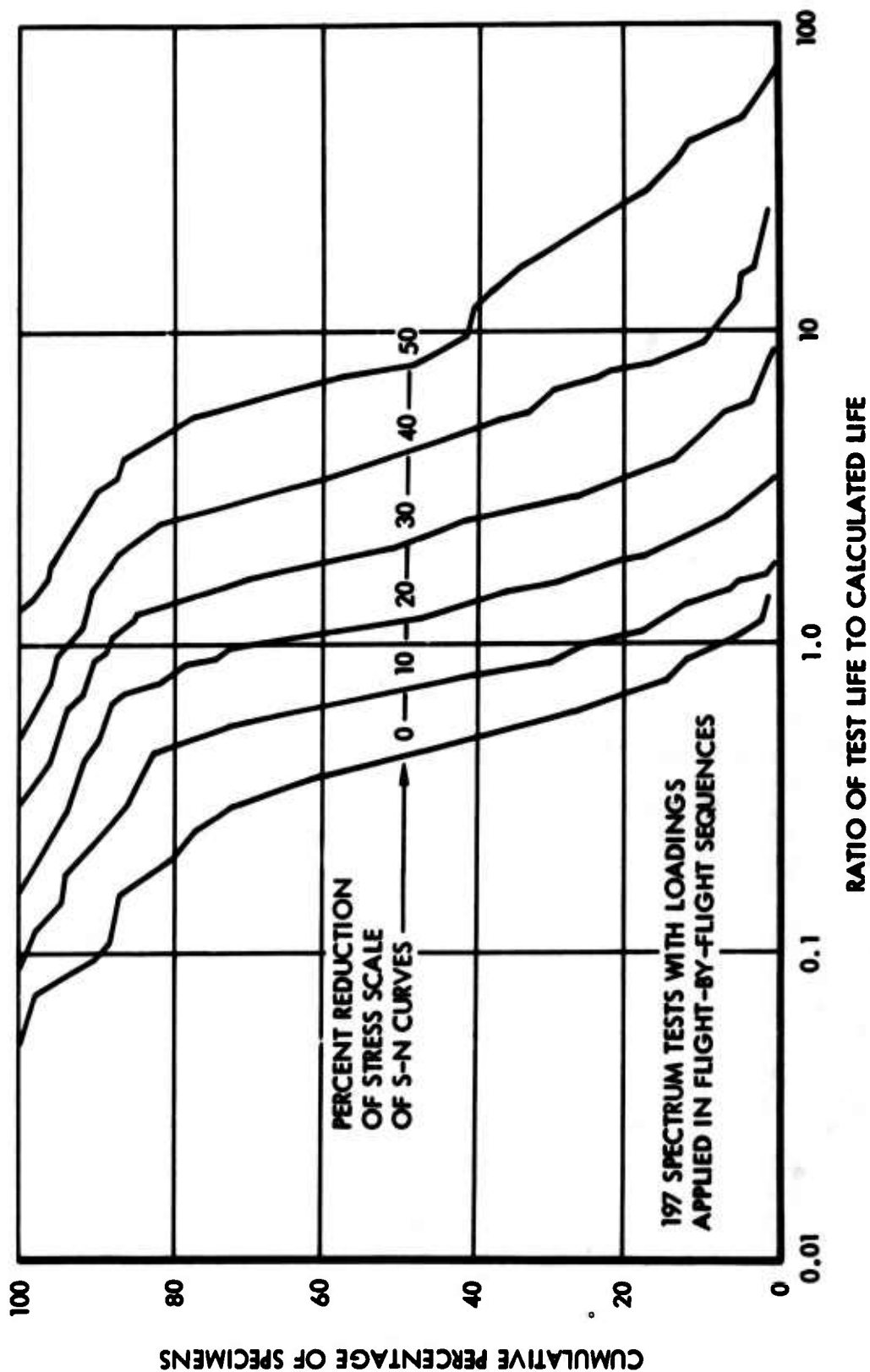


Figure 98. Cumulative Percentage of Fatigue Test Specimens Equalling or Exceeding a Ratio of Test Life to Calculated Life

reduction of the S-N data was used which gives reasonable assurance that tests conducted under simulated service loading will equal or exceed the calculated life.

A range of design stresses and fatigue quality indices, K, was selected to establish a design stress which was compatible with the required service life and projected detail design development. This procedure resulted in a fatigue index corresponding to  $K = 2.5$  for the spectra of loadings shown in Figures 83 through 86.

The spectra of stresses shown in Figures 99 and 100 are for 3600 hours for each type of mission. They represent the stresses at the corner of the structural sections of the flexure and blade, if it is assumed that 80 percent of the chordwise loading magnitudes are in phase with the flapping loads. These stresses appear reasonable in relation to stress spectra of existing rigid rotors.

#### Fatigue Life Prediction

The effects of design stress level and design fatigue quality indices on calculated life are shown in Figures 101 through 110. These are cumulative damage calculations converted to life in hours. In each of these figures, the 100 percent of design stress level corresponds to the spectra of loadings and structural sections used to obtain the stress spectra shown in Figures 99 and 100.

The effect of three different composites of the basic missions on calculated life is illustrated in Figures 109 and 110. The most critical composite, number 2 as indicated by the  $K = 2$  curves, is used to represent the anticipated service usage for 3600 hours. A design fatigue quality index of approximately 2.5, as shown in Figures 111 and 112, is required. Local stress concentrations which exceed this value must be restricted to areas having a correspondingly lower stress field.

#### ROTOR SYSTEM CHARACTERISTICS

The weight, bending stiffness, and torsional stiffness distribution of the rotor system is shown in Figure 113. The pitch mass moment of inertia is shown in Figure 114.

#### ROTOR BLADE TIP DEFLECTION

The static droop, or rotor blade tip deflection for the lg condition, computed from the weight and stiffness distribution shown in

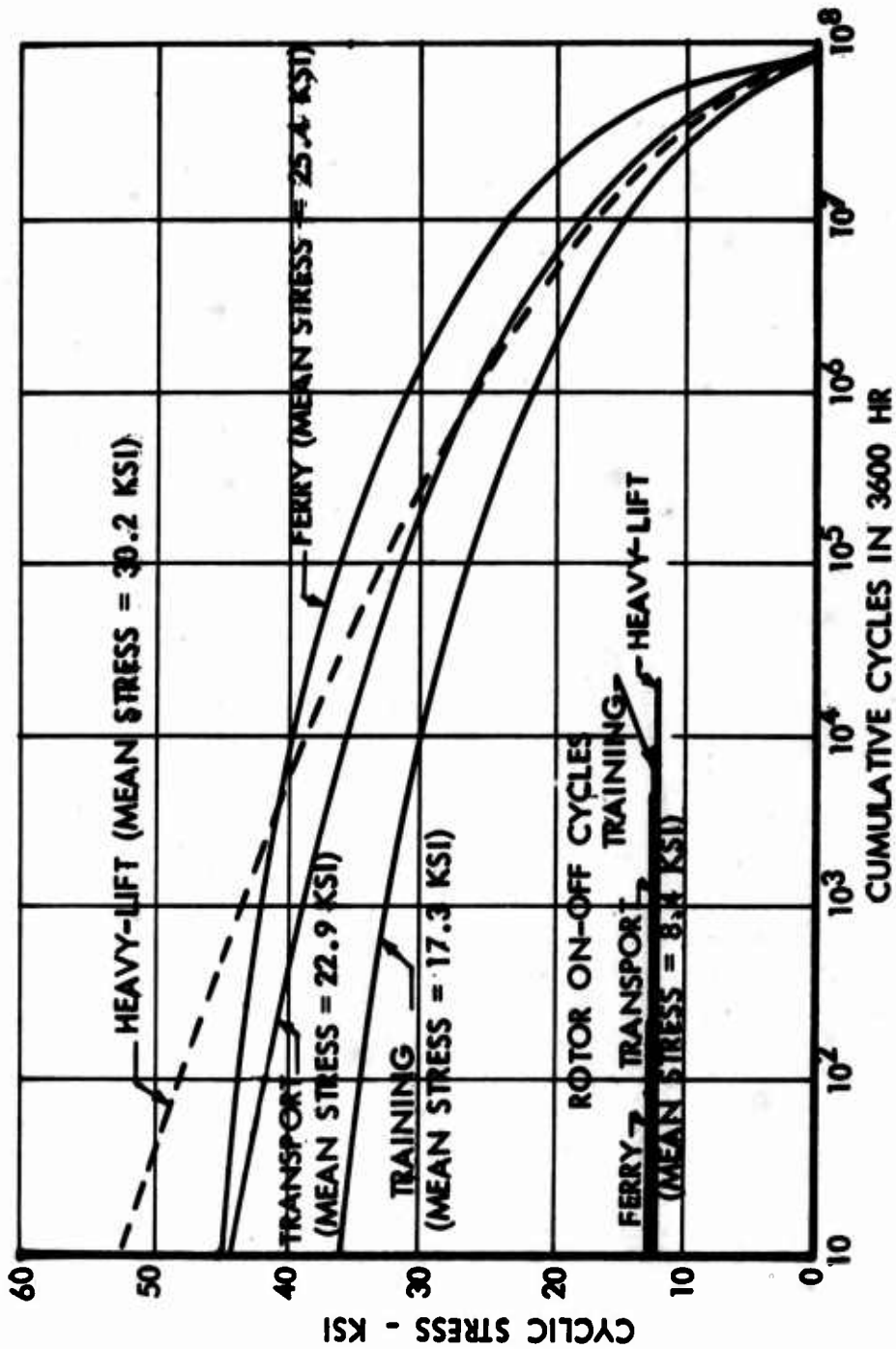


Figure 99. Stress Spectra at Main Rotor Blade Station 75

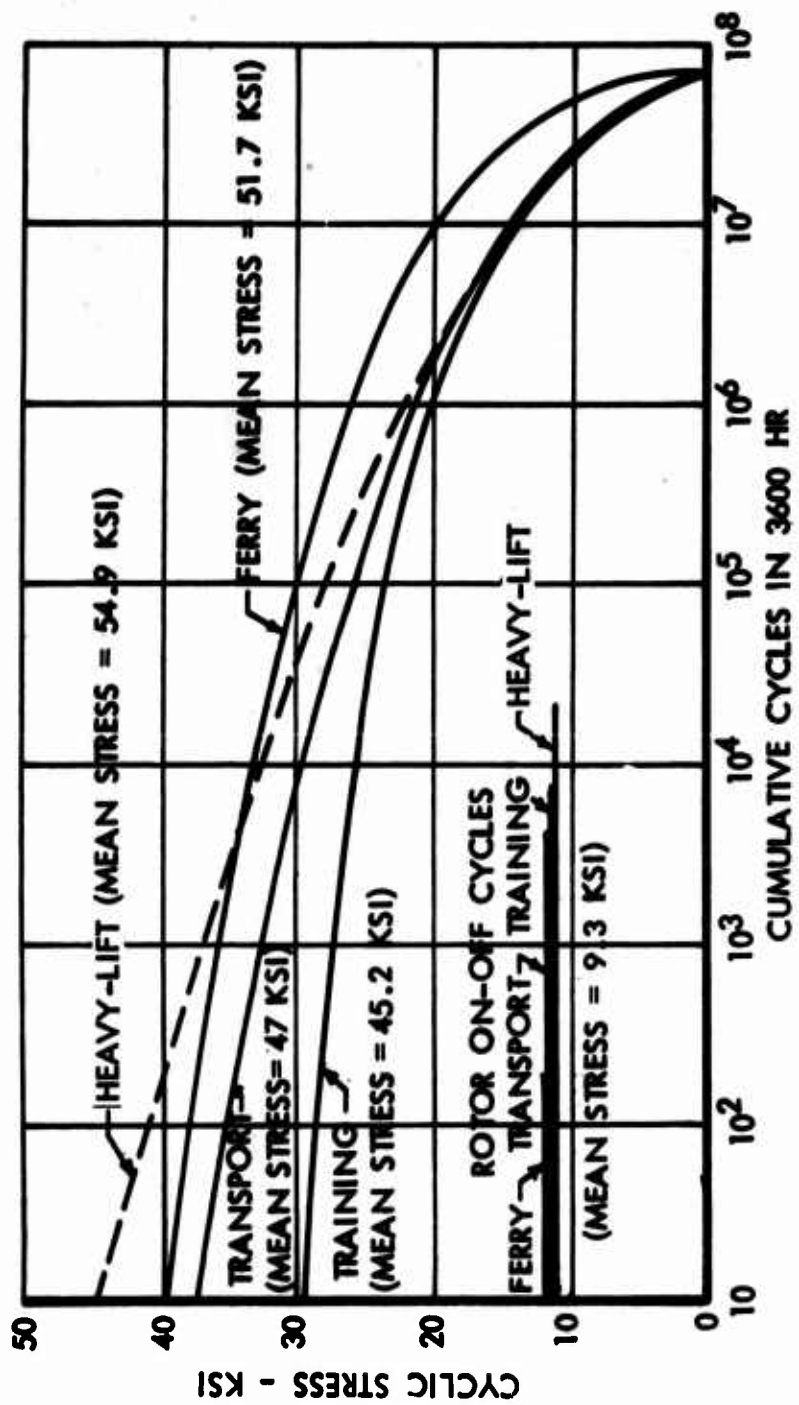


Figure 100. Stress Spectra at Main Rotor Blade Station 165

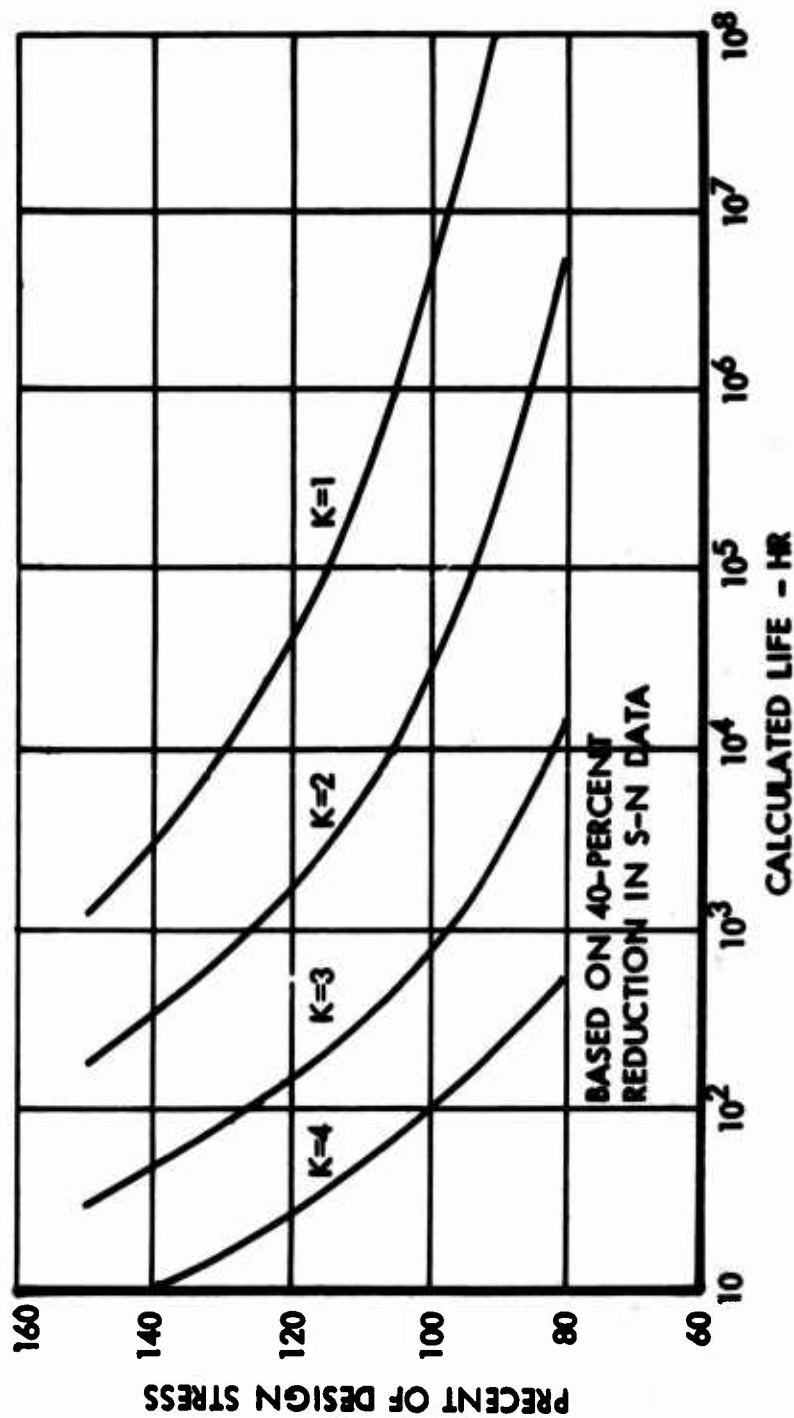


Figure 101. Calculated Life at Main Rotor Blade Station 75 - Transport Mission



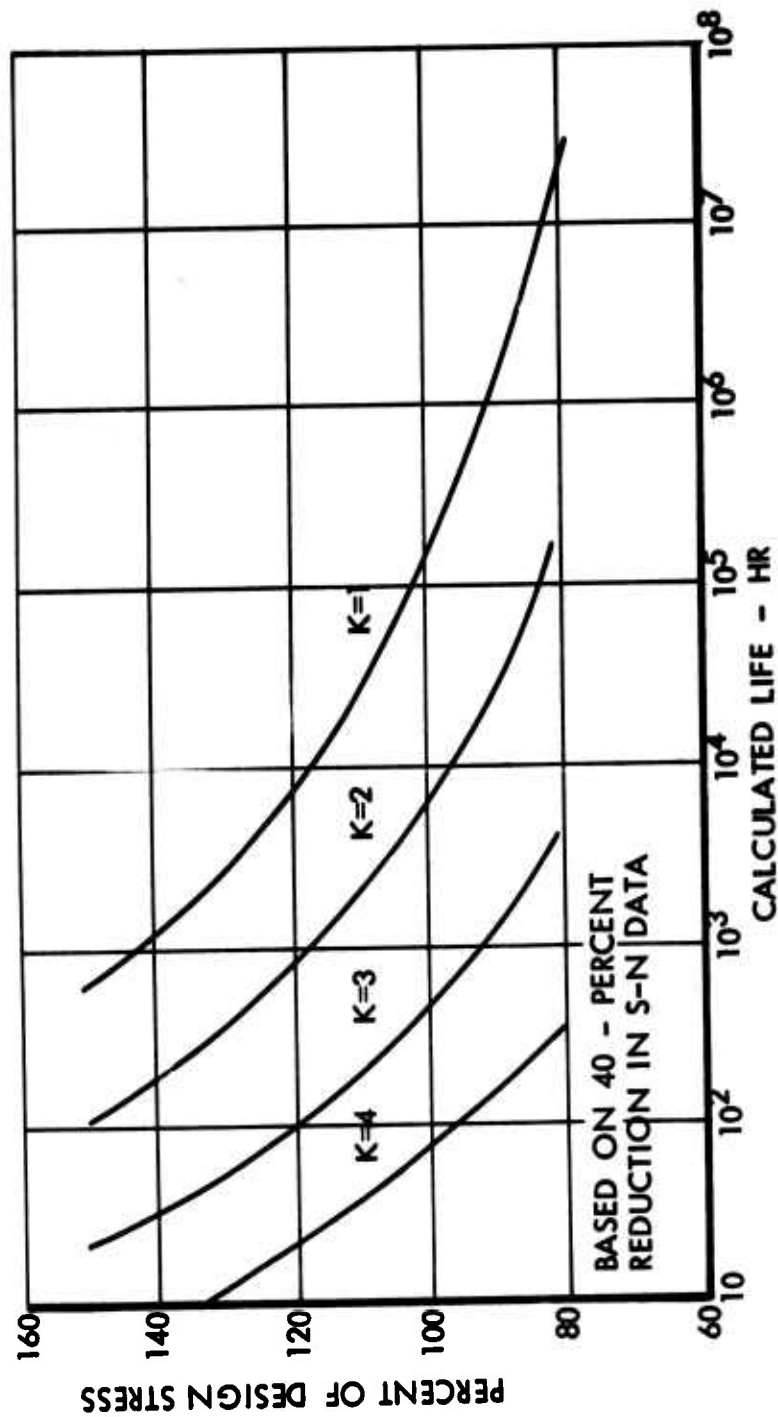


Figure 102. Calculated Life at Main Rotor Blade Station 75 - Heavy-Lift Mission

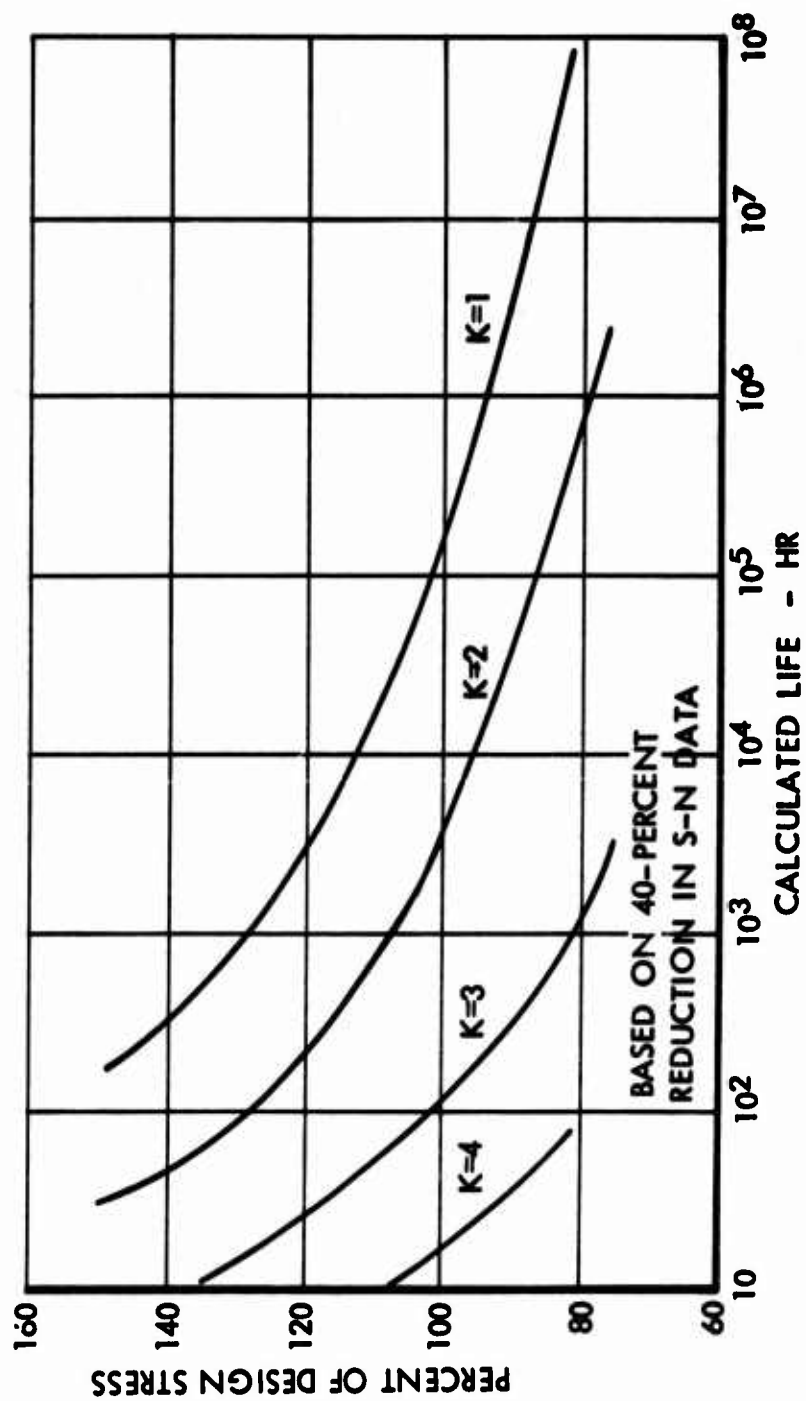


Figure 103. Calculated Life at Main Rotor Blade Station 75 - Ferry Mission

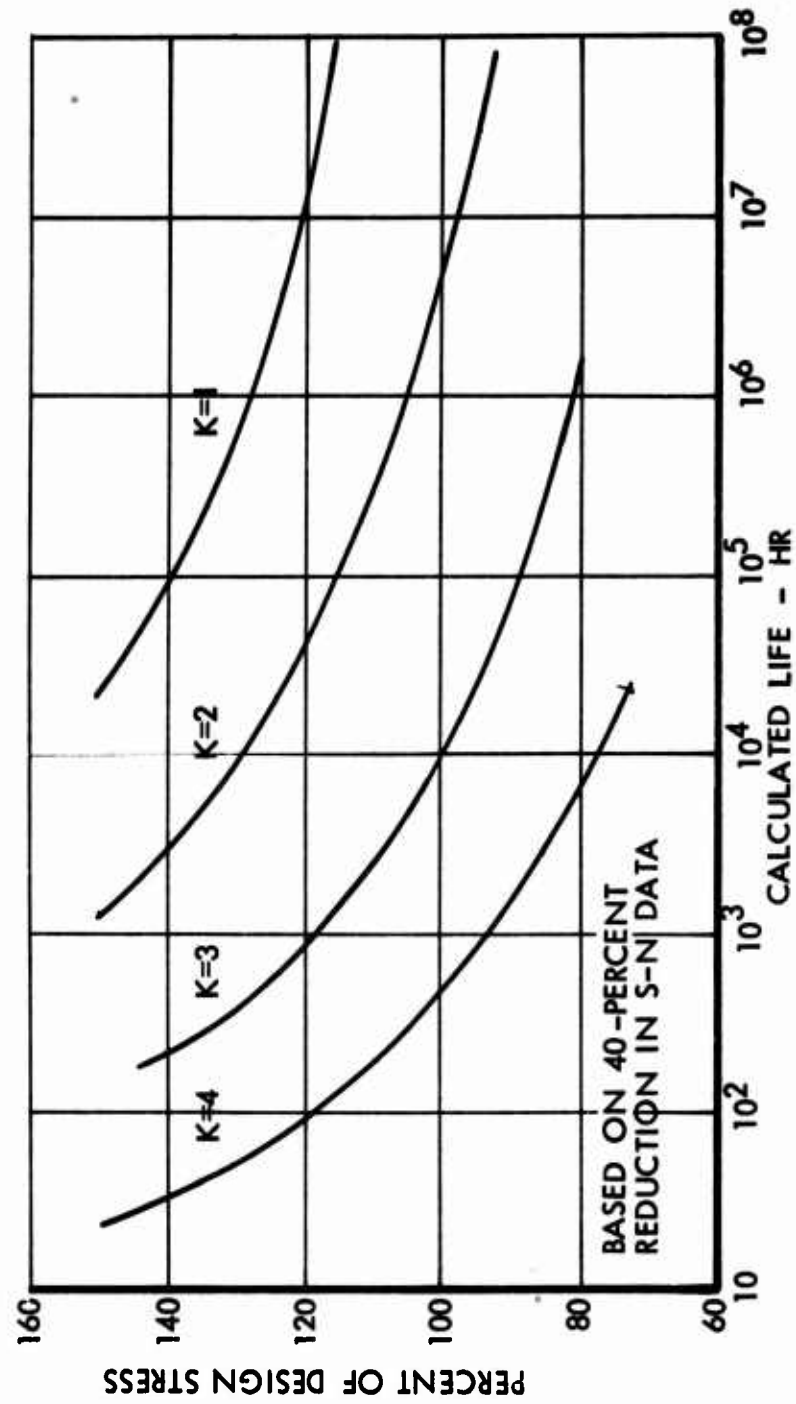


Figure 104. Calculated Life at Main Rotor Blade Station 75 - Training

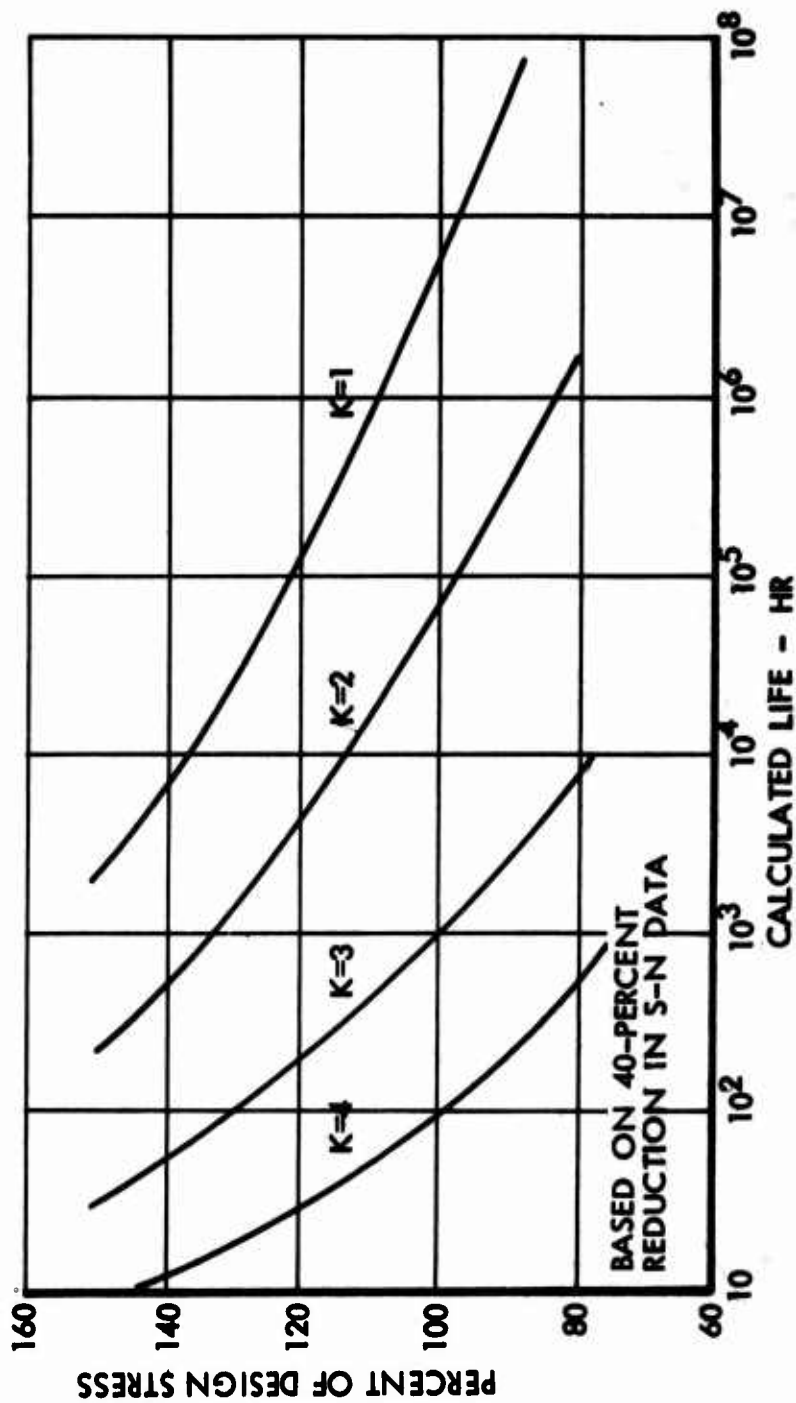


Figure 105. Calculated Life at Main Rotor Blade Station 165 - Transport Mission

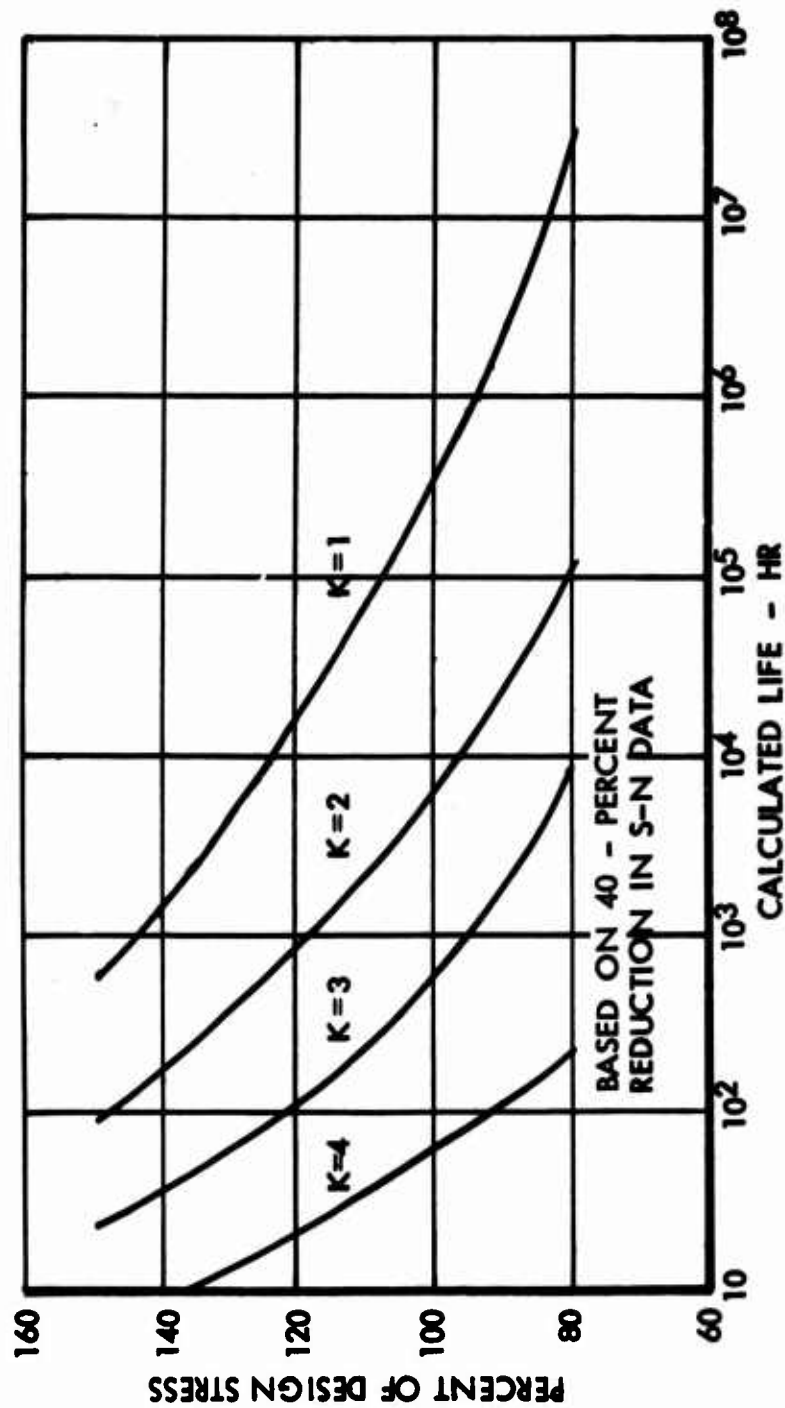


Figure 106. Calculated Life at Main Rotor Blade Station 165 - Heavy-Lift Mission

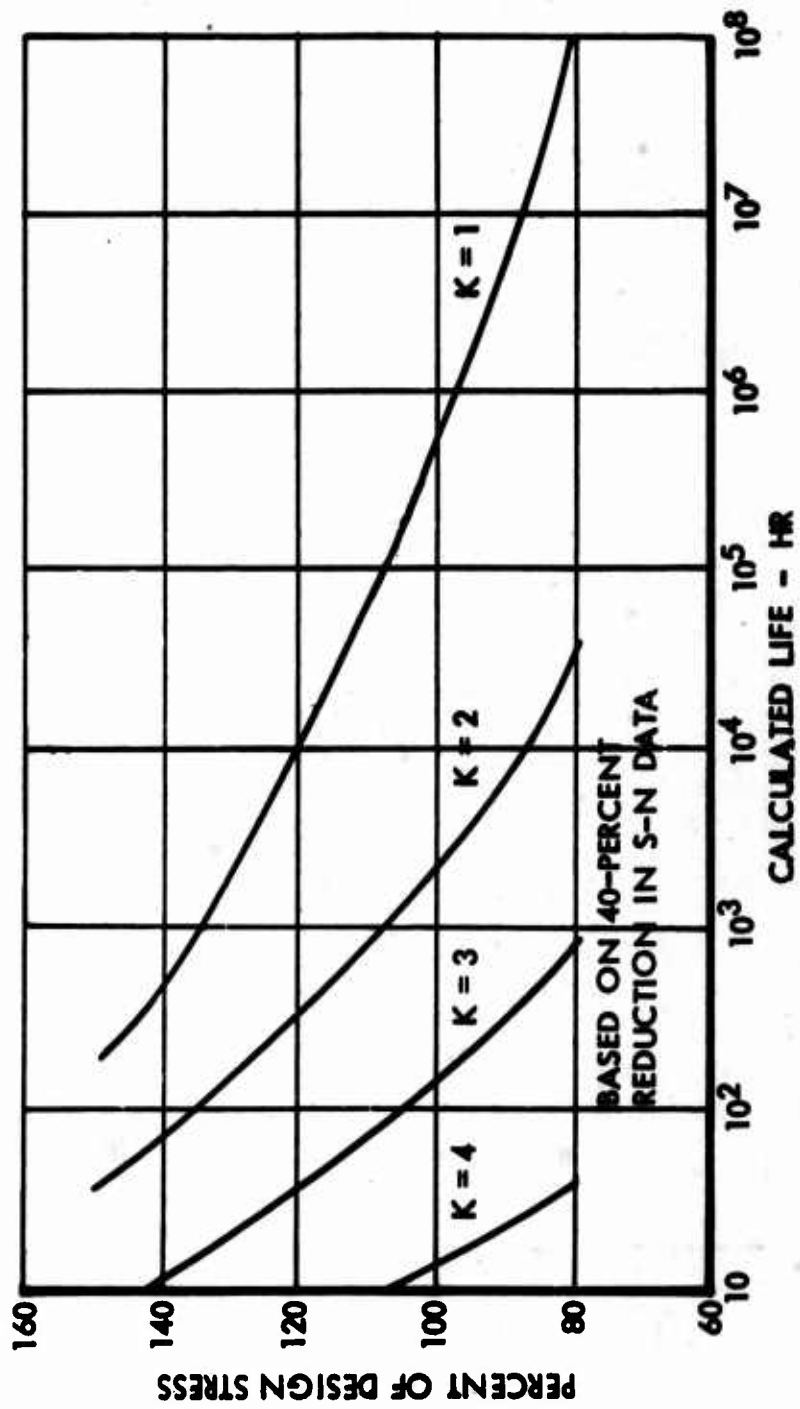


Figure 107. Calculated Life at Main Rotor Blade Station 165 - Ferry Mission

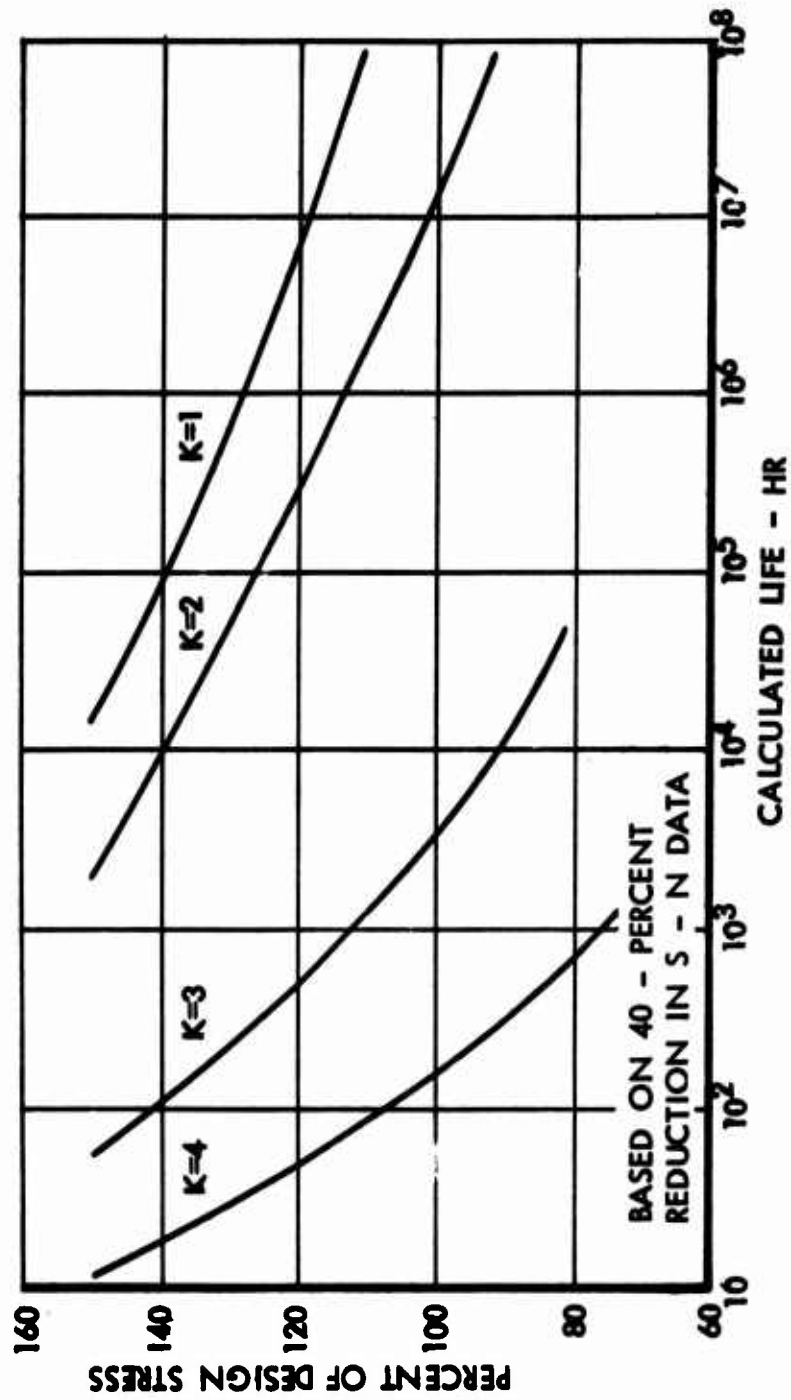


Figure 108. Calculated Life at Main Rotor Blade Station 165 - Training

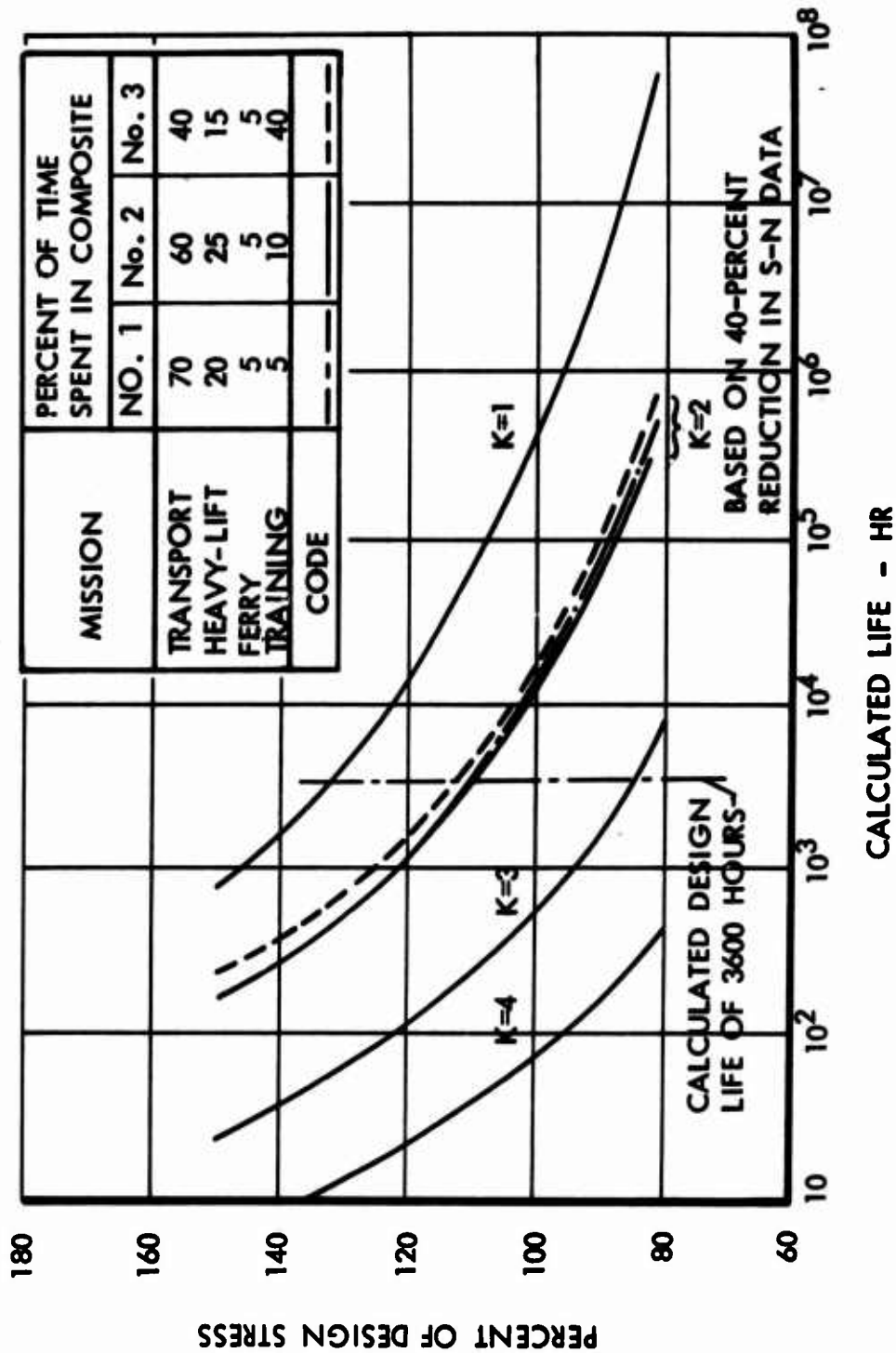


Figure 109. Calculated Life at Main Rotor Blade Station 75 - Composite



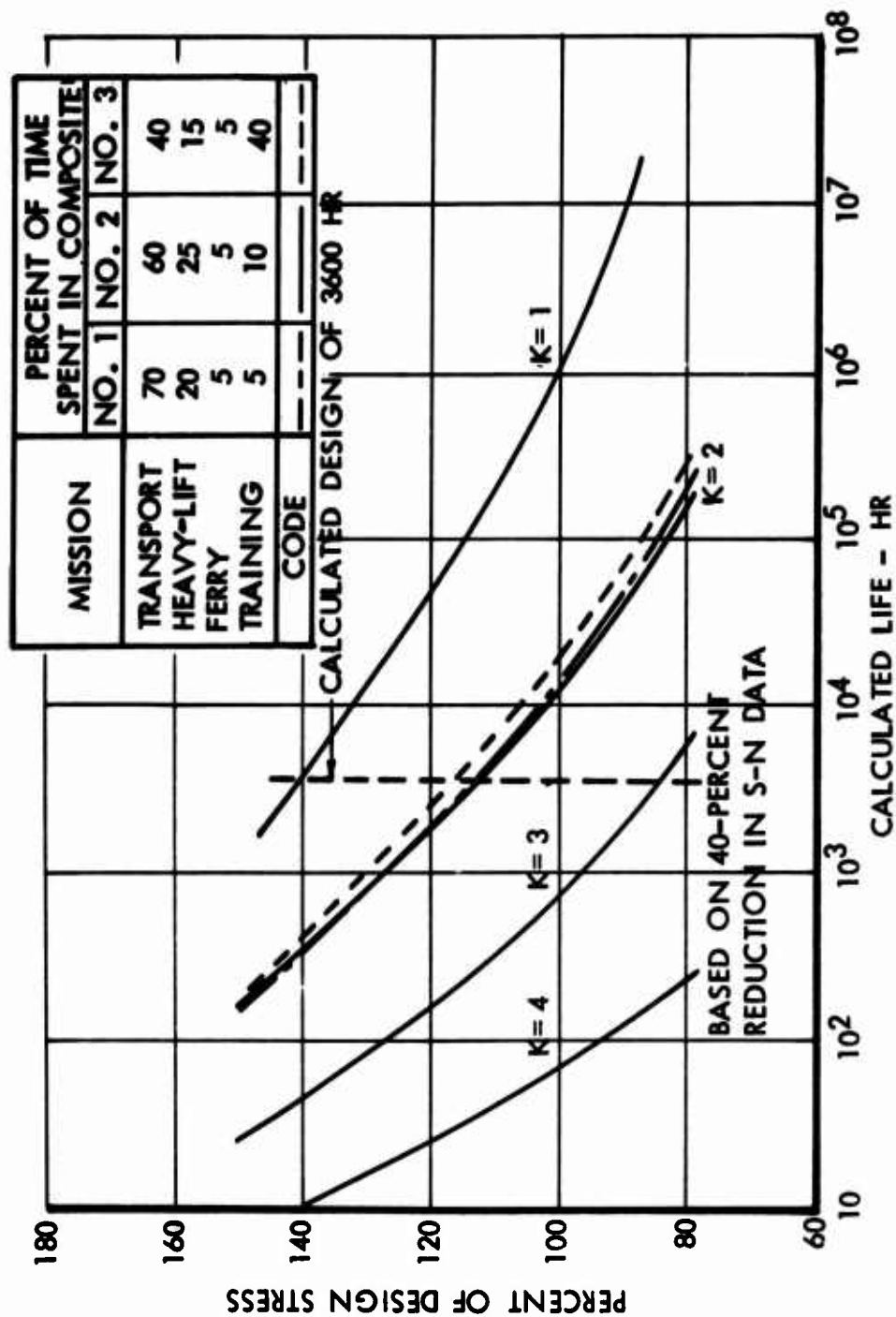


Figure 110. Calculated Life at Main Rotor Blade Station 165 - Composite

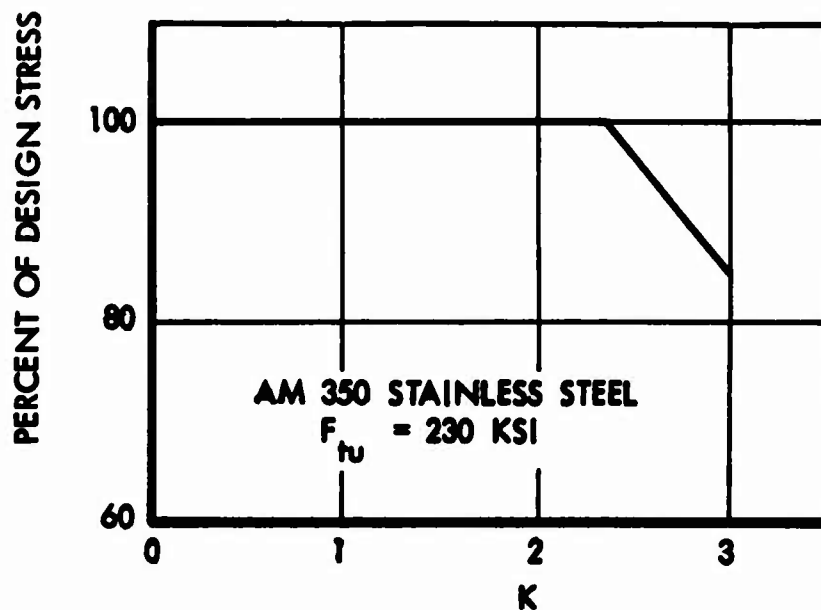


Figure 111. Variation in Design Stress at Main Rotor Blade Station 75 with K - 3600-Hour Life for Composite Mission Profile No. 2, 40-Percent Reduction in S-N Data

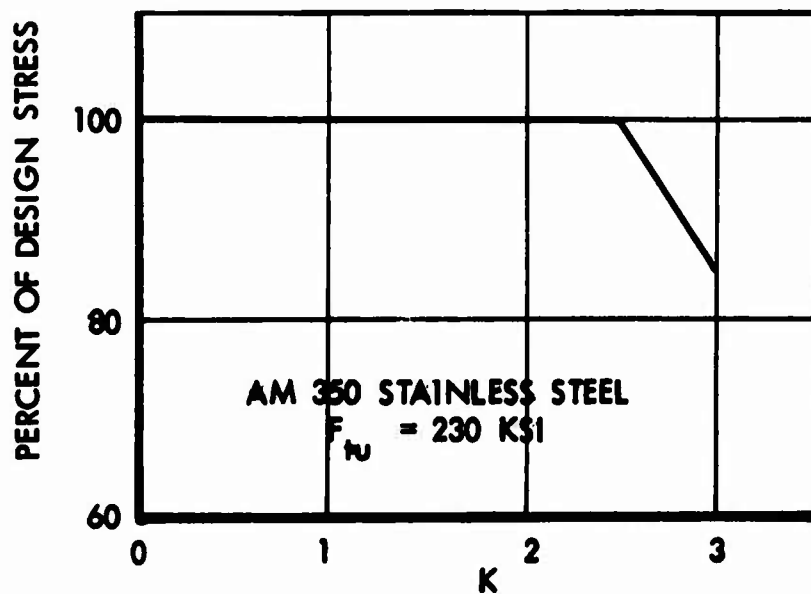


Figure 112. Variation in Design Stress at Main Rotor Blade Station 165 with K - 3600-Hour Life for Composite Mission Profile No. 2, 40-Percent Reduction in S-N Data

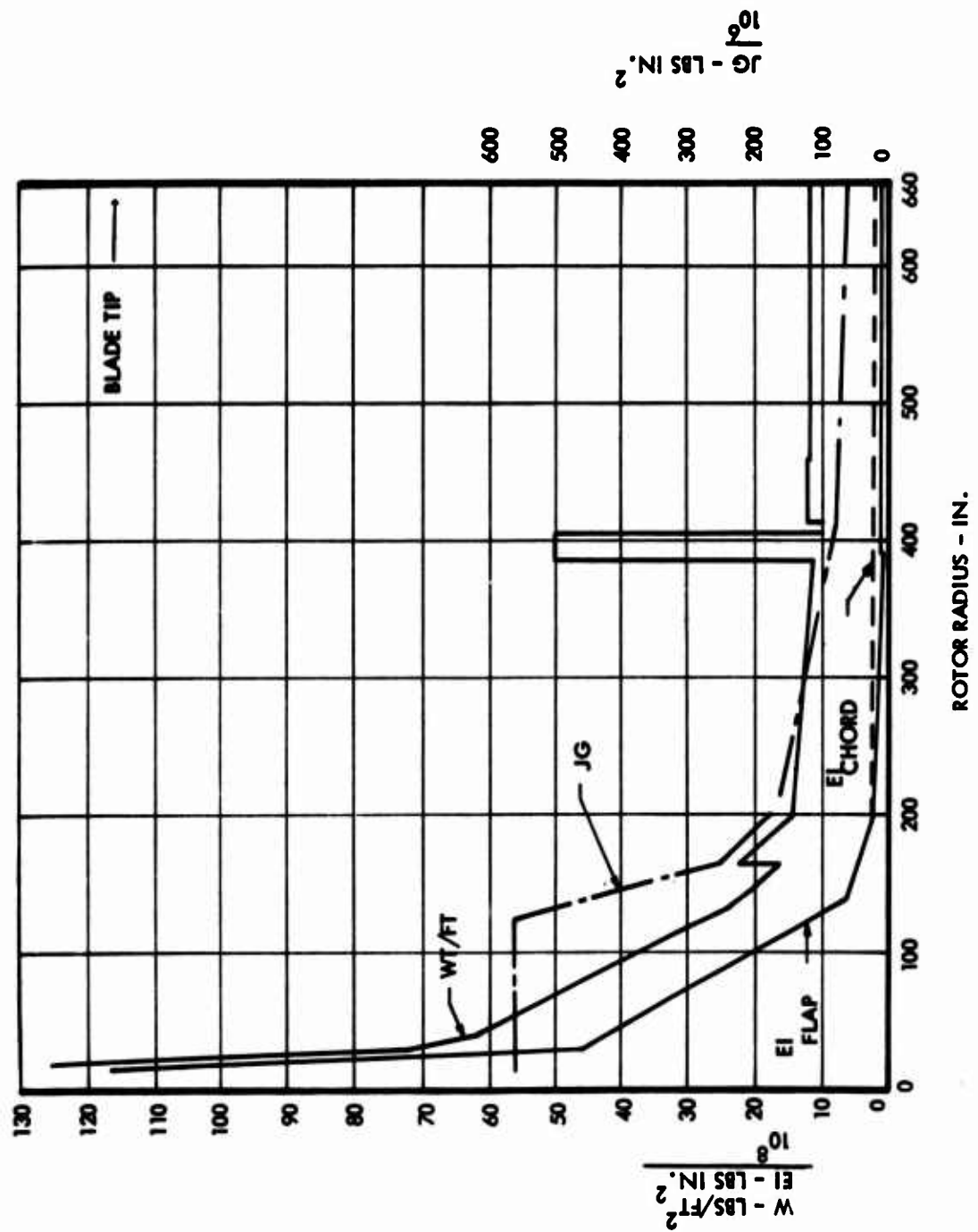


Figure 113. Rotor Blade Stiffness and Weight Distribution

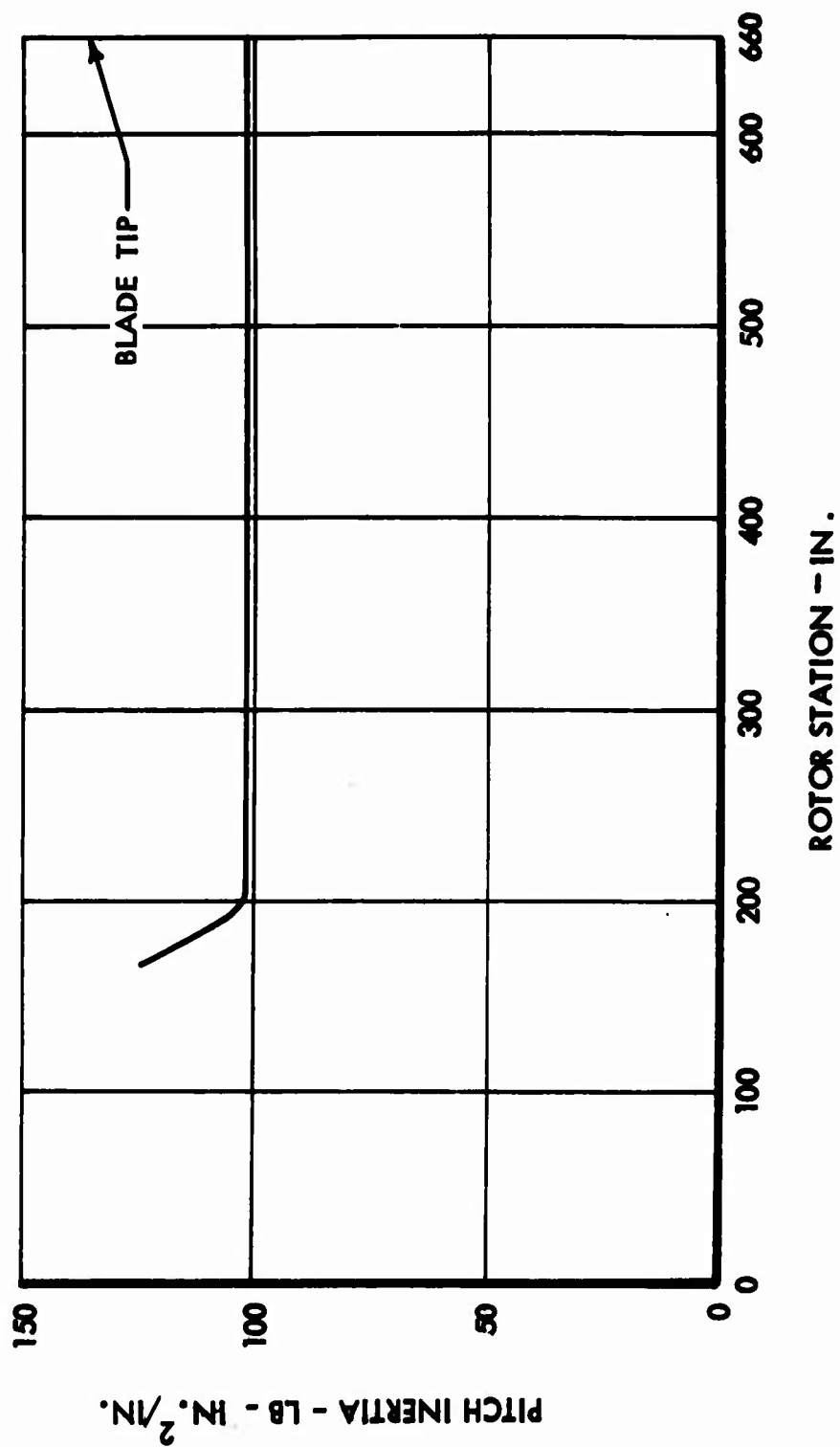


Figure 114. Main Rotor Pitch Mass Moment of Inertia

Figure 113, is 53 inches. The built-in coning angle results in an upward offset of the tip of 82 inches. Therefore, the blade tips are 29 inches above the rotor plane in the static condition.

#### WEIGHT ANALYSIS

Weight studies were conducted in conjunction with the preliminary design of the matched-stiffness rotor system.

The weight analysis of the rotor system components, as defined by the configuration shown in Figures 50 through 54, is as follows (all weights in pounds):

Main Rotor Assembly	6945
Blade (5)	1460
Hub (1)	480
Flexure (5)	3405
Spar (5)	1175
Control Torque Tube (5)	425

Each main rotor blade consists of 12 segmented airfoil sections as shown in Figure 51. The segments are built-up composite sections. All segments are identical except the 6 outboard segments per blade, which incorporate leading-edge ballast for chordwise balance. The outboard segments weigh 30 pounds each and the inboard segments weigh 18.7 pounds each.

The main rotor hub is a one-piece titanium forging, as shown in Figure 53. The hub weight listed includes flexure-attaching bolts.

The flexure is a built-up bonded stainless steel assembly, as shown in Figure 52. The flexure extends from the hub and attaches to the blade spar by bonding at rotor station 165.

The blade spar is a square stainless steel tube with bonded external plate to control weight distribution, material area, and stiffness, as shown in Figure 52. The spar is a constant section extending from rotor station 165 to the blade tip. The spar weight includes the tube, plates, antinodal weight, and blade segment centrifugal force stops.

The control torque tube is a formed aluminum section extending from the rotor hub to the blade root, as shown in Figure 54. The weight listed includes the inboard support bearing and the flexible coupling for attachment to the blade.

A detailed weight breakdown of the components of the heavy-lift helicopter on Form MIL-STD-451 is provided in Figure 132 of Section 6.

## SECTION 5

### STABILITY AND CONTROL STUDY

#### INTRODUCTION

The Lockheed Model CL 875 heavy-lift helicopter uses the same combination of a rigid rotor and a control gyro as the Lockheed XH-51A and Model 286 helicopters. Since the concept can be applied to any size helicopter, the CL 875 will exhibit the same excellent flying qualities as the smaller vehicles even though it is an order of magnitude larger.

#### DESCRIPTION OF THE CONTROL SYSTEM

A schematic of the cyclic control system is shown in Figure 115. To establish an understanding of the operation of the cyclic control system, it is appropriate to outline the sequence of events which occurs following a pilot input:

- Assume that the pilot pushes the cyclic stick forward 1 inch.
- The valve on the boost cylinder is displaced and the boost cylinder compresses the longitudinal spring, to apply a rolling moment to the swash plate.
- The rolling moment is transferred to the gyro through the parallel linkage and causes the control gyro to develop a precession rate in the nose-down direction. The gyro displacement is not hindered by the spring in the lateral control system because the force in the negative actuator balances the effect of the spring.
- Displacement of the gyro with respect to the rotor shaft produces a cyclic feathering of the blades about their feathering axes, with the blade pitch decreased on the right side and increased on the left side.

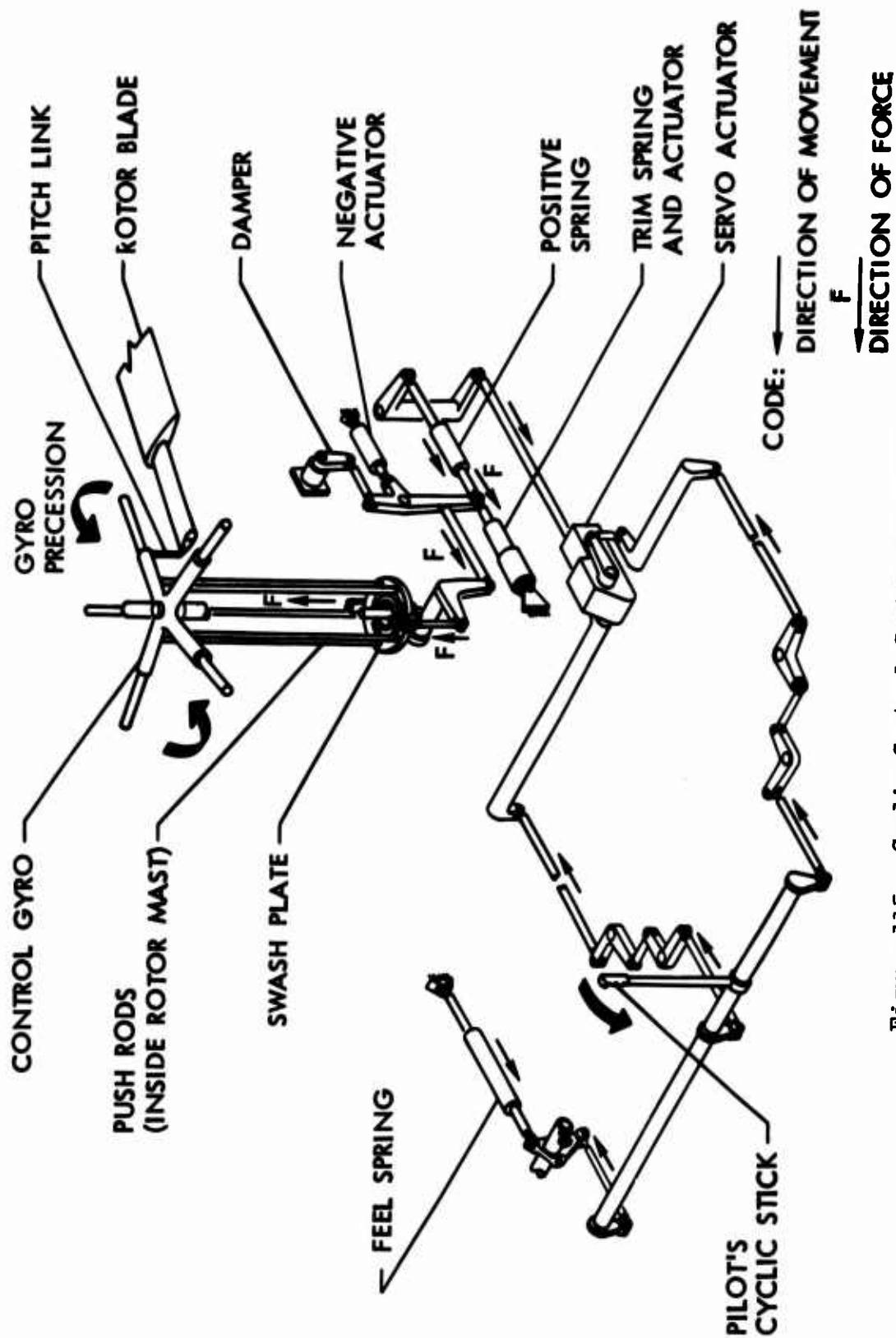


Figure 115. Cyclic Control System Schematic



- The cyclic pitch produced by the gyro displacement causes the rotor blades to flap down in the 180-degree azimuth position and up in the 0-degree azimuth position.
- A nose-down hub moment is developed by the rotor flapping which accelerates the helicopter nose-down until the airframe rate of pitch is equal to the rate of precession of the gyro.
- When the aircraft has pitched nose-down to the attitude the pilot desires, he then returns the control stick to neutral, thus relieving the servo load on the gyro and stopping its rate of precession.
- As the gyro ceases to precess, the vehicle ceases to pitch and remains in a nose-down attitude while it accelerates into forward flight.
- A reversal of the process will bring the aircraft back to hover.

The cyclic systems are provided with feel springs at the stick and trim systems between the boost cylinder and the swash plate. The trim systems consist of springs attached to linear electromechanical actuators which are controlled by switches on the cyclic stick. With these systems, the pilot can balance any moments applied to the gyro by gyro aerodynamics or by blade bending moments acting through the blade forward sweep.

A schematic of the directional control system is shown in Figure 116. This system consists of adjustable rudder pedals, a dual hydraulic actuator at the tail rotor, and linkage for moving the tail rotor blades in collective pitch. The linkage between the pedals and actuator is duplicated, and the actuator is operated by two separate transmission-mounted hydraulic pumps. The trim and feel system on the pedals is similar to that on the cyclic stick.

#### CONTROL POWER AND DAMPING REQUIREMENTS

The requirements for control power and damping of helicopters are given in MIL-H-8501A, "General Requirements for Helicopter Flying and Ground Handling Qualities," as a function of gross weight and moment of inertia. These requirements were used in this study as minimums. The reasonableness of these requirements for helicopters in the size class of the heavy-lift helicopter have not yet been established by flight test. No attempt was made in this study to

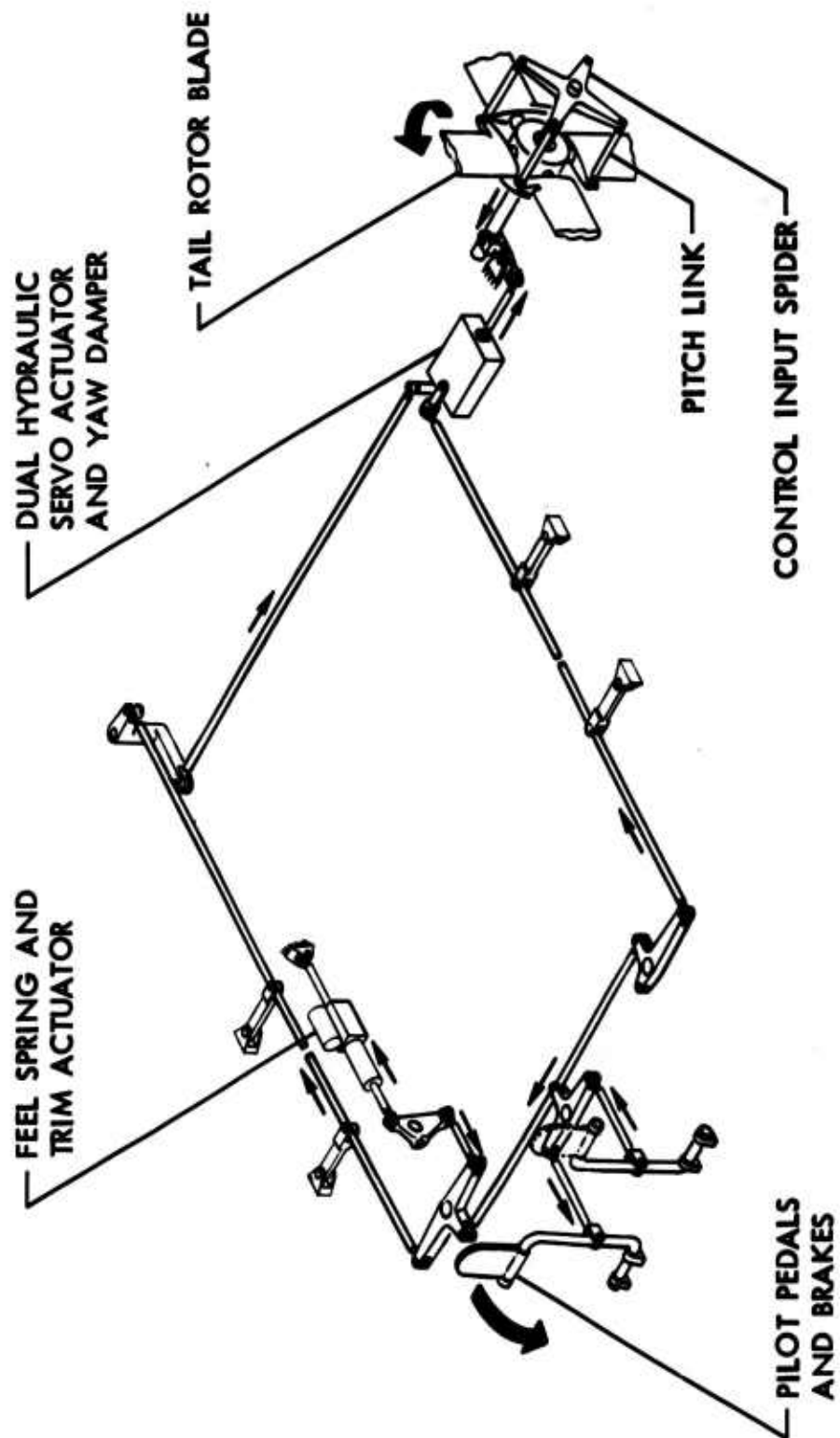


Figure 116. Directional Control System Schematic

analyze the validity of this requirement. The characteristics of the Lockheed rotor system permit control power and damping to be changed with relatively minor changes in the geometry of the control system.

The gross weight and moments of inertia which were used in this study are:

$$\begin{aligned}\text{Gross weight, } W &= 72,325 \text{ lb} \\ \text{Pitch moment of inertia, } I_Y &= 932,000 \text{ slug-ft}^2 \\ \text{Roll moment of inertia, } I_X &= 154,000 \text{ slug-ft}^2 \\ \text{Yaw moment of inertia, } I_Z &= 1,100,000 \text{ slug-ft}^2\end{aligned}$$

The requirements of MIL-H-8501A which must be met in hovering, based on the above weight and inertias, are tabulated in Table XVII.

The compliance of the CL 875 with these pitch-and-roll hovering requirements has been verified by the analog computer studies which are described in the following paragraphs. The hovering yaw compliance has been determined by an uncoupled yaw analysis.

#### ANALOG COMPUTER RESULTS

The equations of motion of the CL 875 have been programmed on Lockheed's analog computer and responses to step- and pulse-control inputs have been determined. The cases which have been investigated are listed in Table XVIII.

The responses to 1-inch control step and pulse inputs for the six cases are shown in Figures 117 to 122.

Figure 121 shows that for both pulse and step control inputs, the displacement requirements of Table XVII have been satisfied. In forward flight, the time histories show that the helicopter has a high degree of dynamic stability consistent with the demonstrated stability of previous Lockheed helicopters.

The equation for damping in pitch in hover of a helicopter using the Lockheed control gyro concept can be derived by noting that at the condition in which the helicopter is forced to pitch, the rate of pitch,  $q$ , is equal to the rate of precession of the gyro,  $q_g$ , and

TABLE XVII  
INSTRUMENT REQUIREMENTS FOR CL 875  
BASED ON MIL-H-8501A

TYPE OF REQUIREMENT	MIL-H-8501A PARAGRAPH	REQUIREMENT
Response to 1-in. Longitude Step Input in 1 sec	3.6.1.1	1.7°
Response to Full Longitude Step Input in 1 sec	3.6.1.1	6.9°
Damping in Pitch	3.6.1.1	222,000 ft-lb/ radian/sec
Response to 1-in. Lateral Step Input in 1/2 sec	3.6.1.1	0.8°
Response to Full Lateral Step Input in 1/2 sec	3.6.1.1	2.3°
Damping in Roll	3.6.1.1	105,000 ft-lb/ radian/sec
Response to 1-in. Pedal Input in 1 sec	3.6.1.1	2.6°
Response to Full Pedal Step Input in 1 sec	3.6.1.1	7.8°
Damping in Yaw	3.6.1.1	457,000 ft-lb/ radian/sec

TABLE XVIII					
CASES INVESTIGATED ON THE ANALOG COMPUTER					
CASE	GROSS WEIGHT (lb)	$f_o$ (sq ft)	V (knots)	LONGITUDINAL CENTER OF GRAVITY (Aft of shaft) (in.)	FIGURE NO.
1	33,000	80	0	+20.0	117
2	33,000	80	130	0	118
3	33,000	80	130	+20.0	119
4	72,325	180	0	+20.0	120
5	72,325	180	95	0	121
6	72,325	180	95	20.0	122

that the gyro precession rate is produced by the rotor moment acting through the blade sweep forward. The precession rate,  $q_g$ , in radians/second is as follows:

$$q_g = \frac{-L_g}{I_{Z_g} \Omega} = \frac{-M_H \psi' \frac{d}{e} \sin \beta}{I_{Z_g} \Omega}$$

where

$L_g$  = rolling moment applied to the gyro to precess in pitch, foot-pounds.

$I_{Z_g}$  = polar moment of inertia of the gyro, slug-feet<sup>2</sup>.

$\Omega$  = rotational velocity of the gyro, radians/second.

$M_H$  = pitching moment of the rotor measured at the hub, foot-pounds.

$\psi'$  = sweep forward of the blade quarter chord with respect to the blade feathering axis, radians.

$\frac{d}{e}$  = mechanical advantage of the blade feathering to gyro tilt motion

$\beta$  = angle between the gyro arm and the blade, degree

The damping, C, in foot-pounds/radian/second is

$$C = \frac{\partial M_H}{\partial q_g} = \frac{\partial M_H}{\partial q} = \frac{-I_{Z_g} \Omega}{\frac{d}{e} \psi' \sin \beta}$$

For the CL 875,

$$I_{Z_g} = 340 \text{ slug-ft}^2$$

$$\Omega = 12.8 \text{ radian/sec}$$

$$\frac{d}{e} = 0.833$$

$$\psi' = 0.0262 \text{ radian}$$

$$\beta = 45 \text{ deg}$$

Using these values, C is 282,000 foot-pounds/radian/second which exceeds the instrument requirement of 222,000 listed in Table XVII. The damping in roll is identical to the damping in pitch and, as such, also exceeds the requirement.

The damping in yaw is produced both by the fuselage and by the tail rotor. The damping of the fuselage has been calculated to be -50,000 foot-pound/radian/second, and the damping contribution of the tail rotor is -257,000 foot-pound/radian/second. The total is -307,000 foot-pound/radian/second which is somewhat short of the -457,000 listed in Table XVII. This difference is typical of all single rotor-tail rotor helicopters but is not prohibitive, since the requirement for yaw damping in paragraph 3.3.19 of MIL-H-8501A is not a firm requirement but only a preference: "The yaw angular velocity damping should preferably be at least 27 (Iz)0.7 foot-pound/radian/second...." If it is required that the yaw damping satisfy the value indicated, a simple yaw damper, operating on the tail rotor control system, can be used.

- (1) MIL SPEC H-8501A PARA 3.6.1.1 (INSTRUMENT FLIGHT) REQUIRES  
2.25 DEG AT 1.0 SEC
- (2) MIL SPEC H-8501A PARA 3.6.1.1 (INSTRUMENT FLIGHT) REQUIRES  
0.99 DEG AT 0.5 SEC

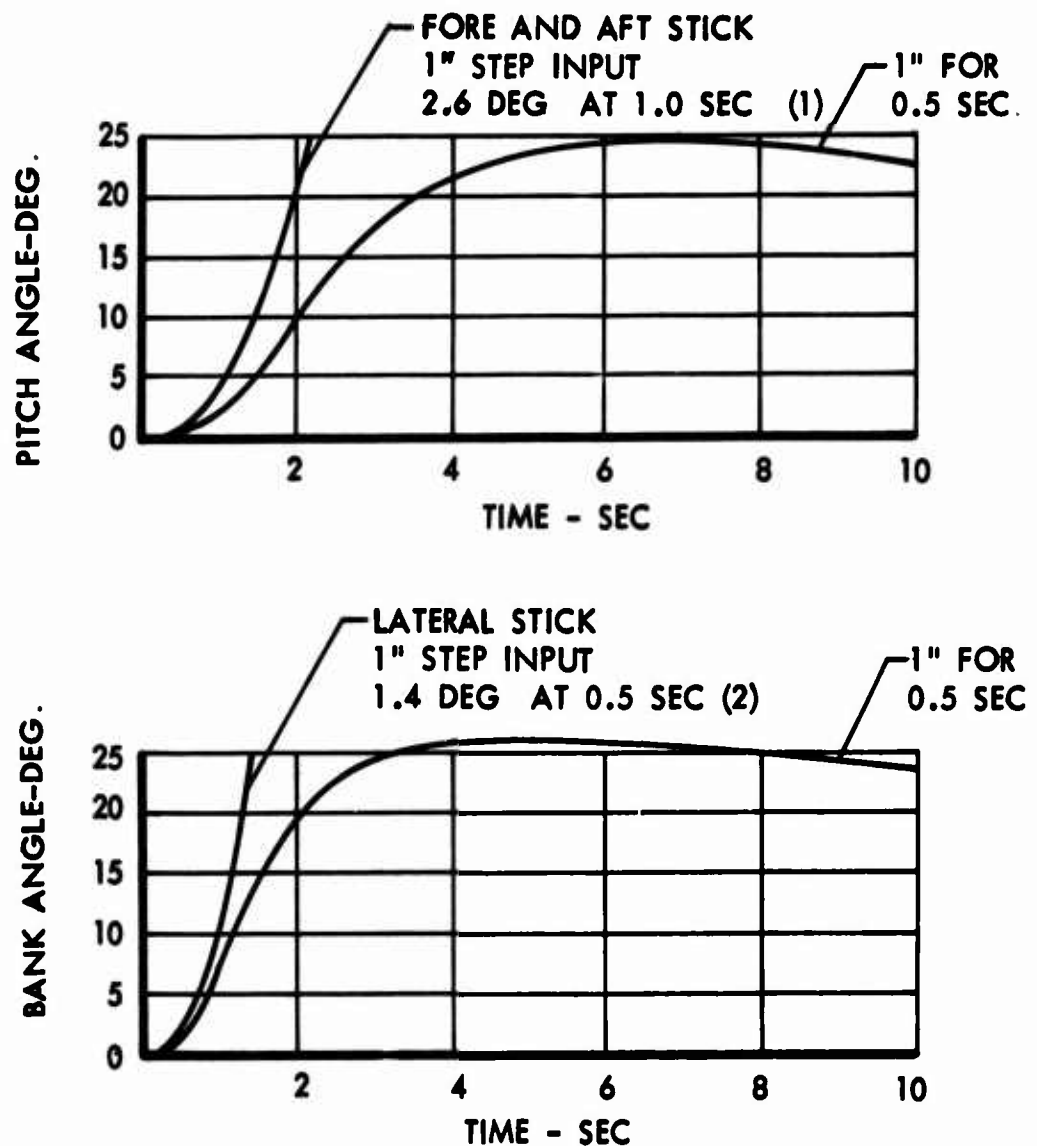
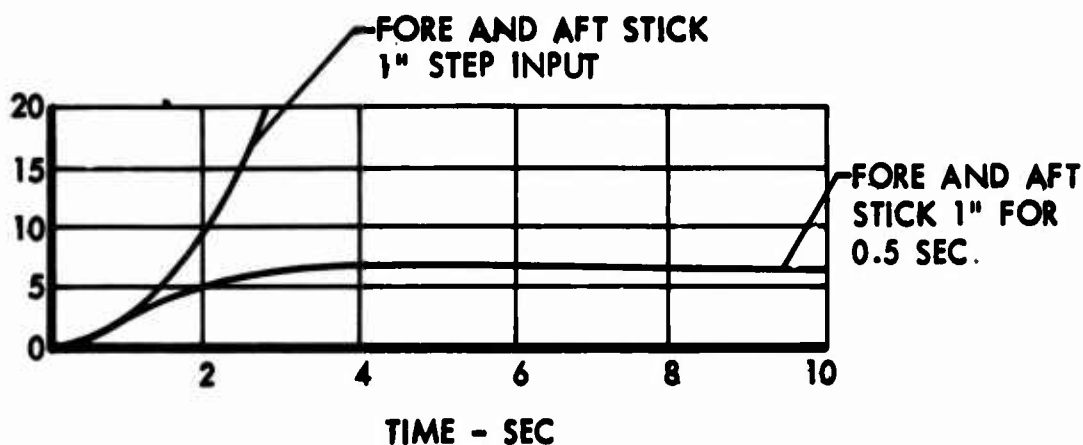
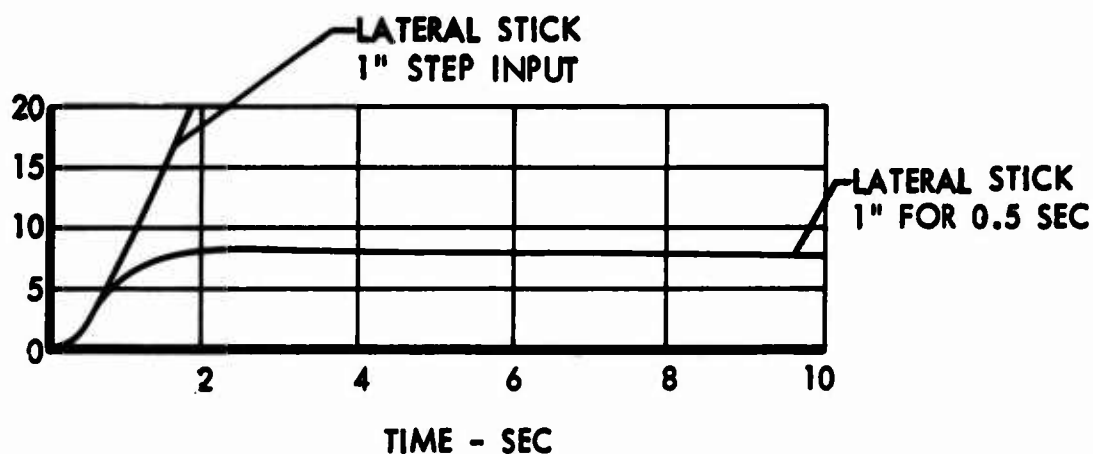


Figure 117. Helicopter Response to Control Inputs - Hovering, 33,000 Pounds, 20-Inch-Aft-Center-of-Gravity Offset

PITCH ANGLE - DEG.



BANK ANGLE - DEG.



YAW ANGLE - DEG.

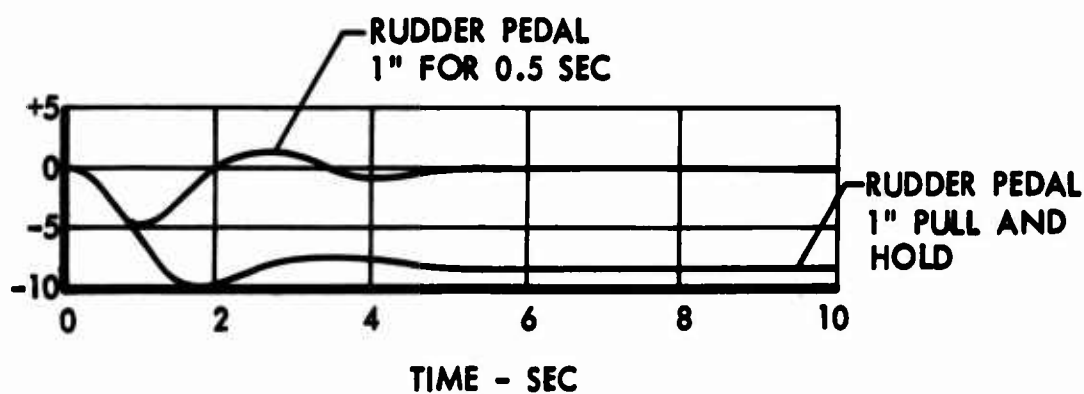


Figure 118. Helicopter Response to Control Inputs - 130 Knots, 33,000 Pounds, 0-Center-of-Gravity Offset



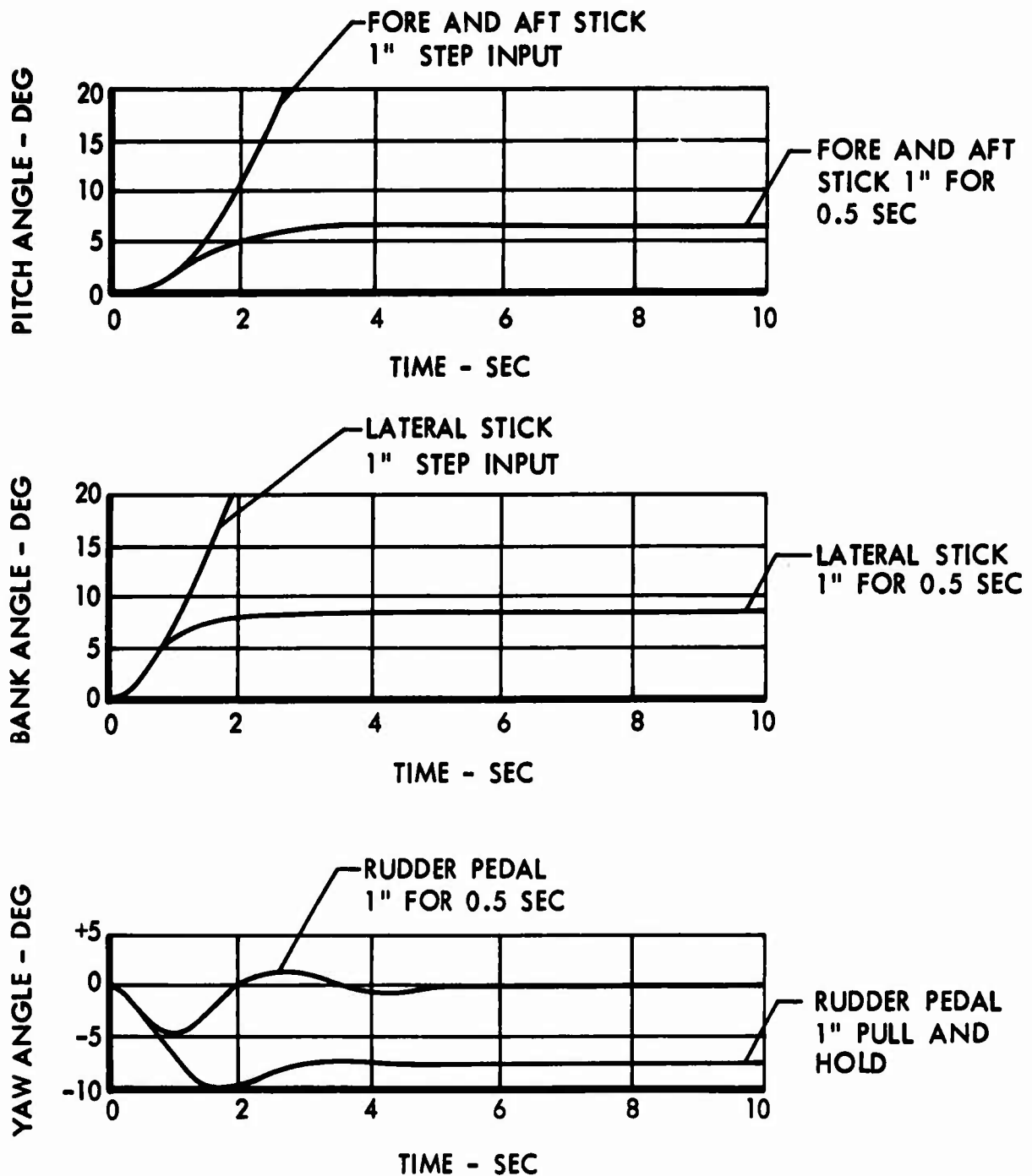


Figure 119. Helicopter Response to Control Inputs - 130 Knots, 33,000 Pounds, 20-Inch-Aft-Center-of-Gravity Offset

- (1) MIL SPEC H-8501A PARA 3.6.1.1 (INSTRUMENT FLIGHT) REQUIRES  
1.73 DEG AT 1.0 SEC
- (2) MIL SPEC H-8501A PARA 3.6.1.1 (INSTRUMENT FLIGHT) REQUIRES  
0.76 DEG AT 0.5 SEC

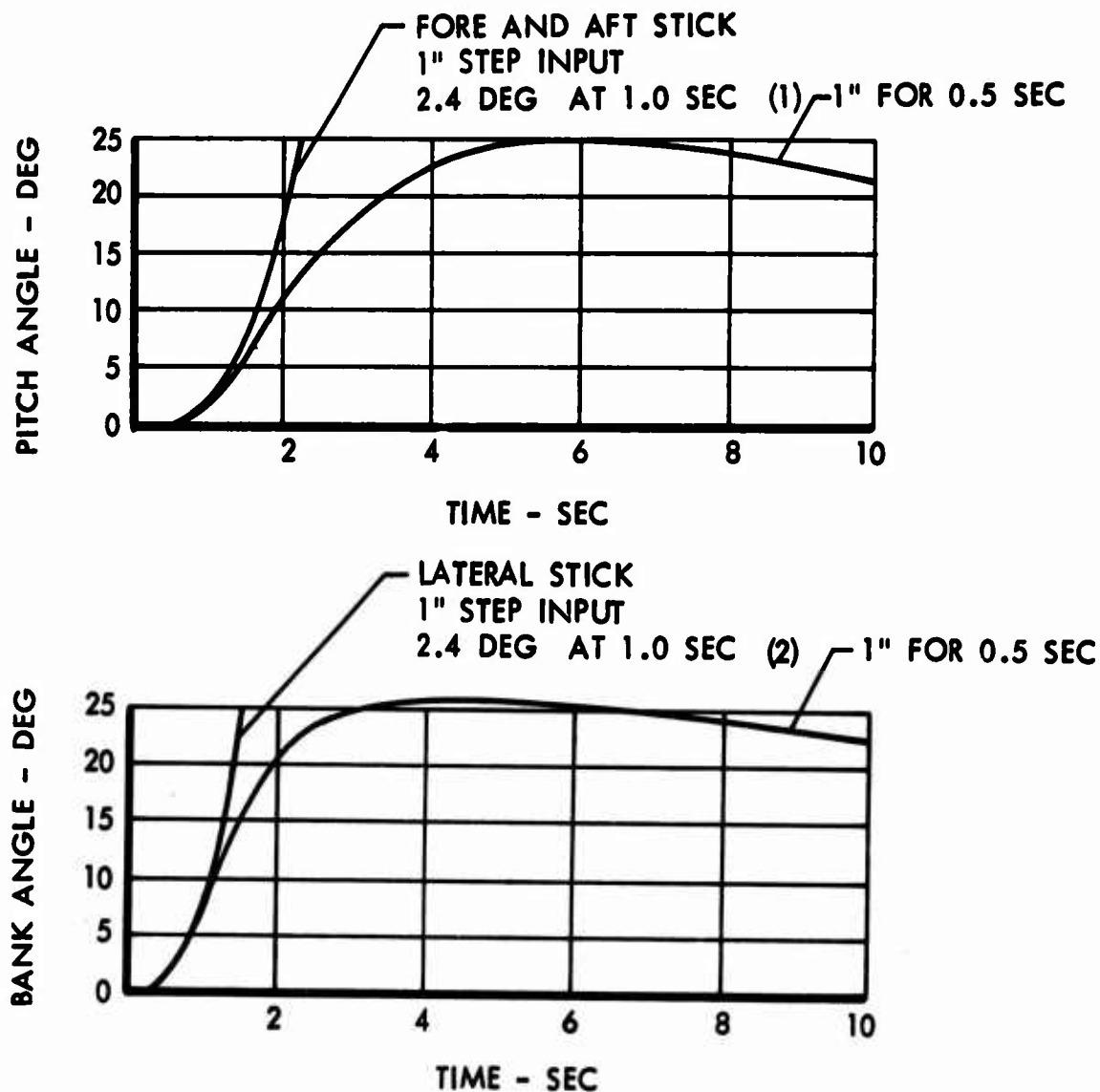


Figure 120. Helicopter Response to Control Inputs - Hovering,  
72,325 Pounds, 20-Inch-Aft-Center-of-Gravity Offset

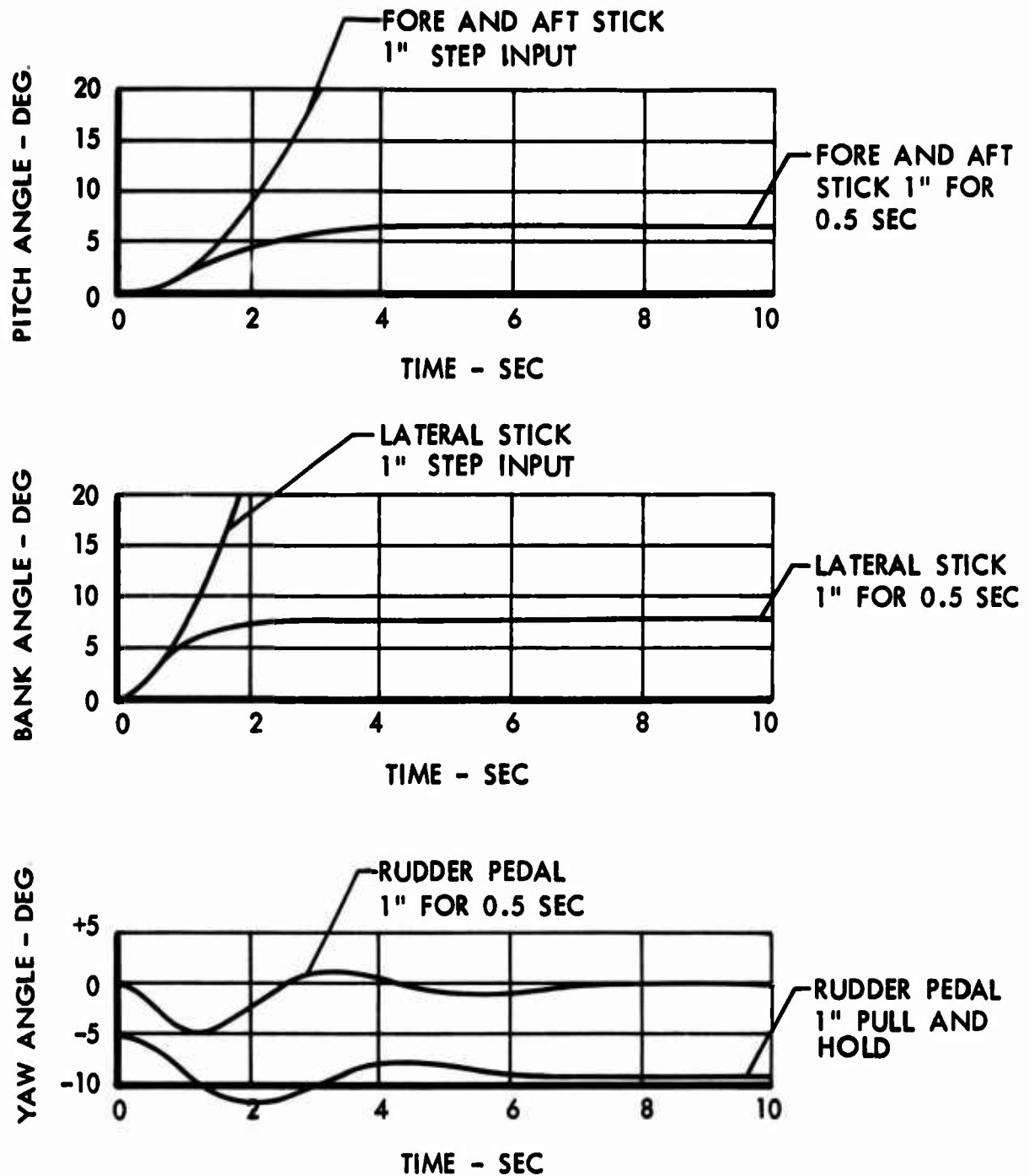


Figure 121. Helicopter Response to Control Inputs - 95 Knots, 72,325 Pounds, 0-Center-of-Gravity Offset

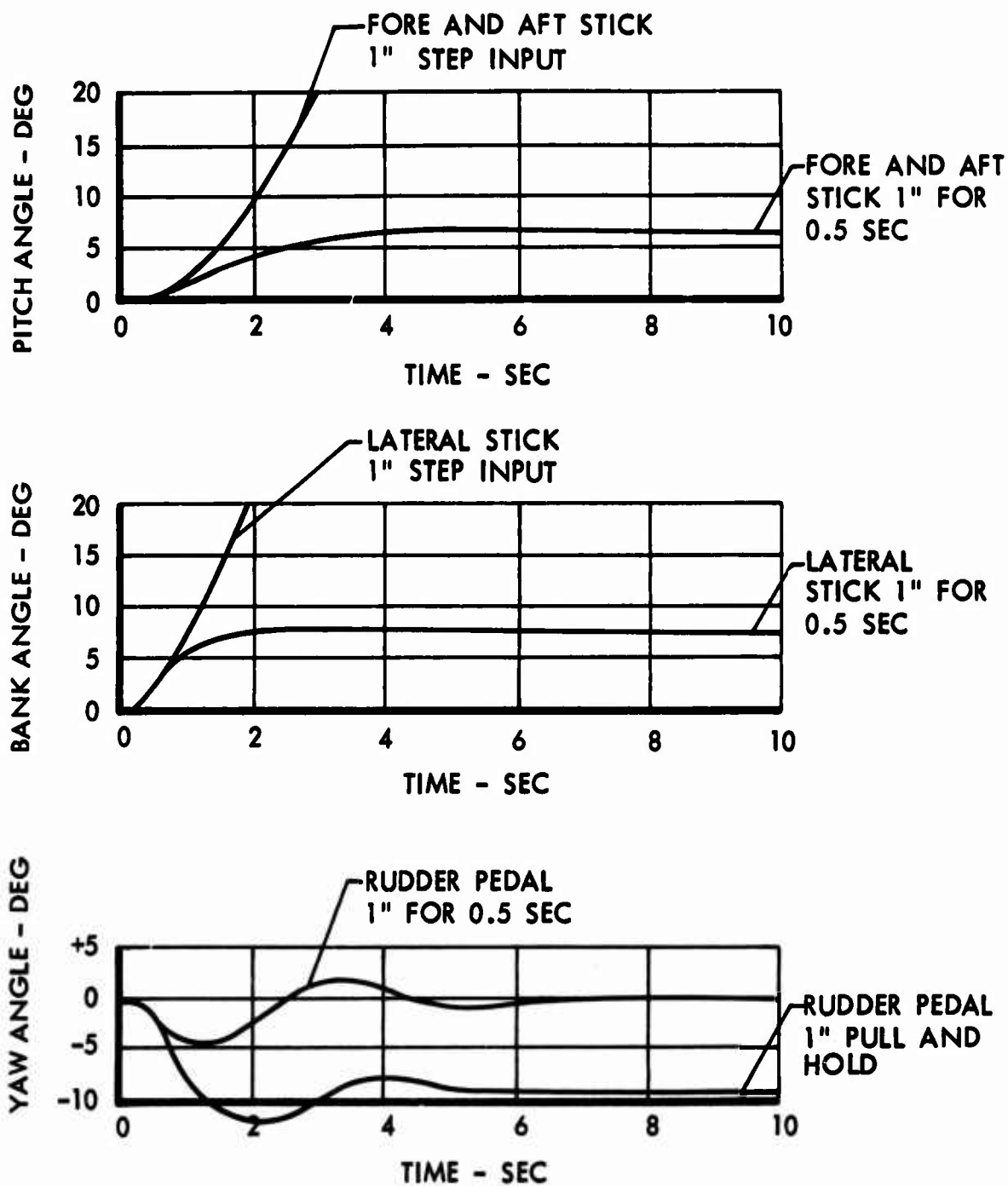


Figure 122. Helicopter Response to Control Inputs - 95 Knots, 72,325 Pounds, 20-Inch-Aft-Center-of-Gravity Offset

## SECTION 6

### CONFIGURATION REFINEMENT

#### INTRODUCTION

In conjunction with the Part 2 rotor system preliminary design study, weight studies were conducted on the preliminary design configurations of the rotor system. Subsequently, weight analyses were also conducted in connection with preliminary design studies of transmission and drive systems for large helicopters; in these analyses additional statistical information was acquired on component weights of contemporary helicopters. The results of these studies indicated that some of the weight equations developed during the Part 1 study did not accurately reflect the component weights for a high gross weight helicopter. Some of the weight equations were rederived or adjusted so that the equations could be used confidently at high gross weights.

During the preliminary design study of the rotor system, an analysis of the effect of blade loading on the matched-stiffness rotor design was conducted. The Part 1 parametric study utilized a blade-loading limit of 77 psf, which was established from wind tunnel tests of a matched-stiffness rotor system model. The results of this study indicated that the blade loading of 77 psf was a valid limit for the conditions of the model tests and that any increase above this blade loading limit without consideration of the advance ratio would result in a rotor weight penalty due to second-harmonic-flapping root-bending stresses. A relationship between blade loading, second-harmonic flapping, and advance ratio was established which permits the use of blade loading in excess of 77 psf without exceeding acceptable design root-bending stresses for the same rotor weight. Justification for this relationship is presented in "Matched-Stiffness Blade Loading Limitations" in this section.

The new weight equations were entered into the solution gross weight determination computer program and, utilizing the change in blade-loading limits, new mission gross weights and rotor system characteristics were established.

For purpose of clarification the configuration resulting from the Part 1 parametric study is referred to as the "recommended configuration," and the configuration resulting from the changes described above is referred to as the "refined configuration."

Characteristics of these two configurations are summarized as follows:

	<u>Recommended Configuration</u>	<u>Refined Configuration</u>
Design gross weight, lb	72,300	74,727
Transport mission weight, lb	59,300	62,500
Number of blades	5	5
Rotor diameter, ft	110	104.4
Blade section	NACA 0012	NACA 0012
Rotor tip speed, fps	650	730
Mean blade lift coefficient	.520	.484
Blade chord, in.	41.0	38.0
Aspect ratio	16.2	16.5
Disc loading, psf	7.60	8.74

The differences in the two configurations are not sufficient to affect the results of the Part 2 preliminary design study but are presented to document the additional studies. However, it is recommended that the refined configuration be utilized for detail design of a shaft-driven rotor system and the general characteristics of a heavy-lift helicopter.

#### WEIGHT ANALYSIS

The rederived or adjusted component weight equations for the heavy-lift helicopter reflecting the latest preliminary design studies and statistical data are presented in the following paragraphs.

The curves and tables showing contemporary helicopter weights and study weights, which substantiate the equations, are included.

A detailed weight analysis of the heavy-lift helicopter on Form MIL-STD-451, Part 1, is also presented.

#### Rotor and Hub Group

The equation for the weight of the rotor and hub group was determined by using a logarithmic least squares curve fit to the data of several contemporary helicopters. The equation giving the best fit was found to be

$$W_{RG} = 1.708 W^{0.342} R^{1.576} \sigma^{0.630}$$

where  $W_{RG}$  is the complete rotor group weight,  $W$  is the design gross weight,  $R$  is the rotor radius, and  $\sigma$  is the main rotor solidity ratio. For tandem rotors, it was assumed that the same equation would hold, with the gross weight replaced by the fraction of the weight which each rotor is required to carry. This value was taken to be 0.60 of the gross weight. The resulting equation for the rotor group of a tandem rotor helicopter is

$$W_{RGT} = 2.87 W^{0.342} R^{1.576} \sigma^{0.630}$$

These equations are valid for articulated, rigid, and teetered rotor systems.

The rotor group weights for various helicopters, along with the weight predicted by the parametric equation, are listed in Table XIX. Figure 123 presents graphically the data of Table XIX.

The rotor group equation provides good correlation with most present-day helicopters. However, it does not reflect improvements due to anticipated advances in both material and design technology. Reference to the data of Figure 123 shows that several of the most recent designs lie below the curve. Using these points as a guide, the rotor group weight equation was reduced uniformly by 10 percent for this study.

The resulting equations are

$$W_{RG} = 1.537 W^{0.342} R^{1.576} \sigma^{0.630}$$

for single-rotor helicopters, and

$$W_{RGT} = 2.58 W^{0.342} R^{1.576} \sigma^{0.630}$$

for tandem rotors.

Another major design advance is the development of the matched-stiffness rotor. Using calculated weights of the present Lockheed designs for a heavy-lift helicopter matched-stiffness rotor, the above rotor group weight equation was modified to reflect the lower weight associated with this type rotor system. The resulting equation is

$$W_{RG} = 1.208 W^{0.342} R^{1.576} \sigma^{0.630}$$

TABLE XIX  
ROTOR GROUP WEIGHT

MODEL		ROTOR GROUP WEIGHT (lb)	EQUATION WEIGHT (lb)
Single Rotor			
Iroquois	UH1B	755	689
LOH	OH4A	250	306
Trooper	47G-3	283	286
Raven	H23D	271	276
LOH	OH5A	233	255
Experimental	Ten-99	346	351
Skyhook	CH1C	351	313
LOH	OH6A	181	216
Aerogyro	XH51A	474	437
Lark	RH3B	396	349
Chickasaw	UH19C	800	764
U.S. Coast Guard	HH52A	838	806
Choctaw	CH34A	1346	1401
Sea King	SH3A	2223	2126
USAF	CH3C	2228	2244
Mohave	H37A	3342	3445
Skycrane	S64	4051	4561
Tandem Rotor			
Sea Knight	CH46A	2275	2180
Chinook	CH47A	2988	3310
Shawnee	CH21C	1344	1620
Transporter	YH16	4777	5420



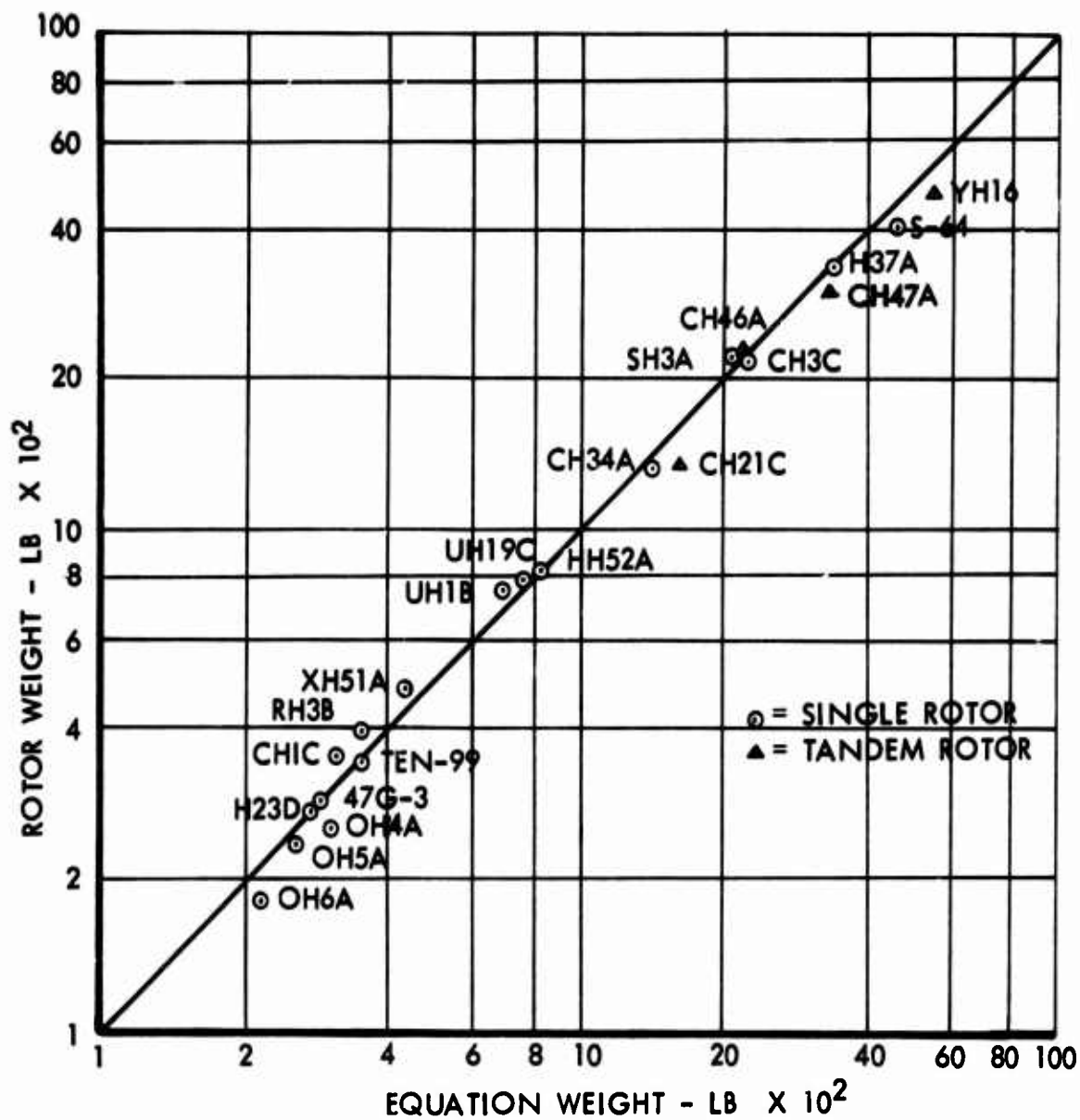


Figure 123. Rotor Group Weight

Use of this equation results in a predicted weight which is approximately 20 percent lower than the weight predicted for an articulated, rigid, or teetered rotor system.

The equation for a tandem matched-stiffness rotor is

$$W_{RGT} = 2.03 W^{0.342} R^{1.576} \sigma^{0.630}$$

The matched-stiffness rotor design weight was determined at a blade loading of 77 psf and a tip speed of 700 fps. This design point was used to establish the constant for the matched-stiffness weight equation. Design studies show that any increase above this blade loading without consideration of the advance ratio would result in a rotor weight penalty due to second-harmonic-flapping root-bending stresses. Therefore, it must be assumed that, for the validity of this equation, a blade loading limit exists at this design point. A relationship between blade loading, second harmonic flapping and advance ratio has been established and is presented in "Matched-Stiffness Blade Loading Limitations" on page 295.

#### Tail Group

The items included in the tail group are the tail rotor and the horizontal stabilizer. The vertical stabilizer weight is included in the fuselage weight.

A statistical study of horizontal stabilizers shows that the weight can be estimated by

$$W_{ST} = 0.000264 W^{0.724} V_C$$

where  $W$  is the design gross weight and  $V_C$  is the cruise speed in knots.

The stabilizer weights and equation weights for the helicopters for which information is available are shown in Figure 124.

The tail rotor weight is estimated by

$$W_{TR} = 0.000456 W^{1.295}$$

where  $W_{TR}$  is the tail rotor weight and  $W$  is the design gross weight.

The tail rotor weights and equation weights for the tail rotors of various helicopters are listed in Table XX. Figure 125 presents the data graphically.

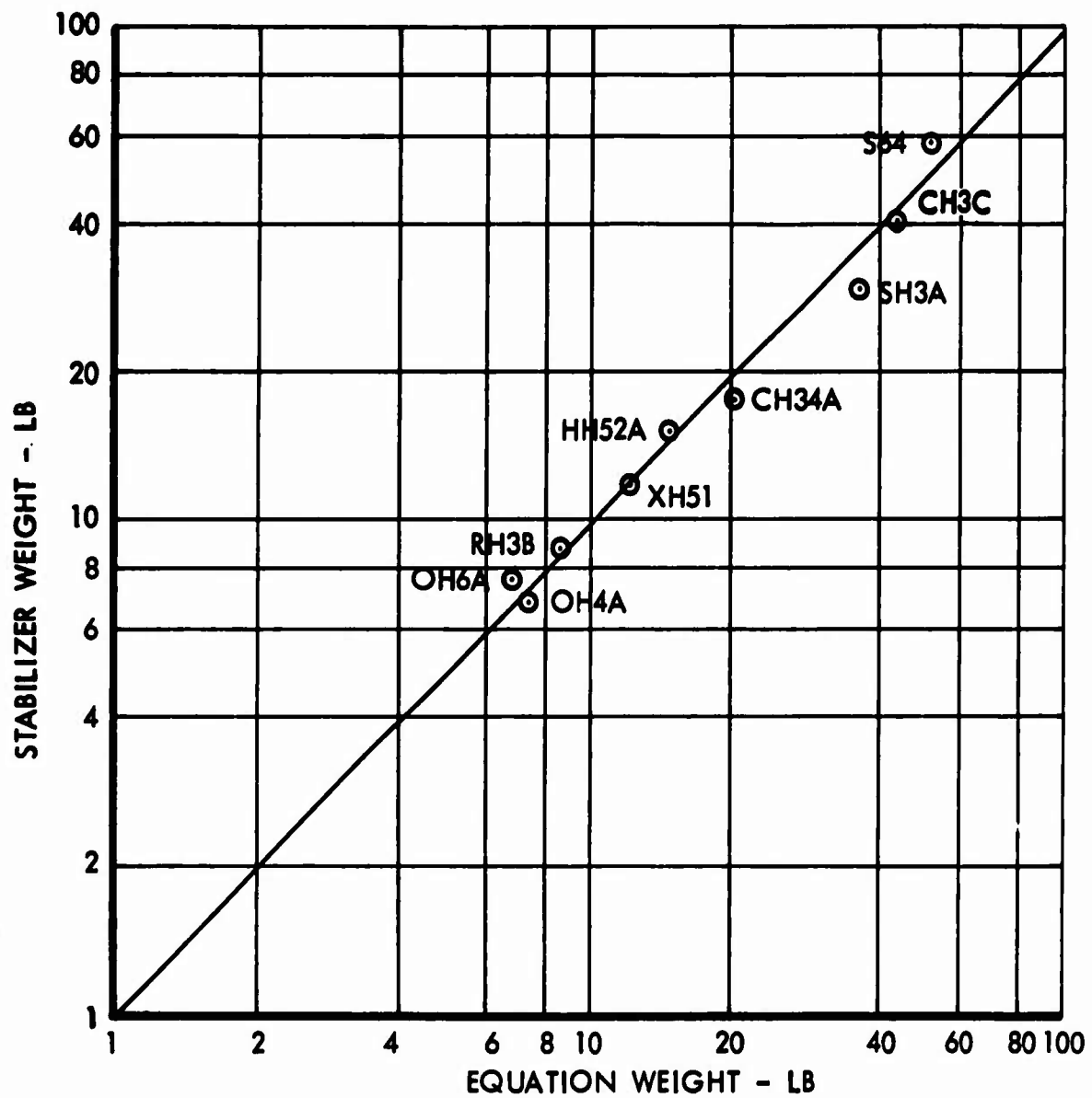


Figure 124 Horizontal Stabilizer Weight

**TABLE XX**  
**TAIL ROTOR WEIGHT**

MODEL		TAIL ROTOR WEIGHT (lb)	EQUATION WEIGHT (lb)
LOH	OH4A	11.0	11.2
Iroquois	UH1B	34.0	40.3
Ranger	47J-1	8.0	11.8
Raven	H23D	14.0	13.0
Raven	H23B	11.0	11.5
Experimental	Ten-99	14.0	17.7
LOH	OH6A	7.0	9.1
Aerogyro	XH51	28.0	17.7
Experimental	XH51A (Compound)	28.0	24.5
Lark	RH3B	14.0	16.4
Commerical	S51	49.0	28.3
Commercial	S55	49.0	44.3
Commercial	S62	62.0	47.5
Sea King	SH3A	108.0	132.0
USAF	CH3C	118.0	161.7
U.S. Marine	CH53A	370.0	330.2
Skycrane	S64	370.0	388.8

As in the case of the main rotor, it is felt that advances in the state of the art in material and design technology will result in a lower tail rotor weight; hence, a 10-percent reduction was applied uniformly to the tail rotor weight, resulting in the equation

$$W_{TR} = 0.000410 W^{1.295}$$

It is assumed that for the tandem configurations no horizontal stabilizer is required. Since the vertical stabilizer weight is

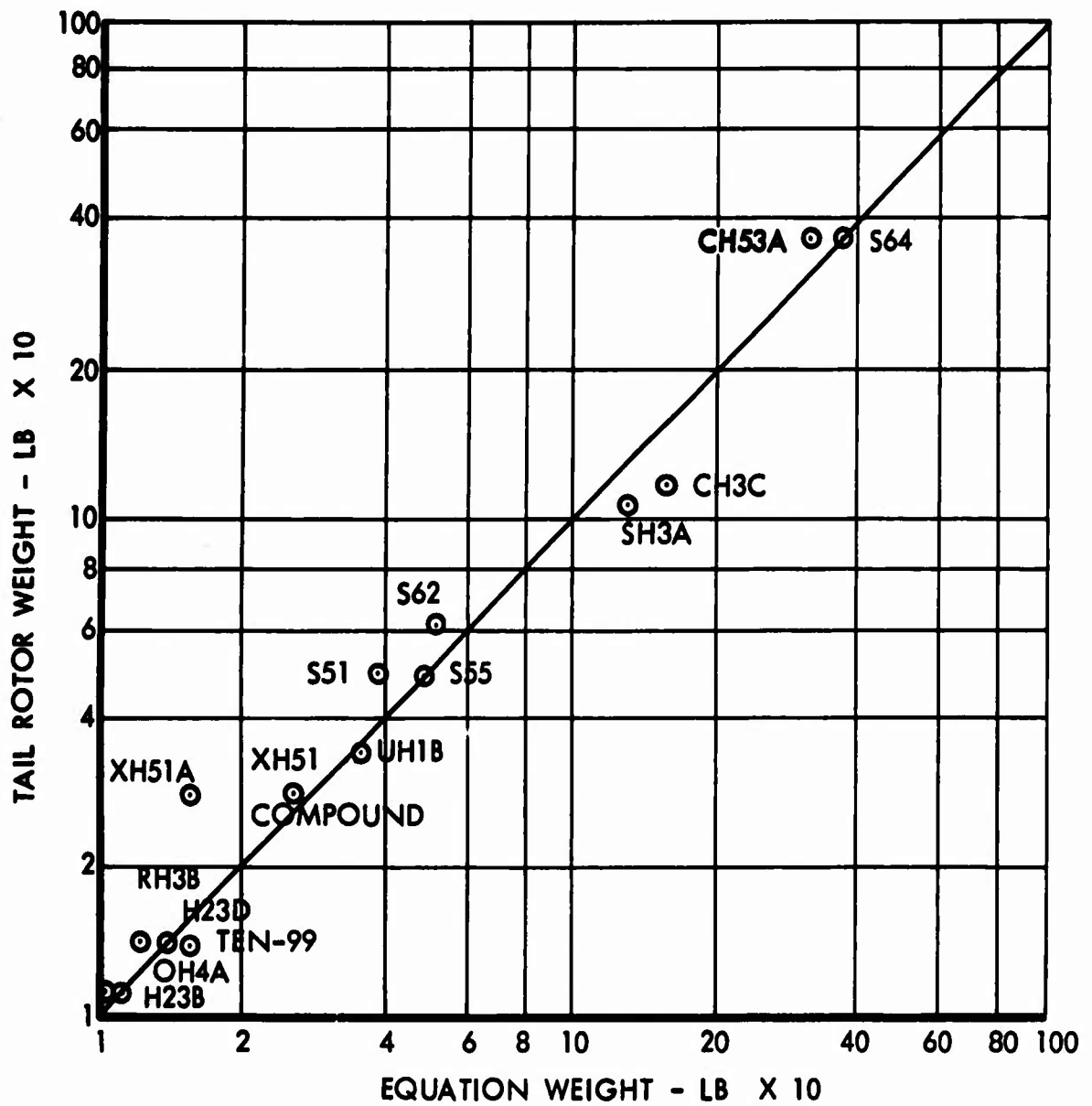


Figure 125. Tail Rotor Weight

included as part of the fuselage group, there will be no weight included in the tandem rotor tail group.

### Fuselage Group

The equations for the fuselage weight were derived by a design synthesis technique. The total fuselage weight can be expressed as

$$W_B = f(W, R, n)$$

where  $W$  = design gross weight  
 $R$  = rotor radius  
 $n$  = load factor

Expressions were found for the variation of unit weight and circumference for the types of helicopters being considered in this study. The resulting equations are:

#### Single Rotor

Internal cargo:  $W_{BI} = 0.202 (R+32) \sqrt{Wn}$

External cargo:  $W_{BE} = 0.261 R \sqrt{Wn}$

#### Tandem Rotor

Internal cargo:  $W_{BTI} = 0.218 (L_R+38.4) \sqrt{Wn}$

External cargo:  $W_{BTE} = 0.308 L_R \sqrt{Wn}$

In these equations,  $W$  is the design gross weight,  $n$  is the design limit load factor,  $R$  is the rotor radius, and  $L_R$  is the distance between rotors. The fuselage weights and equation weights for various helicopters are shown in Table XXI.

In this analysis, several assumptions were made regarding the configuration and the construction. Since these assumptions apply mainly to heavy (i.e., greater than about 20,000-pound gross weight) cargo helicopters, these equations are not expected to give accurate fuselage weight estimates for lightweight helicopters.

TABLE XXI				
FUSELAGE WEIGHT				
MODEL		CARGO	FUSELAGE WEIGHT (lb)	EQUATION WEIGHT (lb)
Single Rotor				
Skycrane	S64	External	2888	2900
USAF	CH3C	Internal	2784	2810
U.S. Marine	CH53A	Internal	5438	4630.
Tandem Rotor				
Transporter	XR16	External	4204	4200
Chinook	HC-1B	Internal	4180	4310
Chinook	CH47A	Internal	4225	4310
Transporter	YH16	Internal	5950	5450

#### Landing Gear Group

Two landing gear configurations were considered in this study: the straddle type (for external cargo helicopters) and the conventional tri-cycle or quadricycle type. Since both single- and tandem-rotor helicopters were to be considered, there are four separate equations for landing gear weight:

##### Single Rotor

Conventional:  $W_{LG} = 0.0696 W^{0.922}$

Straddle:  $W_{LGS} = 0.0960 W^{0.922}$

##### Tandem Rotor

Conventional:  $W_{LGT} = 0.0750 W^{0.922}$

Straddle:  $W_{LGST} = 0.112 W^{0.922}$

The landing gear weights and equation weights are listed in Table XXII, and Figure 126 presents the data graphically.

TABLE XXII			
LANDING GEAR WEIGHT			
MODEL		LANDING GEAR WEIGHT (1b)	EQUATION WEIGHT (1b)
Conventional Gear			
Tandem Rotor			
Experimental	HSL-1	524	510
Chinook	CH47A	856	850
Commercial	107	557	540
Experimental	YCH1B	938	875
Experimental	YH21D	475	525
Sea Knight	CH46A	591	645
Transporter	YH16	1101	1030
Single Rotor			
Choctaw	CH34A	401	395
Commercial	S55	264	228
USAF	CH3C	630	620
U.S. Marine	CH53A	1004	1020
Straddle Gear			
Single Rotor			
Skycrane	S64	1675	1600

#### Propulsion Group

The propulsion group has been divided into four sections: engine, engine accessories, drive system, and fuel tanks. Each of these items is treated separately.



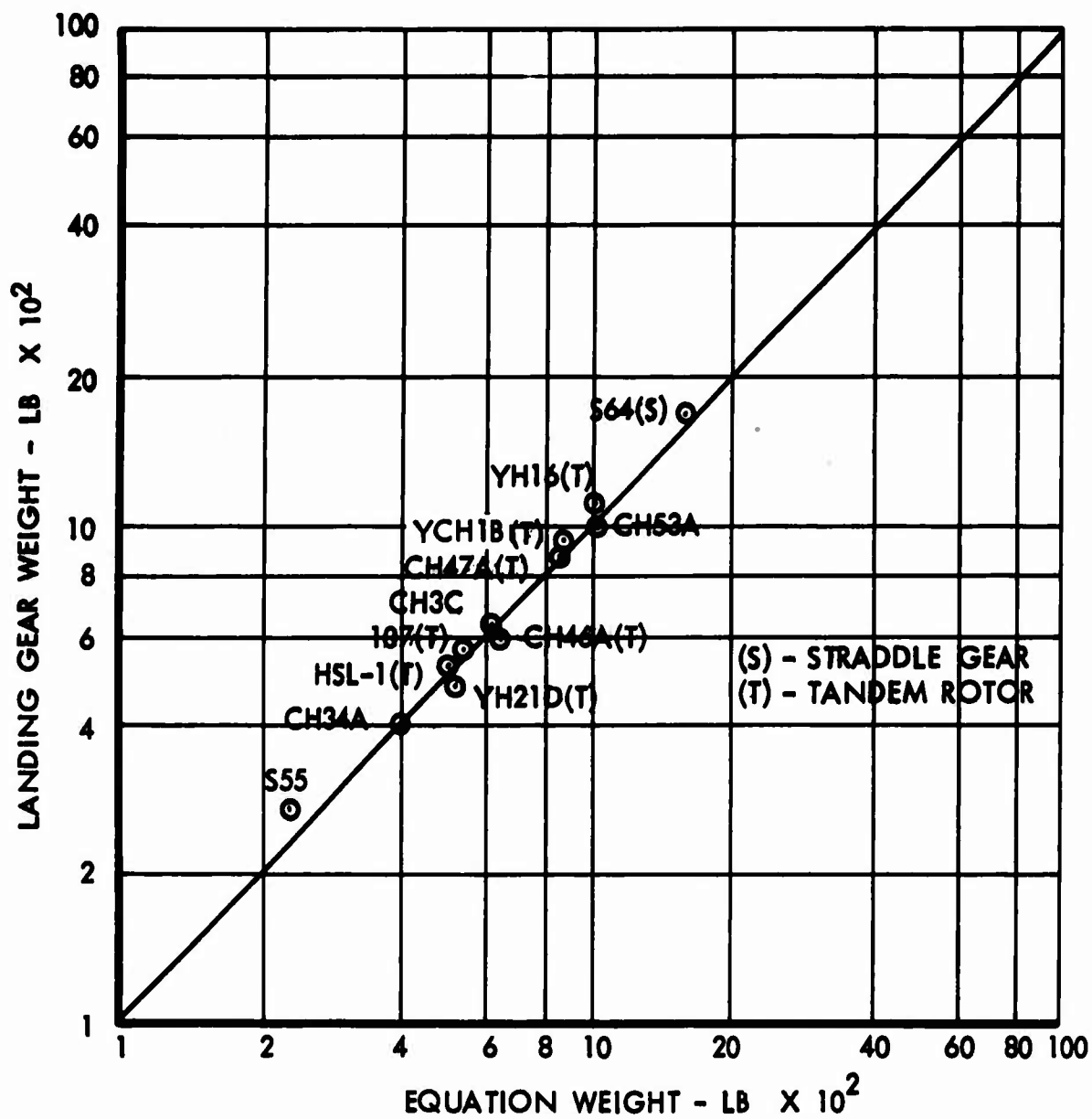


Figure 126. Landing Gear Weight

Engine - In this study, the engine used was to be either a present engine or a growth version thereof. Therefore, actual engine weight to horsepower ratios have been used in the parametric study, and actual engine weights were used in the helicopter weight breakdown.

Engine Accessories - The engine accessories group includes the air induction, exhaust and cooling systems, engine lubrication system, engine controls, starting system, and engine section or nacelle group. Although there appears to be no reliable method for predicting the weight of each of these items separately, their total weight can be reasonably estimated by the following equation:

$$W_{ACC} = 0.425 W_E$$

where  $W_E$  is the engine weight and  $W_{ACC}$  is the total engine accessories weight.

The engine accessories weights and equation weights are listed in Table XXIII, and Figure 127 presents the data graphically.

Fuel System - The fuel system weight is dependent upon the amount of fuel and the construction and location of the fuel tanks. For the helicopter configuration used in this study, the fuel tanks are located in close proximity to the engines and are of a crash-resistant type with fiber glass or foam backup supports. The fuel system weight was found to be

$$W_{FS} = 0.073 W_F$$

where  $W_F$  is the fuel capacity in pounds and  $W_{FS}$  is the total fuel system weight, including tanks and plumbing.

The fuel system weights and equation weights for several helicopters using this method of containment are listed in Table XXIV.

Drive System - The drive system weight was found to be strongly dependent on main rotor torque. The data of several contemporary helicopters were analyzed; the analysis resulted in the expression

$$W_{DS} = 42.4 \left[ \frac{HP \times R}{V_T} \right] 0.763$$

TABLE XXIII			
ENGINE ACCESSORIES AND NACELLE GROUP			
MODEL		ENGINE ACCESSORIES WEIGHT (lb)	EQUATION WEIGHT (lb)
<b>Single Rotor</b>			
Iroquois	UH1B	291	205
LOH	OH4A	121	58
Ranger	47J-2	184	190
Experimental	Ten-99	118	95
Raven	H23D	150	167
Commercial	UH12E4	144	183
LOH	OH6A	51	58
Aerogyro	XH51A	122	103
Lark	RH3B	78	83
U.S. Coast Guard	HH52A	130	130
Sea King	SH3A	253	248
USAF	CH3C	224	258
U.S. Marine	CH53A	568	600
<b>Tandem Rotor</b>			
Chinook	CH47A	339	475
Sea Knight	CH46A	293	248
Sea Knight	HRB-1	242	248
Experimental	YH21D	333	276

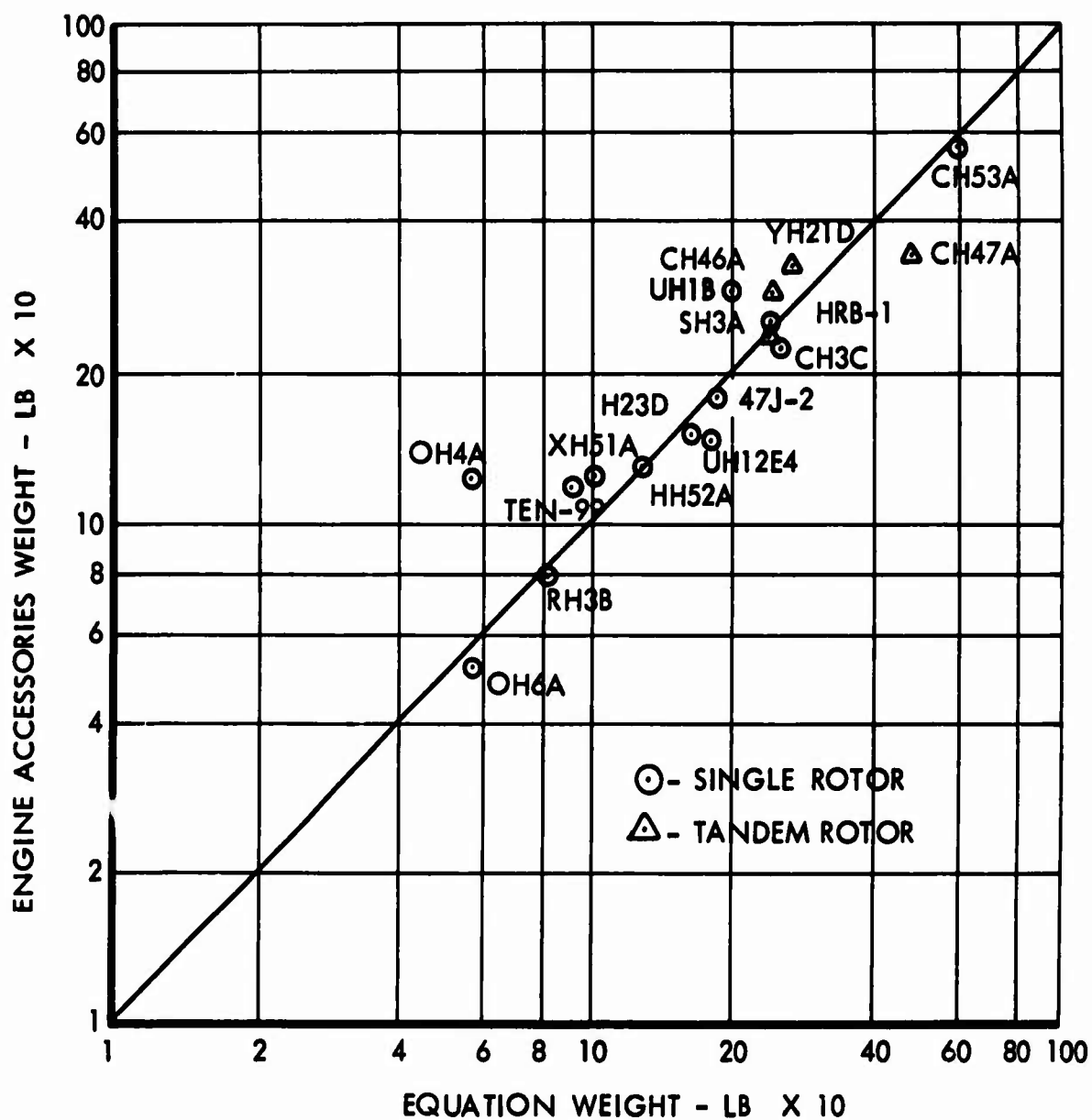


Figure 127. Engine Accessories Weight

TABLE XXIV			
FUEL SYSTEM WEIGHT			
MODEL		FUEL SYSTEM WEIGHT (lb)	EQUATION WEIGHT (lb)
LOH	OH4A	32	36
Experimental	HSL-1 (Tandem)	215	201
Commercial	UH12E4	19	21
LOH	OH6A	30	28
Aerogyro	XH51A	42	39

for single-rotor helicopters, and

$$W_{DST} = 63.8 \left[ \frac{HP \times R}{V_T} \right]^{0.763}$$

for tandem-rotor helicopters.

In these expressions,  $W_{DS}$  and  $W_{DST}$  are the total drive system weights. For single-rotor helicopters, the weight includes main rotor and tail rotor gearboxes, interconnecting shafts, and all mounting provisions; and for tandem-rotor helicopters, it includes both main gearboxes, all interconnect shafts and intermediate gearboxes, and all mounting provisions. Also in the above equations,  $R$  is the main rotor radius for single-rotor helicopters or the radius of one rotor of a tandem-rotor helicopter, and  $V_T$  is the main rotor tip speed.

In determining the equation, the horsepower was taken to be the total maximum rated sea level standard installed horsepower of the engine(s). Using this criterion gave very good results. However, in some cases the engines are not required to deliver maximum horsepower at sea level, but are at some higher altitude and temperature. If it is known that this is the case, the horsepower used in the equation can be the maximum total power delivered by the engines at any one time.

Drive system weights and equation weights for various helicopters are shown in Figure 128 and listed in Table XXV.

In the initial study, an attempt was made to evaluate separate items in the drive system, such as transmission, drive shaft, etc. It

**TABLE XXV**  
**DRIVE SYSTEM WEIGHT**

MODEL		DRIVE SYSTEM WEIGHT (lb)	EQUATION WEIGHT (lb)
<b>Single Rotor</b>			
U.S. Coast Guard	HUL-1G	180	187
Iroquois	UH1C	590	479
Iroquois	UH1D	589	602
LOH	OH4A	171	168
Iroquois	UH1B	575	603
Iroquois	UH1A	529	455
Trooper	47G2	157	171
Trooper	47G3-1	160	169
Skyhook	CH1C	257	193
LOH	OH5A	206	178
Raven	H23B	226	159
Raven	H23D	200	181
Experimental	Ten-99	264	230
LOH	OH6A	113	137
Aerogyro	XH51A	442	339
Russian	Mi-6	7700	7100
Mohave	H37A	2426	2425
U.S. Marine	HUS-1	1044	1039
Chickasaw	UH19C	846	525
Commercial	S56	2478	2546
Commercial	S58	984	1039
U.S. Coast Guard	HH52A	599	859
U.S. Marine	CH53A	3621	3350

TABLE XXV (CONTINUED)			
MODEL		DRIVE SYSTEM WEIGHT (lb)	EQUATION WEIGHT (lb)
Skycrane	S64	3798	3900
USAF	CH3C	1800	1796
Flying Crane	S60	2409	2546
Commercial	S61L	1622	1618
Sea King	SH3A	1715	1796
Commercial	S55	546	525
USAF	H5G	383	443
Tandem Rotor			
Experimental	HSL-1	2001	1600
Sea Knight	HRB-1	1894	1810
Commercial	107	1747	1920
Chinook	HC-1B	3378	3400
Sea Knight	CH46A	1931	1810
Chinook	CH47A	3531	3900
Transporter	YH16	3595	3100
Retriever	HUP-2	608	480
Experimental	YH21D	1521	1390
Shawnee	CH21C	1180	1200
Studies			
Boeing-Vertol:			
Single		6795	6830
Tandem		7265	8430
Sikorsky:			
Single		8700	8610
Tandem		7350	8790

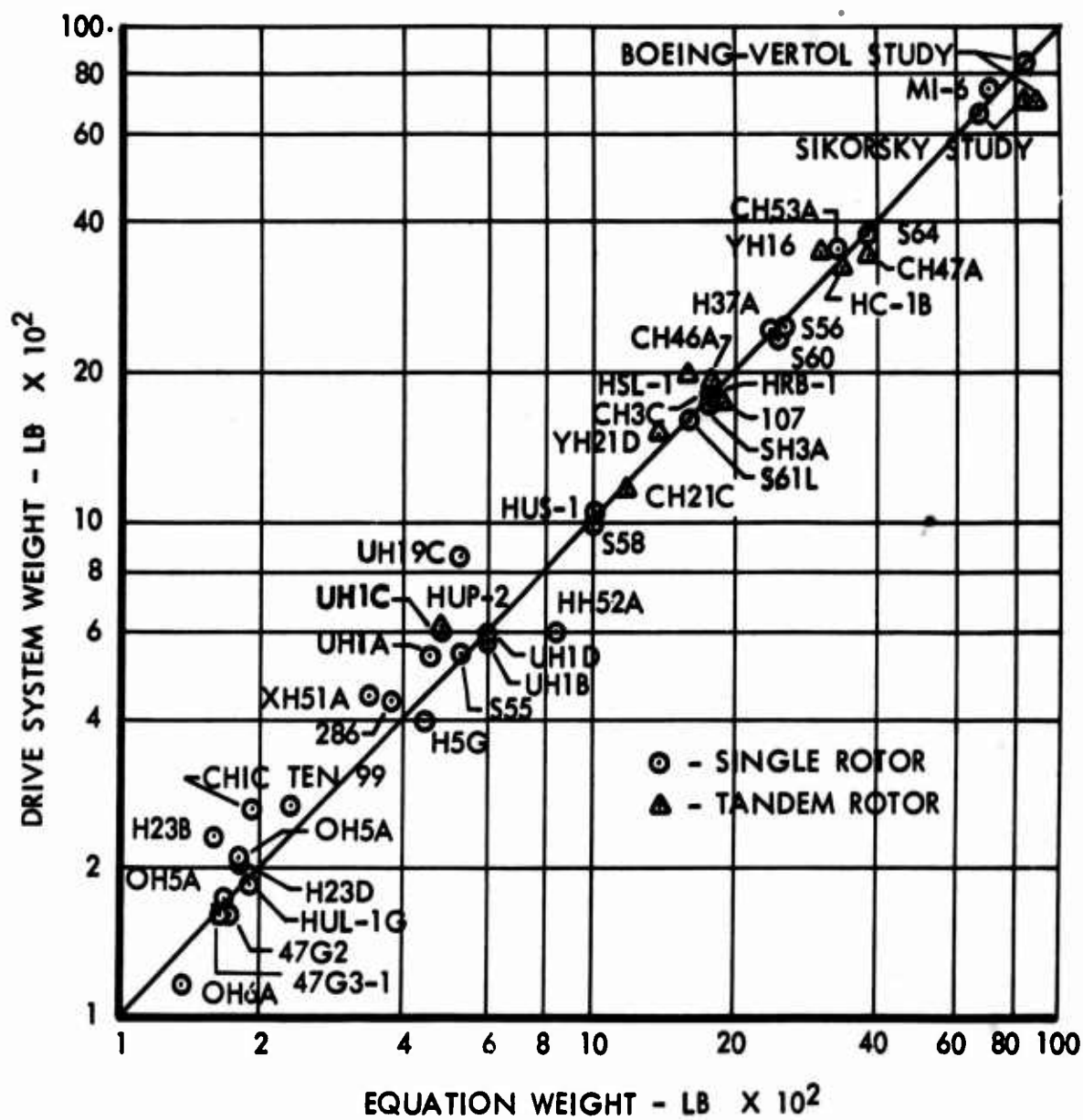


Figure 128. Drive System Weight



was later found that a more reliable estimate could be made if the entire drive system were used. Recent proposed designs for heavy-lift helicopter transmissions indicate that a drive system built today would be somewhat lighter than the preceding equation would indicate; weight savings of as much as 50 percent of the transmission weight have been proposed. At this time, however, a reduction of 10 percent seems a realizable goal for the 1966-1968 period; therefore the resulting equations are

$$W_{DS} = 38.16 \left[ \frac{HP \times R}{V_T} \right]^{0.763}$$

for single-rotor helicopters, and

$$W_{DST} = 57.4 \left[ \frac{HP \times R}{V_T} \right]^{0.763}$$

for tandem-rotor helicopters.

#### Flight Controls Group

A logarithmic least squares fit was made to the data of several contemporary helicopters to determine the best equation for predicting flight controls weight. The equations resulting from this study are

$$W_{FC} = 0.02256 W^{0.712} V_C^{0.653}$$

for single-rotor helicopters, and

$$W_{FCT} = 0.0321 W^{0.712} V_C^{0.653}$$

for tandem-rotor helicopters. In these expressions W is the design gross weight,  $V_C$  is the design cruise speed and  $W_{FC}$  is total flight controls weight for single-rotor and  $W_{FCT}$  is for tandem-rotor helicopters.

The flight controls weights and equation weights for various helicopters are shown in Figure 129 and are listed in Table XXVI.

#### Hydraulics and Electrical Group

An attempt was made to determine statistical weight trends for each of these systems separately. It was found that the equations thus found were unreliable when applied to a helicopter of the size considered in this study. However, when the two groups were combined, the

TABLE XXVI  
FLIGHT CONTROLS WEIGHT

MODEL		FLIGHT CONTROLS WEIGHT (lb)	EQUATION WEIGHT (lb)
Single Rotor			
LOH	OH4A	137	116
Iroquois	UH1B	353	256
Trooper	47G-3	128	105
Skyhook	CH1C	123	115
LOH	OH5A	116	118
Raven	H23D	142	110
Commercial	UH12L4	122	131
LOH	OH6A	52	106
Commercial	286	304	215
Lark	RH3B	120	139
Sea King	SH3A	457	535
USAF	CH3C	490	582
U.S. Marine	CH53A	1085	998
Skycrane	S64	1161	1092
Tandem Rotor			
Sea Knight	HRB-1	827	860
Commercial	107	723	729
Commercial	107 (Adv.)	758	815
Sea Knight	CH46A	838	854
Chinook	CH47A	1201	1036
Chinook	HC-1B	1289	1036
Shawnee	CH21C	502	513

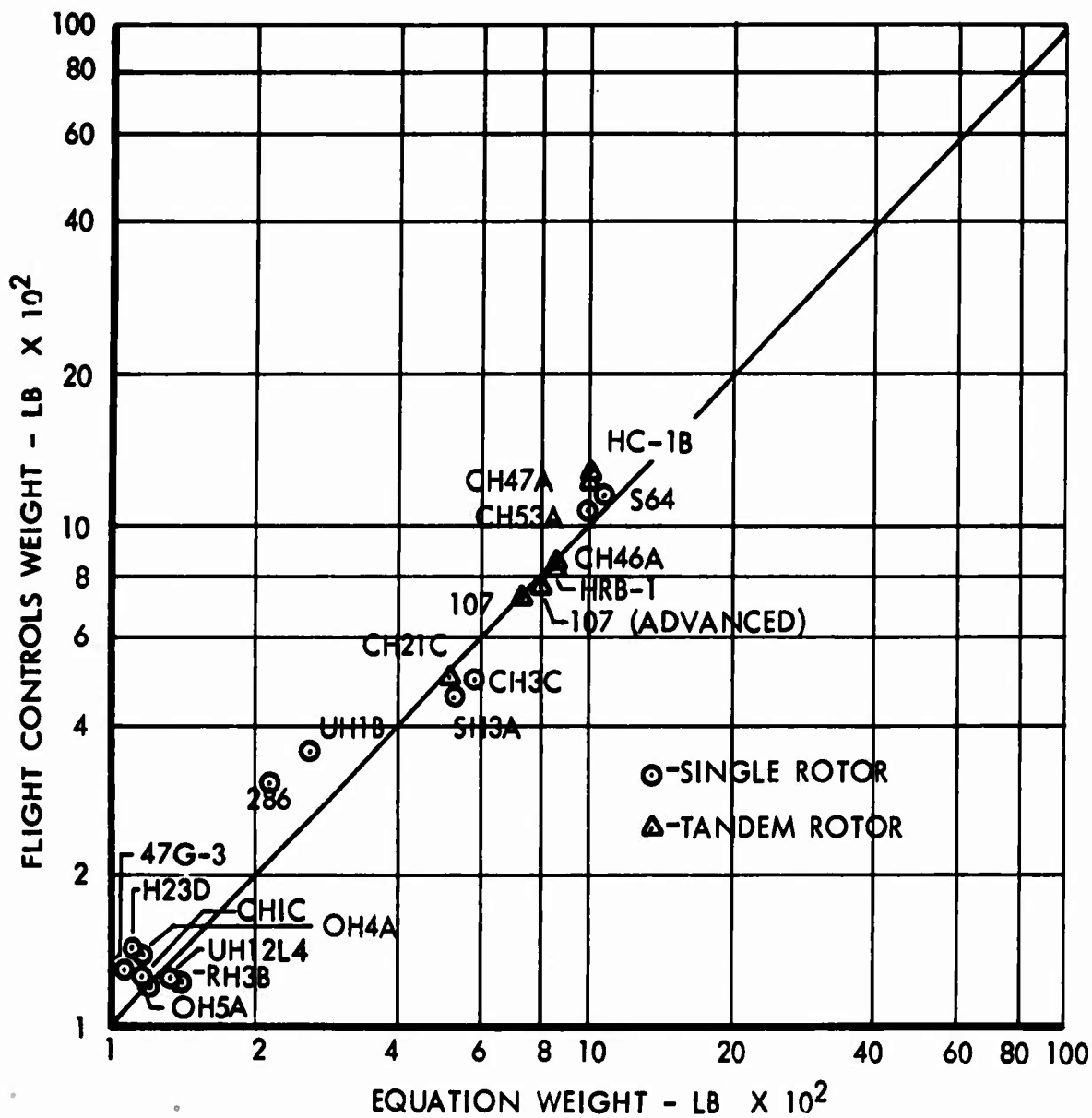


Figure 129. Flight Controls Weight

resulting equation was a better approximation than the sum of the two individual equations. The equation thus found was

$$W_{HE} = 0.153 W^{0.813}$$

for single-rotor helicopters, and

$$W_{HET} = 0.206 W^{0.813}$$

for tandem-rotor helicopters, where  $W$  is the design gross weight and  $W_{HE}$  is total hydraulic and electrical group weight for single-rotor and  $W_{HET}$  is for tandem-rotor helicopters.

Hydraulic and electrical system weights and equation weights for various helicopters are shown in Figure 130 and are listed in Table XXVII.

### Furnishings

For an external cargo helicopter, the furnishings weight is concentrated in the crew compartment; hence, given a crew size, the weight would be approximately constant for either a single- or a tandem-rotor external cargo helicopter. The weight used in this study is

$$W_{FE} = 450 \text{ lb}$$

where  $W_{FE}$  is the furnishings weight for an external cargo helicopter.

For an internal cargo helicopter, it was assumed that soundproofing and insulation will be required over the entire fuselage. Applying a unit weight to an estimated wetted area results in the expression

$$W_{FI} = 180 + .012W$$

where  $W_{FI}$  is the furnishing weight of an internal cargo helicopter and  $W$  is the design gross weight. This equation is valid only for cargo-type helicopters and assumes no fixed seating for personnel.

### Instruments and Electronics

The weights of the instruments and electronics equipment are not explicitly dependent on a size parameter such as gross weight, but are more closely associated with the mission requirements. Therefore, a nominal value was assumed which is felt to be adequate:

$$W_{IE} = 450 \text{ lb}$$

This includes 200 pounds for electronics (radio, navigation, etc.) and 250 pounds for instrument.

TABLE XXVII

## HYDRAULICS AND ELECTRICAL SYSTEM WEIGHT

MODEL		HYDRAULICS AND ELECTRICAL SYSTEM WEIGHT (lb)	EQUATION WEIGHT (lb)
Single Rotor			
LOH	OH4A	79	87
Ranger	47J-2	103	99
Iroquois	UH1B	390	195
Commercial	UH12E	90	95
Raven	H23D	112	95
LOH	OH6A	61	76
Aerogyro	XH51A	134	116
Lark	RH3B	191	111
Skyhook	CH1C	80	105
U.S. Marine	CH53A	605	710
Sea King	SH3A	492	410
USAF	CH3C	522	470
Skycrane	S64	610	810
Tanden Rotor			
Experimental	HSL-1	610	500
Sea Knight	CH46A	777	610
Sea Knight	HRB-1	681	610
Chinook	CH47A	760	770
Chinook	HC-1B	719	770
Experimental	UH21D	377	500

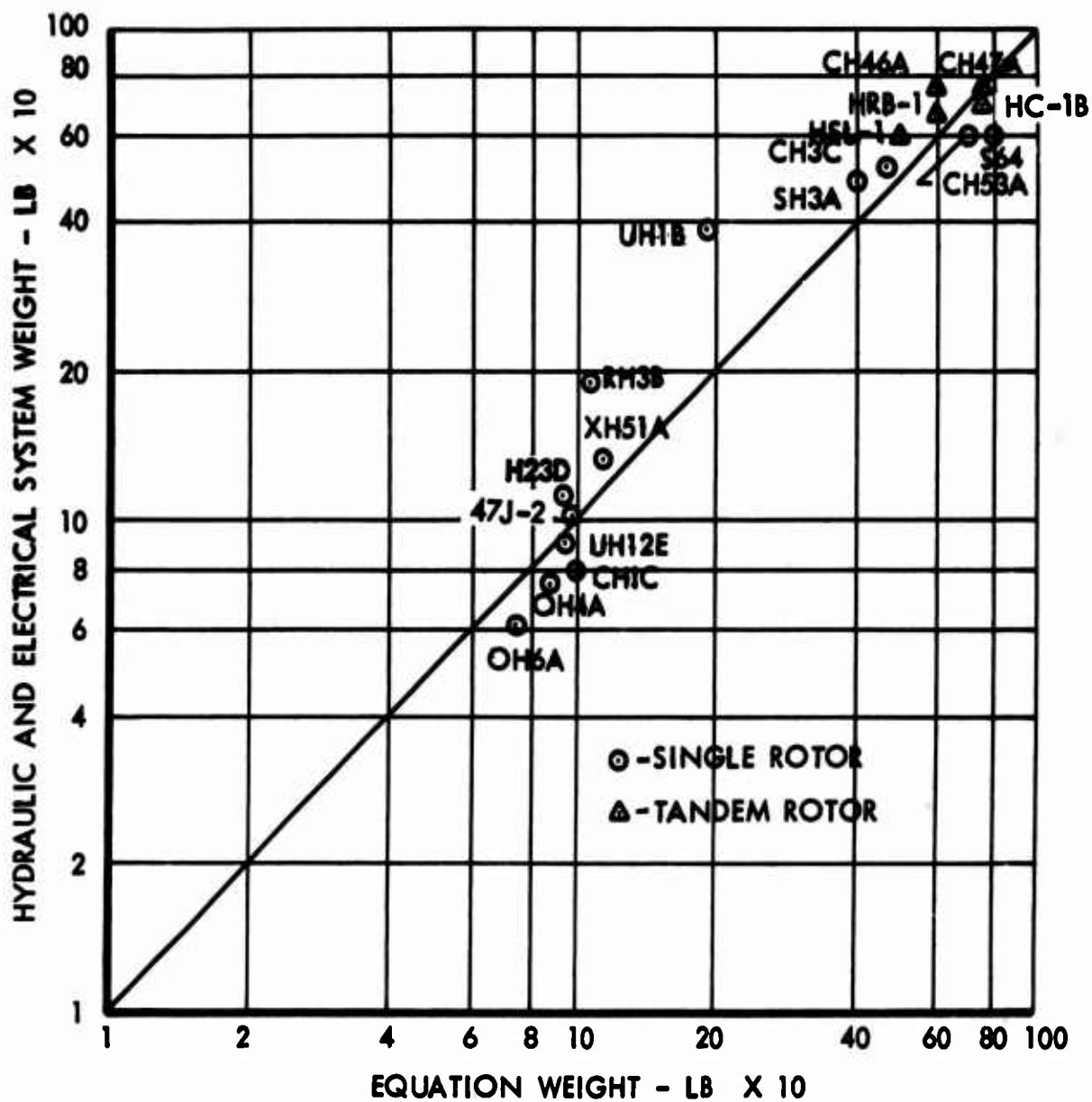


Figure 130. Hydraulics and Electrical Group Weight

### Air Conditioning

For external cargo helicopters, air conditioning will consist of engine bleed air ducting and valves necessary for windshield defogging and crew compartment heating and cooling. The necessary weight is

$$W_{ACE} = 50 \text{ lb}$$

where  $W_{ACE}$  is the air conditioning system weight for an external cargo helicopter.

For an internal cargo helicopter, where a controlled environment may be required in the cargo compartment, the additional ducting will increase the air conditioning system weight by approximately 100 pounds. Therefore, for internal cargo helicopters

$$W_{ACI} = 150 \text{ lb}$$

### Auxiliary Gear Group

The requirement for auxiliary gear was not specified as part of this study, but for a helicopter of this type it is required. The auxiliary gear group consists of a cargo sling and hoist and cargo handling equipment. In addition to being a function of the cargo weight, the weight of these items is a function of the length of the cable required, the reeling speed, the type and number of cargo-attaching devices required, etc. At the present time, it is felt that a weight of 1000 pounds will be sufficient to cover a cargo-handling system with a capacity of 40,000 pounds, and this weight has been included in the weight empty for this study. Therefore,

$$W_{AUX} = 1000 \text{ lb}$$

### Gross Weight

The sum of the preceding items represents the empty weight of the helicopter. The gross weight is found by adding to this weight the weight of the crew, oil and residual fuel, fuel, and payload.

The crew consists of three men; at 200 pounds each, the crew weight is

$$W_C = 600 \text{ lb}$$

It is felt that an allotment of 120 pounds is sufficient to cover residual fuel and engine oil

$$W_{RO} = 120 \text{ lb}$$

In the determination of the gross weight, the fuel is a variable and the fuel tank weight is also a variable. For this program, the basic weight is defined as the weight of all weight - empty items (except the fuel tanks) plus the crew and engine oil. If this definition of basic weight is used, the gross weight is then the sum of the basic weight, fuel and fuel tank weight, and the payload weight.

#### WEIGHT SUMMARY

The Statement of Work required that statistical trend studies be made to estimate a weight breakdown of the systems of an operational helicopter, i.e., transmission, tail rotor and drive, landing gear, etc. for the Part 1 rotor system parametric and configuration determination. This procedure was used as discussed in Section 1 for the parametric study. All of the required work for the Part 2 rotor system preliminary design study was conducted using the helicopter weights as determined in the Part 1 study.

Since the weight studies discussed in this section reflect more accurately the component weights of a high gross-weight helicopter, the detailed weight analysis was made based on the new weight equations and the corresponding rotor characteristics of the refined configuration. The gross weight difference between the Part 1 study and the refined configuration is only 3.4 percent and, as such, would not invalidate any of the results of the parametric or preliminary design study.

The weight breakdown on Form MIL-STD-451, Part 1, is shown in Figure 131. The main rotor assembly weight for the refined configuration is summarized as follows (all weights in pounds):

Main Rotor Assembly	6543
Blade (5)	1380
Hub (1)	454
Flexure (5)	3200
Spar (5)	1110
Control Torque Tube (5)	399

The development of the main rotor assembly weights was an iterative procedure resulting in different rotor weights depending on certain conditions. A summary of this iteration and resulting weights follows.



MIL-STD-491 PART 1  
NAME  
DATE

ROTORCRAFT  
SUMMARY WEIGHT STATEMENT  
WEIGHT EMPTY

PAGE  
MODEL  
REPORT

1									
2	ROTOR GROUP								6513
3	BLADE ASSEMBLY						5690		
4	HUB						419		
5	HINGE AND BLADE RETENTION						424		
6									
7					FLAPPING				
8					LEAD LAG				
9					PITCH				
10					FOLDING				
11	WING GROUP								
12	WING PANELS-BASIC STRUCTURE								
13	CENTER SECTION-BASIC STRUCTURE								
14	INTERMEDIATE PANEL-BASIC STRUCTURE								
15	OUTER PANEL-BASIC STRUCTURE-INCL TIPS					LBS			
16	SECONDARY STRUCT-INCL FOLD MECH					LBS			
17	ATTACHERS - INCL BALANCE WTS					LBS			
18	FLAPS								
19	-TRAILING EDGE								
20	-LEADING EDGE								
21	SLATS								
22	SPOILERS								
23	TAIL GROUP								955
24	TAIL ROTOR						839		
25	- BLADES								
26	- HUB								
27	STABILIZER - BASIC STRUCTURE						116		
28	FINS - BASIC STRUCTURE - INCL DORSAL					LBS			
29	SECONDARY STRUCTURE - STABILIZER AND FINS								
30	ELEVATOR - INCL BALANCE WEIGHT					LBS			
31	RUDDER - INCL BALANCE WEIGHT					LBS			
32									
33	BODY GROUP								5889
34	FUSELAGE OR HULL - BASIC STRUCTURE								
35	BOOMS - BASIC STRUCTURE								
36	SECONDARY STRUCTURE - FUSELAGE OR HULL								
37	- BOOMS								
38	- DOORS, PANELS & MISC								
39									
40									
41	ALIGNING GEAR - LAND TYPE								2990
42	LOCATION				ROLLING	STRUCT	CONTROLS		
43					ASSEMBLY				
44									
45									
46									
47									
48									
49									
50	ALIGNING GEAR GROUP - WATER TYPE								
51	LOCATION				FLOATS	STRUTS	CONTROL:		
52									
53									
54									
55									
56									
57									16,377

\* WHEELS, BRAKES, TIRES, TUBES AND AIR

Figure 131. Weight Summary (1 of 5)

MIL-STD-491 PART 1  
NAME  
DATE

ROTORCRAFT  
SUMMARY WEIGHT STATEMENT  
WEIGHT EMPTY

PAGE  
MODEL  
REPORT

1							
2	FLIGHT CONTROLS GROUP						1590
3	COCKPIT CONTROLS						
4	AUTOMATIC STABILIZATION						
5	SYSTEM CONTROLS - ROTOR	NON ROTATING					
6		ROTATING					
7	- FIXED WING						
8							
9							
10	ENGINE SECTION OR NACELLE GROUP	(INCL. IN ENGINE ACCESSORIES)					
11	INBOARD						
12	CENTER						
13	OUTBOARD						
14	DOORS, PANELS AND MISC						
15							
16	PROPULSION GROUP						9125
17		X AUXILIARY XX	MAIN	X			
18	ENGINE INSTALLATION					2090	
19	ENGINE						
20	TIP BURNERS						
21	LOAD COMPRESSOR						
22	REDUCTION GEAR BOX, ETC						
23	ACCESSORY GEAR BOXES AND DRIVES						
24	SUPERCHARGER-FOR TURBOS						
25	AIR INDUCTION SYSTEM						
26	EXHAUST SYSTEM						
27	COOLING SYSTEM		ENGINE ACCESSORIES			1025	
28	LUBRICATING SYSTEM						
29	TANKS						
30	BACKING BD, TANK SUP & PADDING						
31	COOLING INSTALLATION						
32	PLUMBING, ETC						
33	FUEL SYSTEM					470	
34	TANKS - UNPROTECTED						
35	- PROTECTED						
36	BACKING BD, TANK SUP & PADDING						
37	PLUMBING, ETC						
38	WATER INJECTION SYSTEM						
39	ENGINE CONTROLS		(INCL. IN ENGINE ACCESSORIES)				
40	STARTING SYSTEM						
41	PROPELLER INSTALLATION						
42	DRIVE SYSTEM					5510	
43	GEAR BOXES						
44	CLUTCH SYSTEM						
45	CLUTCH AND MISC						
46	TRANSMISSION DRIVE						
47	ROTOR SHAFT						
48	JET DRIVE						
49							
50							
51							
52	AUXILIARY POWER PLANT GROUP						125
53							
54							
55							
56							
57							10819

Figure 131. Weight Summary (2 of 5)

MIL-STD-491 PART 1  
NAME  
DATE

ROTORCRAFT  
SUMMARY WEIGHT STATEMENT  
WEIGHT EMPTY

PAGE  
MODEL  
REPORT

1							
2							
3							
4	INSTRUMENT AND NAVIGATIONAL EQUIPMENT GROUP						250
5	INSTRUMENTS						
6	NAVIGATIONAL EQUIPMENT						
7							
8							
9	HYDRAULIC AND PNEUMATIC GROUP						
10	HYDRAULIC						
11	PNEUMATIC						
12							100
13							
14	ELECTRICAL GROUP						
15	A C SYSTEM						
16	D C SYSTEM						
17							
18							
19	ELECTRONICS GROUP						200
20	EQUIPMENT						
21	INSTALLATION						
22							
23							
24	ARMAMENT GROUP - INCL GUNFIRE PROTECTION					100	
25							
26	FURNISHINGS AND EQUIPMENT GROUP						150
27	ACCOMMODATIONS FOR PERSONNEL						
28	MISCELLANEOUS EQUIPMENT & INCL				100	BALLAST	
29	FURNISHINGS						
30	EMERGENCY EQUIPMENT						
31							
32							
33							
34	AIR CONDITIONING AND ANTI-ICING EQUIPMENT						50
35	AIR CONDITIONING					50	
36	ANTI-ICING						
37							
38							
39	PHOTOGRAPHIC GROUP						
40	EQUIPMENT						
41	INSTALLATION						
42							
43	AUXILIARY GEAR GROUP						1000
44	AIRCRAFT HANDLING GEAR						
45	LOAD HANDLING GEAR						
46	ATO GEAR						
47							
48							
49							
50							
51							
52							
53							
54	MANUFACTURING VARIATION						
55							
56							1350
57	TOTAL-WEIGHT EMPTY - PAGES 2, 3 AND 4						30,570

Figure 131. Weight Summary (3 of 5)

MIL-STD-881 PART 1  
NAME  
DATE

SUMMARY WEIGHT STATEMENT  
USEFUL LOAD GROSS WEIGHT

PAGE  
MODEL  
REPORT

1	LOAD CONDITION				WEIGHT POUNDS	WEIGHT KILOGRAMS	WEIGHT KILOGRAMS
2							
3	CREW - NO. 3				600	600	600
4	PASSENGERS - NO.						
5	FUEL	LOCATION	TYPE	GALLONS			
6	UNUSABLE				0	0	0
7	INTERNAL				600	200	570.2
8	AUXILIARY TANKS						3700
9							
10							
11	EXTERNAL						
12							
13							
14							
15	BOMB BAY						
16							
17							
18							
19	OIL				10	10	10
20	UNUSABLE						
21	ENGINE						
22							
23							
24							
25	PASSENGER						
26	CARGO				26702	60519	
27							
28	ARMAMENT						
29	GUNS-LOCATION	TYPE	QUANTITY	CALIBER			
30							
31							
32							
33							
34	AMM						
35							
36							
37							
38	BOMB INSTL.						
39	BOMBS						
40							
41	TORPEDO INSTL.						
42	TORPEDOES						
43							
44	ROCKET INSTL.						
45	ROCKETS						
46							
47	EQUIPMENT-PYROTECHNICS						
48	-PHOTOGRAPHIC						
49							
50	-OXYGEN						
51							
52	-MISCELLANEOUS						
53							
54							
55	USEFUL LOAD				31022	15119	62322
56							
57	GROSS WEIGHTS - PAGES 2-3				65,300	75,727	98,900

\* IF NOT SPECIFIED AS WEIGHT EMPTY OR FIRED, FLEXIBLE, ETC.

Figure 131. Weight Summary (4 of 5)

MIL-STD-491 PART 1  
NAME  
DATE

SUMMARY WEIGHT STATEMENT  
DIMENSIONAL STRUCTURAL DATA  
ROTORCRAFT

PAGE  
MODEL  
REPORT

1	LENGTH - OVERALL	X BLADES FOLDED			
2	GENERAL DATA	BOOM	FUS	MAC	CABIN
3	LENGTH - MAXIMUM FEET				
4	DEPTH - MAXIMUM FEET				
5	WIDTH - MAXIMUM FEET				
6	WETTED AREA TOTAL				
7	WETTED AREA GLASS				
8	WING TAIL & FLOOR DATA	WING	H TAIL	V TAIL	FLOOR
9	GROSS AREA - SQUARE FEET				
10	WEIGHT/GROSS AREA - POUNDS PER SQUARE FEET				
11	SPAN - FEET				
12	FOLDED SPAN - FEET				
13	THEORETICAL ROOT CHORD - INCHES				
14	MAXIMUM THICKNESS - INCHES				
15	CHORD AT PLANFORM BREAK - INCHES				
16	MAXIMUM THICKNESS - INCHES				
17	THEORETICAL TIP CHORD - INCHES				
18	MAXIMUM THICKNESS - INCHES				
19	DORSAL AREA INCLUDED IN FUSELAGE	SO FT	TAIL		SO FT
20	TAIL LENGTH 25% MAC WING TO 25% MAC HORIZONTAL TAIL				FEET
21	AREA - SO FT PER ROTORCRAFT	FLAPS	AILERONS	SPOILERS	
22		SLATS	WING LE	WING TE	
23	ROTOR DATA - TYPE -	RIGID			
24		MAIN ROTOR	TAIL ROTOR		
25	FROM CL ROTATION - INCHES	ROOT	TIP	ROOT	TIP
26	CHORD - INCHES	37.90	37.90	23.17	23.17
27	THICKNESS - INCHES	6.50	6.50		
28			MAIN-FWD	MAIN-APT	TAIL
29	BLADE RADIUS - FEET		52.2		9.09
30	NUMBER BLADES		5		6
31	BLADE AREA-TOTAL-OUTBOARD	125	INCHES RADIUS	659	
32	DISC AREA - TOTAL SHEET	8560	SQUARE FEET - OVERLAP		SQUARE FEET
33	TIP SPEED AT DESIGN LIMIT ROTOR-SPEED-POWER-FT/SEC	730			
34	DESIGN FACTOR USED BY CONTRACTOR				
35	LOCATION FROM HORIZONTAL REF DATUM	INCHES			
36	PRESSURE JET & BLADE SECTION AREA FOR DUCT				
37	TIP JET THRUST	GEAR			
38	POWER TRANSMISSION DATA	HP			
39	MAX POWER - TAKE-OFF	21,700			
40	ALTITUDE GEAR TYPE	QUADRICYCLE-GEAR			
41	GEAR LENGTH - OLEO EXTND CL AXLE TO CL TRUNNION				
42	OLEO TRAVEL - FULL EXTENDED TO COMPRESSED	INCHES			
43	WHEEL SIZE AND NUMBER REQUIRED				
44	FUEL AND OIL SYSTEM	LOCATION	NO. TANKS	GALS	NO. TANKS
45			UNPRCTCD		PROTECTED
46	FUEL - BUTLY IN				
47	FUEL - EXTERNAL				
48	LUBRICATING SYSTEM				
49	HYDRAULIC SYSTEM				
50	STRUCTURAL DATA - CONDITION	FUEL IN DESIGN STRESS			
51		WINGS-LGROSS WY GROSS WY			
52	FLIGHT	71,727			
53	LANDING	3.75			
54	S DESIGN LOAD	WING	FWD RTR	APT RTR	
55					
56	TYPE OF POWER TRANSMISSION - GEARED -	HARDCORE			
57					

\* PARALLEL TO CL & CL ROTORCRAFT \*\*\* GEAR RATIOS ENG TO ROTOR  
 \*\* CROSS OUT NON-APPLICABLE TYPE \*\*\* TOTAL USEABLE CAPACITY  
 \*\*\*\*\* REFER TO PARA. 9-1-1-3-ITEMS 6-33 & 6-34 \*\*\* GOVERNMENT PROPERTY OFFICE - FPO 9-1-1-3-34 -06-

Figure 131. Weight Summary. (5 of 5)

In the Part 1 parametric study, weight equations were derived based entirely on statistical data for helicopters up to a weight class of 38,000-pound gross weight. The equation for the matched-stiffness rotor system indicated that the main rotor weight would be 5578 pounds.

The actual weight analysis of the preliminary designs shown in Section 2 for the helicopter characteristics resulting from the Part 1 parametric study resulted in a 6945-pound weight for the matched-stiffness rotor system. This indicated that the weight equations derived from statistical data for contemporary helicopters did not accurately reflect component weights for helicopters in the heavy-lift gross weight category. As such the weight equation was rederived to reflect the preliminary design weight of 6945 pounds.

Based on the rotor characteristics resulting from the refined configuration parametric study of this section and the rederived weight equation, the matched-stiffness rotor system weight is 6543 pounds.

#### PARAMETRIC ANALYSIS PROCEDURE

The procedure followed for the solution gross weight determination of the refined configuration followed the computer program described in "Parametric Analysis Procedure" of Section 1. The matched-stiffness single and tandem rotors were the only configurations that were analyzed under the new conditions. The rederived weight equations and a change in the blade loading limit as discussed below were used.

Figure 132 is an output summary sheet for the solution gross weight determination program for the refined configuration.

#### Matched-Stiffness Blade Loading Limitations

As discussed in Section 1, a blade loading limit of 77 psf was used in determining the characteristics of the rotor system. An analysis of this condition was made during the preliminary design study. It was determined that for the design condition of a center-of-gravity offset for the helicopter of  $\pm 30$  inches, the resultant combination of first- and second-harmonic flapping loads was greater than the in-plane loads. Since the first-harmonic flapping is set by center-of-gravity offset, the blade loading limit was made to correspond to a constant

# MOFH ROTOR

TWETA= -5.3

CT/SIGMA	RADIUS	TIP SPEED	SIGMA	TRANSPORT WT. LBS	HEAVY LIFT WT. LBS	MAX RATED POWER	MAX ALPHA 270. DEG.	CLROT	CLROML	BLADES	B.L.
0.030	45.0	600.0	0.2634	69614.1	81290.7	15048.9	8.007	0.32870	0.38354	13.00000	48.50738
0.065	45.0	600.0	0.1878	64513.9	76972.0	13680.3	10.220	0.42732	0.50916	9.00000	64.36419
0.090	45.0	600.0	0.1471	62188.9	74863.2	13124.7	12.446	0.52593	0.63311	7.00000	80.00920
0.095	45.0	600.0	0.1217	61117.8	73950.0	13103.1	14.658	0.62454	0.75567	6.00000	95.49677
0.050	50.0	600.0	0.2150	70154.3	82000.4	14718.3	7.762	0.32870	0.38421	11.00000	48.55413
0.065	50.0	600.0	0.1531	64929.0	77427.5	12829.1	9.990	0.42732	0.50954	8.00000	64.40374
0.090	50.0	600.0	0.1200	62643.5	75452.1	12157.7	12.211	0.52593	0.63344	6.00000	80.05342
0.095	50.0	600.0	0.0991	61454.1	74413.6	12155.9	14.439	0.62454	0.75624	5.00000	95.56948
0.030	55.0	600.0	0.1798	70977.6	82932.7	13887.3	7.570	0.32870	0.38407	9.00000	48.53657
0.065	55.0	600.0	0.1287	64062.0	76637.9	12221.0	9.789	0.42732	0.50864	6.00000	64.28174
0.090	55.0	600.0	0.1002	63298.6	76198.8	11440.0	12.031	0.52593	0.63311	5.00000	80.00888
0.095	55.0	600.0	0.0829	62154.4	75184.1	11550.2	14.251	0.62454	0.75344	4.00000	95.47111
0.030	45.0	650.0	0.2161	67010.1	78824.9	15123.8	7.442	0.32870	0.38464	11.00000	57.34710
0.065	45.0	650.0	0.1550	62482.4	74936.0	13321.2	9.570	0.42732	0.51249	8.00000	76.00895
0.090	45.0	650.0	0.1224	60730.5	73448.3	12903.1	11.683	0.52593	0.63804	6.00000	94.33733
0.095	45.0	650.0	0.1022	60194.6	72977.0	13435.3	13.744	0.62454	0.75716	5.00000	112.29761
0.030	50.0	650.0	0.1763	67501.2	79471.5	14063.7	7.226	0.32870	0.38700	9.00000	57.39695
0.065	50.0	650.0	0.1263	62843.3	75435.1	12370.8	9.367	0.42732	0.51294	8.00000	76.07354
0.090	50.0	650.0	0.0998	61149.5	73996.6	11981.7	11.484	0.52593	0.63442	5.00000	94.39024
0.095	50.0	650.0	0.0834	60701.9	73595.2	12640.8	13.561	0.62454	0.75719	4.00000	112.30265
0.035	55.0	650.0	0.1674	68293.8	80361.2	13292.9	7.057	0.32870	0.38879	7.00000	57.36533
0.065	55.0	650.0	0.1061	63917.5	76574.6	11759.6	9.189	0.42732	0.51193	5.00000	75.92715
0.090	55.0	650.0	0.0834	61787.6	74718.8	11323.5	11.322	0.52593	0.63400	4.00000	94.32724
0.095	55.0	650.0	0.0697	61343.0	74363.9	11765.5	13.406	0.62454	0.75884	3.00000	112.25284
0.050	45.0	700.0	0.1814	65243.6	77033.0	14701.9	6.967	0.32870	0.38810	9.00000	64.75702
0.065	45.0	700.0	0.1310	61250.4	73667.4	13113.9	9.017	0.42732	0.51394	7.00000	88.40320
0.090	45.0	700.0	0.1043	60015.8	72660.3	13128.4	11.029	0.52593	0.63673	5.00000	109.52408
0.095	45.0	700.0	0.0868	60710.5	73240.3	15015.0	12.939	0.62454	0.75344	4.00000	129.59788
0.050	50.0	700.0	0.1478	65625.1	77564.6	13677.8	6.776	0.32870	0.38851	7.00000	64.82697
0.065	50.0	700.0	0.1048	61631.8	74180.9	12233.2	8.830	0.42732	0.51427	5.00000	88.45985
0.090	50.0	700.0	0.0851	60489.1	73253.2	12280.4	10.847	0.52593	0.63691	4.00000	109.55392
0.095	50.0	700.0	0.0717	60488.1	73241.7	13439.5	12.806	0.62454	0.75621	4.00000	130.07487
0.030	55.0	700.0	0.1229	66050.7	78102.8	12936.3	6.632	0.32870	0.38868	5.00000	64.85704
0.065	55.0	700.0	0.0891	62268.8	74893.6	11554.7	8.683	0.42732	0.51397	4.00000	88.40778
0.090	55.0	700.0	0.0708	60878.3	73748.0	11416.4	10.714	0.52593	0.63711	4.00000	109.58867
0.095	55.0	700.0	0.0604	61632.5	74387.9	13376.1	12.622	0.62454	0.75379	3.00000	129.65928

Figure 132. Output Summary Sheet for Solution Gross Weight Determination Program - Refined Configuration

second-harmonic-flapping angle,  $a_2$  (the  $a_2$  for 95 knots with the blade loading of 77 psf and a tip speed of 700 fps), using the equations

$$\frac{a_2}{\mu^2} = (t_{2,1}) \lambda + (t_{2,2}) \theta_0 + (t_{2,3}) \theta_1$$

and

$$\frac{2C_T}{a\sigma} = (t_{3,1}) \lambda + (t_{3,2}) \theta_0 + (t_{3,3}) \theta_1$$

where

$$\frac{C_T}{\sigma} = \frac{W}{\rho \pi R^2 \sigma (\Omega R)^2} = \frac{BL}{\rho (\Omega R)^2}$$

and using the relationship for  $(t_{i,j})$  given by Bailey's work in NACA Report 716 (Reference 21).

This relationship between blade loading and tip speed is shown in Figure 133. The blade loading limit for each tip speed was established on the corresponding solution plot (Figure 134) using Figure 135.

#### RESULTS OF PARAMETRIC ANALYSIS - REFINED CONFIGURATION

For a given set of rotor parameters and a given helicopter configuration, the computer program printed out the takeoff gross weight for the heavy-lift mission and the required sea level rating of the power plant. These values were then entered on plots such as shown in Figure 134. The rotor radius, thrust/solidity coefficient, and tip speed can be chosen from these plots, for a given configuration and engine size, which will result in the lowest helicopter gross weight. This gross weight and the corresponding rotor parameters represent the optimum matching of the helicopter to the power plants considered for the mission requirements used in the study.

#### Parameters Used in the Computer Program

Solution gross weights were determined for the matched-stiffness single- and tandem-rotor configurations. The basic parameters consisting of tip speed, rotor radius, and thrust/solidity coefficient were entered into the program utilizing combinations of several values of these parameters. The values used were

- Tip speed,  $\Omega R = 600, 650, 700, 750, \text{ and } 800 \text{ fps}$



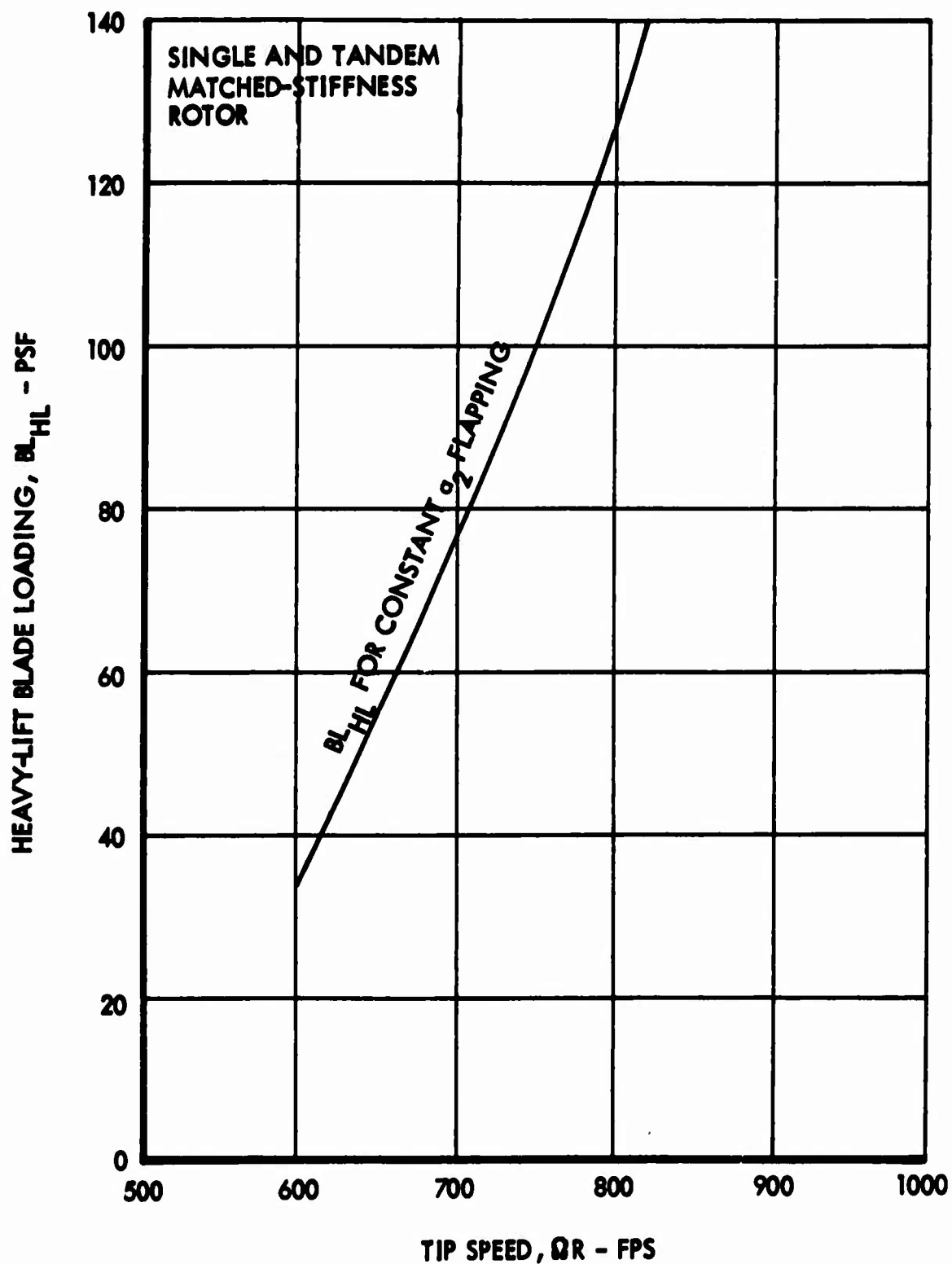


Figure 133. Matched-Stiffness Blade Loading Limit - Tip Speed Relationship

$C_T/\sigma$	B.L.	SINGLE MATCHED-STIFFNESS ROTOR
○ 0.050	66.8	$\Omega R = 700 \text{ FPS}$
□ 0.065	88.4	
◇ 0.080	109.5	
▽ 0.095	129.6	

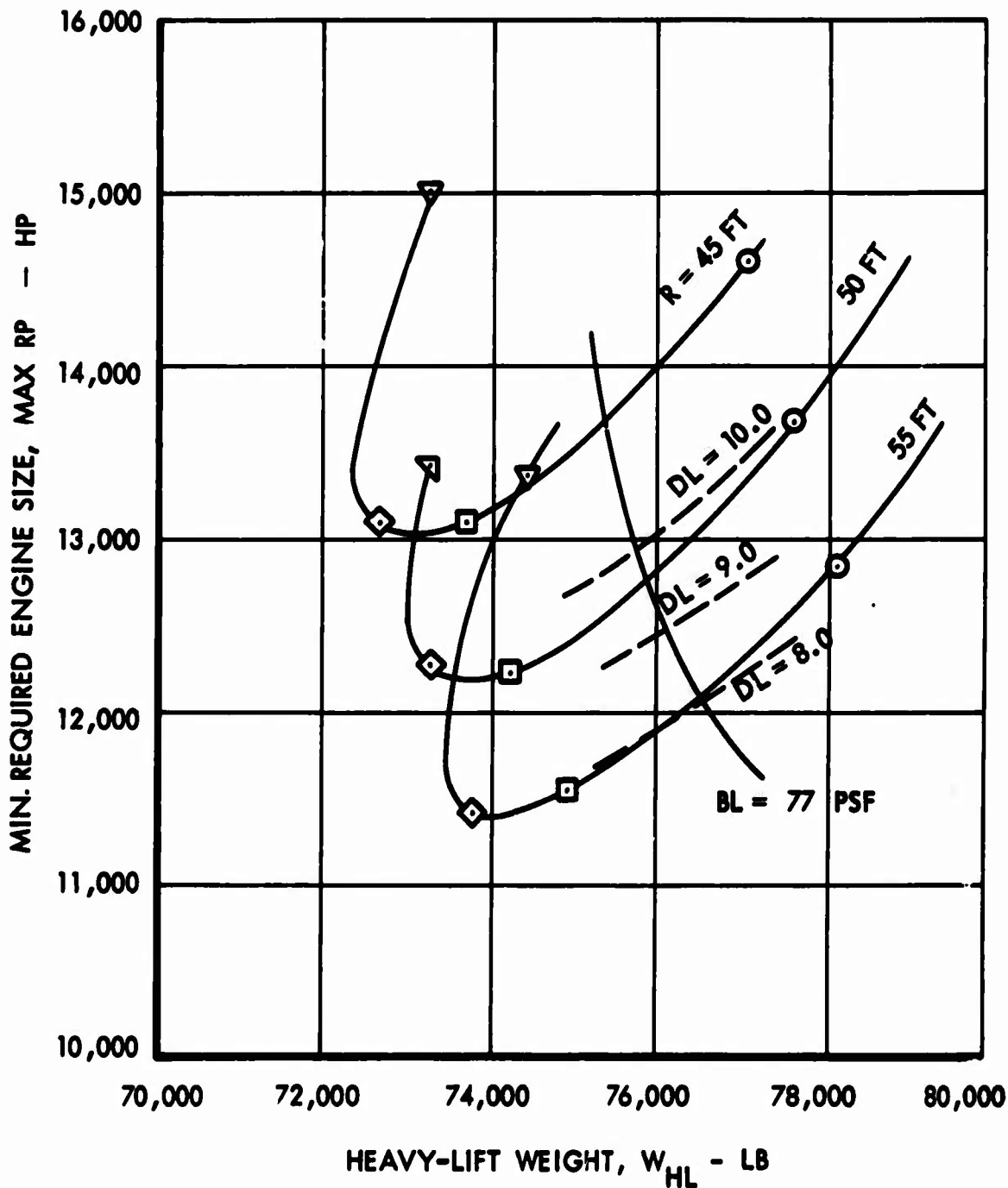


Figure 134. Typical Plot of Solution Gross Weight Determination Program - Refined Configuration

- Thrust/solidity coefficient,  $C_{T/\sigma} = .050, .065, .080, \text{ and } .095$
- Rotor radius:

Single rotor,  $R = 45.50 \text{ and } 55 \text{ ft}$

Tandem rotor,  $R = 37.5, 40, \text{ and } 42.5 \text{ ft}$

Parameter values other than the foregoing were submitted when necessary to fill in areas needing better definition.

#### Use of Computer Results

The results of the solution gross weight determination program were plotted as maximum rated power (Max RP) versus heavy-lift gross weight ( $W_{HL}$ ) at constant tip speeds ( $\Omega R$ ) as shown in Figure 134.

Solution limit lines of blade loading for the matched-stiffness single and tandem-rotor configurations were established on these plots using such plots as are shown in Figure 135. The blade loading limit was determined from Figure 133.

Figure 136 shows a combined plot of the blade loading limited weights and engine sizes required. This plot was used in determining the optimum characteristics for the matched-stiffness single-rotor system, which resulted in the lightest gross weight vehicle. A limiting advancing tip Mach number of 0.85 for the 130-knot outbound cruise speed was used to establish the 730 fps tip speed solution limiting line on this plot.

As a check, and to obtain complete weight and mission breakdowns, the resulting characteristics were submitted to the solution gross weight determination program, and output sheets were obtained. (See Figure 15 for a typical output sheet used in the Section 1 parametric study).

The rotor parameters indicated as the optimum point on Figure 136 were selected on the basis of the best matching with an existing or growth version of an existing engine. In this case the maximum equivalent rated power of three T64/S4B engines provided optimum matching within the limits of the rotor system parameters applied to this study. This does not necessarily restrict the use of other engines in the heavy-lift helicopters.

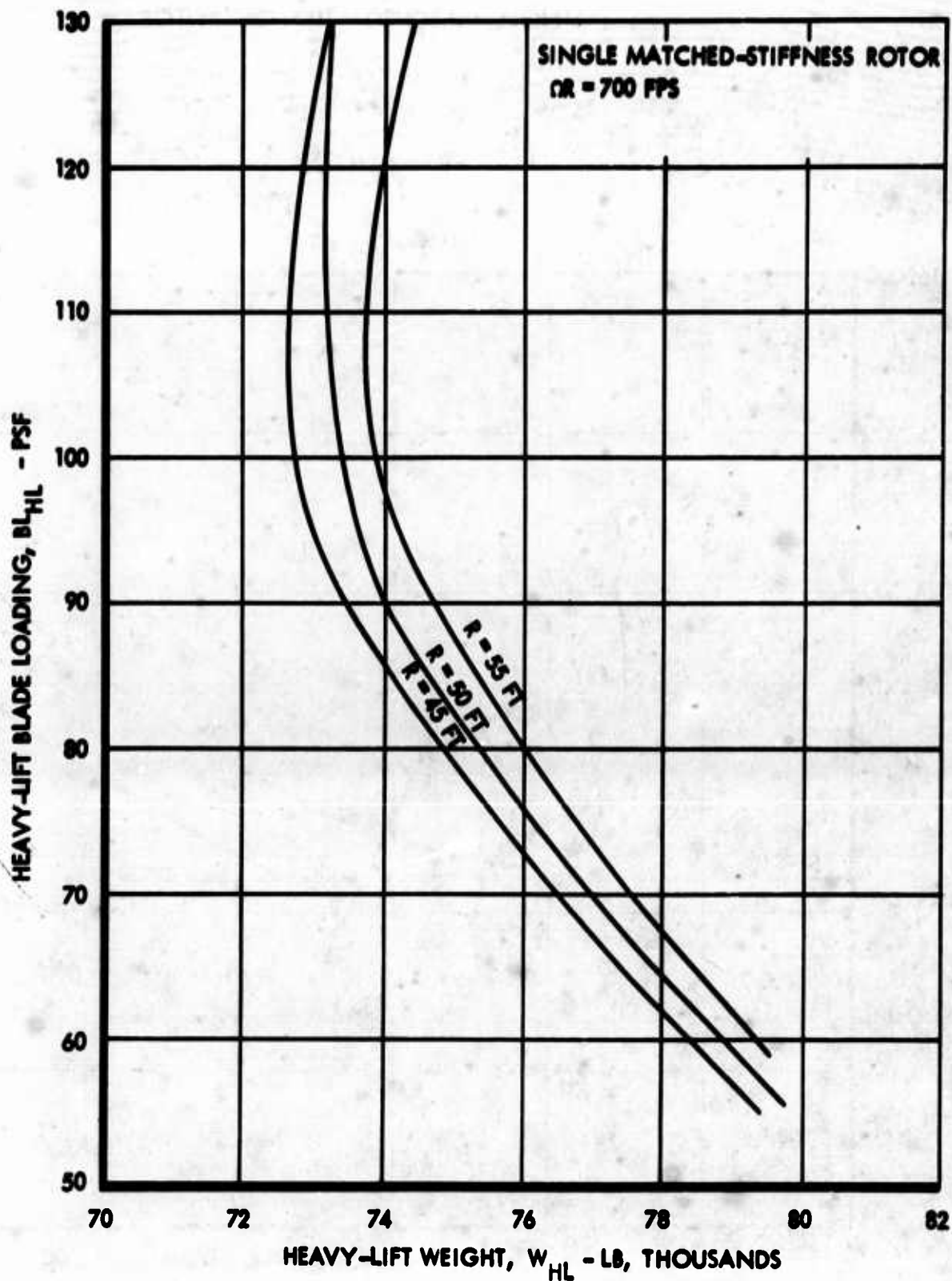


Figure 135. Typical Plot Used In Establishing Solution Limiting Line On Solution Gross Weight Program Results - Refined Configuration

# SINGLE MATCHED-STIFFNESS ROTOR

BLADE LOADING LIMITED  
FOR CONSTANT  $a_2$  FLAPPING

$$\text{AT 95 KNOTS, } \frac{BL}{(\Omega R)^4} = 0.321 \times 10^{-9}$$

$$(BL = 77 \text{ at } \Omega R = 700 \text{ FPS})$$

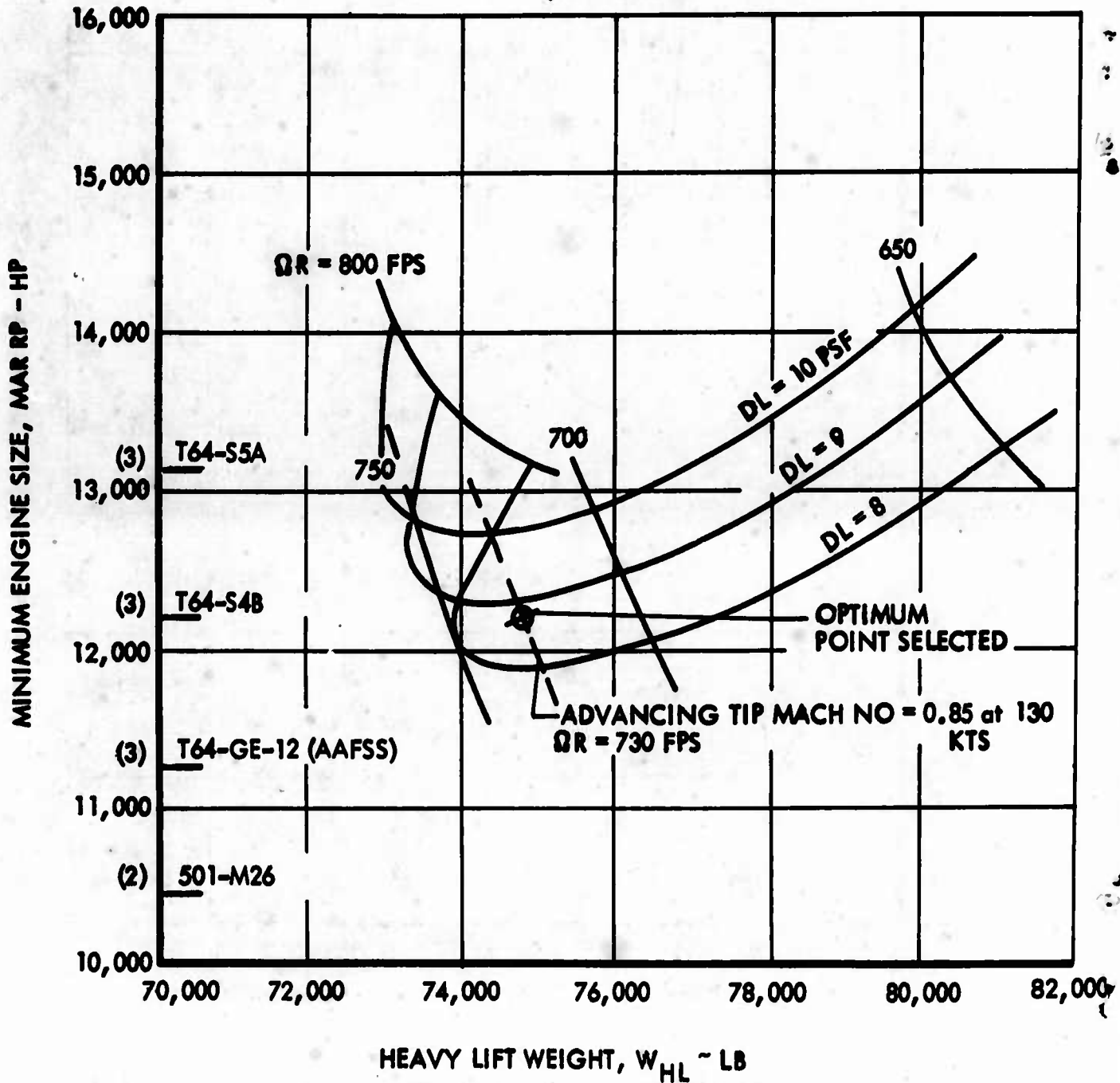


Figure 136. Typical Plot Used in Selecting Refined Configuration

## RESULTS OF COMPUTER ANALYSIS - REFINED CONFIGURATION

A description of the configurations for the matched-stiffness single and tandem rotors as determined by the study conducted in this section is shown in Tables XXVIII and XXIX. A comparison of the results listed in these tables and in Tables IV and V of Section 1 shows that the matched-stiffness single-rotor results in the lightest helicopter gross weight. The gross weight for the matched-stiffness single- and tandem-rotor helicopters has increased from the values shown in the Section 1 study; this is attributed to the use of the rederived weight equations which more accurately reflect component weights for the high gross weight vehicles.

As noted in Section 1, there was negligible weight difference in rotor weights between the articulated, teetered, and rigid rotor systems, and the matched-stiffness rotor resulted in an 8-percent to 12-percent reduction in vehicle gross weight. The study, as defined by this section, results in a 4-percent to 6-percent reduction in vehicle gross weight for the matched-stiffness rotor. The principal areas contributing to the gross weight difference are the rotor system, propulsion system including fuel, and the fuselage.

The complete weight breakdown and description of the matched-stiffness single- and tandem-rotor systems resulting from the parametric study of this section is presented in Table XXX.

### Single-Point Variation

The single-point variation study conducted in Section 1 would apply, in principle, to the study of this section with respect to fuel required, airfoil sections, and airfoil twist and taper.

A comparison of the significant components was made of the internal cargo and external cargo helicopters, based on the weight equations of this section, with the following results:

	<u>External Cargo</u>	<u>Internal Cargo</u>
Body	5,889	7,360
Landing Gear	2,990	2,158
Furnishings	<u>450</u>	<u>1,076</u>
Total	9,329	10,594

From this comparison, it is apparent that the weight penalty associated with the internal cargo fuselage is 1,265 pounds. Some of this could be recovered for the transport mission payload by drag reduction. However, drag reduction would have little effect on the reduced heavy-lift payload capability.

TABLE XXVIII											
CONFIGURATION DESCRIPTION											
EXTERNAL CARGO HELICOPTER, $\theta_1 = -5$ Degrees											
(REFINED CONFIGURATION)											
CONFIGURATION	$W_{HL}$ (lb)	$W_T$ (lb)	NO. OF ENGINES AND TYPE	R (ft)	$\sigma$	$\Omega$ R (fps)	BL (lb/ft <sup>2</sup> )	$C_{LrO_T}$	$C_{LrO_{HL}}$	NO. BLADES	DL (lb/ft <sup>2</sup> )
Single Matched-Stiffness Rotor	74,727	62,500	(3)T64/S4B	52.2	.0964	730	90.6	.405	.484	5	8.74
Tandem Matched-Stiffness Rotor	78,678	66,650	(3)T64/S4B	40.2	.0855	730	90.6	.410	.484	4	8.78

TABLE XXIX							
ADJUSTMENTS OF COMPUTER RESULTS SHOWN IN TABLE XXVIII							
CONFIGURATION	FUSELAGE (lb)	CROSS SHAFT (lb)	ENGINE (lb)	FUEL & FUEL TANK (lb)		PAYLOAD (lb)	
				HEAVY-LIFT MISSION	TRANSPORT MISSION	HEAVY-LIFT MISSION	TRANSPORT MISSION
Single Matched- Stiffness Rotor	0	0	-320	-200	-420	520	740
Tandem Matched- Stiffness Rotor	0	0	-320	-200	-420	520	740



TABLE XXX

DESCRIPTION OF MATCHED-STIFFNESS SINGLE- AND TANDEM-ROTOR SYSTEMS  
AND WEIGHT BREAKDOWN COMPARISON (REFINED CONFIGURATION)

<u>ITEM</u>	<u>SINGLE-ROTOR</u>	<u>TANDEM-ROTOR</u>
Gross Weight, lb:		
Heavy-Lift Mission (Load Factor = 2.5)	74,727	78,678
Transport Mission	62,500	66,650
Ferry Mission (load Factor = 2.0)	92,900	98,400
Power Plant:		
Engine Number and Type (or Equivalent)	Three (3) T64/S4B	Three (3) T64/S4B
Total Rated Power		
Sea Level Uncorrected	11,700 (10 min)	11,700 (10 min)
6000 ft, 95°F Uncorrected	8,700 (10 min)	8,700 (10 min)
Power Correction	-(2.4% + 240 hp)	-(2.4% + 240 hp)
Fuel Flow Increased by	5%	5%
Transmission:		
Design Horsepower (3600-hr Life)	9,529	9,383
Main Rotor:		
Radius, ft	52.2	40.2
Solidity	.09637	.0855
Number of Blades	5	4
Blade Chord, in.	38.0	32.4
Blade Aspect Ratio	16.5	14.9
Tip Speed, fps	730	730
Disc Loading (Heavy-Lift), psf	8.74	8.74
Design Mean Blade Lift Coefficient		
Transport	.405	.410
Heavy-Lift	.484	.484
Hover Horsepower, Transport, 6000 ft, 95°F (Main Rotor Only)	7,525	8,253
Blade Loading, psf	90.6	90.6
Overlap ( $1 - \frac{d}{2R}$ )	-	.35
Tail Rotor:		
Radius, ft	9.89	-
Solidity	.2486	-
Main Rotor to Tail Rotor Hub Distance, ft	63.09	-
Hover Horsepower, Transport, 6000 ft, 95°F (T.R. Only)	741	-
Front to Rear Rotor Hub Distance, ft	-	52.3
Equivalent Drag Areas:		
Inbound (Transport and Heavy-Lift) and Ferry, sq ft	80	80
Outbound Transport, sq ft	100	100
Outbound Heavy-Lift, sq ft	180	180



TABLE XXX (CONTINUED)

<u>ITEM</u>	<u>SINGLE-ROTOR</u>	<u>TANDEM-ROTOR</u>
<b>Component Weights, lb:</b>		
Rotor Group	6,543	6,877
Tail Group	955	-
Tail Rotor	(839)	-
Horizontal Stabilizer	(116)	-
Body Group	5,889	7,139
Landing Gear Group	2,990	3,658
Flight Controls Group	1,598	2,358
Propulsion Group	9,126	10,354
Engines	(2,090)	(2,090)
Engines Accessories	(1,026)	(1,025)
Fuel System	(470)	(492)
Drive System	(5,540)	(6,747)
Equipment	3,477	4,044
Auxiliary Power Unit	(125)	(125)
Instruments and Navigation	(250)	(250)
Hydraulics and Electrical	(1,402)	(1,969)
Electronics	(200)	(200)
Furnishings	(450)	(450)
Air Conditioning	(50)	(50)
Auxiliary Gear	(1,000)	(1,000)
<b>Total (Weight Empty)</b>	<b>30,578</b>	<b>34,430</b>
<b>Mission Weights, lb:</b>		
<b>Transport Mission</b>		
Crew	600	600
Fuel	6,460	6,750
Oil and Residual Fuel	120	120
Payload	24,742	24,750
Gross Weight	62,500	66,650
<b>Heavy-Lift Mission</b>		
Crew	600	600
Fuel	2,910	2,996
Oil and Residual Fuel	120	120
Payload	40,519	40,532
Gross Weight	74,727	78,678
<b>Ferry Mission</b>		
Crew	600	600
Fuel	57,842	59,440
Oil and Residual Fuel	120	120
Auxiliary Tanks	3,760	3,840
Gross Weight	92,900	98,430

A design such as is shown in Figure 59, which has a straddle gear but some internal payload capability, might be represented by the external landing gear and fuselage weight and the internal cargo furnishing weight. Such a configuration would have half (626 pounds) the weight increment of the full internal cargo version.

## CONCLUSIONS

The parametric study and preliminary design of a shaft-driven rotor system for a heavy-lift helicopter, as conducted in Sections 1 through 5 of this report, adequately define and substantiate a rotor system that will meet the requirements specified in the Statement of Work. The configuration resulting in the lightest gross weight helicopter is the single matched-stiffness rotor system.

The additional parametric studies conducted in Section 6 refined the weight equations developed previously. These were based on later statistical data and preliminary design studies, which provided more reliable component weight data at the high gross weights associated with the heavy-lift helicopter. These rederived weight equations were used when the rotor parameters were restudied; the configuration described in Section 6 resulted. It is recommended that the detail design of a shaft-driven rotor system utilize the configuration as determined in Section 6.

## BIBLIOGRAPHY

1. Carpenter, Paul J., Lift and Profile Drag Characteristics of a NACA 0012 Airfoil Section as Derived from Measured Helicopter-Rotor Hovering Performance, NACA TN 4357, Langley Aeronautical Laboratory, Langley Field, Virginia, 1958.
2. Citzos, C. C., et al., Aerodynamic Characteristics of NACA 0012 Airfoil Section at Angles of Attack from 0° to 180°, NACA TN 3361, Langley Aeronautical Laboratory, Langley Field, Virginia, 1955.
3. Gessow, A. and Tapscott, R., Charts for Estimating Performance of High-Performance Helicopters, NACA Report No. 1266, Langley Aeronautical Laboratory, Langley Field, Virginia, 1956.
4. Gustafson, F. B. and Gessow, A., Effect of Blade Stalling on the Efficiency of a Helicopter-Rotor as Measured in Flight, NACA TN 1250, Langley Aeronautical Laboratory, Langley Field, Virginia, April 1947.
5. Gessow, A., and Crim, A. D., A Theoretical Estimate of the Effects of Compressibility on the Performance of a Helicopter-Rotor in Various Flight Conditions, NACA TN 3798, Langley Aeronautical Laboratory, Langley Field, Virginia, 1956.
6. Heyson, Harry H., An Evaluation of Linearized Vortex Theory as Applied to Single and Multiple Rotors Hovering In and Out of Ground Effect, NASA TN-D-43, Langley Research Center, Langley Field, Virginia, September 1959, Figure 7, Page 37.
7. Sweet, George E., Hovering Measurements for Twin-Rotor Configurations With and Without Overlap, NASA TN-D-534, Langley Research Center, Langley Field, Virginia, November 1960, Figure 9, Page 19.
8. Castles, W. Jr., and DeLeeuw, J. H., The Normal Component of the Induced Velocity in the Vicinity of a Lifting Rotor and Some Examples of Its Application, TR-1194, Georgia Institute of Technology, Atlanta, Georgia, March 1953, Figure 4a-g.
9. McKee, John W., and Naeseth, Roger L., Experimental Investigation of the Drag of Flatplates and Cylinders in the Slipstream of a Hovering Rotor, NACA TN 4239, Langley Aeronautical Laboratory, Langley Field, Virginia, April 1958.

10. Pruyn, R. R., and Miller, N. J., Studies of Rotorcraft Aerodynamic Problems Aimed at Reducing Parasite Drag Rotor-Airframe Interference Effects, and Improving Airframe Static Stability, WADD TR 61-124, Wright-Patterson Air Force Base, Ohio, 1961.
11. Wind Tunnel Tests of an Optimized, Matched-Stiffness Rigid Rotor, TRECOM Technical Report 64-56, Lockheed-California Company, U. S. Army Transportation Research Command,\* Fort Eustis, Virginia, November 1964.
12. Gessow, A. and Myers, G. C., Aerodynamics of the Helicopter, The MacMillan Company, New York, 1952.
13. Investigation of Elastic Coupling Phenomena of High-Speed Rigid Rotor Systems, TRECOM Technical Report 63-75, Lockheed-California Company, U. S. Army Transportation Research Command,\* Fort Eustis, Virginia, June 1964.
14. Gustafson, F. B. and Crim, A. D., Flight Measurements and Analysis of Helicopter Normal Load Factors in Maneuvers, NACA TN 2990, Langley Aeronautical Laboratory, Langley Field, Virginia, 1953.
15. Beavan, J. A., et al., Measurements of Maximum Lift on 26 Aerofoil Sections at High Mach Numbers, A.R.C. Technical Report R & M No. 2678, Her Majesty's Stationery Office, London, England, 1953.
16. Sasaki, D. T., Analytical Studies Report for Matched Stiffness/Flexure Root Blade Rotor System,\*\* LR 19057, Lockheed-California Company, 1 October 1965.
17. Coleman, R. P. and Feingold, A. M., Theory of Self-Excited Mechanical Oscillations of Helicopter Rotors with Hinged Blades, NACA Report 1351, Langley Aeronautical Laboratory, Langley Field, Virginia, 1958.

\* Name changed to U. S. Army Aviation Materiel Laboratories in March 1965

\*\* Limited Distribution - Not available to general public

18. Brooks, George W., The Mechanical Instability and Forced Response of Rotors on Multiple-Degree-of-Freedom Supports, Doctoral Dissertation, Princeton University, Princeton, New Jersey, 1961.
19. Bielawa, Richard L., An Experimental and Analytical Study of the Mechanical Instability of Rotors on Multiple-Degree-of-Freedom Supports, Report No. 612, Department of Aeronautical Engineering, Princeton University, Princeton, New Jersey, June 1962.
20. Roark, Raymond J., Formulas for Stress and Strain, McGraw-Hill Book Company, Inc., New York, 1954.
21. Bailey, F. J. Jr., A Simplified Theoretical Method of Determining the Characteristics of a Lifting Rotor in Forward Flight, NACA Report No. 716, Langley Aeronautical Laboratory, Langley Field, Virginia, 1941.



### DISTRIBUTION

US Army Materiel Command	5
US Army Aviation Materiel Command	6
Chief of R&D, DA	1
US Army Aviation Materiel Laboratories	29
US Army R&D Group (Europe)	2
US Army Engineer R&D Laboratories	2
US Army Limited War Laboratory	1
US Army Human Engineering Laboratories	1
US Army Research Office-Durham	1
US Army Test and Evaluation Command	1
Plastics Technical Evaluation Center	1
US Army Medical R&D Command	1
US Army Engineer Waterways Experiment Station	1
US Army Combat Developments Command, Fort Belvoir	2
US Army Combat Developments Command Experimentation Command	3
US Army War College	1
US Army Command and General Staff College	1
US Army Aviation School	1
US Army Infantry Center	2
US Army Tank-Automotive Center	2
US Army Aviation Maintenance Center	2
US Army Armor and Engineer Board	1
US Army Electronics Command	2
US Army Aviation Test Activity	2
Air Force Flight Test Center, Edwards AFB	2
US Army Field Office, AFSC, Andrews AFB	1
Air Force Aeropropulsion Laboratory, Wright-Patterson AFB	1
Air Force Flight Dynamics Laboratory, Wright-Patterson AFB	1
Systems Engineering Group (RTD), Wright-Patterson AFB	3
Air Proving Ground Center, Eglin AFB	1
Bureau of Ships, DN	1
Naval Air Systems Command, DN	6
Chief of Naval Research	6
David Taylor Model Basin	1
Commandant of the Marine Corps	1
Marine Corps Liaison Officer, US Army Transportation School	1
Testing and Development Division, US Coast Guard	1
Ames Research Center, NASA	1
Lewis Research Center, NASA	1
Manned Spacecraft Center, NASA	1
NASA Representative, Scientific and Technical Information Facility	2
NAFEC Library (FAA)	2
National Tillage Machinery Laboratory	1
US Army Aviation Human Research Unit	2
US Army Board for Aviation Accident Research	1
Bureau of Safety, Civil Aeronautics Board	2

US Naval Aviation Safety Center, Norfolk	2
Federal Aviation Agency, Washington, D. C.	1
Bureau of Flight Standards, FAA	1
Civil Aeromedical Research Institute, FAA	2
The Surgeon General	1
Defense Documentation Center	20
US Government Printing Office	1

UNCLASSIFIED

Security Classification

DOCUMENT CONTROL DATA - R&D		
(Security classification of title, body of abstract and indexing annotation must be entered when the overall report is classified)		
1. ORIGINATING ACTIVITY (Corporate author)		2a. REPORT SECURITY CLASSIFICATION
Lockheed California Company		UNCLASSIFIED
		2b. GROUP
3. REPORT TITLE		
PARAMETRIC ANALYSIS AND PRELIMINARY DESIGN OF A SHAFT-DRIVE ROTOR SYSTEM FOR A HEAVY-LIFT HELICOPTER		
4. DESCRIPTIVE NOTES (Type of report and inclusive dates)		
Final		
5. AUTHOR(S) (Last name, first name, initial)		
Bilezikjian, Vahe Conway, William J. Huss, Ronald E. Varner, Charles E. Brye, James M. Goldstein, Harry D. Kaysing, Charles W. Wilson, James R. Childers, Harry M. Hanson, Thomas F. Sacks, Ivan B.		
6. REPORT DATE	7a. TOTAL NO. OF PAGES	7b. NO. OF REFS
August 1966	342	21
8a. CONTRACT OR GRANT NO.	9a. ORIGINATOR'S REPORT NUMBER(S)	
DA 44-177-AMC-276(T)	USAAVLABS Technical Report 66-48	
8b. PROJECT NO.	9b. OTHER REPORT NO(S) (Any other numbers that may be assigned this report)	
Project 1F131001D157	LR 19143	
10. AVAILABILITY/LIMITATION NOTICES		
Distribution of this document is unlimited.		
11. SUPPLEMENTARY NOTES		12. SPONSORING MILITARY ACTIVITY
		U.S. Army Aviation Materiel Laboratories, Fort Eustis, Virginia
13. ABSTRACT		
<p>A parametric analysis and a preliminary design study were conducted to determine the optimum characteristics of a shaft-driven rotor which would result in the lightest gross weight helicopter capable of lifting military loads in the 12- to 20-ton range. The study considered single- and tandem-rotor helicopters with internal cargo and cargo pod. Types of rotors analyzed were articulated, teetered, rigid, and matched-stiffness. Existing turbine engines or growth versions thereof were considered.</p> <p>In the parametric analysis, component weight equations were developed and a computer program was utilized to determine the rotor characteristics for each helicopter configuration. For a given set of rotor parameters, the program computed the power plant rating, fuel required, and the empty weight corresponding to the helicopter which would satisfy the most critical mission requirements with the minimum gross weight. The performance of the resulting configuration was determined. Preliminary design studies of the rotor system, rotor controls, rotor/propulsion arrangement, and the general arrangement were made. Rotor loads were developed and a structural design analysis of the rotor system, including fatigue and weight analyses, was prepared. A dynamic and aeroelastic investigation of the rotor system and a stability and control study of the helicopter were conducted.</p> <p>The study indicates that the single-rotor helicopter incorporating a matched-stiffness rotor system would have a gross weight of 62,500 pounds for 12-ton payload range and 74,727 pounds for the 20-ton payload range. These gross weights are 4- to 6-percent less than the other configurations studied.</p>		

DD FORM 1 JAN 64 1473

UNCLASSIFIED

Security Classification



**UNCLASSIFIED**  
Security Classification

14. KEY WORDS	LINK A		LINK B		LINK C	
	ROLE	WT	ROLE	WT	ROLE	WT
Parametric study						
Design layout						
Static and dynamic analyses						
Stability and control study						
Structural design and weight analyses						
Configuration						

**INSTRUCTIONS**

**1. ORIGINATING ACTIVITY:** Enter the name and address of the contractor, subcontractor, grantee, Department of Defense activity or other organization (*corporate author*) issuing the report.

**2a. REPORT SECURITY CLASSIFICATION:** Enter the overall security classification of the report. Indicate whether "Restricted Data" is included. Marking is to be in accordance with appropriate security regulations.

**2b. GROUP:** Automatic downgrading is specified in DoD Directive 5200.10 and Armed Forces Industrial Manual. Enter the group number. Also, when applicable, show that optional markings have been used for Group 3 and Group 4 as authorized.

**3. REPORT TITLE:** Enter the complete report title in all capital letters. Titles in all cases should be unclassified. If a meaningful title cannot be selected without classification, show title classification in all capitals in parenthesis immediately following the title.

**4. DESCRIPTIVE NOTES:** If appropriate, enter the type of report, e.g., interim, progress, summary, annual, or final. Give the inclusive dates when a specific reporting period is covered.

**5. AUTHOR(S):** Enter the name(s) of author(s) as shown on or in the report. Enter last name, first name, middle initial. If military, show rank and branch of service. The name of the principal author is an absolute minimum requirement.

**6. REPORT DATE:** Enter the date of the report as day, month, year, or month, year. If more than one date appears on the report, use date of publication.

**7a. TOTAL NUMBER OF PAGES:** The total page count should follow normal pagination procedures, i.e., enter the number of pages containing information.

**7b. NUMBER OF REFERENCES:** Enter the total number of references cited in the report.

**8a. CONTRACT OR GRANT NUMBER:** If appropriate, enter the applicable number of the contract or grant under which the report was written.

**8b, 8c, & 8d. PROJECT NUMBER:** Enter the appropriate military department identification, such as project number, subproject number, system numbers, task number, etc.

**9a. ORIGINATOR'S REPORT NUMBER(S):** Enter the official report number by which the document will be identified and controlled by the originating activity. This number must be unique to this report.

**9b. OTHER REPORT NUMBER(S):** If the report has been assigned any other report numbers (*either by the originator or by the sponsor*), also enter this number(s).

**10. AVAILABILITY/LIMITATION NOTICES:** Enter any limitations on further dissemination of the report, other than those imposed by security classification, using standard statements such as:

- (1) "Qualified requesters may obtain copies of this report from DDC."
- (2) "Foreign announcement and dissemination of this report by DDC is not authorized."
- (3) "U. S. Government agencies may obtain copies of this report directly from DDC. Other qualified DDC users shall request through \_\_\_\_\_."
- (4) "U. S. military agencies may obtain copies of this report directly from DDC. Other qualified users shall request through \_\_\_\_\_."
- (5) "All distribution of this report is controlled. Qualified DDC users shall request through \_\_\_\_\_."

If the report has been furnished to the Office of Technical Services, Department of Commerce, for sale to the public, indicate this fact and enter the price, if known.

**11. SUPPLEMENTARY NOTES:** Use for additional explanatory notes.

**12. SPONSORING MILITARY ACTIVITY:** Enter the name of the departmental project office or laboratory sponsoring (paying for) the research and development. Include address.

**13. ABSTRACT:** Enter an abstract giving a brief and factual summary of the document indicative of the report, even though it may also appear elsewhere in the body of the technical report. If additional space is required, a continuation sheet shall be attached.

It is highly desirable that the abstract of classified reports be unclassified. Each paragraph of the abstract shall end with an indication of the military security classification of the information in the paragraph, represented as (TS), (S), (C), or (U).

There is no limitation on the length of the abstract. However, the suggested length is from 150 to 225 words.

**14. KEY WORDS:** Key words are technically meaningful terms or short phrases that characterize a report and may be used as index entries for cataloging the report. Key words must be selected so that no security classification is required. Identifiers, such as equipment model designation, trade name, military project code name, geographic location, may be used as key words but will be followed by an indication of technical context. The assignment of links, rules, and weights is optional.